Fermentative production of chlorinated and brominated L-tryptophan by metabolically engineered *Corynebacterium glutamicum*

DISSERTATION

Submitted by
Kareen Hildegard Veldmann

for the degree of Doctor of Science
Bielefeld University,
Faculty of Biology

Bielefeld, November 2019

The practical work of this thesis has been performed at Bielefeld University in the Institute of the Genetics of Prokaryotes, from October 2016 until September 2019 under the supervision of Prof. Dr. Volker. F. Wendisch.

Examiners

Prof. Dr. Volker F. Wendisch
Chair of Genetics of Prokaryotes
Faculty of Biology & CeBiTec, Bielefeld University

apl. Prof. Dr. Jörn Kalinowski
Chair Microbial Genomics and Biotechnology
CeBiTec, Bielefeld University

Parts of this thesis have been published in:

1. **Veldmann K.H.**, Minges H., Sewald N., Wendisch V.F. 2019. Metabolic engineering of *Corynebacterium glutamicum* fort he fermentative production of halogenated L-tryptophan. J. Biotechnol. 291, 7-16. https://doi.org/10.1016/j.jbiotec.2018.12.008

2. **Veldmann K.H.**, Dachwitz S., Risse J.M., Sewald N., Lee J.H., Wendisch V.F. 2019. Bromination of L-tryptophan in a fermentative process with *Corynebacterium glutamicum*. Front. Bioeng. Biotechnol. 7, 219. https://doi.org/10.3389/fbioe.2019.00219.

Parts of this thesis appear in form of a manuscript:

3. **Veldmann K.H.**, Lee J.H., Wendisch V.F. 2019. Fermentative production of halogenated L-tryptophan by recombinant *Corynebacterium glutamicum* using feedback resistant anthranilate phosphoribosyltransferases. To be submitted.

4. **Veldmann K.H.**, Kerbs A., Schnepel C., Sewald N., Lee J.H., Wendisch V.F. 2019. Fermentative production of indole with *Corynebacterium glutamicum* overexpressing different tryptophanases. To be submitted.

Abstract

Halogenated compounds, like 7-chloro-L-tryptophan and 7-bromo-L-tryptophan, are important building blocks for bioactive substances and have applications in agriculture, chemical and pharmaceutical industries. Around 20% of the pharmaceutical and 30% of the agrochemical compounds are halogenated. The chemical synthesis is characterized as hazardous and highly toxic. Mild halogenation by cross-linked enzyme aggregates containing FAD-dependent halogenase, NADH-dependent flavin reductase, and alcohol dehydrogenase has been described but requires a co-factor regeneration system. Until now, the microbial fermentative production of halogenated L-tryptophan has not been described. In this study, the fermentative synthesis of halogenated L-tryptophan was investigated. *Corynebacterium glutamicum* is a well-studied production host in the white biotechnology. Its a workhorse of the industrial amino acid production and is used since decades in the food and feed industry.

The main objectives of this study were i) establishment of a halogenated L-tryptophan producing *C. glutamicum* strain by overexpressing the genes coding for the FAD-dependent halogenase RebH and the NADH-dependent flavin reductase RebF from *Lechevalieria aerocolonigenes*, ii) extension of the concept regarding another halogenated Trp derivative 7-bromo-L-tryptophan, iii) expansion of the product portfolio deriving from L-tryptophan by fermentative production of indole in an L-tryptophan overproducing *C. glutamicum* strain.

The results presented in this work can be summarized as follows:

- Characterization of *C. glutamicum* indicated its suitability as production host since its tolerance for chloride and bromide salt is high and it is incapable to utilize the products L-tryptophan and halogenated L-tryptophan. The tolerance to 7-chloro-L-tryptophan and 7-bromo-L-tryptophan is moderate.
- Overexpression of *rebH* and *rebF* from *L. aerocolonigenes* in an L-tryptophan overproducing *C. glutamicum* strain enabled the production of 57 mg L^{-1} 7-chloro-L-tryptophan from glucose, ammonia and calcium chloride. Moreover, production of 7-chloro-L-tryptophan was established from the alternative, non-food competing carbon sources arabinose, glucosamine, and xylose.

- The 7-chloro-L-tryptophan producing strain was further engineered for production by optimizing the ribosome binding site of *rebH*. The improved strain HalT2 produced up to 108 mg L^{-1} 7-chloro-L-tryptophan.
- Fermentative production of 7-bromo-L-tryptophan with HalT2 was achieved by addition of sodium bromide to a low chloride medium culture. In a batch fermentation in 2 L minimal medium, a titer of 0.3 g L^{-1} 7-bromo-L-tryptophan was observed. The process was optimized in a fed-batch fermentation with HSG complex medium yielding in 1.2 g L^{-1} 7-bromo-L-tryptophan. The product was isolated to high purity by reverse phase chromatography.
- The *rebH* and *rebF* overexpressing *C. glutamicum* strain was further improved to prevent the feedback inhibition of anthranilate phosphoribosyltransferase, an enzyme of the L-tryptophan biosynthetic pathway, by 7-chloro-L-tryptophan and 7-bromo-L-tryptophan. This was achieved by the expression of feedback resistant anthranilate phosphoribosyltransferase genes. This led to improved production titers in shake flasks for both halogenated compounds.
- The product portfolio was expanded by indole. Implementation of various tryptophanases in the L-tryptophan overproducing *C. glutamicum* strain yielded in indole production. The highest production of 329 mg L^{-1} indole was reached by expression of the tryptophanase from *Proteus vulgaris*. Moreover, by characterization of the tryptophanases from *Escherichia coli* and *P. vulgaris* the new substrates 7-chloro-L-tryptophan and 7-bromo-L-tryptophan were identified.

In this study, the fermentative production of 7-chloro-L-tryptophan and 7-bromo-L-tryptophan in an L-tryptophan overproducing *C. glutamicum* strain overexpressing the genes for the FAD-dependent halogenase RebH and the NADH-dependent flavin reductase RebF was established for the first time. The production could be improved by an optimized ribosome binding site of *rebH*, optimized cultivation conditions, and up-scaling in a fed-batch fermentation. Furthermore, the product portfolio of *C. glutamicum* could be expanded towards indole with tryptophanases with a broad substrate spectrum, including halogenated L-tryptophan.

Abbreviations

7-Br-Trp	7-bromo-L-tryptophan
7-Cl-Trp	7-chloro-L-tryptophan
Ant	Anthranilate
ATCC	American Type Culture Collection
ATP	Adenosine triphosphate
bp	Base pair
cAA	Canonical amino acid
CDW	Cell dry weight
DAD	Diode array detector
Da	Dalton
DNA	Deoxyribonucleic acid
E4P	Erythrose 4-phosphate
EC	Enzyme commission number
ESI	Electrospray ionization
FAD	Flavin adenine dinucleotide
FLD	Fluorescence detector
Fmoc-Cl	9-fluorenylmethyl chlorocarbonate
GRAS	General recognized as save
HPLC	High-performance liquid chromatography
IPTG	Isopropyl-D-β-thiogalactopyranoside
Km	Kanamycin
LB	Lysogeny broth
MS	Mass spectrometry
NADH	Nicotinamide adenine dinucleotide
ncAA	Non-canonical amino acid
NMR	Nuclear magnetic resonance
OD	Optical density
OPA	*Ortho*-phthaldialdehyde
PEP	Phosphoenolpyruvate
RBS	Ribosome binding site

RID	refractive index detector
RNA	Ribonucleic acid
Rpm	revolutions per minute
SAM	*S*-Adenosyl-L-methionine
SDS PAGE	Sodium dodecyl sulfate polyacrylamide gel electrophoresis
Spec	Spectinomycin
Tet	Tetracycline
tRNA	transfer ribonucleic acid
Tris	Tris(hydroxymethyl)-aminomethan
Trp	L-tryptophan
UV	Ultraviolet
WT	Wild type

Common abbreviations, chemical formulas, units, and gene and protein names are not included.

Table of content

1 Introduction

1.1 Relevance of functionalized amino acids

In nature, functionalized amino acids show usually advantages over unmodified amino acids. They have applications in the pharmaceutical, chemical, and food industries. Functionalization of amino acids can enhance, for example, their bioactivity, bioavailability, and stability (Topall and Laborit, 1989), thus, they have often improved pharmacokinetic properties compared to their natural counterparts (Grauer and König, 2009). Various functionalizations are known with different effects, for example, i) the bacterium *Bacillus thuringiensis* strain 2e2 AKU 0251 hydroxylates isoleucine to 4-hydroxyisoleucine, a promising compound for drugs and functional foods because of its antidiabetic activity (Hibi et al., 2011), ii) the fungus *Acremonium* sp. BCC 2629 methylates L-phenylalanine to *N*-methyl-L-phenylalanine, a precursor of the antibiotic and insecticidal beauvericin (Bunyapaiboonsri et al., 2012; Urbaniak et al., 2019), or iii) L-theanine a ethylated glutamine derivative, which was isolated from green tea leaves and has flavour enhancing properties (Sakato, 1950; Nakagawa, 1970). This study focuses on the functionalization of L-tryptophan (Trp) by halogenation at the C7 position to achieve halogenated Trp.

1.1.1 Applications and properties of halogenated compounds

Halogenation describes a reaction of a halogen (chlorine, bromine, iodine or fluorine) with an alkane in which the halogen is introduced into the organic molecule via either an addition or a substitution reaction (Weissermel and Arpe, 2008). Chlorination and bromination reactions of natural products are the most common reactions, while fluorination and iodination rarely occur (Cantillo and Kappe, 2017). Halogenated compounds represent around 20% of the pharmaceutical and 30% of the agrochemical substances (Cantillo and Kappe, 2017). For example, vancomycin has antibiotic activity against Gram-positive bacteria (Bruniera et al., 2015), the herbicide metazosulfuron controls annual and perennial weed in paddy rice fields (Jeschke, 2017), and the sulfoxaflor has insecticidal activity against the green peach aphid (Loso et al., 2016). Additionally, halogenated compounds have applications such as flame retardants, imaging agents in medical diagnosis, dyes, antifouling,

pesticides, and in materials science (Hudlicky and Hudlicky, 1983; Sasson, 1995; Herrera-Rodriguez et al., 2011). Until now, almost 5000 halogenated natural compounds have been identified (Chung and Vanderwal, 2016). The advantages of halogenated substances are higher bioactivity, stability against biodegradation and oxidation (Blasiak and Drennan, 2008; Neumann et al., 2008).

An important part of halogenated compounds are the halogenated amino acids. They are important building blocks in the organic synthesis and precursor of complex molecules (Strickland and Willis, 2010). The halogenation step often occurs at the amino acid level in complex structures (van Pée, 1996). The effects of various halogenated amino acids are known, for example, the agent 2-fluoro-histidine, based on the α-amino acid histidine, inhibits cytopathogenicity of a variety of RNA and DNA viruses (De Clercq et al., 1978) or the halogenated L-phenylalanine derivatives 3,5-diiodo-tyrosine and 3,5-dibromo-tyrosine, which have antiglutamatergic activity, are neuroprotective agents for brain ischemia (Kagiyama et al., 2004). Moreover, halogenated amino acids can be fed in biotransformation processes to generate new halogenated compounds. In 2018 the biosynthesis pathway of the anticancer compound noscapine was transferred to the yeast *Saccharomyces cerevisiae* by Li and co-workers (Li et al., 2018). Noscapine derives from the precursor L-tyrosine and 4-hydroxyphenylacetaldehyde. By feeding 3-fluoro-tyrosine and 3-chloro-tyrosine to the metabolic engineered *S. cerevisae* strain, 8-fluoro-reticuline and 8-chloro-reticuline, the halogenated derivatives of the benzylisoquinoline alkaloid reticuline the precursor of noscapine, were produced.

1.1.2 Biosynthesis of halogenated compounds by halogenases and haloperoxidases

In nature, halogenation reactions are catalyzed by two enzyme classes. Haloperoxidases use hydrogen peroxide as oxidant while the halogenases are dependent on molecular oxygen (Neumann et al., 2008). These enzymes are further divided by their reaction mechanisms into three groups where the halogenation is carried out i) via a halide (X^-), ii) via a halogen ($X\bullet$), or iii) via a hypohalite (X^+) (Neumann et al., 2008).

The enzymatic halogenation via the nucleophilic halide is an *S*-adenosylmethionine (SAM) dependent reaction and is limited by its small substrates spectrum (O'Hagan et al., 2002; Eustáquio et al., 2008) (Fig. 1.1) (Table 1.1). The fluorinase from *Streptomyces cattleya*, for example, catalyzes the first reaction of the multistep pathway producing the pesticide fluoroacetate and 4-fluorothreonine (Sanada et al., 1986; Leong et al., 2017). The halogenase catalyzes the transfer of a fluoride anion to the electrophilic 5' carbon of SAM yielding 5-fluoroadenosine under the release of methionine (O'Hagan et al., 2002).

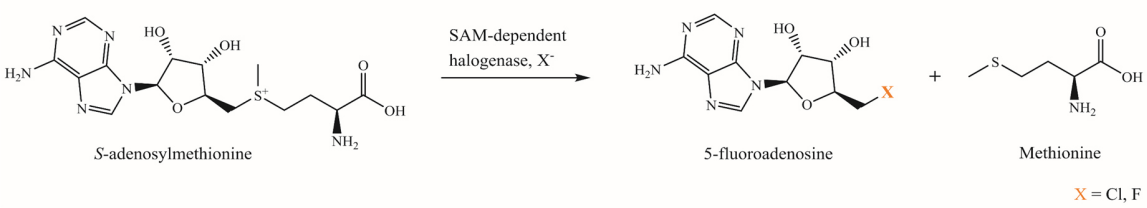

Figure 1.1: Schematic reaction of a SAM-dependent halogenase. The first reaction step of a SAM-dependent halogenase is the transfer of the halide anion to the electrophilic 5' carbon of the SAM, releasing the methionine residue. In further steps, the halogenase is not involved.

The second halogenation functions via a halogen and is a non-heme Fe^{II} dependent halogenation (Table 1.1). The halogenation is regio- and stereospecific on carrier tethered and free substrates (Hillwig and Liu, 2014). Due to the lack of an activated carbon atom, substrates in these reactions cannot be halogenated using an electrophilic agent. An example of this type is the trichlorination of the C5 methyl group L-leucine, the initial step of the biosynthesis of the lipopeptide barbamide (Sitachitta et al., 2000; Chang et al., 2002). The amino acid substrate is attached to the peptidyl carrier protein BarA (Galonić et al., 2006) (Fig. 1.2). For the halogenation two non-heme Fe^{II} dependent halogenases, BarB1 and BarB2 from *Lyngbya majuscula* 19L, are required. These are activated through oxygen, α-ketoglutarate, and a halogen (Galonić et al., 2006). The co-substrate Fe^{II} of the non-heme Fe^{II} dependent halogenases is decarboxylated by α-ketoglutarate to a Fe^{IV}=O species, which abstracts the hydrogen atom from an aliphatic carbon center in the substrate forming a radical. The formed Fe^{III} builts with the Cl• the Fe^{III}-Cl complex. In the next step, the substrate radical is chlorinated by accepting Cl from a Fe^{III}-Cl complex (Vaillancourt et al., 2006). The first two chlorinations are carried out by BarB1 and the third chlorination by BarB2 (Galonić et al., 2006).

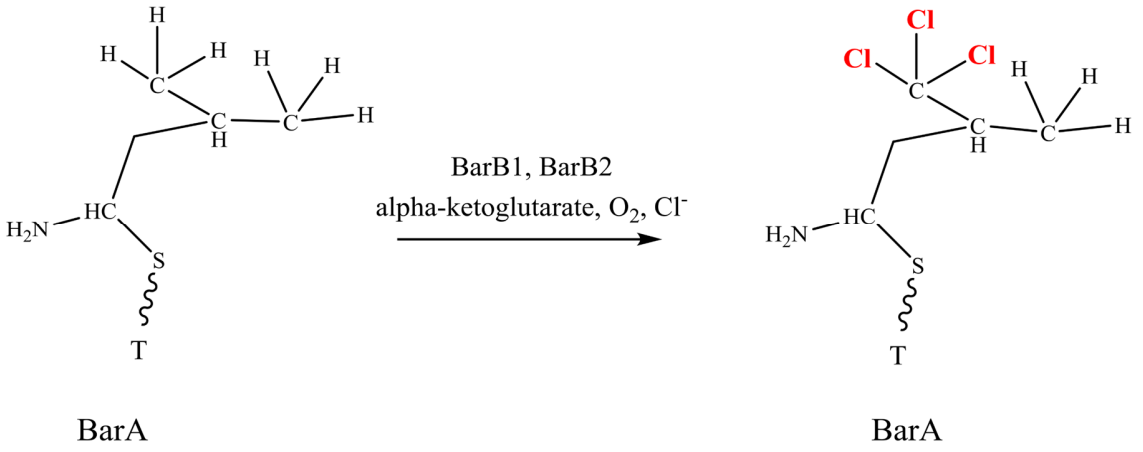

Figure 1.2: Schematic reaction of the non-heme Fe^{II} dependent halogenases BarB1 and BarB2. The hydrogen atoms of the C5 methyl group of L-leucine, which is attached to the peptide carrier protein BarA, are removed by the halogenase. The resulting substrate radical is chlorinated.

The third class of enzymatic halogenases is characterized by the reaction via a hypohalite (X^+). This class is further divided into 3 subclasses: the heme-Fe-dependent haloperoxidase (Hager et al., 1966), the vanadium-dependent haloperoxidase (Wever et al., 1985) and the flavin-dependent halogenases (Dairi et al., 1995; Hammer et al., 1997). All of them form a hypohalous acid (HO-X) as halogenating agent (Grüschow et al., 2014) (Table 1.1.).

The first heme-Fe-dependent haloperoxidase was discovered in *Caldariomyces fumago*, which produces the chlorinated antibiotic caldariomycin (Hager et al., 1966; Morris and Hager, 1966). The halogenation occurs unspecific and the haloperoxidases accept a broad range of substrates (Sundaramoorthy et al., 1995; Latham et al., 2017; Timmins and de Visser, 2018). The formation of the hypohalous acid (HO-X) occurs in several steps. It starts with the resting state of the haloperoxidase, where iron is in the ferric form with four coordination sites and a cysteine ligand bound at the heme prosthetic group (Leak et al., 2009). When hydrogen peroxide (H_2O_2) binds to the haloperoxidase an active ferryl-oxo species is formed and water is eliminated through heterolytic O-O bond cleavage (Neumann et al., 2008). This intermediate is reacting with a halide ion to generate a Fe(III) hypohalide. Either this formed Fe(III) hypohalide executes the halogenation of the substrate or a free hypohalous acid is released and performs the halogenation with a higher distance to the Fe center (Libby et al., 1982; Neumann et al., 2008) (Fig. 1.3 A).

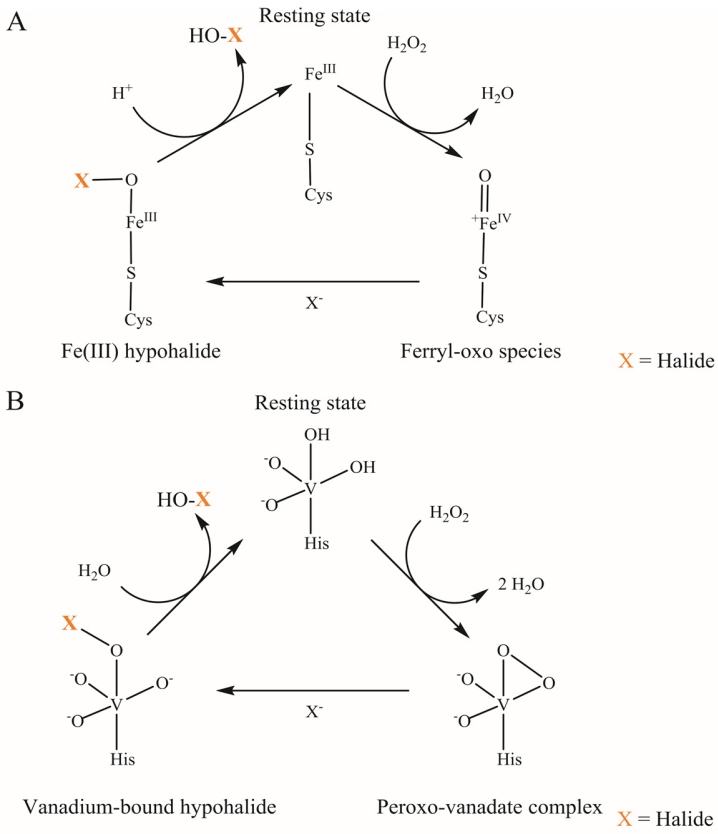

Figure 1.3: Schematic reaction of the heme-Fe-dependent (A) and vanadium-dependent (B) haloperoxidases. **A**: The hypohalous acid is formed in several steps. The resting state of the haloperoxidase is activated by hydrogen peroxide (H_2O_2) to form a ferryl-oxo species after the elimination of water. Through the reaction with the halide ion (X^-) Fe(III) hypohalide is formed. The resting state is reached by release of the hypohalous acid. Either the Fe(III) hypohalide or the released hypohalous acid performs the halogenation. **B**: The vanadium dependent halogenation takes place in multiple steps. Three of the vanadium-bound oxygen atoms interact with the haloperoxidase. The peroxo-vanadate complex is built by reduction of H_2O_2. The complex reacts with the halide ion (X^-) and the vanadium-bound hypohalide is formed. By release of the hypohalous acid the resting state is entered. Either the vanadium-bound hypohalide or the released hypohalous acid performs the halogenation.

The first vanadium-dependent haloperoxidase was discovered in 1985 in the brown algae *Ascophyllum nodosum* (Wever et al., 1985). The bromoperoxidases are mostly found in marine seaweeds (Butler and Carter-Franklin, 2004) and chloroperoxidases in terrestrial fungi and bacteria (Winter et al., 2007). The vanadium-dependent haloperoxidases catalyze the halogenation of electron-rich substrates (Blasiak and Drennan, 2008). The reaction of the vanadium-dependent haloperoxidase proceeds in several steps and the halogenation of the substrate is unspecific (Fig. 1.3 B) (Timmins and de Visser, 2018). The vanadium atom is

bound in the active site to a conserved histidine residue and forms a complex with four oxygen atoms. Three of the oxygen atoms interact with the amino acid moieties of the enzyme while one oxygen atom is involved in the reaction (Messerschmidt and Wever, 1996; Weyand et al., 1999). When hydrogen peroxide binds the vanadate complex a peroxo-vanadate complex is built, which then oxidizes with the halide ion to a vanadium-bound hypohalide (Neumann et al., 2008). The mechanism of the halogenation reaction itself remains still unknown. It is possible, that the built vanadium-bound hypohalide execute the halogenation or the hypohalous acid is released and performs the halogenation (Grüschow et al., 2014).

The last form of the enzymatic halogenation is the flavin-dependent or FAD-dependent reaction (Table 1.1). The first FAD-dependent halogenase was discovered in 1995 in *Streptomyces aureofaciens* NRRL3203, which chlorinates tetracycline to chlortetracycline (Dairi et al., 1995). The halogenases can be divided into two groups due to their substrates. One group catalyzes the halogenation of free small-substrates (Dong et al., 2005; Yeh et al., 2005) and the other requires carrier-bound substrates from non-ribosomal polypeptide synthetase (NRPS) systems (Lin et al., 2007). The FAD-dependent reaction is characterized by several steps (Fig. 1.4). First, flavin adenine dinucleotide (FAD) is reduced by an NADH-dependent flavin reductase to dihydroflavine adenine dinucleotide ($FADH_2$) (Yeh et al., 2005). The $FADH_2$ reacts with molecular oxygen to a peroxo species (FAD(C4a)-OOH) (Hering et al., 2016). In the next step a nucleophilic attack of the halide ion takes place and the hypohalous acid and FAD(C4a)-OH are built. The FAD(C4a)-OH is recycled to FAD through hydration and enters the reaction cycle (Yeh et al., 2006). The hypohalous acid is further channeled from the $FADH_2$ binding site of the halogenase through a 10 Å tunnel to the substrate-binding site. Here, the hypohalous acid is interacting with a lysine residue, which is conserved in most FAD-dependent halogenases and forms an *N*-haloamine. In the last step the *N*-haloamine halogenates the substrate and the halogenated product is released. The halogenation reaction is regiospecific (Yeh et al., 2007) (Fig. 1.4).

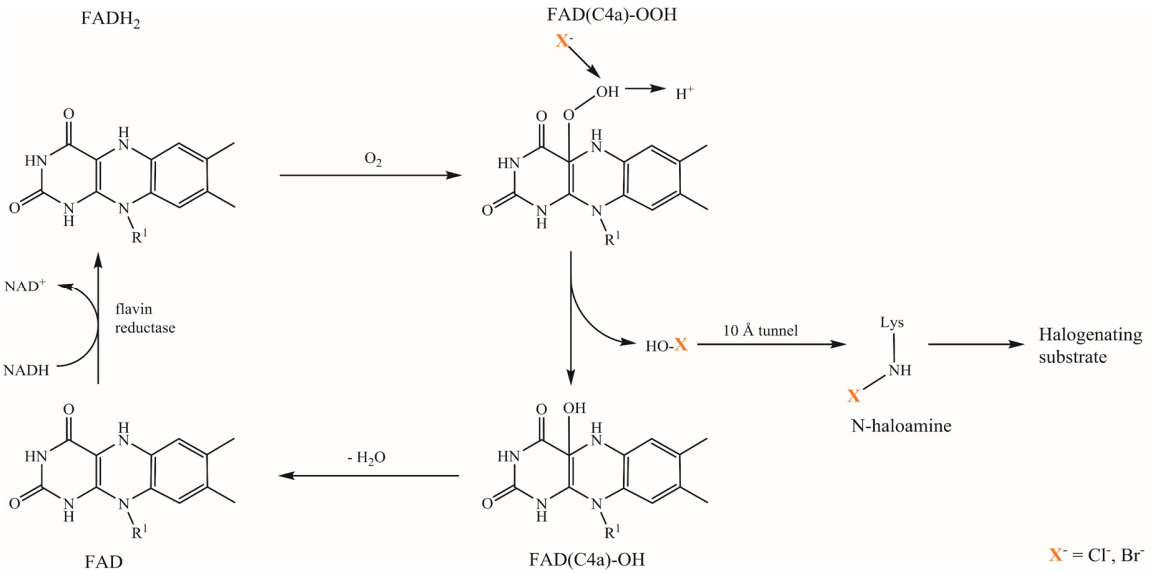

Figure 1.4: Schematic reaction of a FAD-dependent halogenase. The mechanism of the FAD-dependent halogenation includes multiple steps to halogenate the target substrate and to regenerate the cofactor $FADH_2$. $FADH_2$ reacts with molecular oxygen to FAD(C4a)-OOH. In the next step, a nucleophilic attack by the halide ion (X^-) takes place and a hypohalous acid is released. This interacts with a lysine residue to form an *N*-haloamine, which halogenates the substrate. For regeneration the $FADH_2$ FAD(C4a)-OH is dehydrated to FAD, which is reduced to $FADH_2$ by an NADH dependent flavin reductase.

1.1.2.1 FAD-dependent halogenase RebH and NADH-dependent flavin reductase RebF

The gene of the halogenase RebH is encoded in the *reb* operon of *Lechevalieria aerocolonigenes* (strain C-38383-RK2, DSMZ-No. 44217), which was discovered in 1986 and isolated from soil in Japan (Labeda, 1986; Sánchez et al., 2002). This operon encodes 18 genes, with functions in the rebeccamycin biosynthesis, however, the function of six genes remains still unknown (Fig. 1.5). RebH has a molecular weight of 60 kDa and forms a homodimer (Bitto et al., 2008). The two monomers are connected by Van der Waals contacts, 14 hydrogen bonds and one salt bridge (Bitto et al., 2008). RebH has two active sites, the $FADH_2$ and the Trp binding site (Yeh et al., 2005) (Fig. 1.6). They are separated by a 10 Å tunnel (Bitto et al., 2008). RebH performs a FAD-dependent halogenation of Trp (Chapter 1.1.2). The temperature optimum of RebH lies between 30 – 35°C (Poor et al., 2014). RebH catalyzes the chlorination as well as the bromination of its substrate, however, the chlorination is the preferred reaction (Yeh et al., 2005).

Table 1.1: Overview of the various subclasses of the halogenases.

Halogenase	Reaction type/ Co-substrate	Description	Specificity
SAM-dependent halogenase	Nucleophilic/ SAM, F^- or Cl^-	Nucleophilic attack of X^- on SAM yielding in 5-haloadenosine, which causes further biosynthetic halogenation of metabolites	Limited by a few substrates and end products
Non-heme Fe^{II} dependent halogenases	Radical/ O_2, α-ketoglutarate, halogen	Fe^{II}=O species abstract hydrogen from substrate forming a radical, the radical is halogenated by accepting X from Fe^{III}-X species	Regio- and stereospecific halogenation on carrier tethered and free substrates
Heme-Fe-dependent haloperoxidase	Oxidative/ H_2O_2, halide	H_2O_2 activates the resting Fe^{III} state to a ferry-oxo species (Fe^{IV}=O), reaction with halide forms Fe^{III} hypohalide, HOX is released	Unspecific halogenation
Vanadium-dependent haloperoxidase	Oxidative/ H_2O_2, halide	H_2O_2 activates the vanadium resting state to a peroxo-vanadate complex, reaction with the halide to form the vanadium-bound hypohalide, HOX is released	Unspecific halogenation
FAD-dependent halogenase	Oxidative/ O_2, Br^- or Cl^-	$FADH_2$ reacts with O_2 to FAD(C4a)-OOH, reaction with the halide to form the FAD(C4a)-peroxide, release of the HOX, which is channeled to the substrate-binding site	Regioselective halogenation for free and carrier bound substrates

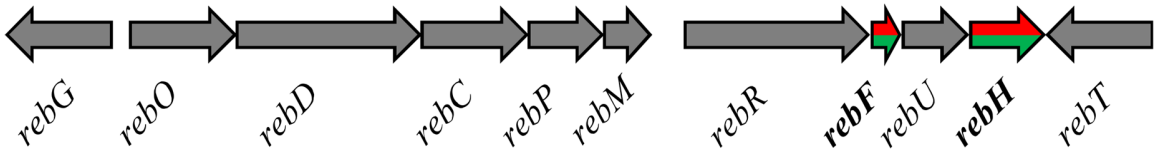

Figure 1.5: Schematic representation of the annotated *reb* operon. *N*-glycosyltransferase (encoded by *rebG*), L-amino acid oxidase (encoded by *rebO*), *bis*-indole formation (encoded by *rebD*), FAD-containing monooxygenase (encoded by *rebC*), P450 heme-thiolate protein (encoded by *rebP*), methyltransferase (encoded by *rebM*), regulatory protein (encoded by *rebR*), NADH dependent flavin reductase (encoded by *rebF*), integral membrane transporter (encoded by *rebU*), FAD-dependent 7-halogenase (encoded by *rebH*), integral membrane transporter (encoded by *rebT*). RebH and RebF are responsible for the chlorination (red) and bromination (green) of Trp.

RebH has a turnover number of 0.29 s^{-1} with the natural substrate Trp and has a K_m value for Trp of 2 µM (Yeh et al., 2007). Interestingly, RebH accepts also other substrates, like D-tryptophan, 5-hydroxy-tryptophan,

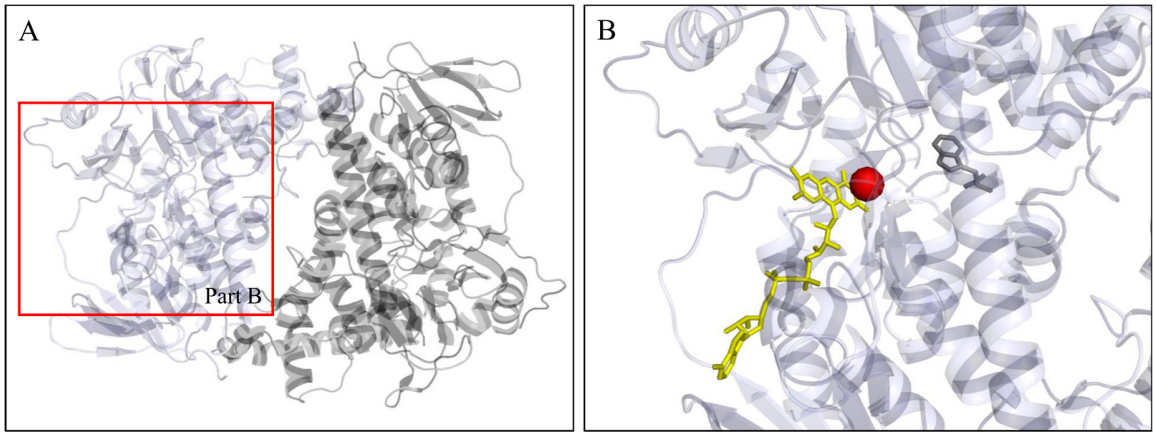

Figure 1.6: Structure of RebH (PDB 2OA1, (Bitto et al., 2008)). A: Whole structure of the homodimer RebH with both monomers (in light blue and black) **B**: Zoom of the left monomer with bond FAD (yellow), Trp (dark grey) and chlorine (red).

5-methyl-tryptophan, 5-fluoro-tryptophan, tryptamine, and tryptophol, however, with a lower conversation rate (Payne et al., 2013; Frese et al., 2014; Frese and Sewald, 2015). Further, the substrate spectrum of RebH could be extended by directed evolution. Different mutants are able to accept various substrates, which are similar in size to Trp, like tryptoline, eleagnine and yohimbine (Payne et al., 2015). Additionally, the thermostability was changed by directed evolution, as a result, the temperature optimum of wild type RebH increased by 5°C (Poor et al., 2014). $FADH_2$ regeneration is performed by the NADH-dependent flavin

reductase RebF, which is also encoded in the *reb* operon of *L. aerocolonigenes* (Sánchez et al., 2002) (Fig. 1.5). The enzyme has a molecular size of 18 kDa. RebF oxidizes NADH with a turnover of 1.8 s^{-1} in presence of FAD or FMN. The K_m for FAD is 0.7 µM and for FMN 1.3 µM (Yeh et al., 2005).

1.3 L-tryptophan biosynthesis

Trp is an essential aromatic amino acid. It was discovered by Frederick G. Hopkins and Sydney W. Cole in 1901 (Hopkins and Cole, 1901). Trp is characterized by an indole ring, a bicyclic ring formed by benzene and a pyrrole group, and connected to an α-carbon, which attaches a carboxyl group and an amine group. It has unique properties in proteins and peptides interactions through the indole ring, which stabilizes structures, domains, and interactions by Van der Waals force (Betti et al., 2016). In membrane proteins, for example, Trp stabilizes the transmembrane domains to the phospholipid bilayer (de Jesus and Allen, 2013). It is also used in food, feed, and pharmaceuticals since it can improve the sleep state and mood (Ikeda, 2006). It is assumed, that a Trp-enriched diet can prevent cognitive decline (Musumeci et al., 2017), has the potential to reduce depressive symptoms and anxiety (Lindseth et al., 2015), and can have an effect on inflammatory bowel disease and Crohn disease (Nikolaus et al., 2017). Several Trp derivatives are formed by enzymatic reactions: decarboxylation of Trp yields tryptamine, the precursor of serotonin (Facchini et al., 2000; Park et al., 2011) and by an α,β-elimination of the side chain the signal molecule indole is built (Newton and Snell, 1965; Lee and Lee, 2010).

The biosynthesis pathway to produce the essential aromatic amino acid Trp can be divided into two parts: i) the shikimate pathway starting from the condensation of phosphoenolpyruvate (PEP) and erythrose-4-phosphate (E4P) and ending with chorismate, and ii) the Trp pathway which starts with chorismate and ends with Trp (Fig. 1.7).

Both the precursors of the shikimate pathway derive from glucose-6-phosphate, which is either converted to PEP via glycolysis or via pentose-phosphate pathway yielding E4P (Eggeling and Bott, 2005). The first step of the shikimate pathway starts with the 3-deoxy-D-arabino-heptulosonate 7-phosphate synthase (encoded by *aro*, *aroII* or *aroF*, *aroH*, and *aroG* depending on the microoragnism) driven aldol-like condensation of PEP and

E4P to generate 3-Deoxy-D-arabino-heptulosonate-7-phosphate (DAHP). In the next step, the 3-dehydroquinate synthase (encoded by *aroB*) catalyzes the conversion of the seven-carbon keto acid DAHP to 3-dehydroquinate via oxidation, elimination of a phosphate, reduction, ring-opening and aldol reaction (Turner et al., 1975; Han et al., 1999; Negron et al., 2011). The third step is the dehydration of 3-dehydroquinate to 3-dehydroshikimate, which is catalyzed by the 3-dehydroquinate dehydratase (encoded by *aroD*) (Herrmann and Weaver, 1999; Liu et al., 2015). Subsequently the NADPH-dependent shikimate dehydrogenase (encoded by *aroE*) reduces 3-dehydroshikimate to shikimate (Ye et al., 2003; Kubota et al., 2013). Shikimate is further phosphorylated to shikimate-3-phosphate catalyzed by the shikimate kinase (encoded by *aroK*) under consumption of adenosine triphosphate (ATP) (Herrmann and Weaver, 1999). In the sixth step the 5-enolpyruvylshikimate 3-phosphate synthase (encoded by *aroA*), which belongs to the transferases, catalyzes the transfer of the enolpyruvyl part of PEP to shikimate-3-phosphate to form 5-enolpyruvylshikimate 3-phosphate (EPSP) and inorganic phosphate (Levin and Sprinson, 1964; Bentley and Haslam, 1990). In the last step of the shikimate pathway the chorismate synthase (encoed by *aroC*) catalyzes the 1,4-*anti*-elimination of the 3-phosphate group and C-(*6proR*) hydrogen from EPSP to form chorismate and orthophosphate (Morell et al., 1967; Floss et al., 1972). Here, a branched point is reached: chorismate can be further converted to L-phenylalanine and L-tyrosine or to Trp (Fig. 1.7). The chorismate mutase (encoded by *csm*) catalyzes the conversion of chorismate to prephenate (Guilford et al., 1987). This is either converted to phenylpyruvate by the prephenate dehydratase (encoed by *pheA*) and further to L-phenylalanine (Follettie and Sinskey, 1986; Zhang et al., 2013) or to pretyrosine, which is then converted

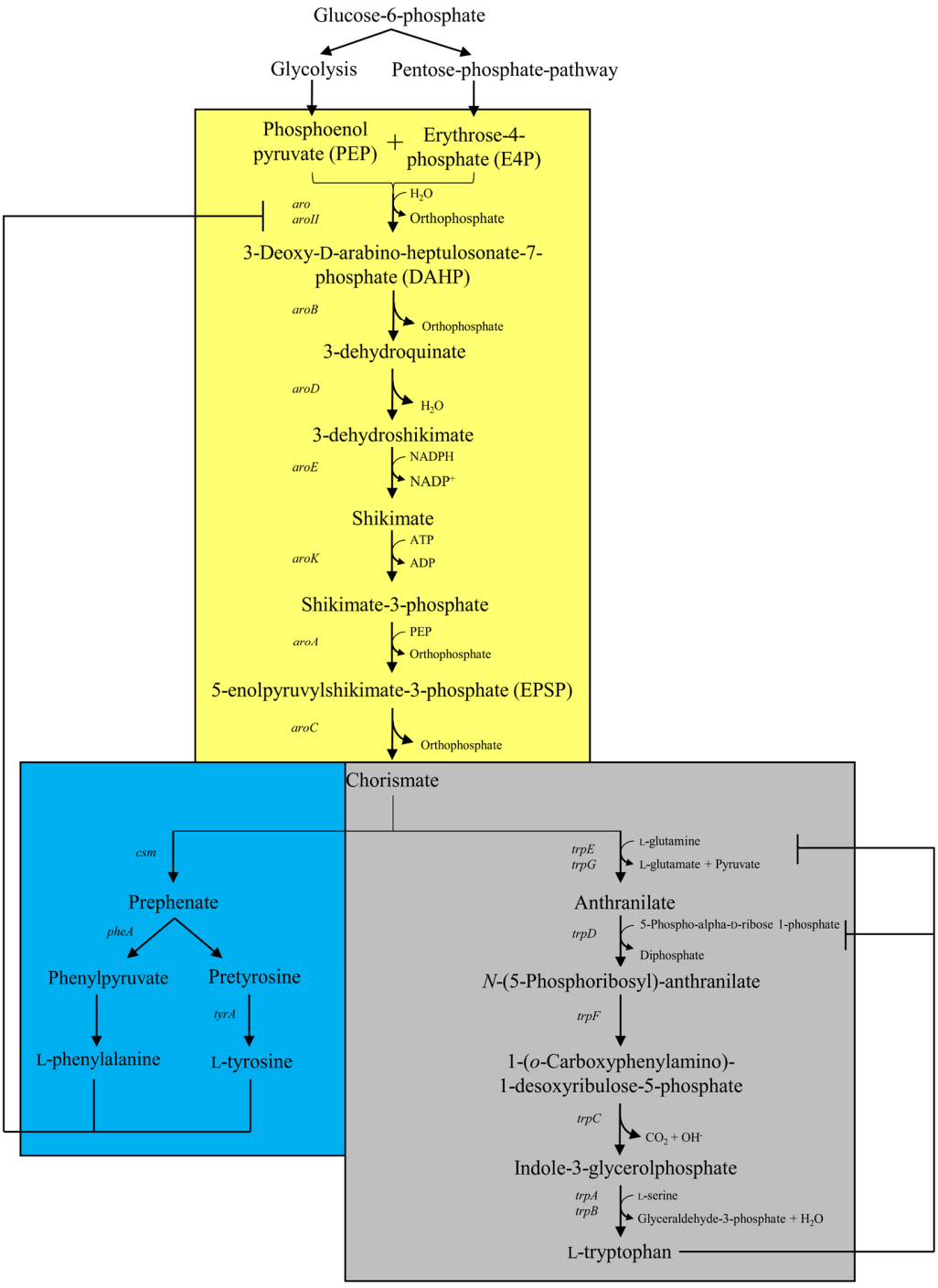

Figure 1.7: Schematic representation of the biosynthetic Trp as well as other aromatic amino acids pathway in *C. glutamicum*. The pathway is divided into shikimate pathway (yellow), which starts from phosphoenolpyruvate (PEP) and erythrose-4-phopshate (E4P) and ends with chorismate, and the Trp pathway from chorismate to Trp (grey). The L-phenylalanine and L-tyrosine pathway starts from chorismate and ends with L-phenylalanine and L-tyrosine (blue). The lines indicate product feedback inhibition. Shikimate pathway

(yellow): 3-deoxy-D-arabino-heptulosonate 7-phosphate synthase (encoded by *aroI*,*aroII*), 3-dehydroquinate synthase (encoded by *aroB*), 3-dehydroquinate dehydratase (encoded by *aroD*), NADPH-dependent shikimate dehydrogenase (encoded by *aroE*), shikimate kinase (encoded by *aroK*), 5-enolpyruvylshikimate 3-phosphate synthase (encoded by *aroA*), chorismate synthase (encoded by *aroC*); L-phenylanine and L-tyrosine pathway (blue): prephenate dehydratase (encoded by *pheA*), pretyrosine dehydrogenase (encoded by *tyrA*); Trp pathway (grey): anthranilate synthase (encoded by *trpG, trpE*), anthranilate phosphoribosyltransferase (encoded by *trpD*), phosphoribosyl anthranilate isomerase (encoded by *trpF*), indole-3-glycerol phosphate synthase (encoded by *trpC*), tryptophan synthase (encoded by *trpB, trpA*).

to L-tyrosine by the pretyrosine dehydrogenase (Hagino et al., 1973; Jensen and Pierson, 1975). The biosynthesis pathway in the direction of Trp starts with the conversion of chorismate to anthranilate. For this step the anthranilate synthase (encoded by *trpE* (component I) and *trpG* (component II)) is responsible, which requires chorismate and L-glutamine as substrates. First, an amine is transferred from L-glutamine to the C2 position of the chorismate and L-glutamate is released. In the next step, an enolpyruvate group is removed by protonation from the intermediate to form pyruvate and anthranilate (Tamir and Srinivasan, 1970). The anthranilate phosphoribosyltransferase (encoded by *trpD*) transfers a phosphoribosyl group from 5-phospho-α-D-ribose 1-diphosphate (PRPP) to anthranilate forming *N*-(5-phospho-β-D-ribosyl)-anthranilate and diphosphate (Lambrecht and Downs, 2012). The third and the fourth step of the Trp biosynthesis is catalyzed by a bifunctional enzyme complex: the phosphoribosyl anthranilate isomerase (encoded by *trpF*; component I) rearranges irreversible *N*-(5-phospho-β-D-ribosyl)-anthranilate to 1-(*o*-carboxyphenylamino)-1-deoxy-D-ribulose 5-phosphate (Wilmanns et al., 1992), which is further converted to indole-3-glycerol phosphate by a ring closure reaction which is catalyzed by the indole-3-glycerol phosphate synthase (encoded by *trpC*), the second component of the complex (Parry, 1971; Hennig et al., 2002). The last step of the Trp biosynthesis is catalyzed by the tryptophan synthase, which consists of an $\alpha_2\beta_2$ complex formed by TrpA and TrpB (Crawford and Yanofsky, 1958). In the first reaction the α subunit (encoded by *trpA*) cleaves the indole-3-glycerol-phosphate to indole and D-glyceraldehyde 3-phosphate, without releasing the intermediates (Lane and Kirschner, 1991). In the next step, the β subunit (encoded by *trpB*) catalyzes in a pyridoxal 5-phosphate dependent reaction the condensation of L-serine and indole to Trp (Lane and Kirschner, 1983) (Fig. 1.7).

1.4 Biosynthesis and applications of halogenated L-tryptophan

Trp can be further processed by enzymtic halogenation to halogenated Trp. This reaction is catalyzed by different halogenases, which halogenate the Trp regioselective at a carbon atom. The enzymatic halogenations at the C5, C6, and C7 positions were already described in previous studies (Keller et al., 2000; Yeh et al., 2005; Zehner et al., 2005; Zeng and Zhan, 2011) (Fig. 1.8). The FAD-dependent 5-halogenases PyrH and FHal16 from *Streptomyces rugosporus* LL-42D005 and *Xenorhabdus szentirmaii* DSM 16338, respectively, chlorinate Trp at the C5 position to obtain 5-chloro-tryptophan (Zehner et al., 2005; Domergue et al., 2019). In *Streptomyces rugosporus* LL-42D005 5-chloro-tryptophan is a precursor of the antibiotic compound pyrroindomycin B (Zehner et al., 2005).

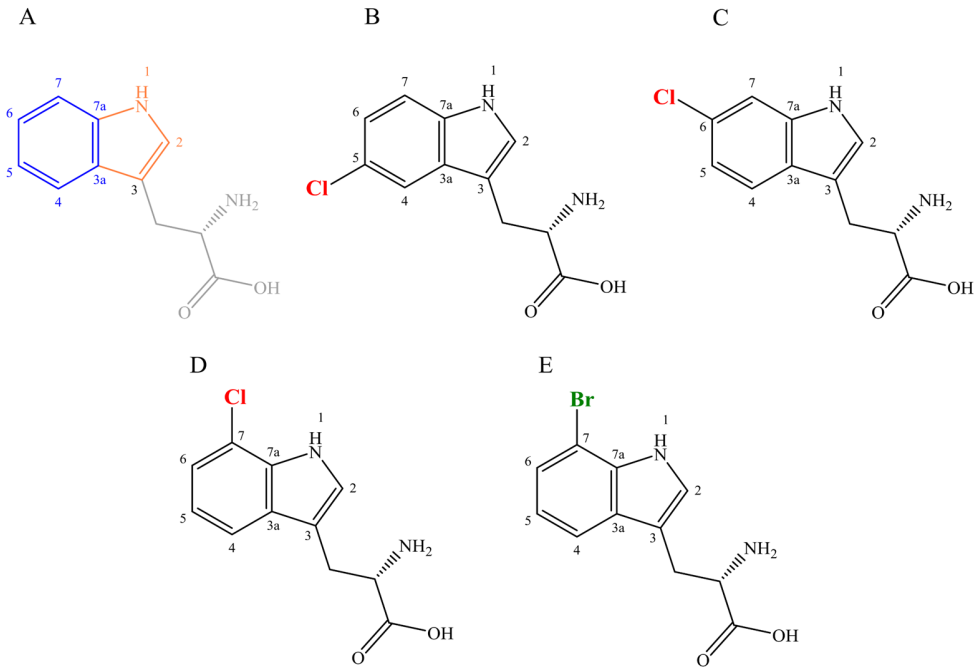

Figure 1.8: Structure of Trp, 5-chloro-tryptophan, 6-chloro-trptophan, 7-chloro-L-tryptophan (7-Cl-Trp), and 7-bromo-L-tryptophan (7-Br-Trp): A: Trp The benzene ring is marked in blue, the pyrrol group in orange and side chain in grey. **B**: 5-chloro-tryptophan **C**: 6-chloro-tryptophan **D**: 7-Cl-Trp. **E**: 7-Br-Trp.

Halogenation at position 6 is catalyzed by the FAD-dependent 6-halogenases ThaI (ThdH) and SttH, which derive from *Streptomyces rugosporus* and *Streptomyces toxytricini*, respectively (Zeng and Zhan, 2011; Milbredt et al., 2014) (Fig. 1.8). 6-chloro-tryptophan is

the precursor of the plant growth-regulating substance thienodolin (Kanbe et al., 1993; Milbredt et al., 2014). Both tryptophan 6-halogenases accept also bromide ions, whereby 6-bromo-tryptophan the precursor of barettin, a compound with antioxidant activity, is formed (Bittner et al., 2007). For the halogenation of the C7 position two halogenases from the same enzyme class are known. In *P. fluorescens* BL915ΔORF1-4 the FAD-dependent 7-halogenase PrnA chlorinates Trp (Keller et al., 2000; Dong et al., 2005). The resulting 7-chloro-L-tryptophan (7-Cl-Trp) (Fig. 1.9) serves as a precursor for the antifungal antibiotic pyrrolnitrin (Hammer et al., 1997). A second FAD-dependent 7-halogenase is RebH from *L. aerocolonigenes*. Here, 7-Cl-Trp (Fig. 1.9) serves as a precursor of the indolocarbazole antitumor agent rebeccamycin (Bush et al., 1987; Nishizawa et al., 2005).

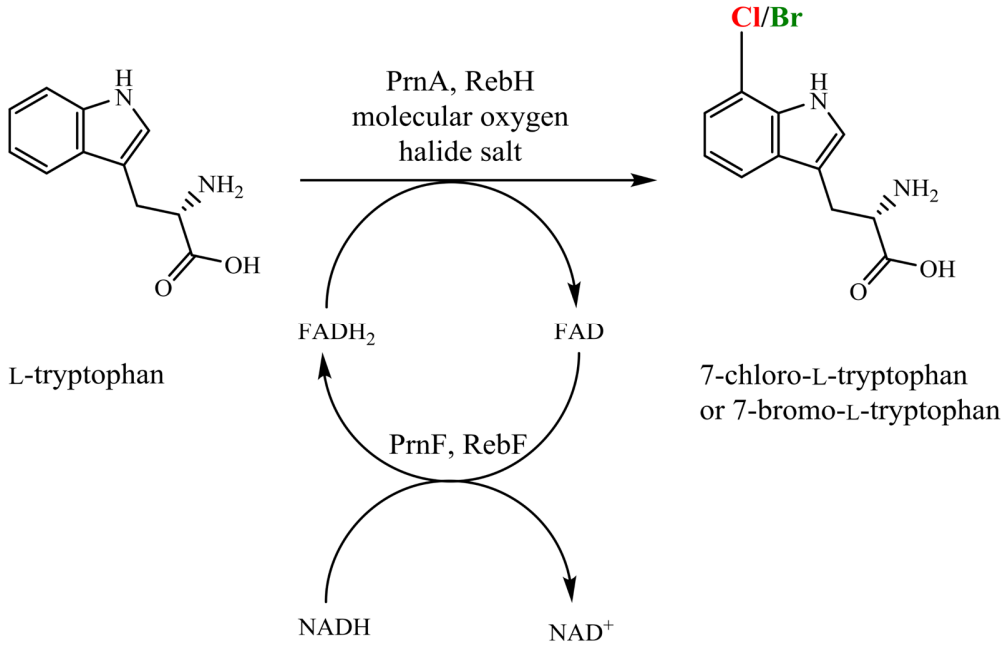

Figure 1.9: Schematic reaction from Trp to 7-Cl-Trp or 7-Br-Trp. Trp is either chlorinated or brominated by the FAD-dependent tryptophan halogenase PrnA or RebH. For the regeneration of the $FADH_2$, the NADH dependent flavin reductase PrnF or RebF are responsible.

Next to the chlorination of Trp, the bromination at position 7 was described as well. 7-bromo-L-tryptophan (7-Br-Trp) (Fig. 1.9) is a precursor of the 20S proteasome protease inhibitor TMC-95A (Koguchi et al., 2000). Another application of 7-Cl-Trp and 7-Br-Trp is the use in cross-linking reactions. In the Suzuki–Miyaura cross-coupling reaction, which uses palladium catalyst the C7 position of Trp shows the highest reactivity compared to the C5

and C6 position (Roy et al., 2008; Schnepel and Sewald, 2017). In this reaction the halogen is exchanged by an acryl substituent to form various acryl-substituted Trps (Frese et al., 2016), but for most of the cross-linking reactions the brominated Trp is preferred due to its higher reactivity (Corr et al., 2017). Another crosslinking reaction is the Mizoroki–Heck cross-coupling, which is also palladium-catalyzed. In this reaction the halogen of 7-Br-Trp substituted by different styrenes to build styryltryptophans (Gruß et al., 2019). This styryltryptophans have fluorescence properties and the potential to be used in the labeling of biomolecules (Gruß et al., 2019). In both cross-linking reactions the halogenated amino acid is protected by an N^{α}-*tert*-butoxycarbonyl (Boc) group to obtain Trp derivatives used for peptide chemistry (Frese et al., 2014; Schnepel and Sewald, 2017; Gruß et al., 2019). A third option to process 7-Br-Trp is the Sonogashira cross-coupling reaction, which is palladium-catalyzed (Corr et al., 2017). Here, 7-Br-Trp is bound to a tripeptide at the N-terminal position, and the bromine is substituted by a 3-fluorophenylacetylene, which has a potential in ^{19}F-labelling of peptides. Due to the short time of cross-coupling it may be a tool for the Positron Emission Tomography (PET) (Krapf et al., 2016; Corr et al., 2017).
Until now, three methods are established to obtain halogenated Trp. One is the chemical halogenation, which is mostly hazardous and highly toxic. The second one is a biocatalytic process, where the FAD-dependent halogenase RebH, NADH dependent flavin reductase PrnF (*Pseudomonas fluorecens*) and an alcohol dehydrogenase ADH (*Rhodococcus sp*.) are cross-linked in CLEA (cross-linked enzyme aggregates). Through this biocatalytic strategy, the regioselective halogenation of Trp in gram scale is possible (Frese and Sewald, 2015). The third method is the production by plants by heterologous expression of *rebH* and *rebF* in *Catharanthus roseus* or *Nicotiana benthamiana* (Runguphan et al., 2010; Fräbel et al., 2016).

1.4.1 Indole and halogenated indole

One important derivative of Trp is indole. Indole and its derivatives are an important class of heterocyclic aromatic compounds, which have a wide range of biological activities (Ghinea and Dinica, 2016). Indole is produced in various species, like plants (Zhang et al., 2008; Warskulat et al., 2016), Gram-positive (DeMoss and Moser, 1969; Elsden et al., 1976) and

Gram-negative bacteria (Smith, 1897; Mueller et al., 2009). Indole has a variety of functions in nature: it serves as a signal molecule (Vega et al., 2012), affects biofilm formation (Hu et al., 2010) and modulates antibiotic resistance (Lee et al., 2010). In mammals, including humans, indole was detected, however, they lack the ability to produce it themselves. Indole derives from commensal bacteria, which naturally occur in the bodies of mammals (Tlaskalová-Hogenová et al., 2004; Wikoff et al., 2009; Bansal et al., 2010). The influence of indole and its derivatives in humans is poorly understood, but it may influence human diseases, like bacterial infections, intestinal inflammation, neurological diseases, diabetes and cancer (Lee et al., 2015). Indole and its derivatives also have applications in different industries: they are used for pharmaceuticals and in medicine because they have anti-inflammatory (da Silva Guerra et al., 2011), antitumor (Dadashpour and Emami, 2018) or antiviral activities (Giampieri et al., 2009). In the dye industry the indole derivatives indigo and LI-3 or LI-4 (organic dyes for dye-sensitized solar cells) are produced (Li et al., 2009; Sánchez-Viesca et al., 2016). In black and green tea indole is responsible for the volatile aroma (Ho et al., 2015). The production of indole in microorganisms was described via α,β-elimination of Trp catalyzed by a tryptophanase (TnaA, EC 4.1.99.1) yielding next to indole also pyruvate and ammonia (Newton and Snell, 1965). In plants indole-3-glycerol phosphate is converted to free indole by the indole-3-glycerol phosphate lyase (Frey et al., 1997; Frey et al., 2000)

Also, halogenated indole derivatives have various functions: fluorinated and iodinated indole show nematicidal and insecticidal activities (Rajasekharan et al., 2019), which is used in the control of parasitic nematodes, which cause infection in humans, animals, and plants (Jasmer et al., 2003). The halogenated indole derivatives, 7-chloroindole, 7-bromoindole and, 5-iodoindole have a strong toxic effect to the persister cells of *E. coli*. Formation of bacterial persister cells occurs often together with multidrug resistance and hence, halogenated indoles are potential compounds targeting the persister cells (Lewis, 2008; Lee et al., 2016). Different halogenases or haloperoxidases were described, which catalyze the halogenation of indole and indole derivatives, like the *Xcc* halogenases from *Xanthomonas campestris* pv. *campestris* B100 (Butler, 1998; Martinez et al., 2001; Neubauer et al., 2018; Ismail et al., 2019).

1.5 *Corynebacterium glutamicum* as production host for halogenated L-tryptophan

C. glutamicum is a Gram-positive, non-pathogenic and non-motile rode shaped soil bacterium (Eggeling and Bott, 2015). It was discovered in the 1950s in Japan (Kinoshita et al., 1957) and is classified taxonomically in the class *Actinobacteria* and the order *Actinomycetales* on the basis of the (16S) rRNA and the genes coding for this molecule (rDNA) (Stackebrandt et al., 1997). The whole genome of *C. glutamicum* ATCC 13032 was sequenced in 2003 (Ikeda and Nakagawa, 2003; Kalinowski et al., 2003). It is used for large-scale industrial production of the flavor enhancer L-glutamate and the food and feed additive L-lysine (Wendisch, 2019). Products produced with *C. glutamicum* are recognized as GRAS (generally recognized as safe). A toolbox with different techniques, like DNA transfer techniques (Dunican and Shivnan, 1989; Schäfer et al., 1990), gene expression systems (Kirchner and Tauch, 2003; Eggeling and Bott, 2015) and gene deletion and integration (Schäfer et al., 1994) exist. The product portfolio was expanded by metabolic engineering, to the natural amino acids L-ornithine and L-arginine (Schneider et al., 2011; Peters-Wendisch et al., 2014), the cyclic amino acid pipecolic acid (Pérez-García et al., 2016), terpenoids (Heider et al., 2014; Henke et al., 2016; Henke et al., 2018), the alkylated amino acid *N*-methylalanine (Mindt et al., 2018) or sarcosine (Mindt et al., 2019) and *para*-hydroxybenzoic acid (Purwanto et al., 2018). *C. glutamicum* has natural access to different carbon sources, like the sugars glucose, sucrose and fructose (Zahoor et al., 2012), but by metabolic engineering, the range of carbon sources was extended to various alternative carbon sources, which are not competing with the food and feed industries. For example, the polymer starch (Seibold et al., 2006; Tateno et al., 2007; Tateno et al., 2009), *N*-acetyl-glucosamine (Matano et al., 2014) *N*-acetylmuramic acid (Sgobba et al., 2018), the sugars xylose (Kawaguchi et al., 2006) and arabinose (Kawaguchi et al., 2008), the dicarboxylic acids fumaric and malic acid (Teramoto et al., 2008; Youn et al., 2009) are accessible for engineered *C. glutamicum* strains.

Moreover, *C. glutamicum* is an ideal host for the production of aromatic amino acids. On the one hand is the shikimate pathway and its regulation well studied (Bongaerts et al., 2001)

and on the other hand it has been already engineered towards the production of the aromatic amino acids (Ikeda and Katsumata, 1992), like Trp (Ikeda and Katsumata, 1999). In the industry, Trp is produced in large amounts by microbial fermentation with, for example, *C. glutamicum* and *E. coli* (Liu et al., 2019; Wendisch, 2019). Further, Trp produced by *C. glutamicum* was recognized as safe and effective (Additives et al., 2019), hence, *C. glutamicum* is a suitable host for the production of Trp and Trp derivatives.

1.5.1 Regulation of the L-tryptophan biosynthesis in *Corynebacterium glutamicum*

The biosynthesis of Trp is regulated by feedback inhibition and feedback repression in *C. glutamicum*. First, feedback inhibition is considered here in more detail. The first step of the Trp biosynthesis catalyzed by Aro and AroII is feedback regulated by the two aromatic amino acids L-phenylalanine and L-tyrosine. In *C. glutamicum* these compounds inhibit the wildtype enzymes to prevent the overproduction of aromatic amino acids (Liu et al., 2008) (Fig. 1.7). In other microorganisms, for example *E. coli*, this step, catalyzed by the 3-deoxy-D-arabino-heptulosonate 7-phosphate synthases AroF, AroH, and AroG (encoded by *aroF*, *aroH,* and *aroG*), is feedback regulated as well. Each enzyme is inhibited by one of the aromatic amino acids: AroF by L-tyrosine (Schoner and Herrmann, 1976), AroH by Trp (Akowski and Bauerle, 1997) and AroG by L-phenylalanine (McCandliss et al., 1978). Further, AroE is feedback inhibited by its product shikimate in both *C. glutamicum* and *E. coli* (Dell and Frost, 1993; Kubota et al., 2013). In the second part of the Trp biosynthesis the TrpE and TrpD are feedback inhibited by different compounds. In *C. glutamicum* the TrpE and TrpD are strongly inhibited by Trp and its derivatives, ensuring a tight regulation of the Trp biosynthesis (Hagino and Nakayama, 1975) (Fig. 1.7). Already at a concentration of 0.83 mM Trp or 0.32 mM 5-methyl-trpytophan, the enzyme activity of TrpD decreased around 4.5 times (O'Gara and Dunican, 1995). In *E. coli* TrpE, TrpG and TrpD form a complex, which is feedback regulated by Trp. However, if TrpD is not bound in the complex it is less inhibited by Trp, hence TrpEG is the regulated subunit (Ito and Yanofsky, 1969). Furthermore, the Trp biosynthesis is regulated at the transcriptional level. Both *C. glutamicum* and *E. coli* are regulated by a repressor and an attenuator (Brune et al., 2007).

In *E. coli* the repressor is encoded by the *trpR* gene. If the intracellular concentration of Trp is high, Trp binds to TrpR, which binds reversibly to the operator sequence of the *trp* operon to prevent the transcription. At low Trp concentration the repression is paused (Yanofsky and Crawford, 1987) (Fig. 1.10). In *C. glutamicum* the repressor LtbR binds to a 12 bp motif between the -10 promoter region and the ribosome binding site of the *trpL* gene and prevents the transcription of the *trp* operon. The deletion of the LtbR repressor leads to enhanced expression of the *trp* operon (Brune et al., 2007). Until now the regulation of the LtbR repressor is unknown (Fig. 1.10). Additionally, in *C. glutamicum* a putative operator sequence, which shows similarity to the operator DNA binding sequence of the TrpR repressor of *E. coli*, was detected upstream of the -10 promoter region of the *trp* operon (Matsui et al., 1987; Sano and Matsui, 1987). However, *C. glutamicum* is not encoding a TrpR related protein nor showed the sequence a regulatory role (Guerrero et al., 1994; Brune et al., 2005). For the second transcriptional regulation in *E. coli*, the attenuation, the synchronization of the translation of the leader peptide sequence, TrpL, and the transcription of the operon´s leader sequence plays an important role. During the transcription of *trpL* the formed mRNA can build a hairpin structure, the anti-antiterminator, which causes a transcriptional pause. By binding of the ribosome, the RNA-polymerase is released, and the anti-antiterminator structure is disrupted. After this step two following events are possible, which depend on the availability of charged $tRNA^{Trp}$. If the concentration of the $tRNA^{Trp}$ is low, the ribosome stalls during translation of the two Trp codons of the *trpL* mRNA. An antiterminator hairpin structure is formed in the leader mRNA, which prevents the formation of the terminator hairpin structure. Hence, the transcription of the *trp* operon continues. If the concentration of $tRNA^{Trp}$ is high, the ribosome translates the *trpL* mRNA without stalling and declines at the *trpL* stop codon. This enables the leader mRNA to form an anti-antiterminator hairpin and a terminator hairpin structure and the transcription termination is initiated (Morse and Morse, 1976; Yanofsky and Soll, 1977; Zurawski et al., 1978; Oxender et al., 1979; Zurawski and Yanofsky, 1980) (Fig. 1.10).

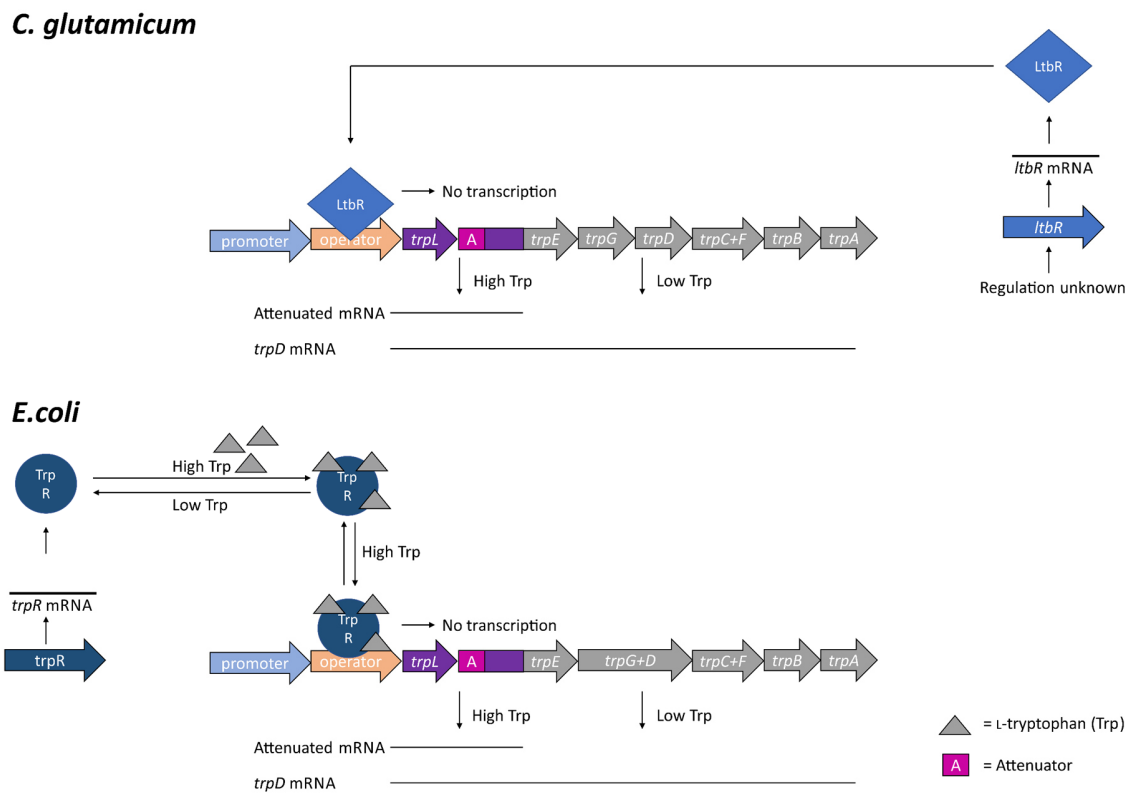

Figure 1.10: Transcriptional regulation of the *trp* operon in *C. glutamicum* and *E. coli*. In *C. glutamicum* the transcription is regulated by the repressor LtbR and by attenuation, whereby both are not complete investigated. The transcription of *E. coli* is regulated by the repressor TrpR, which is regulated by the intracellular concentration of Trp. Additionally, the transcription is regulated by attenuation.

The transcription of the *trp* operon of *C. glutamicum* is controlled by attenuation, but this is not as well investigated as in *E. coli*. The attenuator region contains a short leader peptide region of 17-codon open reading frame (ORF) containing three consecutive Trp codons (Herry and Dunican, 1993). A non-sense mutation can lead to a constitutive antiterminator formation (Herry and Dunican, 1993). A point mutation in the attenuator region may destabilize the terminator structure and hence, the transcription level of the *trp* operon was increased (Matsui et al., 1987) (Fig. 1.10).

1.5.1 Production of L-tryptophan by *Corynebacterium glutamicum*

In the *C. glutamicum* ATCC 13032 wildtype no accumulation of Trp or the precursors chorismate and anthranilate could be detected (Katsumata and Ikeda, 1993). In 2018, a Trp overproducing strain was generated by metabolic engineering by Purwanto and co-workers

(Purwanto et al., 2018). They achieved high Trp titers by engineering of four metabolic steps: i) overexpression of a feedback resistant AroG gene from *E. coli*, thus avoiding the inhibition by L-phenylalanine and L-tyrosine, ii) prohibit by-product formation of L-phenylalanine and L-tyrosine by deletion of *csm,* resulting as well in an L-phenylalanine and L-tyrosine auxotrophic strain, iii) integrating a homologous feedback resistant TrpE into the genome channeling the flux to anthranilate and preventing inhibition by Trp, and iv) plasmid-based overexpression of *trpD* from *E. coli* converting the produced anthranilate to Trp. The resulting strain Tp679 (pCES208-*trpD*) produces 2 g L^{-1} Trp (Purwanto et al., 2018). The highest Trp production by *C. glutamicum* so far was reached by Ikeda et al., 1999. Here, a Trp overproducing *C. glutamicum* strain produced in a fed-batch cultivation up to 58 g L^{-1} (Ikeda and Katsumata, 1999; Ikeda, 2006). This titer was reached by overexpression of the 3-deoxy-D-arabino-heptulosonate 7-phosphate synthase gene (*aroII*) from *C. glutamiucum*, the Trp biosynthesis operon (*trp* operon), the phosphoglycerate dehydrogenase gene(*serA*) and the transketolase gene (*tkt*), and by a plasmid stabilization system (Ikeda and Katsumata, 1999).

Taken together, because of the great availability of tools for strain development and the establishment in the food and feed industries *C. glutamicum* is a suitable host for the production Trp and its derivatives.

1.5 Objectives

Halogenated compounds, like 7-Cl-Trp and 7-Br-Trp, are important building blocks of bioactive substances. The chemical halogenation is characterized as hazardous and highly toxic. The greener alternative is the halogenation by biocatalysis, however, it requires a co-factor regeneration system. Hence, the aim of this study was to establish a *de novo* synthesis of halogenated Trp and the Trp derivative indole using the industrial relevant production host *C. glutamicum*.

The fermentative production of Trp derivatives was accomplished by: i) production of halogenated Trp (7-Cl-Trp) by overexpression the genes for the FAD-dependent halogenase RebH and the NADH-dependent flavin reductase RebF, both derived from *L. aerocolonigenes* in a Trp overproducing *C. glutamicum* strain, ii) extension of the concept regarding another halogenated Trp derivative (7-Br-Trp), iii) expansion of product portfolio deriving from Trp by fermentative production of indole in a Trp overproducing *C. glutamicum* strain.

1.6 References

Additives, E.P.o., Products or Substances used in Animal, F., Bampidis, V., Azimonti, G., de Lourdes Bastos, M., Christensen, H., et al. (2019). Safety and efficacy of L-tryptophan produced by fermentation with *Corynebacterium glutamicum* KCCM 80176 for all animal species. EFSA Journal 17**,** e05729. doi:10.2903/j.efsa.2019.5729.

Akowski, J.P., and Bauerle, R. (1997). Steady-state kinetics and inhibitor binding of 3-deoxy-D-arabino-heptulosonate-7-phosphate synthase (tryptophan sensitive) from *Escherichia coli*. Biochem. 36**,** 15817-15822. doi:10.1021/bi971135t.

Bansal, T., Alaniz, R.C., Wood, T.K., and Jayaraman, A. (2010). The bacterial signal indole increases epithelial-cell tight-junction resistance and attenuates indicators of inflammation. Proc. Natl. Acad. Sci. 107**,** 228-233. doi:10.1073/pnas.0906112107.

Bentley, R., and Haslam, E. (1990). The shikimate pathway—a metabolic tree with many branche. Crit. Rev. Biochem. Mol. Biol 25**,** 307-384. doi:10.3109/10409239009090615.

Betti, L., Rossi, A., and Giannaccini, G. (2016). Tryptophan biochemistry: structural, nutritional, metabolic, and medical aspects in humans. J. amino acids 2016. doi:10.1155/2016/8952520.

Bittner, S., Scherzer, R., and Harlev, E. (2007). The five bromotryptophans. Amino acids. 33**,** 19-42. doi:10.1007/s00726-006-0441-8.

Bitto, E., Huang, Y., Bingman, C.A., Singh, S., Thorson, J.S., and Phillips, G.N. (2008). The structure of flavin-dependent tryptophan 7-halogenase RebH. Proteins: Struct., Funct., Bioinf. 70**,** 289-293. doi:10.1002/prot.21627.

Blasiak, L.C., and Drennan, C.L. (2008). Structural perspective on enzymatic halogenation. Acc. Chem. Res. 42**,** 147-155. doi:10.1002/anie.201506388.

Bongaerts, J., Krämer, M., Müller, U., Raeven, L., and Wubbolts, M. (2001). Metabolic engineering for microbial production of aromatic amino acids and derived compounds. Metab. Eng. 3**,** 289-300. doi:10.1006/mben.2001.0196.

Brune, I., Brinkrolf, K., Kalinowski, J., Pühler, A., and Tauch, A. (2005). The individual and common repertoire of DNA-binding transcriptional regulators of *Corynebacterium glutamicum*, *Corynebacterium efficiens*, *Corynebacterium diphtheriae* and *Corynebacterium jeikeium* deduced from the complete genome sequences. BMC genomics 6**,** 86. doi:10.1186/1471-2164-6-86.

Brune, I., Jochmann, N., Brinkrolf, K., Hüser, A.T., Gerstmeir, R., Eikmanns, B.J., et al. (2007). The IclR-type transcriptional repressor LtbR regulates the expression of leucine and tryptophan biosynthesis genes in the amino acid producer *Corynebacterium glutamicum*. J. Bacteriol. 189**,** 2720-2733. doi:10.1128/JB.01876-06.

Bruniera, F.R., Ferreira, F.M., Saviolli, L.R., Bacci, M.R., Feder, D., da Luz Goncalves Pedreira, M., et al. (2015). The use of vancomycin with its therapeutic and adverse effects: a review. Eur Rev Med Pharmacol Sci 19**,** 694-700.

Bunyapaiboonsri, T., Vongvilai, P., Auncharoen, P., and Isaka, M. (2012). Cyclohexadepsipeptides from the filamentous fungus *Acremonium sp*. BCC 2629. Helv. Chim. Acta 95**,** 963-972. doi:10.1002/hlca.201100482.

Bush, J.A., Long, B.H., Catino, J.J., and Bradner, W.T. (1987). Production and biological activity of rebeccamycin, a novel antitumor agent. J. Antibiot. 40**,** 668-678. doi:10.7164/antibiotics.40.668.

Butler, A. (1998). Vanadium haloperoxidases. Curr. Opin. Chem. Biol. 2**,** 279-285. doi:10.1016/S1367-5931(98)80070-7.

Butler, A., and Carter-Franklin, J.N. (2004). The role of vanadium bromoperoxidase in the biosynthesis of halogenated marine natural products. Nat. Prod. Rep. 21**,** 180-188. doi:10.1039/b302337k.

Cantillo, D., and Kappe, C.O. (2017). Halogenation of organic compounds using continuous flow and microreactor technology. React. Chem. Eng. 2**,** 7-19. doi:10.1039/C6RE00186F.

Chang, Z., Flatt, P., Gerwick, W.H., Nguyen, V.-A., Willis, C.L., and Sherman, D.H. (2002). The barbamide biosynthetic gene cluster: a novel marine cyanobacterial system of mixed polyketide synthase (PKS)-non-ribosomal peptide synthetase (NRPS) origin involving an unusual trichloroleucyl starter unit. Gene 296**,** 235-247. doi:10.1016/S0378-1119(02)00860-0.

Chung, W.j., and Vanderwal, C.D. (2016). Stereoselective halogenation in natural product synthesis. Angew. Chem. Int. Ed. 55**,** 4396-4434. doi:10.1002/anie.201506388.

Corr, M.J., Sharma, S.V., Pubill-Ulldemolins, C., Bown, R.T., Poirot, P., Smith, D.R.M., et al. (2017). Sonogashira diversification of unprotected halotryptophans, halotryptophan containing tripeptides; and generation of a new to nature bromo-natural product and its diversification in water. Chem. Sci. 8**,** 2039-2046. doi:10.1039/C6SC04423A.

Crawford, I.P., and Yanofsky, C. (1958). On the separation of the tryptophan synthetase of *Escherichia coli* into two protein components. Proc. Natl. Acad. Sci. U. S. A. 44**,** 1161. doi:10.1073/pnas.44.12.1161.

da Silva Guerra, A.S.H., do Nascimento Malta, D.J., Laranjeira, L.P.M., Maia, M.B.S., Colaço, N.C., de Lima, M.d.C.A., et al. (2011). Anti-inflammatory and antinociceptive activities of indole–imidazolidine derivatives. Int. Immunopharmacol. 11**,** 1816-1822. doi:10.1016/j.intimp.2011.07.010.

Dadashpour, S., and Emami, S. (2018). Indole in the target-based design of anticancer agents: A versatile scaffold with diverse mechanisms. Eur. J. Med. Chem. 150**,** 9-29. doi:10.1016/j.ejmech.2018.02.065.

Dairi, T., Nakano, T., Mizukami, T., Aisaka, K., Hasegawa, M., and Katsumata, R. (1995). Conserved organization of genes for biosynthesis of chlortetracycline in *Streptomyces* strains. Biosci. Biotechnol. Biochem. 59**,** 1360-1361. doi:10.1271/bbb.59.1360.

De Clercq, E., Billiau, A., Edy, V.G., Kirk, K.L., and Cohen, L.A. (1978). Antimetabolic activities of 2-fluoro-L-histidine. Biochem. Biophys. Res. Commun. 82**,** 840-846. doi:10.1016/0006-291X(78)90859-8.

de Jesus, A.J., and Allen, T.W. (2013). The role of tryptophan side chains in membrane protein anchoring and hydrophobic mismatch. Biochim. Biophys. Acta (BBA)-Biomembranes 1828**,** 864-876. doi:10.1016/j.bbamem.2012.09.009.

Dell, K.A., and Frost, J.W. (1993). Identification and removal of impediments to biocatalytic synthesis of aromatics from D-glucose: rate-limiting enzymes in the common pathway of aromatic amino acid biosynthesis. J. Am. Chem. Soc. 115**,** 11581-11589.

DeMoss, R.D., and Moser, K. (1969). Tryptophanase in diverse bacterial species. J. Bacteriol. 98**,** 167-171.

Domergue, J., Erdmann, D., Fossey-Jouenne, A., Petit, J.-L., Debard, A., de Berardinis, V., et al. (2019). *Xszen*FHal, a novel tryptophan 5-halogenase from *Xenorhabdus szentirmaii*. AMB Express 9**,** 1-11. doi:10.1186/s13568-019-0898-y.

Dong, C., Flecks, S., Unversucht, S., Haupt, C., Van Pee, K.-H., and Naismith, J.H. (2005). Tryptophan 7-halogenase (PrnA) structure suggests a mechanism for regioselective chlorination. Science 309**,** 2216-2219. doi:10.1126/science.1116510.

Dunican, L.K., and Shivnan, E. (1989). High Frequency Transformation of Whole Cells of Amino Acid Producing Coryneform Bacteria Using High Voltage Electroporation. Bio/Technology 7**,** 1067-1070. doi:10.1038/nbt1089-1067.

Eggeling, L., and Bott, M. (2005). Handbook of *Corynebacterium glutamicum.* CRC press.

Eggeling, L., and Bott, M. (2015). A giant market and a powerful metabolism: L-lysine provided by *Corynebacterium glutamicum*. Appl. Microbiol. Biotechnol. 99**,** 3387-3394. doi:10.1007/s00253-015-6508-2.

Elsden, S.R., Hilton, M.G., and Waller, J.M. (1976). The end products of the metabolism of aromatic amino acids by *Clostridia*. Arch. Microbiol. 107**,** 283-288. doi:10.1007/BF00425340.

Eustáquio, A.S., Pojer, F., Noel, J.P., and Moore, B.S. (2008). Discovery and characterization of a marine bacterial SAM-dependent chlorinase. Nat. Chem. Biol. 4**,** 69. doi:10.1038/nchembio.2007.56.

Facchini, P.J., Huber-Allanach, K.L., and Tari, L.W. (2000). Plant aromatic L-amino acid decarboxylases: evolution, biochemistry, regulation, and metabolic engineering applications. Phytochemistry 54**,** 121-138. doi:10.1016/S0031-9422(00)00050-9.

Floss, H.G., Onderka, D.K., and Carroll, M. (1972). Stereochemistry of the 3-deoxy-D-arabino-heptulosonate 7-phosphate synthetase reaction and the chorismate synthetase reaction. J. Biol. Chem. 247**,** 736-744.

Follettie, M.T., and Sinskey, A.J. (1986). Molecular cloning and nucleotide sequence of the *Corynebacterium glutamicum pheA* gene. J. Bacteriol. 167**,** 695-702. doi:10.1128/jb.167.2.695-702.1986.

Fräbel, S., Krischke, M., Staniek, A., and Warzecha, H. (2016). Recombinant flavin-dependent halogenases are functional in tobacco chloroplasts without co-expression of flavin reductase genes. Biotechnol. J. 11**,** 1586-1594. doi:10.1002/biot.201600337.

Frese, M., Guzowska, P.H., Voss, H., and Sewald, N. (2014). Regioselective Enzymatic Halogenation of Substituted Tryptophan Derivatives using the FAD-Dependent Halogenase RebH. ChemCatChem. 6**,** 1270-1276. doi:10.1002/cctc.201301090.

Frese, M., Schnepel, C., Minges, H., Voss, H., Feiner, R., and Sewald, N. (2016). Modular Combination of Enzymatic Halogenation of Tryptophan with Suzuki–Miyaura Cross-Coupling Reactions. ChemCatChem. 8**,** 1799-1803. doi:10.1002/cctc.201600317.

Frese, M., and Sewald, N. (2015). Enzymatic Halogenation of Tryptophan on a Gram Scale. Angew. Chem. Int. Ed. 54**,** 298-301. doi:10.1002/anie.201408561.

Frey, M., Chomet, P., Glawischnig, E., Stettner, C., Grün, S., Winklmair, A., et al. (1997). Analysis of a chemical plant defense mechanism in grasses. Science 277**,** 696-699. doi:10.1126/science.277.5326.696.

Frey, M., Stettner, C., Paré, P.W., Schmelz, E.A., Tumlinson, J.H., and Gierl, A. (2000). An herbivore elicitor activates the gene for indole emission in maize. Proc. Natl. Acad. Sci. 97**,** 14801-14806. doi:10.1073/pnas.260499897.

Galonić, D.P., Vaillancourt, F.H., and Walsh, C.T. (2006). Halogenation of unactivated carbon centers in natural product biosynthesis: trichlorination of leucine during barbamide biosynthesis. J. Am. Chem. Soc. 128**,** 3900-3901. doi:10.1021/ja060151n.

Ghinea, I.O., and Dinica, R.M. (2016). Breakthroughs in Indole and Indolizine Chemistry–New Synthetic Pathways, New Applications. Scope of Selective Heterocycles from Organic and Pharmaceutical Perspective**,** 115. doi:10.5772/62079.

Giampieri, M., Balbi, A., Mazzei, M., La Colla, P., Ibba, C., and Loddo, R. (2009). Antiviral activity of indole derivatives. Antiviral. Res. 83**,** 179-185. doi:10.1016/j.antiviral.2009.05.001.

Grauer, A., and König, B. (2009). Peptidomimetics–a versatile route to biologically active compounds. Eur. J. Org. Chem. 2009**,** 5099-5111. doi:10.1002/ejoc.200900599.

Grüschow, S., Smith, D.R.M., Gkotsi, D.S., and Goss, R.J.M. (2014). Halogenases. Biocatalysis in Organic Synthesis 3**,** 313-359.

Gruß, H., Belu, C., Bernhard, L.M., Merschel, A., and Sewald, N. (2019). Fluorogenic Diversification of Unprotected Bromotryptophan by Aqueous Mizoroki–Heck Cross-Coupling. Chem. Eur. J. 25**,** 5880-5883. doi:10.1002/chem.201900437.

Guerrero, C., Mateos, L.M., Malumbres, M., and Martin, J.F. (1994). Directed mutagenesis of a regulatory palindromic sequence upstream from the *Brevibacterium lactofermentum* tryptophan operon. Gene 138**,** 35-41. doi:10.1016/0378-1119(94)90780-3.

Guilford, W.J., Copley, S.D., and Knowles, J.R. (1987). The mechanism of the chorismate mutase reaction. J. Am. Chem. Soc. 109**,** 5013-5019. doi:10.1021/bi00611a004.

Hager, L.P., Morris, D.R., Brown, F.S., and Eberwein, H. (1966). Chloroperoxidase II. Utilization of halogen anions. J. Biol. Chem. 241**,** 1769-1777.

Hagino, H., and Nakayama, K. (1975). Regulatory properties of anthranilate synthetase from *Corynebacterium glutamicum*. Agric. Biol. Chem. 39**,** 323-330. doi:10.1080/00021369.1975.10861619.

Hagino, H., Yoshida, H., Kato, F., Arai, Y., Katsumata, R., and Nakayama, K. (1973). L-Tyrosine Production by Polyauxotrophic Mutants of *Corynebacterium glutamicum*. Agric. Biol. Chem. 37**,** 2001-2005. doi:10.1080/00021369.1973.10860956.

Hammer, P.E., Hill, D.S., Lam, S.T., Van Pée, K.-H., and Ligon, J.M. (1997). Four genes from *Pseudomonas fluorescens* that encode the biosynthesis of pyrrolnitrin. Appl. Environ. Microbiol. 63**,** 2147-2154.

Han, M.-A., Lee, H.-S., Cheon, C.-I., Min, K.-H., and Lee, M.-S. (1999). Cloning and analysis of the *aroB* gene encoding dehydroquinate synthase from *Corynebacterium glutamicum*. Can. J. Microbiol. 45**,** 885-890. doi:10.1139/w99-076.

Heider, S.A.E., Peters-Wendisch, P., Wendisch, V.F., Beekwilder, J., and Brautaset, T. (2014). Metabolic engineering for the microbial production of carotenoids and related products with a focus on the rare C50 carotenoids. Appl. Microbiol. Biotechnol. 98**,** 4355-4368. doi:10.1007/s00253-014-5693-8.

Henke, N.A., Heider, S.A.E., Peters-Wendisch, P., and Wendisch, V.F. (2016). Production of the marine carotenoid astaxanthin by metabolically engineered *Corynebacterium glutamicum*. Mar. Drugs 14**,** 124. doi:10.3390/md14070124.

Henke, N.A., Wiebe, D., Pérez-García, F., Peters-Wendisch, P., and Wendisch, V.F. (2018). Coproduction of cell-bound and secreted value-added compounds: Simultaneous production of carotenoids and amino acids by *Corynebacterium glutamicum*. Bioresour. Technol. 247**,** 744-752. doi:10.1016/j.biortech.2017.09.167.

Hennig, M., Darimont, B.D., Jansonius, J.N., and Kirschner, K. (2002). The catalytic mechanism of indole-3-glycerol phosphate synthase: crystal structures of complexes of the enzyme from *Sulfolobus solfataricus* with substrate analogue, substrate, and product. J. Mol. Biol. 319**,** 757-766. doi:10.1016/S0022-2836(02)00378-9.

Hering, T., Mühldorf, B., Wolf, R., and König, B. (2016). Halogenase-Inspired Oxidative Chlorination Using Flavin Photocatalysis. Angew. Chem. Int. Ed. 55**,** 5342-5345. doi:10.1002/ange.201600783

Herrera-Rodriguez, L.N., Meyer, H.-P., Robins, K.T., and Khan, F. (2011). Perspectives on biotechnological halogenation. Chim. Oggi. 29.

Herrmann, K.M., and Weaver, L.M. (1999). The shikimate pathway. Annu. Rev. Plant Biol. 50**,** 473-503. doi:10.1146/annurev.arplant.50.1.473.

Herry, D.M., and Dunican, L.K. (1993). Cloning of the *trp* gene cluster from a tryptophan-hyperproducing strain of *Corynebacterium glutamicum*: identification of a mutation in the *trp* leader sequence. Appl. Environ. Microbiol. 59**,** 791-799.

Hibi, M., Kawashima, T., Kodera, T., Smirnov, S.V., Sokolov, P.M., Sugiyama, M., et al. (2011). Characterization of *Bacillus thuringiensis* L-isoleucine dioxygenase for production of useful amino acids. Appl. Environ. Microbiol. 77**,** 6926-6930. doi:10.1016/j.bbrc.2009.09.126.

Hillwig, M.L., and Liu, X. (2014). A new family of iron-dependent halogenases acts on freestanding substrates. Nat. Chem. Biol. 10**,** 921. doi:10.1038/nchembio.1625.

Ho, C.-T., Zheng, X., and Li, S. (2015). Tea aroma formation. Food Science and Human Wellness 4**,** 9-27. doi:10.1016/j.fshw.2015.04.001.

Hopkins, F.G., and Cole, S.W. (1901). A contribution to the chemistry of proteins: Part I. A preliminary study of a hitherto undescribed product of tryptic digestion. J. Physiol. 27**,** 418. doi:10.1113/jphysiol.1901.sp000880.

Hu, M., Zhang, C., Mu, Y., Shen, Q., and Feng, Y. (2010). Indole affects biofilm formation in bacteria. Indian J. Microbiol. 50**,** 362-368. doi:10.1007/s12088-011-0142-1.

Hudlicky, M., and Hudlicky, T. (1983). Formation of carbon–halogen bonds. Halides, Pseudo-Halides and Azides (1983) Part 2 2**,** 1021-1172. doi:10.1002/9780470771723.ch3.

Ikeda, M. (2006). Towards bacterial strains overproducing L-tryptophan and other aromatics by metabolic engineering. Appl. Microbiol. Biotechnol. 69**,** 615. doi:10.1007/s00253-005-0252-y.

Ikeda, M., and Katsumata, R. (1992). Metabolic engineering to produce tyrosine or phenylalanine in a tryptophan-producing *Corynebacterium glutamicum* strain. Appl. Environ. Microbiol. 58**,** 781-785.

Ikeda, M., and Katsumata, R. (1999). Hyperproduction of Tryptophan by *Corynebacterium glutamicum* with the Modified Pentose Phosphate Pathway. Appl. Environ. Microbiol. 65**,** 2497-2502.

Ikeda, M., and Nakagawa, S. (2003). The *Corynebacterium glutamicum* genome: features and impacts on biotechnological processes. Appl. Microbiol. Biotechnol. 62**,** 99-109. doi:10.1007/s00253-003-1328-1.

Ismail, M., Frese, M., Patschkowski, T., Ortseifen, V., Niehaus, K., and Sewald, N. (2019). Flavin-Dependent Halogenases from *Xanthomonas campestris* pv. campestris B100 Prefer Bromination over Chlorination. Adv. Synth. Catal. doi:10.1002/adsc.201801591.

Ito, J., and Yanofsky, C. (1969). Anthranilate synthetase, an enzyme specified by the tryptophan operon of *Escherichia coli*: Comparative studies on the complex and the subunits. J. Bacteriol. 97**,** 734-742.

Jasmer, D.P., Goverse, A., and Smant, G. (2003). Parasitic nematode interactions with mammals and plants. Annu. Rev. Phytopathol. 41**,** 245-270. doi:10.1146/annurev.phyto.41.052102.104023.

Jensen, R.A., and Pierson, D.L. (1975). Evolutionary implications of different types of microbial enzymology for L-tyrosine biosynthesis. Nature. 254**,** 667. doi:10.1038/254667a0.

Jeschke, P. (2017). Latest generation of halogen-containing pesticides. Pest Manag. Sci. 73**,** 1053-1066. doi:10.1002/ps.4540.

Kagiyama, T., Glushakov, A.V., Sumners, C., Roose, B., Dennis, D.M., Phillips, M.I., et al. (2004). Neuroprotective action of halogenated derivatives of L-phenylalanine. Stroke 35**,** 1192-1196.

Kalinowski, J., Bathe, B., Bartels, D., Bischoff, N., Bott, M., Burkovski, A., et al. (2003). The complete *Corynebacterium glutamicum* ATCC 13032 genome sequence and its impact on the production of L-aspartate-derived amino acids and vitamins. J. Biotechnol. 104**,** 5-25. doi:10.1016/S0168-1656(03)00154-8.

Kanbe, K., Naganawa, H., Nakamura, K.T., Okami, Y., and Takeuchi, T. (1993). Thienodolin, a new plant growth-regulating substance produced by a Streptomycete strain: II. Structure of thienodolin. Biosci. Biotechnol. Biochem. 57**,** 636-637. doi:10.1271/bbb.57.636.

Katsumata, R., and Ikeda, M. (1993). Hyperproduction of tryptophan in *Corynebacterium glutamicum* by pathway engineering. Bio/Technology 11**,** 921. doi:10.1038/nbt0893-921.

Kawaguchi, H., Sasaki, M., Vertès, A.A., Inui, M., and Yukawa, H. (2008). Engineering of an L-arabinose metabolic pathway in *Corynebacterium glutamicum*. Appl. Microbiol. Biotechnol. 77**,** 1053-1062. doi:10.1007/s00253-007-1244-x.

Kawaguchi, H., Vertès, A.A., Okino, S., Inui, M., and Yukawa, H. (2006). Engineering of a xylose metabolic pathway in *Corynebacterium glutamicum*. Appl. Environ. Microbiol. 72**,** 3418-3428. doi:10.1128/AEM.72.5.3418-3428.2006.

Keller, S., Wage, T., Hohaus, K., Hölzer, M., Eichhorn, E., and van Pée, K.H. (2000). Purification and partial characterization of tryptophan 7-halogenase (PrnA) from *Pseudomonas fluorescens*. Angew. Chem. Int. Ed. 39**,** 2300-2302. doi:10.1002/1521-3773(20000703)39:13<2300::AID-ANIE2300>3.0.CO;2-I.

Kinoshita, S., Udaka, S., and Shimono, M. (1957). Studies on the amino acid fermentation. J. Gen. Appl. Microbiol. 3**,** 193-205. doi:10.2323/jgam.3.193.

Kirchner, O., and Tauch, A. (2003). Tools for genetic engineering in the amino acid-producing bacterium *Corynebacterium glutamicum*. J. Biotechnol. 104**,** 287-299. doi:10.1016/S0168-1656(03)00148-2.

Koguchi, Y., Kohno, J., Nishio, M., Takahashi, K., Okuda, T., Ohnuki, T., et al. (2000). TMC-95A, B, C, and D, novel proteasome inhibitors produced by *Apiospora montagnei* Sacc. TC 1093. J. Antibiot. 53**,** 105-109. doi:10.7164/antibiotics.53.105.

Krapf, P., Richarz, R., Urusova, E.A., Neumaier, B., and Zlatopolskiy, B.D. (2016). Seyferth–Gilbert Homologation as a Route to ^{18}F-Labeled Building Blocks: Preparation of Radiofluorinated Phenylacetylenes and Their Application in PET Chemistry. Eur. J. Org. Chem. 2016**,** 430-433. doi:10.1002/ejoc.201501377.

Kubota, T., Tanaka, Y., Hiraga, K., Inui, M., and Yukawa, H. (2013). Characterization of shikimate dehydrogenase homologues of *Corynebacterium glutamicum*. Appl. Microbiol. Biotechnol. 97**,** 8139-8149. doi:10.1007/s00253-012-4659-y.

Labeda, D.P. (1986). Transfer of "*Nocardia aerocolonigenes*"(Shinobu and Kawato 1960) Pridham 1970 into the Genus *Saccharothrix* Labeda, Testa, Lechevalier, and Lechevalier 1984 as *Saccharothrix aerocolonigenes* sp. nov. Int. J. Syst. Evol. Microbiol. 36**,** 109-110.

Lambrecht, J.A., and Downs, D.M. (2012). Anthranilate phosphoribosyl transferase (TrpD) generates phosphoribosylamine for thiamine synthesis from enamines and phosphoribosyl pyrophosphate. ACS Chem. Biol. 8**,** 242-248. doi:10.1021/cb300364k.

Lane, A.N., and Kirschner, K. (1983). The Catalytic Mechanism of Tryptophan Synthase from Escherichia coli: Kinetics of the Reaction of Indole with the Enzyme—l-Serine Complexes. Eur. J. Biochem. 129**,** 571-582. doi:10.1111/j.1432-1033.1983.tb07087.x.

Lane, A.N., and Kirschner, K. (1991). Mechanism of the physiological reaction catalyzed by tryptophan synthase from *Escherichia coli*. Biochem. 30**,** 479-484. doi:10.1021/bi00216a025.

Latham, J., Brandenburger, E., Shepherd, S.A., Menon, B.R.K., and Micklefield, J. (2017). Development of halogenase enzymes for use in synthesis. Chem. Rev. 118**,** 232-269. doi:10.1021/acs.chemrev.7b00032.

Leak, D.J., Sheldon, R.A., Woodley, J.M., and Adlercreutz, P. (2009). Biocatalysts for selective introduction of oxygen. Biocatal. Biotransform. 27**,** 1-26. doi:10.1080/10242420802393519.

Lee, H.H., Molla, M.N., Cantor, C.R., and Collins, J.J. (2010). Bacterial charity work leads to population-wide resistance. Nature. 467**,** 82. doi:10.1038/nature09354.

Lee, J.-H., Kim, Y.-G., Gwon, G., Wood, T.K., and Lee, J. (2016). Halogenated indoles eradicate bacterial persister cells and biofilms. AMB Express 6**,** 123. doi:10.1186/s13568-016-0297-6.

Lee, J.-H., and Lee, J. (2010). Indole as an intercellular signal in microbial communities. FEMS Microbiol. Rev. 34**,** 426-444. doi:10.1111/j.1574-6976.2009.00204.x.

Lee, J.-H., Wood, T.K., and Lee, J. (2015). Roles of indole as an interspecies and interkingdom signaling molecule. Trends microbiol. 23**,** 707-718. doi:10.1016/j.tim.2015.08.001.

Leong, L.E.X., Khan, S., Davis, C.K., Denman, S.E., and McSweeney, C.S. (2017). Fluoroacetate in plants-a review of its distribution, toxicity to livestock and microbial detoxification. J. Anim. Sci. Biotechnol. 8**,** 55. doi:10.1186/s40104-017-0180-6.

Levin, J.G., and Sprinson, D.B. (1964). The enzymatic formation and isolation of 3-enolpyruvylshikimate 5-phosphate. J. Biol. Chem. 239**,** 1142-1150.

Lewis, K. (2008). Multidrug tolerance of biofilms and persister cells, in Bacterial Biofilms. Springer. 107-131.

Li, Q., Lu, L., Zhong, C., Shi, J., Huang, Q., Jin, X., et al. (2009). New indole-based metal-free organic dyes for dye-sensitized solar cells. J. Phys. Chem. 113**,** 14588-14595. doi:10.1021/jp906334w.

Li, Y., Li, S., Thodey, K., Trenchard, I., Cravens, A., and Smolke, C.D. (2018). Complete biosynthesis of noscapine and halogenated alkaloids in yeast. Proc. Natl. Acad. Sci. 115**,** E3922-E3931. doi:10.1073/pnas.1721469115.

Libby, R.D., Thomas, J.A., Kaiser, L.W., and Hager, L.P. (1982). Chloroperoxidase halogenation reactions. Chemical versus enzymic halogenating intermediates. J. Biol. Chem. 257**,** 5030-5037.

Lin, S., Van Lanen, S.G., and Shen, B. (2007). Regiospecific chlorination of (*S*)-*β*-tyrosyl-S-carrier protein catalyzed by SgcC3 in the biosynthesis of the enediyne antitumor antibiotic C-1027. J. Am. Chem. Soc. 129**,** 12432-12438. doi:10.1021/ja072311g.

Lindseth, G., Helland, B., and Caspers, J. (2015). The effects of dietary tryptophan on affective disorders. Arch. Psychiatr. Nurs. 29**,** 102-107. doi:10.1016/j.apnu.2014.11.008.

Liu, C., Liu, Y.-M., Sun, Q.-L., Jiang, C.-Y., and Liu, S.-J. (2015). Unraveling the kinetic diversity of microbial 3-dehydroquinate dehydratases of shikimate pathway. AMB Express 5**,** 7. doi:10.1186/s13568-014-0087-y.

Liu, L., Bilal, M., Luo, H., Zhao, Y., and Iqbal, H. (2019). Metabolic Engineering and Fermentation Process Strategies for L-Tryptophan Production by *Escherichia coli*. Processes 7**,** 213. doi:10.3390/pr7040213.

Liu, Y.-J., Li, P.-P., Zhao, K.-X., Wang, B.-J., Jiang, C.-Y., Drake, H.L., et al. (2008). *Corynebacterium glutamicum* contains 3-deoxy-D-arabino-heptulosonate 7-phosphate synthases that display novel biochemical features. Appl. Environ. Microbiol. 74**,** 5497-5503. doi:10.1128/AEM.00262-08.

Loso, M.R., Benko, Z., Buysse, A., Johnson, T.C., Nugent, B.M., Rogers, R.B., et al. (2016). SAR studies directed toward the pyridine moiety of the sap-feeding insecticide

sulfoxaflor (Isoclast™ active). Bioorg. Med. Chem. 24**,** 378-382. doi:10.1016/j.bmc.2015.11.022.

Martinez, J.S., Carroll, G.L., Tschirret-Guth, R.A., Altenhoff, G., Little, R.D., and Butler, A. (2001). On the regiospecificity of vanadium bromoperoxidase. J. Am. Chem. Soc. 123**,** 3289-3294. doi:10.1021/ja004176c.

Matano, C., Uhde, A., Youn, J.-W., Maeda, T., Clermont, L., Marin, K., et al. (2014). Engineering of *Corynebacterium glutamicum* for growth and L-lysine and lycopene production from *N*-acetyl-glucosamine. Appl. Microbiol. Biotechnol. 98**,** 5633-5643. doi:10.1007/s00253-014-5676-9.

Matsui, K., Miwa, K., and Sano, K. (1987). Two single-base-pair substitutions causing desensitization to tryptophan feedback inhibition of anthranilate synthase and enhanced expression of tryptophan genes of *Brevibacterium lactofermentum*. J. Bacteriol. 169**,** 5330-5332.

McCandliss, R.J., Poling, M.D., and Herrmann, K.M. (1978). 3-Deoxy-D-arabino-heptulosonate 7-phosphate synthase. Purification and molecular characterization of the phenylalanine-sensitive isoenzyme from *Escherichia coli*. J. Biol. Chem. 253**,** 4259-4265.

Messerschmidt, A., and Wever, R. (1996). X-ray structure of a vanadium-containing enzyme: chloroperoxidase from the fungus *Curvularia inaequalis*. Proc. Natl. Acad. Sci. 93**,** 392. doi:10.1073/pnas.93.1.392.

Milbredt, D., Patallo, E.P., and van Pée, K.H. (2014). A Tryptophan 6-Halogenase and an Amidotransferase are Involved in Thienodolin Biosynthesis. ChemBioChem 15**,** 1011-1020. doi:10.1002/cbic.201400016.

Mindt, M., Heuser, M., and Wendisch, V.F. (2019). Xylose as preferred substrate for sarcosine production by recombinant *Corynebacterium glutamicum*. Bioresour. Technol. 281**,** 135-142. doi:10.1016/j.biortech.2019.02.084.

Mindt, M., Risse, J.M., Gruß, H., Sewald, N., Eikmanns, B.J., and Wendisch, V.F. (2018). One-step process for production of *N*-methylated amino acids from sugars and methylamine using recombinant *Corynebacterium glutamicum* as biocatalyst. Sci. Rep. 8**,** 12895. doi:10.1038/s41598-018-31309-5.

Morell, H., Clark, M.J., Knowles, P.F., and Sprinson, D.B. (1967). The enzymic synthesis of chorismic and prephenic acids from 3-enolpyruvylshikimic acid 5-phosphate. J. Biol. Chem. 242**,** 82-90.

Morris, D.R., and Hager, L.P. (1966). Chloroperoxidase I. Isolation and properties of the crystalline glycoprotein. J. Biol. Chem. 241**,** 1763-1768.

Morse, D.E., and Morse, A.N.C. (1976). Dual-control of the tryptophan operon is mediated by both tryptophanyl-tRNA synthetase and the repressor. J. Mol. Biol. 103**,** 209-226. doi:10.1016/0022-2836(76)90310-7.

Mueller, R.S., Beyhan, S., Saini, S.G., Yildiz, F.H., and Bartlett, D.H. (2009). Indole acts as an extracellular cue regulating gene expression in *Vibrio cholerae*. J. Bacteriol. 191**,** 3504-3516. doi:10.1128/JB.01240-08.

Musumeci, G., Castrogiovanni, P., Szychlinska, M.A., Imbesi, R., Loreto, C., Castorina, S., et al. (2017). Protective effects of high Tryptophan diet on aging-induced passive avoidance impairment and hippocampal apoptosis. Brain Res. Bull. 128**,** 76-82. doi:10.1016/j.brainresbull.2016.11.007.

Nakagawa, M. (1970). Constituents in tea leaf and their contribution to the taste of green tea liquor. Jpn. Agric. Res. Q 5**,** 43-47.

Negron, L., Patchett, M.L., and Parker, E.J. (2011). Expression, purification, and characterisation of dehydroquinate synthase from *Pyrococcus furiosus*. Enzym. Res. 2011. doi:10.4061/2011/134893.

Neubauer, P.R., Widmann, C., Wibberg, D., Schröder, L., Frese, M., Kottke, T., et al. (2018). A flavin-dependent halogenase from metagenomic analysis prefers bromination over chlorination. PloS One 13**,** e0196797. doi:10.1371/journal.pone.0196797.

Neumann, C.S., Fujimori, D.G., and Walsh, C.T. (2008). Halogenation strategies in natural product biosynthesis. Chem. Biol. 15**,** 99-109. doi:10.1016/j.chembiol.2008.01.006.

Newton, W.A., and Snell, E.E. (1965). Formation and interrelationships of tryptophanase and tryptophan synthetases in *Escherichia coli*. J. Bacteriol. 89**,** 355-364.

Nikolaus, S., Schulte, B., Al-Massad, N., Thieme, F., Schulte, D.M., Bethge, J., et al. (2017). Increased tryptophan metabolism is associated with activity of inflammatory bowel diseases. Gastroenterology 153**,** 1504-1516. doi:10.1053/j.gastro.2017.08.028.

Nishizawa, T., Aldrich, C.C., and Sherman, D.H. (2005). Molecular analysis of the rebeccamycin L-amino acid oxidase from *Lechevalieria aerocolonigenes* ATCC 39243. J. Bacteriol. 187**,** 2084-2092. doi:10.1128/JB.187.6.2084-2092.2005.

O'Gara, J.P., and Dunican, L.K. (1995). Mutations in the *trpD* gene of *Corynebacterium glutamicum* confer 5-methyltryptophan resistance by encoding a feedback-resistant anthranilate phosphoribosyltransferase. Appl. Environ. Microbiol. 61**,** 4477-4479.

O'Hagan, D., Schaffrath, C., Cobb, S.L., Hamilton, J.T.G., and Murphy, C.D. (2002). Biochemistry: biosynthesis of an organofluorine molecule. Nature. 416**,** 279. doi:10.1038/416279a.

Oxender, D.L., Zurawski, G., and Yanofsky, C. (1979). Attenuation in the *Escherichia coli* tryptophan operon: role of RNA secondary structure involving the tryptophan codon region. Proc. Natl. Acad. Sci. 76**,** 5524-5528. doi:10.1073/pnas.76.11.5524.

Park, S., Kang, K., Lee, S.W., Ahn, M.-J., Bae, J.-M., and Back, K. (2011). Production of serotonin by dual expression of tryptophan decarboxylase and tryptamine 5-hydroxylase in *Escherichia coli*. Appl. Microbiol. Biotechnol. 89**,** 1387-1394. doi:10.1007/s00253-010-2994-4.

Parry, R.J. (1971). Biosynthesis of compounds containing an indole nucleus. Chemistry of Heterocyclic Compounds: Indoles, Part Two 25**,** 1-64. doi:10.1002/9780470186930.ch1.

Payne, J.T., Andorfer, M.C., and Lewis, J.C. (2013). Regioselective Arene Halogenation using the FAD-Dependent Halogenase RebH. Angew. Chem. 125**,** 5379-5382. doi:10.1002/anie.201300762.

Payne, J.T., Poor, C.B., and Lewis, J.C. (2015). Directed Evolution of RebH for Site-Selective Halogenation of Large Biologically Active Molecules. Angew. Chem. Int. Ed. 54**,** 4226-4230. doi:10.1002/anie.201411901.

Pérez-García, F., Peters-Wendisch, P., and Wendisch, V.F. (2016). Engineering *Corynebacterium glutamicum* for fast production of L-lysine and L-pipecolic acid. Appl. Microbiol. Biotechnol. 100**,** 8075-8090. doi:10.1007/s00253-016-7682-6.

Peters-Wendisch, P., Götker, S., Heider, S.A.E., Reddy, G.K., Nguyen, A.Q., Stansen, K.C., et al. (2014). Engineering biotin prototrophic *Corynebacterium glutamicum* strains for amino acid, diamine and carotenoid production. J. Biotechnol. 192**,** 346-354. doi:10.1016/j.jbiotec.2014.01.023.

Poor, C.B., Andorfer, M.C., and Lewis, J.C. (2014). Improving the stability and catalyst lifetime of the halogenase RebH by directed evolution. ChemBioChem 15**,** 1286-1289. doi:10.1002/cbic.201300780.

Purwanto, H.S., Kang, M.-S., Ferrer, L., Han, S.-S., Lee, J.-Y., Kim, H.-S., et al. (2018). Rational engineering of the shikimate and related pathways in *Corynebacterium glutamicum* for 4-hydroxybenzoate production. J. Biotechnol. doi:10.1016/j.jbiotec.2018.07.016.

Rajasekharan, S.K., Lee, J.-H., Ravichandran, V., Kim, J.-C., Park, J.G., and Lee, J. (2019). Nematicidal and insecticidal activities of halogenated indoles. Sci. Rep. 9**,** 2010. doi:10.1038/s41598-019-38561-3.

Roy, A.D., Goss, R.J.M., Wagner, G.K., and Winn, M. (2008). Development of fluorescent aryltryptophans by Pd mediated cross-coupling of unprotected halotryptophans in water. Chem. Commun. 39**,** 4831-4833. doi:10.1039/B807512C.

Runguphan, W., Qu, X., and O'connor, S.E. (2010). Integrating carbon–halogen bond formation into medicinal plant metabolism. Nature. 468**,** 461. doi:10.1038/nature09524.

Sakato, Y. (1950). Studies on the Chemical Constituents of Tea Part III. . Nippon Nōgeikagaku Kaishi 23**,** 262-267. doi:10.1271/nogeikagaku1924.23.262.

Sanada, M., Miyano, T., Iwadare, S., Williamson, J.M., Arison, B.H., Smith, J.L., et al. (1986). Biosynthesis of fluorothreonine and fluoracetic. J. Antibiot. 39**,** 259-265. doi:10.7164/antibiotics.39.259.

Sánchez-Viesca, F., Berros, M., and Gómez, R. (2016). On the mechanism of the Baeyer-Drewsen synthesis of indigo. Am. J. Chem 6**,** 18-22. doi:10.5923/j.chemistry.20160601.04.

Sánchez, C., Butovich, I.A., Braña, A.F., Rohr, J., Méndez, C., and Salas, J.A. (2002). The biosynthetic gene cluster for the antitumor rebeccamycin: characterization and generation of indolocarbazole derivatives. Chem. Biol. 9**,** 519-531. doi:10.1016/S1074-5521(02)00126-6.

Sano, K., and Matsui, K. (1987). Structure and function of the trp operon control regions of *Brevibacterium lactofermentum*, a glutamic-acid-producing bacterium. Gene 53**,** 191-200. doi:10.1016/0378-1119(87)90007-2.

Sasson, Y. (1995). Formation of carbon–halogen bonds (Cl, Br, I). Supplement D2; The Chemistry of Halides, Pseudo-Halides and Azides**,** 535-628. doi:10.1002/047002349X.ch11.

Schäfer, A., Kalinowski, J., Simon, R., Seep-Feldhaus, A.H., and Pühler, A. (1990). High-frequency conjugal plasmid transfer from gram-negative *Escherichia coli* to various gram-positive coryneform bacteria. J. Bacteriol. 172**,** 1663-1666.

Schäfer, A., Tauch, A., Jäger, W., Kalinowski, J., Thierbach, G., and Pühler, A. (1994). Small mobilizable multi-purpose cloning vectors derived from the *Escherichia coli* plasmids pK18 and pK19: selection of defined deletions in the chromosome of *Corynebacterium glutamicum*. Gene 145**,** 69-73. doi:10.1016/0378-1119(94)90324-7.

Schneider, J., Niermann, K., and Wendisch, V.F. (2011). Production of the amino acids L-glutamate, L-lysine, L-ornithine and L-arginine from arabinose by recombinant *Corynebacterium glutamicum*. J. Biotechnol. 154**,** 191-198. doi:10.1016/j.jbiotec.2010.07.009.

Schnepel, C., and Sewald, N. (2017). Enzymatic Halogenation: A Timely Strategy for Regioselective C− H Activation. Chem. Eur. J. 23**,** 12064-12086. doi:10.1002/chem.201701209

Schoner, R., and Herrmann, K.M. (1976). 3-Deoxy-D-arabino-heptulosonate 7-phosphate synthase. Purification, properties, and kinetics of the tyrosine-sensitive isoenzyme from *Escherichia coli*. J. Biol. Chem. 251**,** 5440-5447.

Seibold, G., Auchter, M., Berens, S., Kalinowski, J., and Eikmanns, B.J. (2006). Utilization of soluble starch by a recombinant *Corynebacterium glutamicum* strain: growth and lysine production. J. Biotechnol. 124**,** 381-391. doi:10.1016/j.jbiotec.2005.12.027.

Sgobba, E., Blöbaum, L., and Wendisch, V.F. (2018). Production of food and feed additives from non-food-competing feedstocks: Valorizing *N*-acetylmuramic acid for amino acid and carotenoid fermentation with *Corynebacterium glutamicum*. Front. Microbiol. 9**,** 2046. doi:10.3389/fmicb.2018.02046.

Sitachitta, N., Márquez, B.L., Williamson, R.T., Rossi, J., Roberts, M.A., Gerwick, W.H., et al. (2000). Biosynthetic pathway and origin of the chlorinated methyl group in barbamide and dechlorobarbamide, metabolites from the marine cyanobacterium *Lyngbya majuscula*. Tetrahedron 56**,** 9103-9113. doi:10.1016/S0040-4020(00)00763-8.

Smith, T. (1897). A modification of the method for determining the production of indol by bacteria. J. Exp. Med. 2**,** 543.

Stackebrandt, E., Rainey, F.A., and Ward-Rainey, N.L. (1997). Proposal for a new hierarchic classification system, *Actinobacteria* classis nov. Int. J. Syst. Evol. Microbiol. 47**,** 479-491. doi:10.1099/00207713-47-2-479.

Strickland, M., and Willis, C.L. (2010). Synthesis of Halogenated α-Amino Acids, in Amino Acids, Peptides and Proteins in Organic Chemistry.

Sundaramoorthy, M., Terner, J., and Poulos, T.L. (1995). The crystal structure of chloroperoxidase: a heme peroxidase–cytochrome P450 functional hybrid. Structure 3**,** 1367-1378. doi:10.1016/S0969-2126(01)00274-X.

Tamir, H., and Srinivasan, P.R. (1970). Studies of the mechanism of anthranilate synthase reaction. Proc. Natl. Acad. Sci. 66**,** 547-551. doi:10.1073/pnas.66.2.547.

Tateno, T., Fukuda, H., and Kondo, A. (2007). Production of L-Lysine from starch by *Corynebacterium glutamicum* displaying α-amylase on its cell surface. Appl. Microbiol. Biotechnol. 74**,** 1213-1220. doi:10.1007/s00253-006-0766-y.

Tateno, T., Okada, Y., Tsuchidate, T., Tanaka, T., Fukuda, H., and Kondo, A. (2009). Direct production of cadaverine from soluble starch using *Corynebacterium glutamicum* coexpressing α-amylase and lysine decarboxylase. Appl. Microbiol. Biotechnol. 82**,** 115. doi:10.1007/s00253-008-1751-4.

Teramoto, H., Shirai, T., Inui, M., and Yukawa, H. (2008). Identification of a gene encoding a transporter essential for utilization of C4 dicarboxylates in *Corynebacterium glutamicum*. Appl. Environ. Microbiol. 74**,** 5290-5296. doi:10.1128/AEM.00832-08.

Timmins, A., and de Visser, S. (2018). A Comparative Review on the Catalytic Mechanism of Nonheme Iron Hydroxylases and Halogenases. Catalysts 8**,** 314. doi:10.3390/catal8080314.

Tlaskalová-Hogenová, H., Štěpánková, R., Hudcovic, T., Tučková, L., Cukrowska, B., Lodinová-Žádnıková, R., et al. (2004). Commensal bacteria (normal microflora), mucosal immunity and chronic inflammatory and autoimmune diseases. Immunol. Lett. 93**,** 97-108. doi:10.1016/j.imlet.2004.02.005.

Topall, G., and Laborit, H. (1989). Brain tyrosine increases after treating with prodrugs: comparison with tyrosine. J. Pharm. Pharmacol. 41**,** 789-791. doi:10.1111/j.2042-7158.1989.tb06368.x.

Turner, M.J., Smith, B.W., and Haslam, E. (1975). The shikimate pathway. Part IV. The stereochemistry of the 3-dehydroquinate dehydratase reaction and observations on 3-dehydroquinate synthetase. J. Chem. Soc., 52-55. doi:10.1039/P19750000052.

Urbaniak, M., Stępień, Ł., and Uhlig, S. (2019). Evidence for Naturally Produced Beauvericins Containing *N*-Methyl-Tyrosine in *Hypocreales* Fungi. Toxins 11, 182. doi:10.3390/toxins11030182.

Vaillancourt, F.H., Yeh, E., Vosburg, D.A., Garneau-Tsodikova, S., and Walsh, C.T. (2006). Nature's inventory of halogenation catalysts: oxidative strategies predominate. Chem. Rev. 106, 3364-3378. doi:10.1021/cr050313i.

van Pée, K.-H. (1996). Biosynthesis of halogenated metabolites by bacteria. Annu. Rev. Microbiol. 50, 375-399. doi:10.1146/annurev.micro.50.1.375.

Vega, N.M., Allison, K.R., Khalil, A.S., and Collins, J.J. (2012). Signaling-mediated bacterial persister formation. Nat. Chem. Biol. 8, 431. doi:10.1038/nchembio.915.

Warskulat, A.C., Tatsis, E.C., Dudek, B., Kai, M., Lorenz, S., and Schneider, B. (2016). Unprecedented utilization of pelargonidin and indole for the biosynthesis of plant indole alkaloids. ChemBioChem 17, 318-327. doi:10.1002/cbic.201500572.

Weissermel, K., and Arpe, H.-J. (2008). Industrial organic chemistry. John Wiley & Sons.

Wendisch, V.F. (2019). Metabolic engineering advances and prospects for amino acid production. Metab. Eng. doi:10.1016/j.ymben.2019.03.008.

Wever, R., Plat, H., and de Boer, E. (1985). Isolation procedure and some properties of the bromoperoxidase from the seaweed *Ascophyllum nodosum*. Biochim. Biophys. Acta (BBA)-Protein Structure and Molecular Enzymology 830, 181-186. doi:10.1016/0167-4838(85)90026-3.

Weyand, M., Hecht, H.J., Kiess, M., Liaud, M.F., Vilter, H., and Schomburg, D. (1999). X-ray structure determination of a vanadium-dependent haloperoxidase from *Ascophyllum nodosum* at 2.0 Å resolution. J. Mol. Biol. 293, 595-611. doi:10.1006/jmbi.1999.3179.

Wikoff, W.R., Anfora, A.T., Liu, J., Schultz, P.G., Lesley, S.A., Peters, E.C., et al. (2009). Metabolomics analysis reveals large effects of gut microflora on mammalian blood metabolites. Proc. Natl. Acad. Sci. 106, 3698-3703. doi:10.1073/pnas.0812874106.

Wilmanns, M., Priestle, J.P., Niermann, T., and Jansonius, J.N. (1992). Three-dimensional structure of the bifunctional enzyme phosphoribosylanthranilate isomerase: indoleglycerolphosphate synthase from *Escherichia coli* refined at 2.0 Å resolution. J. Mol. Biol. 223, 477-507. doi:10.1016/0022-2836(92)90665-7.

Winter, J.M., Moffitt, M.C., Zazopoulos, E., McAlpine, J.B., Dorrestein, P.C., and Moore, B.S. (2007). Molecular Basis for Chloronium-mediated Meroterpene Cyclization cloning, sequencing, and heterologous expression of the napyradiomycin biosynthetic gene cluster. J. Biol. Chem. 282, 16362-16368. doi:10.1074/jbc.M611046200.

Yanofsky, C., and Crawford, I.P. (1987). The tryptophan operon. Escherichia coli and Salmonella typhimurium Cellular and Molecular Biology**,** 1453-1472.

Yanofsky, C., and Soll, L. (1977). Mutations affecting $tRNA^{Trp}$ and its charging and their effect on regulation of transcription termination at the attenuator of the tryptophan operon. J. Mol. Biol. 113**,** 663-677. doi:10.1016/0022-2836(77)90229-7.

Ye, S., von Delft, F., Brooun, A., Knuth, M.W., Swanson, R.V., and McRee, D.E. (2003). The crystal structure of shikimate dehydrogenase (AroE) reveals a unique NADPH binding mode. J. Bacteriol. 185**,** 4144-4151. doi:10.1128/JB.185.14.4144-4151.2003.

Yeh, E., Blasiak, L.C., Koglin, A., Drennan, C.L., and Walsh, C.T. (2007). Chlorination by a Long-Lived Intermediate in the Mechanism of Flavin-Dependent Halogenases. Biochem. 46**,** 1284-1292. doi:10.1021/bi0621213.

Yeh, E., Cole, L.J., Barr, E.W., Bollinger, J.M., Ballou, D.P., and Walsh, C.T. (2006). Flavin redox chemistry precedes substrate chlorination during the reaction of the flavin-dependent halogenase RebH. Biochem. 45**,** 7904-7912. doi:10.1021/bi060607d.

Yeh, E., Garneau, S., and Walsh, C.T. (2005). Robust in vitro activity of RebF and RebH, a two-component reductase/halogenase, generating 7-chlorotryptophan during rebeccamycin biosynthesis. Proc. Natl. Acad. Sci. U. S. A. 102**,** 3960-3965. doi:10.1073/pnas.0500755102.

Youn, J.-W., Jolkver, E., Krämer, R., Marin, K., and Wendisch, V.F. (2009). Characterization of the dicarboxylate transporter DctA in *Corynebacterium glutamicum*. J. Bacteriol. 191**,** 5480-5488. doi:10.1128/JB.00640-09.

Zahoor, A., Lindner, S.N., and Wendisch, V.F. (2012). Metabolic engineering of *Corynebacterium glutamicum* aimed at alternative carbon sources and new products. Comput. Struct. Biotechnol. J. 3**,** e201210004. doi:10.5936/csbj.201210004.

Zehner, S., Kotzsch, A., Bister, B., Süssmuth, R.D., Méndez, C., Salas, J.A., et al. (2005). A regioselective tryptophan 5-halogenase is involved in pyrroindomycin biosynthesis in *Streptomyces rugosporus* LL-42D005. Chem. Biol. 12**,** 445-452. doi:10.1016/j.chembiol.2005.02.005.

Zeng, J., and Zhan, J. (2011). Characterization of a tryptophan 6-halogenase from *Streptomyces toxytricini*. Biotechnol. Lett. 33**,** 1607-1613. doi:10.1007/s10529-011-0595-7.

Zhang, C., Zhang, J., Kang, Z., Du, G., Yu, X., Wang, T., et al. (2013). Enhanced production of L-phenylalanine in *Corynebacterium glutamicum* due to the introduction of *Escherichia coli* wild-type gene *aroH*. J. Ind. Microbiol. Biotechnol. 40**,** 643-651. doi:10.1007/s10295-013-1262-x.

Zhang, R., Wang, B., Ouyang, J., Li, J., and Wang, Y. (2008). *Arabidopsis* indole synthase, a homolog of tryptophan synthase alpha, is an enzyme involved in the Trp-independent indole-containing metabolite biosynthesis. J. Integr. Plant Biol. 50**,** 1070-1077. doi:10.1111/j.1744-7909.2008.00729.x.

Zurawski, G., Elseviers, D., Stauffer, G.V., and Yanofsky, C. (1978). Translational control of transcription termination at the attenuator of the *Escherichia coli* tryptophan operon. Proc. Natl. Acad. Sci. 75**,** 5988-5992. doi:10.1073/pnas.75.12.5988.

Zurawski, G., and Yanofsky, C. (1980). *Escherichia coli* tryptophan operon leader mutations, which relieve transcription termination, are *cis*-dominant to trp leader mutations, which increase transcription termination. J. Mol. Biol. 142**,** 123-129. doi:10.1016/0022-2836(80)90210-7.

2. Results

The results of this thesis are presented within four manuscripts:

The first manuscript ´Metabolic engineering of *Corynebacterium glutamicum* for the fermentative production of halogenated tryptophan´ describes the fermentative production of 7-chloro-L-tryptophan (7-Cl-Trp) by *C. glutamicum*. Therefor the genes coding for the FAD-dependent halogenase RebH and the NADH-dependent flavin reductase RebF from *Lechevalieria aerocolonigenes* were overexpressed in an L-tryptophan (Trp) overproducing *C. glutamicum* strain. By further engineering, the production of 7-Cl-Trp from the alternative carbon sources arabinose, glucosamine and xylose was established.

Since RebH accepts beside chlorine ions as well bromine ions the concept was extended to another halogenated Trp derivative 7-bromo-L-tryptophan (7-Br-Trp). The production of 7-Br-Trp is described in the second manuscript ´Bromination of L-tryptophan in a fermentative process with *Corynebacterium glutamicum*´. The halogenating *C. glutamicum* strain was cultivated with sodium bromide in a low-chloride medium to enable the production of 7-Br-Trp. The fermentative production was scaled up to 2 L in a batch and a fed-batch fermentation. The product 7-Br-Trp was isolated and purified by reverse phase chromatography.

In the first two manuscripts, it was observed, that the products 7-Cl-Trp and 7-Br-Trp inhibited the anthranilate phosphoribosyltransferase (encoded by *trpD*) which lead to an accumulation of anthranilate. Overexpression of feedback resistant *trpDs* from various microorganisms in a *rebH* and *rebF* expressing *C. glutamicum* strain enabled full conversion of anthranilate in the fermentative production of 7-Cl-Trp and 7-Br-Trp. The characterization of the feedback resistant TrpDs are described in the third manuscript ´Fermentative production of halogenated Trp by recombinant *Corynebacterium glutamicum* using feedback resistant anthranilate phosphoribosyltransferases´.
To expanse the product portfolio of *C. glutamicum* towards indole different tryptophanases were overexpressed in the Trp overproducing *C. glutamicum* strain which is described in the

fourth manuscript ´Fermentative production of indole with *Corynebacterium glutamicum* overexpressing different tryptophanases´. Interestingly, the tryptophanases from *E. coli* and *P. vulgaris* showed a wider substrate spectrum containing halogenated Trp.

Editorial changes were done in the manuscripts according to the style of the thesis. Grammar and typos were corrected.

2.1 Metabolic engineering of *Corynebacterium glutamicum* for the fermentative production of halogenated tryptophan

Kareen H. Veldmann[a], Hannah Minges[b], Norbert Sewald[b], Jin-Ho Lee[c], Volker F. Wendisch[a]

[a] Genetics of Prokaryotes, Faculty of Biology & CeBiTec, Bielefeld University, Universitätsstr. 25, 33615 Bielefeld, Germany

[b] Organic Chemistry III, Faculty of Chemistry & CeBiTec, Bielefeld University, Universitätsstr. 25, 33615 Bielefeld, Germany

[c] Major in Food Science & Biotechnology, School of Food Biotechnology & Nutrition, BB21+, Kyungsung University, 309, Suyeong-ro, Nam-gu, Busan 48434, Republic of Korea

2.1.1 Abstract

Halogenated compounds, like 7-chloro-L-tryptophan, are important intermediates or components of bioactive substances relevant for the pharmaceutical, chemical and agrochemical industries. About 20% of all pharmaceutical small molecule drugs and around 30% of all active compounds in agrochemistry are halogenated. Chemical halogenation procedures usually are characterized by the use of hazardous or even highly toxic chemicals. Recently, a biocatalytic process for L-tryptophan halogenation at the gram-scale using FAD-dependent halogenase and NADH-dependent flavin reductase enzymes has been described. Many proteinogenic amino acids are produced by fermentation using *Corynebacterium glutamicum.* The fermentative production of L-glutamate and L-lysine, for example, is operated at the million-ton scale. However, fermentative production of halogenated amino acids has not yet been described. In this study, fermentative production of the halogenated amino acid 7-chloro-L-tryptophan from sugars, ammonium and chloride salts was achieved. This required metabolic engineering of an L-tryptophan producing *C. glutamicum* strain for expression of the genes coding for FAD-dependent halogenase RebH and NADH-dependent flavin reductase RebF from *Lechevalieria aerocolonigenes*. Chlorination of L-tryptophan to 7-chloro-L-tryptophan by recombinant *C. glutamicum* was

improved by optimizing the RBS of *rebH*. Metabolic engineering enabled production of 7-chloro-L-tryptophan and L-tryptophan from the alternative carbon sources arabinose, glucosamine and xylose.

2.1.2 Introduction

Halogenated amino acids are sought after by the pharmaceutical, chemical and agrochemical industries (Diederich and Stang, 2008). They are found in various natural products including the antibiotics chloramphenicol and pyrroindomycin, the plant growth-regulating thienodolin, and the antifungal pyrrolnitrin (Hammer et al., 1997; van Pée and Hölzer, 1999). Rebeccamycin is an indolocarbazole alkaloid antibiotic that inhibits DNA topoisomerase I and is produced naturally by *Lechevalieria aerocolonigenes* (Onaka et al., 2003; Nishizawa et al., 2005). 7-Chloro-L-tryptophan (7-Cl-Trp) is a precursor of rebeccamycin. Halogenation of L-tryptophan (Trp) requires two enzymes encoded in the *reb* cluster of *L. aerocolonigenes*: the FAD-dependent halogenase RebH and NADH-dependent flavin reductase RebF (Nishizawa et al., 2005). Halogenase RebH uses $FADH_2$, molecular oxygen (O_2) and chloride (Cl^-) to halogenate its substrate Trp yielding 7-Cl-Trp. In turn, recycling of the reduced cofactor $FADH_2$ requires nicotinamide adenine dinucleotide (NADH)-dependent flavin reductase RebF. Recently, a biocatalytic process for L-tryptophan halogenation at the gram-scale has been described based on the purified enzymes and cross-linked enzyme aggregates including alcohol dehydrogenase for NADH recycling with isobutanol (Frese and Sewald, 2015; Schnepel and Sewald, 2017). However, production of the halogenated amino acid 7-Cl-Trp by fermentation has neither been described for the native *L. aerocolonigenes* nor for other microorganisms.

Corynebacterium glutamicum is the work horse of fermentative amino acid production (Hermann, 2003; Eggeling and Bott, 2015; Lee et al., 2016; Wendisch et al., 2016). Besides its use in the million-ton scale L-glutamate and L-lysine processes, this bacterium has been engineered for production of various compounds including alcohols (Inui et al., 2004; Jojima et al., 2015; Siebert and Wendisch, 2015; Wendisch et al., 2016), diamines (Wendisch et al., 2018) like putrescine (Schneider and Wendisch, 2010), organic acids (Wieschalka et al.,

2013), terpenoids (Heider et al., 2014) such as patchoulol (Henke et al., 2018) or non-proteinogenic amino acids (Wendisch, 2016) such as GABA (Kim et al., 2013; Jorge et al., 2016; Pérez-García et al., 2016; Jorge et al., 2017). *C. glutamicum* has also been engineered to produce aromatic amino acids including Trp and aromatic compounds amenable from intermediates of the shikimate and chorismate pathways (Lee and Wendisch, 2017).

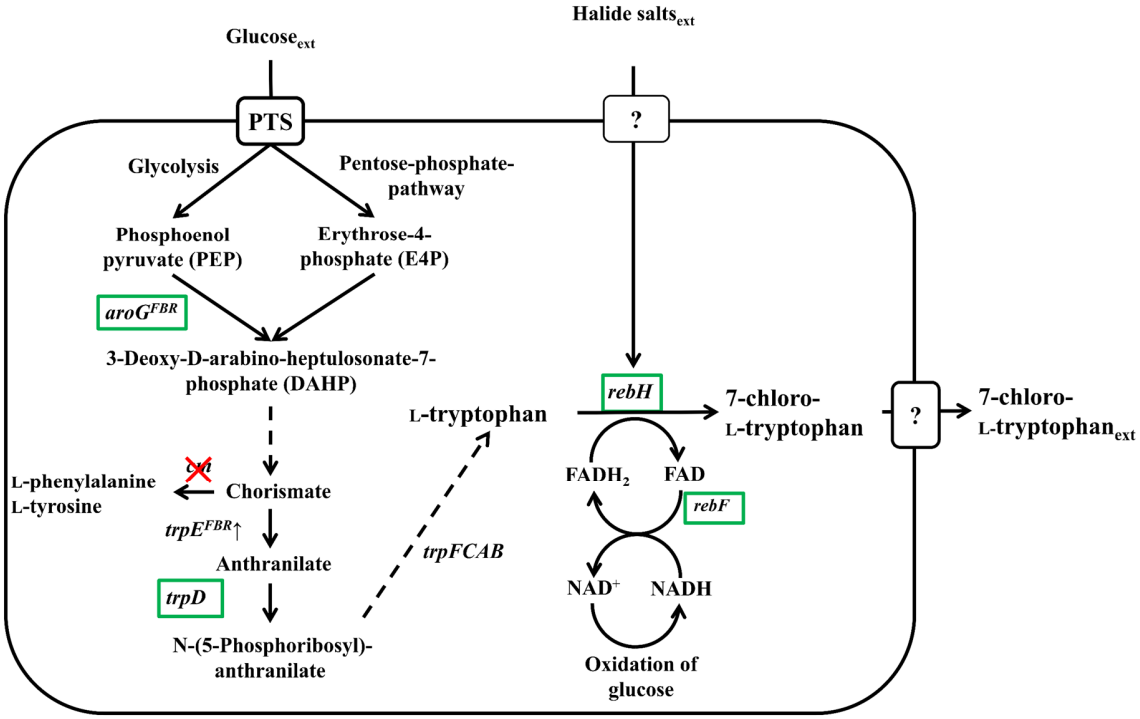

Figure 2.1.1: Schematic representation of reactions in recombinant Trp and 7-Cl-Trp producing *C. glutamicum*. Genes names are shown next to reactions that are represented by arrows. Dashed arrows show several reactions. Overexpression of endogenous genes is indicated (↑), expression of heterologous genes is marked by green boxes, deletions are marked with red crosses. FBR: feedback resistant

Recently, a metabolic engineering strategy to overproduce Trp and related compounds such as 4-hydroxybenzoate has been described (Purwanto et al., 2018). Strain engineering for Trp production included plasmid-based expression of *trpD* from *E. coli* and genome-based expression of *trpE*^{FBR} coding for feedback-resistant anthranilate synthase, together with deletion of *csm* encoding chorismate mutase and expression of *aroG*^{FBR} encoding feedback-resistant 3-deoxy-D-arabinoheptulosonate-7-phosphate synthase from *E. coli* in the *vdh*-deleted genome locus (Purwanto et al., 2018).

Here, we describe metabolic engineering of 7-Cl-Trp producing strains based on the above described Trp producing strain. Overexpression of the genes encoding the FAD-dependent halogenase RebH and the NADH-dependent flavin reductase RebF from *L. aerocolonigenes* enabled halogenation of Trp to 7-Cl-Trp. Moreover, production of 7-Cl-Trp and Trp from the alternative carbon sources like arabinose, xylose and glucosamine that do not have competing uses for human and animal nutrition was established.

2.1.3 Materials and methods

2.1.3.1 Bacterial strains and growth conditions

Bacterial strains and plasmids used in this study are listed in Table 2.1.1. *Escherichia coli* DH5α (Hanahan, 1983) was used for cloning of the plasmid constructs. *E. coli* and *C. glutamicum* were usually grown in lysogeny broth medium (LB) in 500 mL baffled flask at 37 °C and 30 °C, respectively. For growth and production experiments *C. glutamicum* was inoculated in CGXII (Eggeling and Bott, 2005) supplemented with 40 g L^{-1} glucose in 500 mL baffled flasks to an optical density (OD_{600}) of 1 and incubated at 120 rpm (shaking diameter: 16.5 cm) at 30 °C. Growth was followed by measuring the optical density using V-1200 Spectrophotometer at 600 nm (VWR, Radnor, PA, USA). For production of halogenated tryptophan, the minimal medium was supplemented with chloride salts. For all strains derived from Tp679 1.5 mM L-phenylalanine and 1.37 mM L-tyrosine were added to the minimal medium. If necessary, the growth medium was supplemented with kanamycin (25 µg mL^{-1}), spectinomycin (100 µg mL^{-1}) and/ or tetracycline (5 µg mL^{-1}). To induce the gene expression from the vectors pEKEx3 (Stansen et al., 2005) and pECXT99A (Kirchner and Tauch, 2003) isopropyl-β-D-1-thiogalactopyranoside (IPTG) (1 mM) was added.

Table 2.1.1: Strains and vectors used in this work.

Strains	**Description**	**Source**
WT	*C. glutamicum* wild type, ATCC 13032	ATCC
Tp679	*Δcsm ΔtrpL::P_{ilvCM1} $trpE^{fbr}$ Δvdh::P_{ilvC} $aroG^{fbr}$*	(Purwanto et al., 2018)
Tp679 (pCES208-*trpD*)	Tp679 carrying pCES208-*trpD*	(Purwanto et al., 2018)
P. putida KT2440	*P. putida* mt-2 hsdRI hsdM*	(Bagdasarian et al., 1981; Nelson et al., 2002)
P. putida (pCIBhis-*prnF*)	*P. putida* KT2440 carrying pCIBhis-*prnF*	This work
Strains	**Description**	**Source**
E.coli BL21(DE3)	F^- ompT hsdSB(r_B- m_B-) gal dcm (DE3)	Novagen

BL21(DE3) (pET21-ADH)	BL21(DE3) carrying pET21-ADH	This work
Tp679 (pCES208-*trpD*) (pEKEx3)	Tp679 (pCES208-*trpD*) carrying pEKEx3	This work
WT (pEKEx3-*rebH-rebF*)	Wild type carrying pEKEx3-*rebH-rebF*	This work
HalT1	Tp679 (pCES208-*trpD*) carrying pEKEx3-*rebH-rebF*	This work
HalT2	Tp679 (pCES208-*trpD*) carrying pEKEx3-optimRBS-*rebH-rebF*	This work
HalT3	Tp679 (pCES208-*trpD*) carrying pECXT99A-*rebH-rebF*	This work
HalT4	Tp679 (pCES208-*trpD*) carrying pECXT99A-optimRBS-*rebH-rebF*	This work
HalT1 (pECXT99A-*araBAD*)	HalT1 carrying pECXT99A-*araBAD*	This work
HalT1 (pECXT99A-*xylAB*)	HalT1 carrying pECXT99A-*xylAB*	This work
HalT1 (pECXT99A-*nagB*)	HalT1 carrying pECXT99A-*nagB*	This work
Plasmids	**Description**	**Source**
pCLBhis-*prnF*	Tet^R, *E. coli*/*Pseudomonas* shuttle vector (Ptac, *tra*, oriT, oriV, (his)6-tag) overexpressin *prnF* from *P. fluorescens*	(Frese et al., 2014)
pET21-ADH	Amp^R, *E. coli* vector (T7 promotor, *lacI*, pBR322 $Ori_{E.c}$, (his)6-tag) overexpressing alcohol dehydrogenase from *Rhodococcus* sp.	(Frese et al., 2014)
pCES208	Kan^R, *C. glutamicum*/ *E. coli* shuttle vector pCG1 $OriV_{C.g.}$	(Park et al., 2008)
pCES208-*trpD*	Kan^R, pCES208 overexpressing *trpD* from *E. coli*	
pEKEx3	$Spec^R$, *C. glutamicum*/*E. coli* shuttle vector (Ptac, *lacI* , pBL1 $OriV_{C.g.}$)	(Stansen et al., 2005)

Plasmids	Description	Source
pECXT99A	Tet^R, *C. glutamicum*/*E. coli* shuttle vector (Ptrc, *lacI*, pGA1 $OriV_{C.g.}$)	(Kirchner and Tauch, 2003)
pEKEx3-*rebH*-*rebF*	$Spec^R$, pEKEx3 overexpressing *rebH*, *rebF* from *Lechevalieria aerocolonigenes*	This work
pEKEx3-optimRBS-*rebH*-*rebF*	$Spec^R$, pEKEx3 overexpressing *rebH*, *rebF* from *Lechevalieria aerocolonigenes* with optimized RBS for *rebH*	This work
pECXT99A-*rebH*-*rebF*	Tet^R, pECXT99A overexpressing *rebH*, *rebF* from *Lechevalieria aerocolonigenes*	This work
pECXT99A-optimRBS-*rebH*-*rebF*	Tet^R, pECXT99A overexpressing *rebH*, *rebF* from *Lechevalieria aerocolonigenes* with optimized RBS for *rebH*	This work
pEKEx3-$xylA_{Xc}$-$xylB_{Cg}$	$Spec^R$, pEKEx3 overexpressing *xylA* from *Xanthomonas campestris* SCC1758 and *xylB* from *C. glutamicum* ATCC 13032	(Meiswinkel et al., 2013)
pECXT99A-*nagB*	Tet^R, pECXT99A overexpressing *nagB* from *C. glutamicum* ATCC 13032	This work
pECXT99A-*araBAD*	Tet^R, pECXT99A overexpressing *araBAD* from *E. coli* MG1655	(Mindt et al., 2018)
pECXT99A-*xylAB*	Tet^R, pECXT99A overexpressing *xylA* from *Xanthomonas campestris* SCC1758 and *xylB* from *C. glutamicum* ATCC 13032	This work

2.1.3.2 Molecular genetic techniques and strains construction

Standard molecular genetic techniques were carried out as described elsewhere (Sambrook et al., 1989). *E. coli* was transformed by heat shock (Sambrook et al., 1989) and *C. glutamicum* by electroporation (Eggeling and Bott, 2005). The genes *rebH* and *rebF* were amplified from plasmid pET28-*rebH* and pET21-*rebF*, respectively. For amplification of *rebH* different forward primers (fwd) and one reverse (rv) primer were used: pEKEx3-*rebH*-fwd (CATGCCTGCAGGTCGACTCTAGAGGAAAGGAGGCCCTTCAG

ATGTCCGGCAAGATTGACAAG)(HalT1), pEKEx3-optimRBS-*rebH*-fwd (GCCTGCAGGTCGACTCTAGAGCACGCTGTAAGGAGTAACCAAAAAAAGGAGG TTTTTTATGTCCGGCAAGATTGACAAG) (HalT2), pECXT99A-*rebH*-fwd (CATGGAATTCGAGCTCGGTACCCGGGGAAAGGAGGCCCTTCAGATGTCCGGC AAGATTGACAAG)(HalT3), pECXT99A-optimRBS-*rebH*-fwd (CATGGAATTCGAGCTCGGTACCCGGGAATATTCCAATTTAAAGGAGGTTATTT ATGTCCGGCAAGATTGACAAG)(HalT4) and *rebH*-rv (GAACTCGATCGTCATCTGAAGGGCCTCCTTTCTCAGCGGCCGTGCTGTTGCC). RebF was amplified with *rebF*-fwd (CCTGAGGCAACAGCACGGCCGCTGAGAAAGGAGGCCCTTCAGATGACGATCG AGTTCGACAG) and *rebF*-rv (GAATTCGAGCTCGGTACCCGGGGATCTCATCCCTCCGGTGTCCACA). All *rebH*-fwd primers carry the RBS sequence for *rebH* and primer *rebF*-fwd carries the RBS sequence for *rebF*. The vectors pEKEx3 and pECXT99A were restricted with *Bam*HI and incubated in Gibson assembly (Gibson et al., 2009) with the two PCR products for construction of pEKEx3-*rebH-rebF*, pEKEx3-optimRBS-*rebH-rebF*, pECXT99A-*rebH-rebF* and pEKEx3-optimRBS-*rebH-rebF*. These plasmids were used for transformation of *C. glutamicum* strains. For construction of the expression plasmid the genes for xylose degradation *xylA* from *Xanthomonas campestris* SCC1758 and *xylB* from *C. glutamicum* ATCC 13032 were amplified using the plasmid pEKEx3-$xylA_{Xc}$-$xylB_{Cg}$ (Meiswinkel et al., 2013) with the primers pECXT99A-*xylAB*-fwd (CATGGAATTCGAGCTCGGTACCCGGGGAAAGGAGGCCCTTCAGATGAGCAAC ACCGTTTTCATC) and pECXT99A-*xylAB*-rv (GCCTGCAGGTCGACTCTAGAGGATCCTAGTACCAACCCTGCGTTGC); pECXT99A-*xylAB*-fwd carries the RBS sequence. The vector pECXT99A was incubated with *Bam*HI for restriction and incubated with the PCR product in a Gibson assembly for plasmid construction. The constructed plasmid was used to transform *C. glutamicum* strains. For glucosamine degradation *nagB* from *C. glutamicum* ATCC 13032 was amplified using genomic DNA of *C. glutamicum* ATCC 13032 with the primers pECXT99A-*nagB*-fwd (CATGGAATTCGAGCTCGGTACCCGGGGAAAGGAGGCCCTTCAGATGGACATC

ATCATCTGCAAAG) and pECXT99A-*nagB*-rv (GCCTGCAGGTCGACTCTAGAGGATCCTAGCGCAGCTTTAATTGCTC); pECXT99A-*nagB*-fwd carries the RBS sequence. The vector pECXT99A was incubated with *Bam*HI for restriction and incubated with the PCR product in a Gibson assembly for plasmid construction. The constructed plasmid was used to transform *C. glutamicum* strains.

2.1.3.3 Determination of halogenase activity

Cultivation and disruption of halogenase overproducing *C. glutamicum* cells

C. glutamicum HalT1 was inoculated to 50 mL LB from an overnight culture. Expression of *rebH* and *rebF* was induced with 1 mM IPTG and the cells were grown for 24 h at 30 °C before the cells were spun down and stored at -20 °C. To disrupt the cells the pellet was resuspended in 2 mL 100 mM Na_2HPO_4, 300 mM NaCl, pH 7.4 (in case of RebF in 10 mM Na_2HPO_4 pH 7.4 buffer) and sonicated for 9 min 55% amplitude and 0.5 cycles on ice in the UP200S Ultrasonic Processor from Hielsche Ultrasound Technology. The supernatant after centrifugation was used as crude extract for the enzymatic assay.

Determination of the specific activity of RebH

The measurements were done in triplicates. The reaction mixture had a final volume of 0.5 mL and contained 5 mM Trp, 1 U mL^{-1} ADH from *Rhodococcus* sp. (s. below), 2.5 U mL^{-1} PrnF from *P. fluorescens* (s. below), 0.01 mM FAD, 1 mM NAD, 5% isopropanol, 0.005 mM PMSF, 5 mM Na_2HPO_4, 15 mM NaCl and 250 µL of crude extract. It was incubated at 30 °C for 10 min. The reaction was stopped with 187.5 µL methanol. The supernatant was analyzed by HPLC. Product formation was calculated based on the peak area in comparison to a calibration curve of 7-Cl-Trp. Since we and Frese et *al.*2014 observed difficulties in purification of RebF, we used the easily obtainable PrnF for this in vitro assay.

Cultivation of *P. putida* KT2440(pCIBhis-*prnF*) and *E. coli* BL21(DE3) (pET21-ADH)

For the overproduction of PrnF from *P. fluorescens*, *P. putida* KT2440 was transformed with pCIBhis-*prnF*. For the expression, 500 mL LB were inoculated with 5 mL of the *P. putida*

KT2440(pCIBhis-*prnF*) overnight culture. The main culture was cultivated for 1 day at 30 °C with 50 µg mL^{-1} tetracycline. Then the cells were spun down and stored at -20 °C. For overexpression of the alcohol dehydrogenase (ADH), pET21-ADH was transformed in BL21(DE3). After inoculated from an overnight culture to an OD 0.1, the cells were cultivated at 37 °C to an OD of 0.6 before the temperature was lowered to 21 °C and the expression was induced with 0.5 mM IPTG. After 4 h the cells were spun down and stored at -20 °C.

Enzyme purification

All steps during the purification were done at 4 °C. To purify the His_6-tagged PrnF, *P. putida* cells from a 500 mL LB culture were centrifuged and resuspended in TGNI5 buffer (20 mM Tris, 300 mM NaCl, 5% glycerin, 5 mM imidazole). To inhibit the protease activity 1 mM PMSF was added. The cells were disrupted by sonication (UP 200 S, Dr. Hielscher GmbH, Teltow, Germany) on ice at an amplitude of 55% and a duty cycle of 0.5 for 4 min. After centrifugation (20200 × g, 60 min, 4 °C) the supernatant was filtered and poured in Polypropylene columns 5 mL which a had bed volume of 2 mL Ni-NTA Superflow from Qiagen. The column was washed twice with TNGI5 and once with TNGI20 (20 mM Tris, 300 mM NaCl, 5% glycerin, 20 mM imidazole). The protein was eluted with TNGI buffer which contained 200 mM imidazole. The protein was analyzed using a 10% sodium dodecyl sulfate-polyacrylamide gel electrophoresis (SDS-PAGE). For the purification of the ADH, a heat precipitation method was used. The cells were resuspended in 6.6 mL, 10 mM K_2HPO_4, pH 7.4, and disrupted 4 min with 55% amplitude and 0.5 cycles on ice in the UP200S Ultrasonic Processor from Hielsche Ultrasound Technology. The crude extract was taken after centrifugation and heated up to 60 °C for 20 min. The enzyme was stored at -20 °C.

Determination of the alcohol dehydrogenase activity

The specific activity of the overexpressed alcohol dehydrogenase (crude extract) was determined in triplicates by monitoring an increase of absorption at λ = 340 nm due to the oxidation of NADH + H^+ to NAD^+ (ε =6.3 mL $mmol^{-1}$ cm^{-1}) in a final volume of 1 mL. The reaction mixture contained 910 µL of 10 mM K_2HPO_4, pH 7.4, 5% isopropanol (2-Propanol),

250 µM NAD and 20 µL of the crude extract. The cuvette was prewarmed to 30 °C with the Shimadzu UV-1800. The conversion rate of the substrate was determined by regression of the linear range.

Determination of flavin reductase activity

The cultivation and crude extract preparation are described in capture 2.3.1. The specific activities of the overexpressed flavin reductase RebF in *C. glutamicum* (crude extract) and the purified flavin reductase PrnF (see 2.3) were determined in triplicates by monitoring the decrease of absorption at λ = 340 nm due to the oxidation of NADH + H^+ to NAD^+ (ε =6.3 mL $mmol^{-1}$ cm^{-1}). The reaction mixture with a final volume of 1 mL contained 910 µL of 10 mM Na_2HPO_4 (pH 7.4 buffer), 50 µM FAD, 160 µM NADH and 20 µL of the crude extract (or the purified enzyme). The reaction mixture was prewarmed to 30 °C with the Shimadzu UV-1800. The conversion rate of the substrate was determined by regression in the linear range.

2.1.3.4 Analytical procedures

For the quantification of the extracellular and intracellular tryptophan and 7-chloro-tryptophan a high-pressure liquid chromatography (HPLC) system was used (1200 series, Agilent Technologies Deutschland GmbH, Böblingen, Germany). The supernatants of the cell culture were collected by centrifugation (20238 x g, 20 min, RT) and further used for analysis. For detection of L-tryptophan and the derivatives, samples were derivatised with *ortho*-phthaldialdehyde (OPA) (Schneider and Wendisch, 2010). The amino acid separation was performed by a precolumn (LiChrospher 100 RP18 EC-5 µ (40 mm× 4 mm), CS-Chromatographie Service GmbH, Langerwehe, Germany) and a column (Li- Chrospher 100 RP18 EC-5 µ (125 mm× 4 mm), CS Chromatographie Service GmbH). The detection was carried out with a fluorescence detector (FLD G1321A, 1200 series, Agilent Technologies) with the excitation and emission wavelengths of 230 nm and 450 nm, respectively.

2.1.3.5 Internal metabolites extraction

For the quantification of intracellular amino acids 2 mL of broth for each strain grown in minimal medium were collected at 24 h. 1 mL was centrifuged for 10 min at 13,000 rpm and 4°C. Pellets were treated with 5% $HClO_4$ in an ice bath for 20 min. After centrifuging at 13,000 rpm for 10 min and 4°C, the supernatant was neutralized with K_2CO_3 solution and centrifuged again at 13,000 rpm for 10 min and 4°C. The supernatant was then ready for amino acid quantification or to be stored at -20°C (Sun et al., 2016). The biomass concentration was determined according to the correlation CDW = 0.353 OD (Bolten et al., 2007).

2.1.4 Results and discussion

2.1.4.1 *C. glutamicum* is unable to use Trp as nitrogen and carbon sources

For the production of halogenated tryptophans it is beneficial if the production host cannot degrade the final product. As a first approach, it was tested if *C. glutamicum* can use Trp as sole nitrogen source, *C. glutamicum* WT was grown in CGXII minimal medium lacking urea and ammonium sulfate as nitrogen sources but containing 10 g L^{-1} glucose as carbon source and either 10 mM Trp or 10 mM nitrogen (urea + ammonium sulfate) as nitrogen source. While *C. glutamicum* grew with urea + ammonium sulfate as nitrogen source at a specific growth rate of 0.35 ± 0.01 h^{-1}, Trp did not serve as nitrogen for growth (Fig. 2.1.2). Second, it was tested if Trp can be used as sole carbon source, *C. glutamicum* was grown in CGXII minimal medium with either 10 mM Trp or with 10 mM glucose as sole carbon source. No growth with 10 mM Trp as carbon source was observed, whereas *C. glutamicum* grew with a specific growth rate of 0.31 ± 0.01 h^{-1} with 10 mM glucose (Fig. 2.1.2). From the experiments with Trp it was expected that 7-Cl-Trp would serve neither as a carbon nor as a nitrogen source. To test if *C. glutamicum* WT can metabolize 7-Cl-Trp, the WT was cultivated in the presence of 0.1 mM 7-Cl-Trp in CGXII containing 10 mM nitrogen (urea + ammonium sulfate) as nitrogen source and 10 mM glucose as carbon source. *C. glutamicum* WT grew to a biomass concentration of 1.18 ± 0.03 g L^{-1} with a growth rate of 0.17 ± 0.01 h^{-1}. Quantitation of 7-Cl-Trp in the medium supernatant revealed that comparable 7-Cl-Trp concentrations of 0.1 ± 0.01 mM after 0 h, 12 h and 24 h (data not shown). Thus, during growth in minimal medium *C. glutamicum* is unable to metabolize 7-Cl-Trp.

The inability of *C. glutamicum* to use Trp as sole nitrogen or carbon source is likely due to the lack of tryptophan degrading enzyme(s). *E. coli*, for example, is able to use tryptophan as sole carbon source by degrading tryptophan to indole, pyruvate and ammonia by tryptophanase (Yanofsky et al., 1991). Alternatively, tryptophan is degraded by a tryptophan oxygenase as e.g. in *Bacillus megaterium*. Tryptophan oxygenase forms *N*-formyl-L-kynurenine from Trp, which subsequently is catabolized to acetate, succinate and ammonium (Bouknight and Sadoff, 1975).

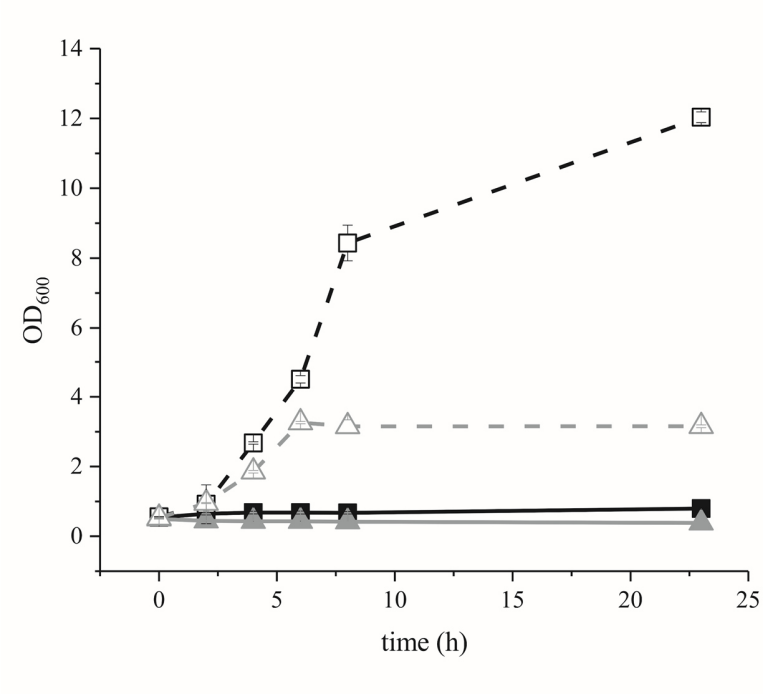

Figure 2.1.2: Growth of *C. glutamicum* WT with Trp as sole nitrogen or carbon source. To test if Trp serves as sole nitrogen source *C. glutamicum* WT was grown in nitrogen source-free CGXII minimal medium and 10 g L^{-1} glucose as carbon source supplemented with either 10 mM Trp (■) or 10 mM nitrogen (urea and ammonium sulfate) (□). To test if Trp serves as sole carbon source *C. glutamicum* WT was cultured in carbon source-free CGXII minimal medium supplemented either with 10 mM Trp (▲) or 10 mM glucose (△). Optical densities are reported as means and standard deviations of triplicate cultivations.

A reduction of the growth rate was observed when 0.1 mM 7-Cl-Trp was added to glucose minimal medium. Therefore, it was tested to what extent 7-Cl-Trp perturbs growth of *C. glutamicum* in glucose minimal medium. The presence of 0.1 mM 7-Cl-Trp reduced the maximal growth rate to 50% and in the presence of 0.5 mM 7-Cl-Trp, no significant growth was observed (data not shown). Therefore, although not metabolized, 7-Cl-Trp inhibits growth of *C. glutamicum*.

2.1.4.2 Heterologous expression of halogenase and flavin reductase genes in a Trp overproducing *C. glutamicum* strain

To enable fermentative production of 7-Cl-Trp by *C. glutamicum,* the genes encoding FAD-dependent halogenase RebH and NADH-dependent flavin reductase RebF from *Lechevalieria aerocolonigenes* were expressed in Trp overproducing strain Tp679. Since

RebH and RebF derive from the same organism and are likely co-evolved for functioning together, we chose to use RebH and RebF in our fementative approach. To confirm that both gene products were functional in the *C. glutamicum* host, crude extracts after growth in LB medium with 1 mM IPTG were assayed for halogenase and flavin reductase activities. While the specific enzyme activity of the purified halogenase RebH has been reported to be 145 mU mg^{-1} at 25 °C (turnover number of 0.29 s^{-1}) (Yeh et al., 2007), a specific enzyme activity of 0.90 ± 0.01 mU mg^{-1} (turnover number of 0.002 ± 0.0005 s^{-1}) was measured in crude extracts of *C. glutamicum*. The low activity in crude extracts (about 0.6% activity of the purified enzyme) was in accordance with protein levels observed in SDS-PAGE of these crude extracts (Supplement data Fig. 2.1.1). Similarly, the specific enzyme activity of flavin reductase RebF in crude extracts (28 ± 4 mU mg^{-1}; turnover number of 0.013 ± 0.002 s^{-1}) was about 1% of that observed for purified flavin reductase RebF (Yeh et al., 2005), which was in accordance with SDS-PAGE analysis of the crude extracts (Supplement data Fig. 2.1.1).

For the fermentative production of 7-Cl-Trp by *C. glutamicum* HalT1 which expresses *rebF* and *rebH,* glucose minimal medium CGXII was tested with different chloride salts as halogen substrates for Trp chlorination. It is known that *C. glutamicum* withstands relatively high concentrations of sodium chloride and potassium chloride (half-maximal growth rates at ~490 mM and ~480 mM, respectively) (Zahoor et al., 2014). Hence, low concentrations of chloride salts (potassium, sodium, calcium, magnesium) added to the growth medium of *C. glutamicum* were expected to have little effect on growth. In minimal medium with 50 mM NaCl *C. glutamicum* HalT1 showed a specific growth rate of 0.08 ± 0.01 h^{-1} and produced 20 ± 1 mg L^{-1} 7-Cl-Trp and 2.0 ± 0.1 g L^{-1} Trp (Fig. 2.1.3; Table 2.1.2). With 50 mM potassium chloride a specific growth rate of 0.08 ± 0.01 h^{-1} and production of 19 ± 2 mg L^{-1} 7-Cl-Trp and 2.0 ± 0.1 g L^{-1} Trp resulted (Fig. 2.1.3; Table 2.1.2). As the minimal medium CGXII contains calcium chloride and magnesium sulfate (Eggeling and Bott, 2005), the calcium chloride was raised to 25 mM and instead of magnesium sulfate 50 mM magnesium chloride, respectively, were used. With 25 mM $CaCl_2$ a growth rate of 0.17 ± 0.01 h^{-1} resulted and the strain produced 62 ± 7 mg L^{-1} 7-Cl-Trp and 2.5 ± 0.2 g L^{-1} Trp. With 25 mM $MgCl_2$ *C. glutamicum* HalT1 produced 54 ± 1 mg L^{-1} 7-Cl-Trp and 2.3 ± 0.1 g L^{-1} Trp with a specific

growth rate of 0.17 ± 0.01 h^{-1}. The negative control strain Tp679 *trpD* (pEKEx3) did not produce 7-Cl-Trp (data not shown) under these conditions. Since $CaCl_2$ resulted in the highest 7-Cl-Trp titers, the following experiments were performed with $CaCl_2$. The improved performance in the presence of calcium ions currently is not understood, but tryptophan 7-halognase was found to contain calcium in one report (Gribble, 2004).

Taken together, fermentative production of 7-Cl-Trp by recombinant *C. glutamicum* has been enabled. However, 7-Cl-Trp titers are around 50 to 100-fold lower than Trp titers produced by the same strain.

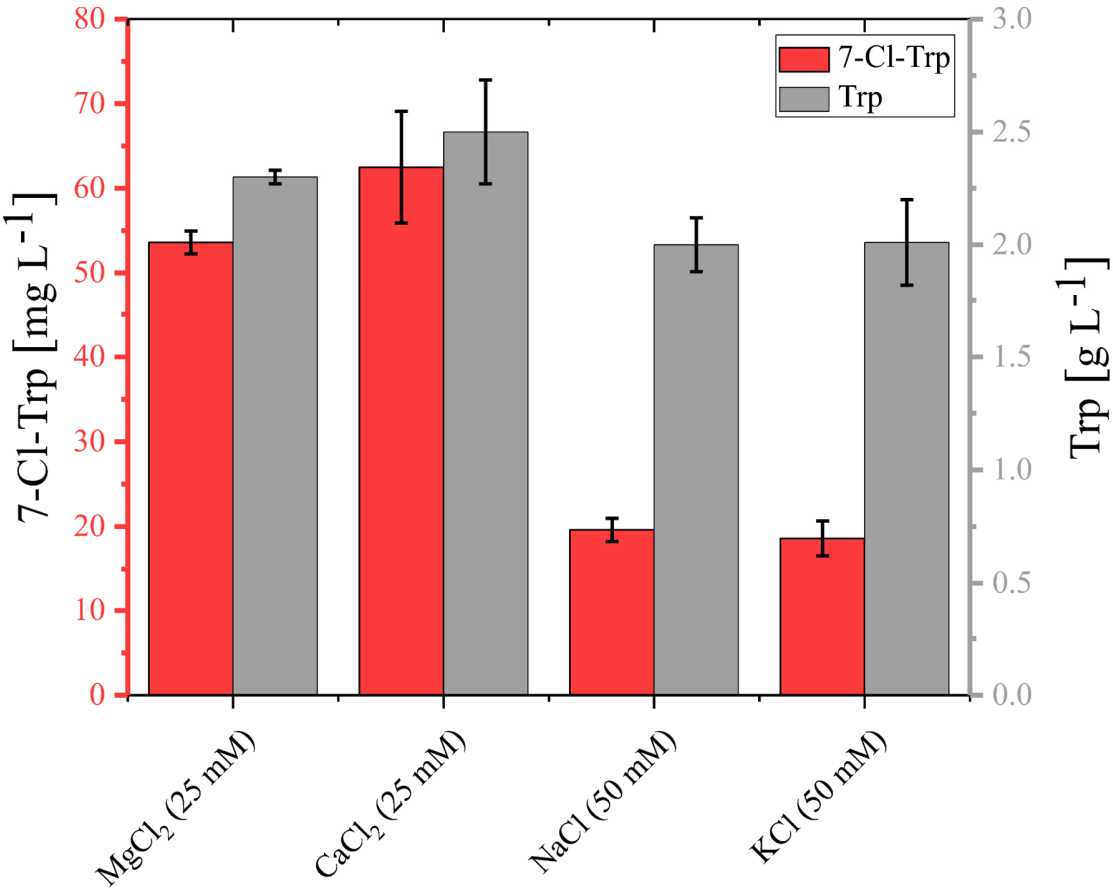

Figure 2.1.3: Influence of various chloride salts on the production of 7-Cl-Trp and Trp by *C. glutamicum* HalT1. Strain HalT1 was grown in CGXII minimal medium with 40 g L^{-1} glucose and the indicated chloride salt concentrations. Means and standard deviations of three replicate cultivations are shown

Table 2.1.1: Growth parameters, production yields and volumetric productivities of *C. glutamicum* HalT1 in the presence of different chloride salts.

Chloride salt	Specific growth rate (h^{-1})	Biomass concentration ($g\ L^{-1}$)	7-Cl-Trp Yield ($mg\ g^{-1}$)	7-Cl-Trp Volumetric productivity ($mg\ L^{-1}h^{-1}$)	Trp Yield ($g\ g^{-1}$)	Trp Volumetric productivity ($g\ L^{-1}h^{-1}$)
$MgCl_2$ (25 mM)	0.17 ± 0.00	10.9 ± 0.5	1.34 ± 0.03	0.74 ± 0.02	0.06 ± 0.00	0.03 ± 0.00
$CaCl_2$ (25 mM)	0.17 ± 0.00	7.8 ± 1.4	1.56 ± 0.16	0.87 ± 0.09	0.06 ± 0.01	0.03 ± 0.00
NaCl (50 mM)	0.08 ± 0.00	10.9 ± 0.3	0.49 ± 0.03	0.27 ± 0.02	0.05 ± 0.0	0.03 ± 0.00
KCl (50 mM)	0.08 ± 0.00	11.5 ± 1.6	0.47 ± 0.05	0.26 ± 0.03	0.05 ± 0.01	0.03 ± 0.00

Means and standard deviations obtained from triplicate shake flask cultivations in CGXII minimal medium after 72 h are given. Product yields are normalized to the glucose concentration utilized

2.1.4.3 Determination of intra- and extracellular 7-Cl-Trp and Trp concentrations during 7-Cl-Trp production by *C. glutamicum* HalT1

One possible explanation of the finding that 7-Cl-Trp titers are around 50 to 100-fold lower than Trp titers may be inefficient export of 7-Cl-Trp out of the *C. glutamicum* cell. Since the genes of *C. glutamicum* coding for export system(s) for Trp and/or 7-Cl-Trp are unknown (Marin and Krämer, 2007), genetic experiments were not possible. Under the assumption that inefficient 7-Cl-Trp export resulted in low extracellular but high intracellular 7-Cl-Trp concentrations, the intracellular Trp and 7-Cl-Trp content and the supernatant concentrations were quantified during 7-Cl-Trp production by *C. glutamicum* HalT1 (Figure 2.1.4).

C. glutamicum HalT1 was cultivated in CGXII with 4% glucose and 50 mM $CaCl_2$ and grew with a specific growth rate of 0.19 ± 0.01 h^{-1}. In the stationary phase from 24 h to 72 h the biomass concentration decreased from 13.2 ± 0.9 g L^{-1} to 7.8 ± 0.5 g L^{-1} (Fig. 2.1.4). During this time the extracellular concentration of 7-Cl-Trp increased from 15 ± 1 mg L^{-1} to 38 ± 1 mg L^{-1} (Figs. 2.1.4 and 2.1.5). The extracellular Trp concentration was 1.3 ± 0.1 g L^{-1} after 24 h and reached a plateau of about 2 g L^{-1} at 36 h to 72 h. The extracellular 7-Cl-Trp concentration increased gradually from 15 ± 1 mg L^{-1} to 38 ± 1 mg L^{-1} in the period from 24 h to 72 h (Fig. 2.1.4). At all time points assayed the extracellular Trp concentration exceeded the extracellular 7-Cl-Trp concentration. For example, at 72 h, the extracellular Trp concentration (2.1 g L^{-1} or about 10 mM) was 65-fold that of 7-Cl-Trp (38 mg L^{-1} or about 0.16 mM; Fig. 2.1.4). After 24 h no intracellular 7-Cl-Trp was detected, although extracellular 7-Cl-Trp was present in the supernatant (s. above; 15 ± 1 mg L^{-1}). At later time points, intracellular 7-Cl-Trp concentrations of 0.34 ± 0.05 mg g[CDW]$^{-1}$ to 0.46 ± 0.05 mg g[CDW]$^{-1}$ were detected (Fig. 2.1.4). During this period, intracellular Trp concentrations ranged between 14 and 19 mg g[CDW]$^{-1}$) (Fig. 2.1.4). Since the *C. glutamicum* cell volume has been determined at 2 µL mg[CDW]$^{-1}$ (Gutmann et al., 1992), intracellular concentrations of about 34 mM Trp (at 72h) and about 1 mM 7-Cl-Trp (at 72 h) were detected. Since the intracellular Trp and 7-Cl-Trp concentrations were about three and about six-fold higher than the respective extracellular concentrations, export of these compounds out of the *C. glutamicum* cell may limit production to some extent. However, as observed for the extracellular concentrations, the intracellular concentration of Trp was much larger (34 fold)

than that of 7-Cl-Trp. Thus, the major bottleneck of 7-Cl-Trp production by *C. glutamicum* is inefficient halogenation of Trp.

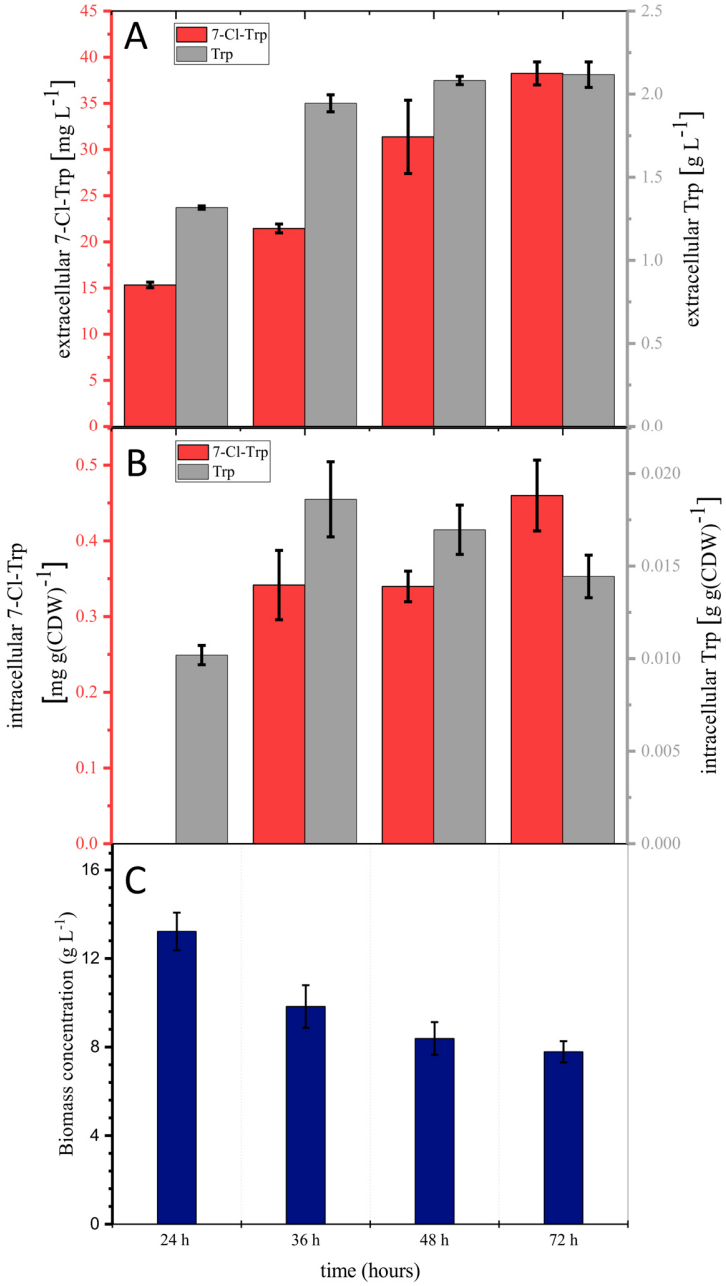

Figure 2.1.4: Extracellular (A) and intracellular (B) product concentrations and biomass concentrations (C) of *C. glutamicum* strain HalT1. Values are given as means and standard deviations of three replicate cultivations in CGXII minimal medium with 40 g L^{-1} glucose.

2.1.4.4 Provision of intracellular Trp by feeding Trp or the dipeptide Ala-Trp

It may be possible that biosynthetic precursors of Trp inhibit chlorination of Trp to 7-Cl-Trp. The biosynthetic precursors are likely present at increased intracellular concentrations in a Trp overproducing strain. Therefore, instead of using a Trp overproducing strain, the plasmid pEKEx3-*rebH-rebF* for expression of the FAD-dependent halogenase and the flavin reductase genes was used to transform *C. glutamicum* WT. To produce 7-Cl-Trp this strain was grown in CGXII 4% glucose with 50 mM $CaCl_2$, and 2 mM Trp was added to the medium. Since import of Trp occurs *via* the importer AroP (Wehrmann et al., 1995), Trp was expected to be available intracellularly for halogenation to 7-Cl-Trp, while the intracellular concentrations of its precursors are not expected to be increased. *C. glutamicum* WT(pEKEx3-*rebH-rebF*) grew with a specific growth rate of 0.15 ± 0.01 h^{-1} and produced 21 ± 1 mg L^{-1} 7-Cl-Trp after 48 h. This 7-Cl-Trp concentration (about 0.1 mM) is much lower than the Trp concentration added to the medium (2 mM).

As an alternative, Trp was provided intracellularly by feeding the dipeptide L-alanyl-L-tryptophan (Ala-Trp). Dipeptides like Ala-Trp are taken up actively into the *C. glutamicum* cell by peptide transport systems before they are hydrolyzed by peptide hydrolases (Trötschel et al., 2005). Whereas alanine is catabolized fast by *C. glutamicum* (Trötschel et al., 2005), Trp is not (s. above, Trp is neither a carbon nor a nitrogen source for growth of *C. glutamicum*). When *C. glutamicum* WT(pEKEx3-*rebH-rebF*) was cultivated in CGXII 4% glucose with 1 mM Ala-Trp and 50 mM $CaCl_2$, it grew with a specific growth rate of 0.15 ± 0.01 h^{-1} to a biomass concentration of 14.4 ± 0.5 g L^{-1} at 48 h (Figure 2.1.5). After 4 h, about 1 mM (256 ± 9 mg L^{-1}) Ala-Trp remained in the supernatant while its intracellular concentration was about 27 mM (14 ± 1 mg g[CDW]$^{-1}$). At 4 h, the intra- and extracellular Trp concentrations were 7 mM (3 ± 1 mg g[CDW]$^{-1}$) and about 0.14 mM (27 ± 2 mg L^{-1}), respectively, while 7-Cl-Trp was neither detected intracellularly nor in the supernatant (Fig. 2.1.5). As expected from the kinetics of dipeptide uptake and hydrolysis (Trötschel et al., 2005), Ala-Trp was completely utilized at 48 h since it could neither be detected intra- nor extracellularly. At 48 h, the intracellular concentrations of Trp and 7-Cl-Trp were very low (below 0.5 mM). 7-Cl-Trp was produced (34 ± 1 mg L^{-1}; 0.14 mM) and its concentration exceeded that of extracellular Trp (9 ± 1 mg L^{-1}; 0.04 mM).

Taken together, the low titers of 7-Cl-Trp that resulted upon addition of Trp or Ala-Trp do not support the notion that biosynthetic precursors of Trp inhibit its chlorination to 7-Cl-Trp.

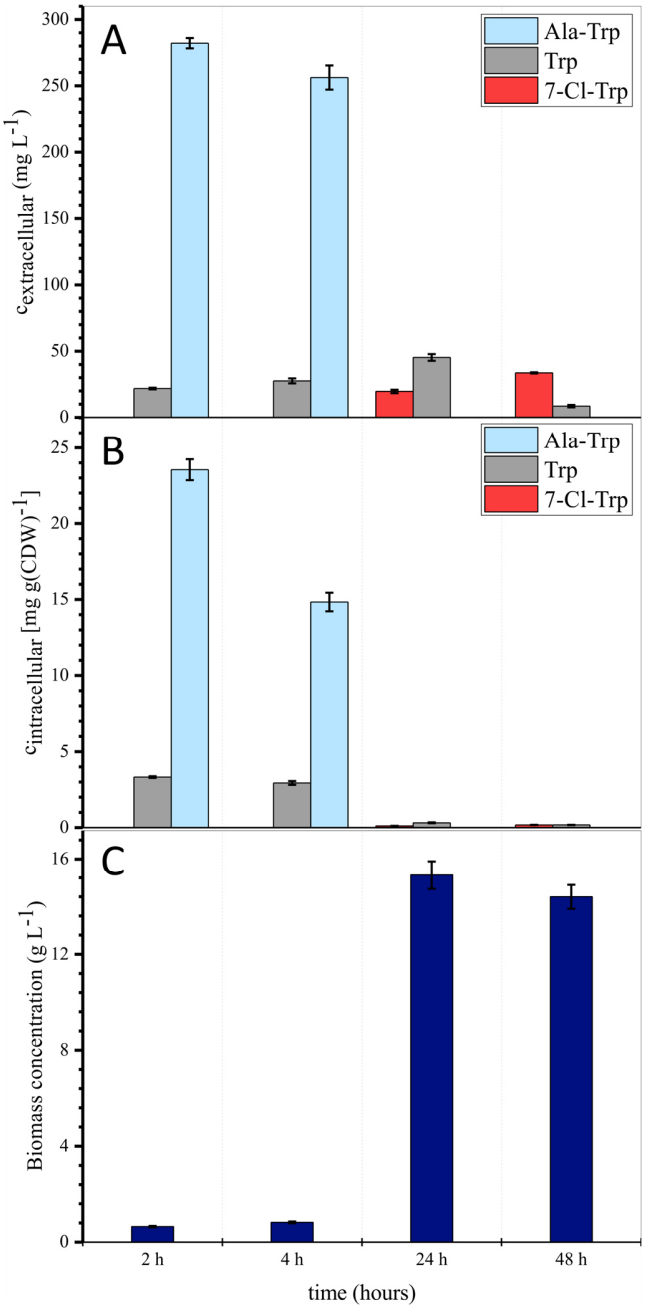

Figure 2.1.5: Extracellular (A) and intracellular (B) product concentrations and biomass concentrations (C) of *C. glutamicum* strain WT (pEKEx3-*rebH-rebF*) after growth in the presence of 1 mM Ala-Trp. Values are given as means and standard deviations of three replicate cultivations in CGXII minimal medium with 40 g L^{-1} glucose.

2.1.4.5 Optimization of the 7-Cl-Trp production

To test if expression of the halogenase and flavin reductase genes is limiting production of 7-Cl-Trp, two expression vectors differing by their origins of replication and copy numbers were compared. In addition, the influence of altering the ribosome binding site (RBS) to support a higher translation initiation rate of *rebH* was tested. The synthetic *rebH-rebF* present in pEKEx3-*rebH-rebF* was cloned into pECXT99A (Kirchner and Tauch, 2003) (Table 2.1.1). The sequence of the RBS of *rebH* was optimized using RBS calculator (https://salislab.net/software/). Based on this optimized RBS, the vectors pEKEx3-optimRBS-*rebH-rebF* and pECXT99A-optimRBS-*rebH-rebF* were constructed. Vectors pECXT99A-*rebH-rebF* and pECXT99A-optimRBS-*rebH-rebF* were used to transform Tp679 (pCES208-*trpD*). The resulting strains were HalT3 and HalT4, respectively (Table 2.1.1). The strain HalT3 was cultivated in CGXII 4% glucose and had a specific growth rate of 0.17 ± 0.004 h^{-1}. HalT3 produced 42 ± 2 mg L^{-1} 7-Cl-Trp and 2.3 ± 0.2 g L^{-1} Trp (Fig. 2.1.6). This was similar to HalT1 which produced 57 ± 1 mg L^{-1} 7-Cl-Trp and 2.2 ± 0.1 g L^{-1} Trp with a specific growth rate of 0.11 ± 0.01 h^{-1}.

A second option to improve the production of 7-Cl-Trp was to optimize the RBS. The genes *rebH* and *rebF* were cloned with the optimized RBS in the pECXT99A vector and transformed Tp679 (pCES208-*trpD*). The build strain HalT4 was grown in CGXII with 4% glucose and 50 mM $CaCl_2$. The specific growth rate was 0.16 ± 0.006 h^{-1}, and 66 ± 1 mg L^{-1} 7-Cl-Trp and 2.3 ± 0.02 g L^{-1} Trp were accumulated. An increase of 7-Cl-Trp production by 56% could be observed between HalT3 and HalT4 which arrived from the optimized RBS. Thus, the RBS in combination with the pEKEx3 vector (Stansen et al., 2005), which is the expression vector of HalT1, was optimized as well. The plasmid pEKEx3-optimRBS-*rebH-rebF* was transformed in Tp679 (pCES208-*trpD*). The resulting strain HalT2 was cultivated in CGXII with 4% glucose and 50 mM $CaCl_2$. HalT2 reached a specific growth rate of 0.11 ± 0.004 h^{-1} and a production of 108 ± 2 mg L^{-1} 7-Cl-Trp and 1.1 ± 0.1 g L^{-1} Trp was measured (Fig. 2.1.6). Hence, there is an improvement in production of 7-Cl-Trp of 56% from HalT1 to HalT2. The production of Trp decreased by 48% from HalT1 to HalT2. But 1.7 ± 0.1 g L^{-1} of the precursor anthranilate (Ant) were detected in HalT2. This can be caused through an inhibitory effect of halogenated compounds on *trpD* (Fig. 2.1.1). It is known that

halogenated Ant is a competitive inhibitor of PqsA, the initial enzyme of 4-hydroxy-2-alkylquinolines biosynthesis in *Pseudomonas aeruginosa*, and that halogenated Ant competitively inhibits Ant converting TrpD (Lesic et al., 2007). Until now, it is not known if 7-Cl-Trp inhibits Trp or other enzymes of the Trp pathway in *C. glutamicum*. The intracellular concentration of the cofactor FAD may be limiting although the intracellular concentrations of FAD or FMN are about 4.5 mM OD_{610}^{-1} or about 2 mM OD_{610}^{-1}, respectively (Toyoda et al., 2014). The addition of 2 mM FMN to the cultivation medium improved 7-Cl-Trp production by about two fold (62 ± 7 mg L^{-1} 7-Cl-Trp for HalT1 with 50 mM $CaCl_2$, 4% glucose without added FMN as compared to 130 ± 1 mg L^{-1} 7-Cl-Trp when 2 mM FMN were added, Fig. 2.1.3 and data not shown). However, the addition of FMN is too costly for fermentative production. Our results clearly show that despite sufficient provision of Trp by the recombinant *C. glutamicum* strains, halogenation proceeds to much lower concentrations as compared to Trp production (Fig. 2.1.3 and 2.1.4). Likewise, classical biocatalytic halogenation stops at a distinct conversion (Schnepel and Sewald, 2017). For example, Frese et *al*. 2014 as well as Payne et *al*.2013 converted Trp at concentrations of only 0.5 mM, which led to almost complete conversion. Up-scaling required to increase the volume while maintaining the low substrate concentration, e.g. Payne et *al*. 2013 converted 100 mg Trp in a volume of 12 L (Payne et al., 2013). Although operated at the gram scale, bromination of Trp using CLEAs also had to be operated at a low concentration (i.e. 1g Trp in 5 L; (Frese and Sewald, 2015)). Possible limitations may be product inhibition of the halogenase, insufficient supply of oxygen and/or redox cofactors. Thus, chlorination of Trp in solution using purified enzymes or preparations such as CLEAs currently is restricted to conversion of few milligrams of substrate (Frese and Sewald, 2015). Fermentation as described here may similarly be limited by product inhibition of the halogenase enzyme, thus, enzyme engineering to overcome such limitation would benefit both biocatalytic and fermentative process. The expression of *rebH* and *rebF* of the strains HalT1 to HalT4 was shown by SDS-PAGE (Supplement Fig. 2.1.1). Strain HalT2, which accumulated the highest concentration of 7-Cl-Trp, showed the highest expression of the *rebH* gene. Thus, future strain development may target further *rebH* overexpression. It may also be important to balance the concentrations of the involved enzymes RebH and RebF.

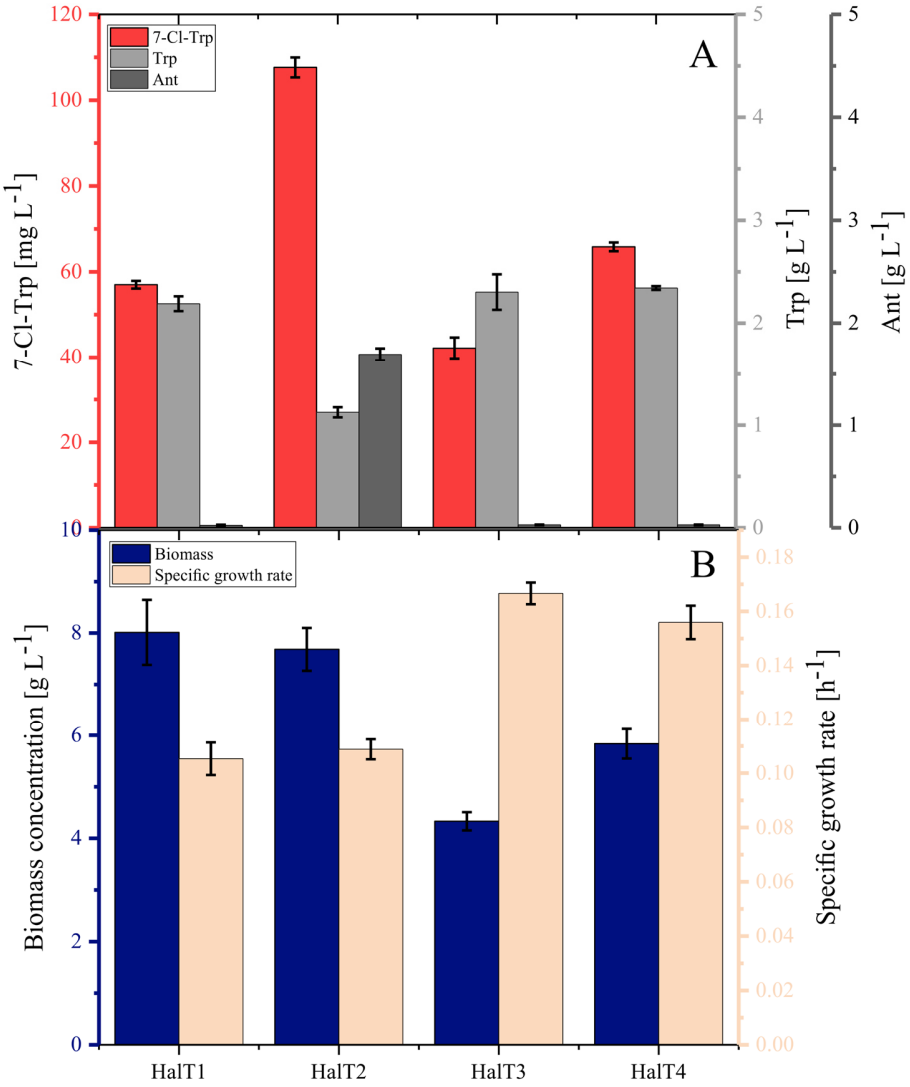

Figure 2.1.6: Product titers and growth parameters of various *C. glutamicum* strains. The *C. glutamicum* strains HalT1, HalT2, HalT3 and HalT4 were grown in CGXII with 4% glucose, 50 mM $CaCl_2$ and were induced with 1 mM IPTG. Means and standard deviations of triplicate cultivations are given for titers of 7-Cl-Trp, Trp, and anthranilate (Ant) (A) and for biomass concentrations and specific growth rates (B).

This may be done e.g. by varying translation initiation rates by changing the sequence and/or position of the ribosome binding sites (Henke et al., 2016). Alternatively, fusion proteins of RebH and RebF may show better performance as shown for (Payne et al., 2013). Higher FAD concentrations within the cell may be reached by deletion of *rshA* as shown by Toyoda et al. 20000 or be overexpression of *ribF* (Taniguchi and Wendisch, 2015). Redox cofactor recycling may be improved by oxygen-deprivation conditions as shown for L-alanine

production by recombinant *C. glutamicum* (Jojima et al., 2010). It may be important to identify the export system for 7-Cl-Trp export. In the case of fermentative L-lysine production, the L-lysine export gene *lysE* was overexpressed in L-lysine producing strains (Unthan et al., 2015). Unfortunately, currently the Trp export system of *C. glutamicum* is unknown (it may also be relevant in 7-Cl-Trp export) (Pérez-García and Wendisch, 2018). Trp transport engineering, however, successfully improved Trp production when the Trp uptake system was deleted (Pérez-García and Wendisch, 2018). Assuming that this system imports 7-Cl-Trp into the *C. glutamicum* cell, deletion of its gene may also be relevant for improved 7-Cl-Trp producing strains.

2.1.4.6 7-Chloro-tryptophan production from alternative carbon sources

Glucose is the preferred carbon and energy source of *C. glutamicum* and a proof-of-concept for glucose-based 7-Cl-Trp production was reached. However, feedstocks that do not have competing uses in human and animal nutrition are preferred for large-scale fermentations. Metabolic engineering strategies for access of *C. glutamicum* to the alternative carbon sources arabinose, xylose and glucosamine have been developed and applied to amino acid production (Sasaki et al., 2011; Schneider et al., 2011; Meiswinkel et al., 2013; Uhde et al., 2013). For access to arabinose *C. glutamicum* HalT1 was transformed with pECXT99A-*araBAD* containing the heterologous operon *araBAD* from *E. coli* for arabinose catabolism (Sasaki et al., 2011; Schneider et al., 2011). The resulting strain grew with a growth rate of 0.08 h^{-1} and produced 52 ± 1 mg L^{-1} 7-Cl-Trp and 2.4 ± 0.1 g L^{-1} Trp (Fig. 2.1.7; Table 2.1.3). Efficient xylose utilization by *C. glutamicum* required heterologous expression of the xylose isomerase XylA gene from *Xanthomonas campestris* and overexpression of the endogenous gene coding for xylulokinase XylB (Meiswinkel et al., 2013). *C. glutamicum* HalT1 (pECXT99A-*xylAB*) showed a specific growth rate of 0.07 ± 0.01 h^{-1} in minimal medium with 40 g L^{-1} Xylose and produced 34 ± 2 mg L^{-1} 7-Cl-Trp and 2.3 ± 0.1 g L^{-1} Trp (Fig. 2.1.7; Table 2.1.3). Glucosamine, a constituent of chitin and one of the most abundant amino sugars in soil, is a poor growth substrate for *C. glutamicum* (Uhde et al., 2013). For efficient glucosamine utilization the endogenous glucosamine-6-phosphate deaminase gene *nagB* was overexpressed (Uhde et al., 2013).

C. glutamicum HalT1 (pECXT99A-*nagB*) grew in CGXII with 40 g L^{-1} glucosamine with a specific growth rate of 0.11 h^{-1} and produced 51 ± 3 mg L^{-1} 7-Cl-Trp and 1.5 ± 0.1 g L^{-1} Trp. For comparison, *C. glutamicum* HalT1 grew in CGXII medium with 40 g L^{-1} glucose with a specific growth rate of 0.13 h^{-1} and produced 56 ± 5 mg L^{-1} 7-Cl-Trp and 2.2 ± 0.1 g L^{-1} Trp (Fig. 2.1.7, Table 2.1.3). Taken together, 7-Cl-Trp production has been shown using glucose as well as the alternative feedstocks glucosamine, arabinose and xylose as growth substrates for the *C. glutamicum* host.

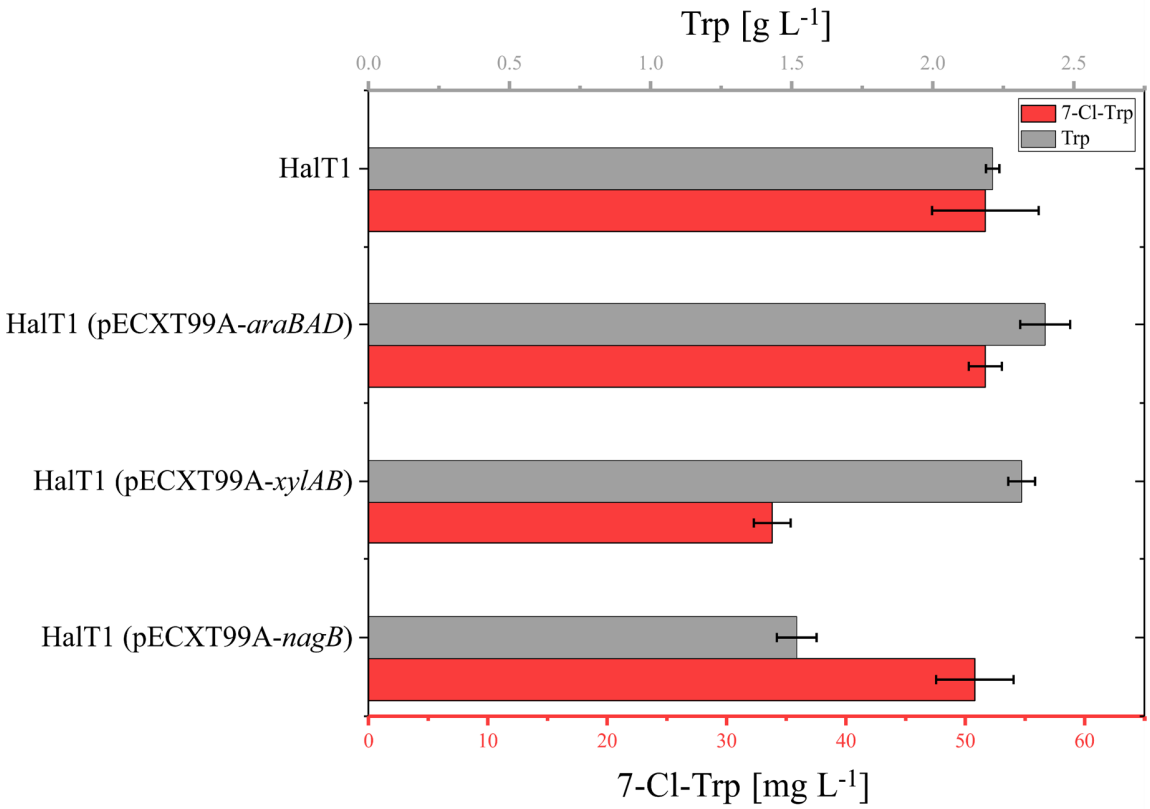

Figure 2.1.7: Production of 7-Cl-Trp and Trp by *C. glutamicum* HalT1 and derived strains with different carbon sources. For HalT1 40 g L^{-1} glucose were used as sole carbon source, 40 g L^{-1} arabinose for HalT1 (pECXT99A-*araBAD*), 40 g L^{-1} Xylose for HalT1 (pECXT99A-*xylAB*) and 40 g L^{-1} glucosamine for HalT1 (pECXT99A-*nagB*). Means and standard deviations of three replicate cultivations are given.

Table 2.1.3: Growth parameters, production yields and volumetric productivities of *C. glutamicum* HalT1 and derived strains with different carbon sources.

Strain	Carbon source	Specific growth rate (h^{-1})	Biomass concentration ($g\ L^{-1}$)	7-Cl-Trp yield ($mg\ g^{-1}$)	7-Cl-Trp volumetric productivity ($mg\ L^{-1}h^{-1}$)	Trp yield ($g\ g^{-1}$)	Trp volumetric productivity ($g\ L^{-1}h^{-1}$)
HalT1	Glucose	0.13 ± 0.00	7.5 ± 0.5	1.41 ± 0.11	0.47 ± 0.04	0.05 ± 0.00	0.02 ± 0.00
HalT1 (pECXT99A-*araBAD*)	Arabinose	0.07 ± 0.01	0.9 ± 0.6	1.30 ± 0.03	0.43 ± 0.01	0.06 ± 0.00	0.02 ± 0.00
HalT1 (pECXT99A-*xylAB*)	Xylose	0.07 ± 0.01	8.8 ± 0.6	0.85 ± 0.04	0.28 ± 0.01	0.06 ± 0.00	0.02 ± 0.00
HalT1 (pECXT99A-nagB)	Glucosamine	0.11 ± 0.00	5.4 ± 0.6	1.27 ± 0.08	0.42 ± 0.03	0.04 ± 0.00	0.01 ± 0.00

Means and standard deviations obtained from triplicate shake flask cultivations in CGXII minimal medium with 40 $g\ L^{-1}$ carbon source after 120 h are given. Product yields are normalized to the carbon source concentration utilized.

2.1.5 Conclusion

Fermentative production of the halogenated amino acid 7-Cl-Trp from sugars, ammonium and chloride salts was enabled by recombinant *C. glutamicum* expressing the genes coding for FAD-dependent halogenase RebH and NADH-dependent flavin reductase RebF from *L. aerocolonigenes*. Chlorination of Trp to 7-Cl-Trp by *C. glutamicum* was improved by optimizing the RBS of *rebH.* Production of 7-Cl-Trp was limited by inhibition of 7-Cl-Trp and the chlorination efficiency. Strains able to produce 7-Cl-Trp and Trp from the alternative carbon sources arabinose, glucosamine and xylose were constructed.

2.1.6 References

Bagdasarian, M., Lurz, R., Rückert, B., Franklin, F.C.H., Bagdasarian, M.M., Frey, J., et al. (1981). Specific-purpose plasmid cloning vectors II. Broad host range, high copy number, RSF 1010-derived vectors, and a host-vector system for gene cloning in *Pseudomonas*. Gene 16**,** 237-247.

Bolten, C.J., Kiefer, P., Letisse, F., Portais, J.-C., and Wittmann, C. (2007). Sampling for Metabolome Analysis of Microorganisms. Anal. Chem. 79**,** 3843-3849. doi:10.1021/ac0623888.

Bouknight, R.R., and Sadoff, H.L. (1975). Tryptophan catabolism in *Bacillus megaterium*. J. Bacteriol. 121**,** 70-76.

Diederich, F., and Stang, P.J. (2008). Metal-Catalyzed Cross-Coupling Reactions. Wiley. doi:DOI:10.1002/9783527619535.

Eggeling, L., and Bott, M. (2005). Handbook of *Corynebacterium glutamicum.* CRC press.

Eggeling, L., and Bott, M. (2015). A giant market and a powerful metabolism: L-lysine provided by *Corynebacterium glutamicum*. Appl. Microbiol. Biotechnol. 99**,** 3387-3394. doi:10.1007/s00253-015-6508-2.

Frese, M., Guzowska, P.H., Voss, H., and Sewald, N. (2014). Regioselective Enzymatic Halogenation of Substituted Tryptophan Derivatives using the FAD-Dependent Halogenase RebH. ChemCatChem. 6**,** 1270-1276. doi:10.1002/cctc.201301090.

Frese, M., and Sewald, N. (2015). Enzymatic Halogenation of Tryptophan on a Gram Scale. Angew. Chem. Int. Ed. 54**,** 298-301. doi:10.1002/anie.201408561.

Gibson, D.G., Young, L., Chuang, R.-Y., Venter, J.C., Hutchison Iii, C.A., and Smith, H.O. (2009). Enzymatic assembly of DNA molecules up to several hundred kilobases. Nat. Methods 6**,** 343. doi:10.1038/nmeth.1318.

Gribble, G.W. (2004). Natural production of organohalogen compounds. Springer.

Gutmann, M., Hoischen, C., and Krämer, R. (1992). Carrier-mediated glutamate secretion by *Corynebacterium glutamicum* under biotin limitation. Biochim. Biophys. Acta (BBA)-Biomembranes 1112**,** 115-123. doi:10.1016/0005-2736(92)90261-J.

Hammer, P.E., Hill, D.S., Lam, S.T., Van Pée, K.-H., and Ligon, J.M. (1997). Four genes from *Pseudomonas fluorescens* that encode the biosynthesis of pyrrolnitrin. Appl. Environ. Microbiol. 63**,** 2147-2154.

Hanahan, D. (1983). Studies on transformation of *Escherichia coli* with plasmids. J. Mol. Biol. 166**,** 557-580. doi:10.1016/S0022-2836(83)80284-8.

Heider, S.A.E., Peters-Wendisch, P., Wendisch, V.F., Beekwilder, J., and Brautaset, T. (2014). Metabolic engineering for the microbial production of carotenoids and related products with a focus on the rare C50 carotenoids. Appl. Microbiol. Biotechnol. 98**,** 4355-4368. doi:10.1007/s00253-014-5693-8.

Henke, N.A., Heider, S.A.E., Peters-Wendisch, P., and Wendisch, V.F. (2016). Production of the marine carotenoid astaxanthin by metabolically engineered *Corynebacterium glutamicum*. Mar. Drugs 14**,** 124. doi:10.3390/md14070124.

Henke, N.A., Wichmann, J., Baier, T., Frohwitter, J., Lauersen, K.J., Risse, J.M., et al. (2018). Patchoulol production with metabolically engineered *Corynebacterium glutamicum*. Genes 9**,** 219. doi:10.3390/genes9040219.

Hermann, T. (2003). Industrial production of amino acids by coryneform bacteria. J. Biotechnol. 104**,** 155-172. doi:10.1016/S0168-1656(03)00149-4.

Inui, M., Kawaguchi, H., Murakami, S., Vertès, A.A., and Yukawa, H. (2004). Metabolic engineering of *Corynebacterium glutamicum* for fuel ethanol production under oxygen-deprivation conditions. J. Mol. Microbiol. Biotechnol. 8**,** 243-254. doi:10.1159/000086705.

Jojima, T., Fujii, M., Mori, E., Inui, M., and Yukawa, H. (2010). Engineering of sugar metabolism of *Corynebacterium glutamicum* for production of amino acid L-alanine under oxygen deprivation. Appl. Microbiol. Biotechnol. 87**,** 159-165. doi:10.1007/s00253-010-2493-7.

Jojima, T., Noburyu, R., Sasaki, M., Tajima, T., Suda, M., Yukawa, H., et al. (2015). Metabolic engineering for improved production of ethanol by *Corynebacterium glutamicum*. Appl. Microbiol. Biotechnol. 99**,** 1165-1172. doi:10.1007/s00253-014-6223-4.

Jorge, J.M.P., Leggewie, C., and Wendisch, V.F. (2016). A new metabolic route for the production of gamma-aminobutyric acid by *Corynebacterium glutamicum* from glucose. Amino acids. 48**,** 2519-2531. doi:10.1007/s00726-016-2272-6.

Jorge, J.M.P., Nguyen, A.Q.D., Pérez-García, F., Kind, S., and Wendisch, V.F. (2017). Improved fermentative production of gamma-aminobutyric acid via the putrescine route: Systems metabolic engineering for production from glucose, amino sugars, and xylose. Biotechnol. Bioeng. 114**,** 862-873. doi:10.1002/bit.26211.

Kim, J.Y., Lee, Y.A., Wittmann, C., and Park, J.B. (2013). Production of non-proteinogenic amino acids from α-keto acid precursors with recombinant *Corynebacterium glutamicum*. Biotechnol. Bioeng. 110**,** 2846-2855. doi:10.1002/bit.24962.

Kirchner, O., and Tauch, A. (2003). Tools for genetic engineering in the amino acid-producing bacterium *Corynebacterium glutamicum*. J. Biotechnol. 104**,** 287-299. doi:10.1016/S0168-1656(03)00148-2.

Lee, J.-H., and Wendisch, V.F. (2017). Biotechnological production of aromatic compounds of the extended shikimate pathway from renewable biomass. J. Biotechnol. 257**,** 211-221. doi:10.1016/j.jbiotec.2016.11.016.

Lee, J.-Y., Na, Y.-A., Kim, E., Lee, H.-S., and Kim, P. (2016). The actinobacterium *Corynebacterium glutamicum*, an industrial workhorse. J. Microbiol. Biotechnol. 26**,** 807-822. doi:10.4014/jmb.1601.01053.

Lesic, B., Lépine, F., Déziel, E., Zhang, J., Zhang, Q., Padfield, K., et al. (2007). Inhibitors of pathogen intercellular signals as selective anti-infective compounds. PLoS Pathog. 3**,** e126. doi:10.1371/journal.ppat.0030126.

Marin, K., and Krämer, R. (2007). Amino acid transport systems in biotechnologically relevant bacteria, in Amino acid biosynthesis pathways, regulation and metabolic engineering. Springer. 289-325.

Meiswinkel, T.M., Gopinath, V., Lindner, S.N., Nampoothiri, K.M., and Wendisch, V.F. (2013). Accelerated pentose utilization by *Corynebacterium glutamicum* for accelerated production of lysine, glutamate, ornithine and putrescine. Microb. Biotechnol. 6**,** 131-140. doi:10.1111/1751-7915.12001.

Mindt, M., Risse, J.M., Gruß, H., Sewald, N., Eikmanns, B.J., and Wendisch, V.F. (2018). One-step process for production of *N*-methylated amino acids from sugars and methylamine using recombinant *Corynebacterium glutamicum* as biocatalyst. Sci. Rep. 8**,** 12895. doi:10.1038/s41598-018-31309-5.

Nelson, K.E., Weinel, C., Paulsen, I.T., Dodson, R.J., Hilbert, H., dos Santos, V.A.P.M., et al. (2002). Complete genome sequence and comparative analysis of the metabolically versatile *Pseudomonas putida* KT2440. Environ. Microbiol. 4**,** 799-808. doi:10.1046/j.1462-2920.2002.00366.x.

Nishizawa, T., Aldrich, C.C., and Sherman, D.H. (2005). Molecular analysis of the rebeccamycin L-amino acid oxidase from *Lechevalieria aerocolonigenes* ATCC 39243. J. Bacteriol. 187**,** 2084-2092. doi:10.1128/JB.187.6.2084-2092.2005.

Onaka, H., Taniguchi, S.-i., Igarashi, Y., and Furumai, T. (2003). Characterization of the biosynthetic gene cluster of rebeccamycin from *Lechevalieria aerocolonigenes* ATCC 39243. Biosci. Biotechnol. Biochem. 67**,** 127-138. doi:10.1271/bbb.67.127.

Park, J.-U., Jo, J.-H., Kim, Y.-J., Chung, S.-S., Lee, J.-H., and Lee, H.H. (2008). Construction of heat-inducible expression vector of *Corynebacterium glutamicum* and *C. ammoniagenes*: fusion of lambda operator with promoters isolated from *C. ammoniagenes*. J. Microbiol. Biotechnol. 18**,** 639-647.

Payne, J.T., Andorfer, M.C., and Lewis, J.C. (2013). Regioselective Arene Halogenation using the FAD-Dependent Halogenase RebH. Angew. Chem. 125**,** 5379-5382. doi:10.1002/anie.201300762.

Pérez-García, F., Peters-Wendisch, P., and Wendisch, V.F. (2016). Engineering *Corynebacterium glutamicum* for fast production of L-lysine and L-pipecolic acid. Appl. Microbiol. Biotechnol. 100**,** 8075-8090. doi:10.1007/s00253-016-7682-6.

Pérez-García, F., and Wendisch, V.F. (2018). Transport and metabolic engineering of the cell factory *Corynebacterium glutamicum*. FEMS Microbiol. Lett. 365**,** fny166. doi:10.1093/femsle/fny166.

Purwanto, H.S., Kang, M.-S., Ferrer, L., Han, S.-S., Lee, J.-Y., Kim, H.-S., et al. (2018). Rational engineering of the shikimate and related pathways in *Corynebacterium glutamicum* for 4-hydroxybenzoate production. J. Biotechnol. doi:10.1016/j.jbiotec.2018.07.016.

Sambrook, Joseph, Fritsch, E. F. (Edward F.), Maniatis, Tom, et al. (1989). Molecular cloning : a laboratory manual. New York : Cold Spring Harbor Laboratory Press 2nd ed.

Sasaki, M., Teramoto, H., Inui, M., and Yukawa, H. (2011). Identification of mannose uptake and catabolism genes in *Corynebacterium glutamicum* and genetic engineering for simultaneous utilization of mannose and glucose. Appl. Microbiol. Biotechnol. 89**,** 1905-1916. doi:10.1007/s00253-010-3002-8.

Schneider, J., Niermann, K., and Wendisch, V.F. (2011). Production of the amino acids L-glutamate, L-lysine, L-ornithine and L-arginine from arabinose by recombinant *Corynebacterium glutamicum*. J. Biotechnol. 154**,** 191-198. doi:10.1016/j.jbiotec.2010.07.009.

Schneider, J., and Wendisch, V.F. (2010). Putrescine production by engineered *Corynebacterium glutamicum*. Appl. Microbiol. Biotechnol. 88**,** 859-868. doi:10.1007/s00253-010-2778-x.

Schnepel, C., and Sewald, N. (2017). Enzymatic Halogenation: A Timely Strategy for Regioselective C− H Activation. Chem. Eur. J. 23**,** 12064-12086. doi:10.1002/chem.201701209

Siebert, D., and Wendisch, V.F. (2015). Metabolic pathway engineering for production of 1, 2-propanediol and 1-propanol by *Corynebacterium glutamicum*. Biotechnol. Biofuels 8**,** 91. doi:10.1186/s13068-015-0269-0.

Stansen, C., Uy, D., Delaunay, S., Eggeling, L., Goergen, J.-L., and Wendisch, V.F. (2005). Characterization of a *Corynebacterium glutamicum* lactate utilization operon induced during temperature-triggered glutamate production. Appl. Environ. Microbiol. 71**,** 5920-5928. doi:10.1128/AEM.71.10.5920-5928.2005.

Sun, Y., Guo, W., Wang, F., Peng, F., Yang, Y., Dai, X., et al. (2016). Transcriptome and multivariable data analysis of *Corynebacterium glutamicum* under different dissolved oxygen conditions in bioreactors. PloS One 11**,** e0167156. doi:10.1371/journal.pone.0167156.

Taniguchi, H., and Wendisch, V.F. (2015). Exploring the role of sigma factor gene expression on production by *Corynebacterium glutamicum*: sigma factor H and FMN as example. Front. Microbiol. 6**,** 740. doi:10.3389/fmicb.2015.00740.

Toyoda, K., Teramoto, H., Yukawa, H., and Inui, M. (2014). Expanding the Regulatory Network Governed by the ECF-family Sigma factor σ^H in *Corynebacterium glutamicum*. J. Bacteriol.**,** JB-02248. doi:10.1128/JB.02248-14.

Trötschel, C., Deutenberg, D., Bathe, B., Burkovski, A., and Krämer, R. (2005). Characterization of methionine export in *Corynebacterium glutamicum*. J. Bacteriol. 187**,** 3786-3794. doi:10.1128/JB.187.11.3786-3794.2005.

Uhde, A., Youn, J.-W., Maeda, T., Clermont, L., Matano, C., Krämer, R., et al. (2013). Glucosamine as carbon source for amino acid-producing *Corynebacterium glutamicum*. Appl. Microbiol. Biotechnol. 97**,** 1679-1687. doi:10.1007/s00253-012-4313-8.

Unthan, S., Baumgart, M., Radek, A., Herbst, M., Siebert, D., Brühl, N., et al. (2015). Chassis organism from *Corynebacterium glutamicum*–a top-down approach to identify and delete irrelevant gene clusters. Biotechnol. J. 10**,** 290-301. doi:10.1002/biot.201400041.

van Pée, K.-H., and Hölzer, M. (1999). Specific enzymatic chlorination of tryptophan and tryptophan derivatives, in Tryptophan, Serotonin, and Melatonin. Springer. 603-609.

Wehrmann, A., Morakkabati, S., Krämer, R., Sahm, H., and Eggeling, L. (1995). Functional analysis of sequences adjacent to *dapE* of *Corynebacterium glutamicum* reveals the presence of *aroP*, which encodes the aromatic amino acid transporter. J. Bacteriol. 177**,** 5991-5993.

Wendisch, V.F. (2016). Microbial production of amino acid-related compounds, in Amino Acid Fermentation. Springer. 255-269.

Wendisch, V.F., Jorge, J.M.P., Pérez-García, F., and Sgobba, E. (2016). Updates on industrial production of amino acids using *Corynebacterium glutamicum*. World J. Microbiol. Biotechnol. 32**,** 1-10. doi:10.1007/s11274-016-2060-1.

Wendisch, V.F., Mindt, M., and Pérez-García, F. (2018). Biotechnological production of mono- and diamines using bacteria: recent progress, applications, and perspectives. Appl. Microbiol. Biotechnol. 102**,** 3583-3594. doi:10.1007/s00253-018-8890-z.

Wieschalka, S., Blombach, B., Bott, M., and Eikmanns, B.J. (2013). Bio-based production of organic acids with *Corynebacterium glutamicum*. Microb. Biotechnol. 6**,** 87-102. doi:10.1111/1751-7915.12013.

Yanofsky, C., Horn, V., and Gollnick, P. (1991). Physiological studies of tryptophan transport and tryptophanase operon induction in *Escherichia coli*. J. Bacteriol. 173**,** 6009-6017.

Yeh, E., Blasiak, L.C., Koglin, A., Drennan, C.L., and Walsh, C.T. (2007). Chlorination by a Long-Lived Intermediate in the Mechanism of Flavin-Dependent Halogenases. Biochem. 46**,** 1284-1292. doi:10.1021/bi0621213.

Yeh, E., Garneau, S., and Walsh, C.T. (2005). Robust in vitro activity of RebF and RebH, a two-component reductase/halogenase, generating 7-chlorotryptophan during

rebeccamycin biosynthesis. Proc. Natl. Acad. Sci. U. S. A. 102**,** 3960-3965. doi:10.1073/pnas.0500755102.

Zahoor, A., Otten, A., and Wendisch, V.F. (2014). Metabolic engineering of *Corynebacterium glutamicum* for glycolate production. J. Biotechnol. 192**,** 366-375. doi:10.1016/j.jbiotec.2013.12.020.

2.1.7 Supplement data

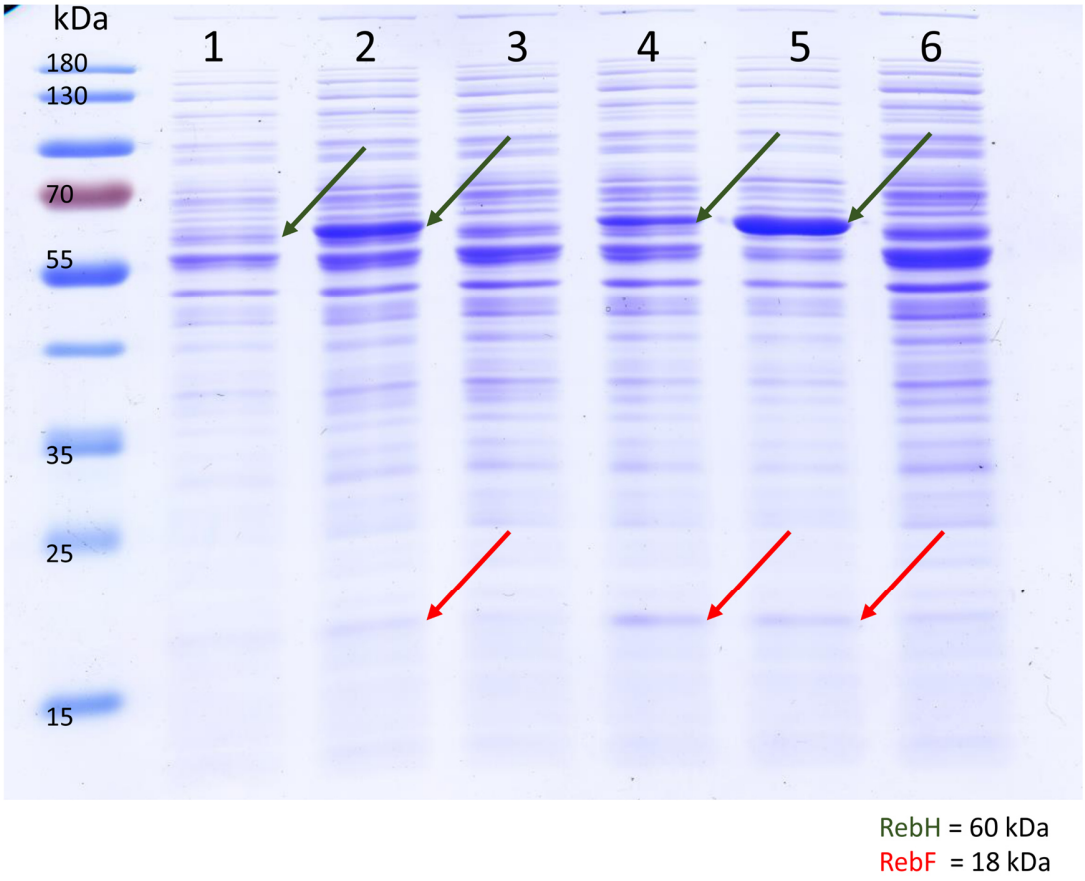

Figure 2.1.1: SDS-PAGE of RebH and RebF overproducing *C. glutamicum* strains. The strains were grown 24 h in LB medium with 1 mM IPTG. The strains were derived from strain Tp679(pCES208-*trpD*) and carried an additional expression plasmid for overproduction of RebH and RebF: pECXT99A-*rebH-rebF* (Lane 1), pECXT99A-optimRBS-*rebH-rebF* (Lane 2), pECXT99A (Line 3), pEKEx3-*rebH-rebF* (Line 4), pEKEx3-optimRBS-*rebH-rebF* (Line 5) or pEKEx3 (Line 6).

2.2 Bromination of L-tryptophan in a fermentative process with *Corynebacterium glutamicum*

Kareen H. Veldmann[a], Steffen Dachwitz[b], Joe Max Risse[c], Jin-Ho Lee[d], Norbert Sewald[b], Volker F. Wendisch[a]

[a] Genetics of Prokaryotes, Faculty of Biology & CeBiTec, Bielefeld University, Universitätsstr. 25, 33615 Bielefeld, Germany

[b] Organic and Bioorganic Chemistry, Faculty of Chemistry & CeBiTec, Bielefeld University, Universitätsstr. 25, 33615 Bielefeld, Germany

[c] Fermentation Technology, Technical Faculty & CeBiTec, Bielefeld University, Universitätsstr. 25, 33615 Bielefeld, Germany

[d] Major in Food Science & Biotechnology, School of Food Biotechnology & Nutrition, BB21+, Kyungsung University, 309, Suyeong-ro, Nam-gu, Busan 48434, Republic of Korea

2.2.1 Abstract

Brominated compounds such as 7-bromo-L-tryptophan (7-Br-Trp) occur in Nature. Many synthetic and natural brominated compounds have applications in the agriculture, food and pharmaceutical industries, for example, the 20S-proteasome inhibitor TMC-95A that may be derived from 7-Br-Trp. Mild halogenation by cross-linked enzyme aggregates containing FAD-dependent halogenase, NADH-dependent flavin reductase, and alcohol dehydrogenase as well as by fermentation with recombinant *Corynebacterium glutamicum* expressing the genes for the FAD-dependent halogenase RebH and the NADH-dependent flavin reductase RebF from *Lechevalieria aerocolonigenes* have recently been developed as green alternatives to more hazardous chemical routes. In this study, the fermentative production of 7-Br-Trp was established. The fermentative process employs an L-tryptophan producing *C. glutamicum* strain expressing *rebH* and *rebF* from *L. aerocolonigenes* for halogenation and is based on glucose, ammonium and sodium bromide. *C. glutamicum* tolerated high

sodium bromide concentrations, but its growth rate was reduced to half-maximal at 0.09 g L^{-1} 7-Br-Trp. This may be, at least in part, due to inhibition of anthranilate phosphoribosyltransferase by 7-Br-Trp since anthranilate phosphoribosyltransferase activity in crude extracts was half-maximal at about 0.03 g L^{-1} 7-Br-Trp. Fermentative production of 7-Br-Trp by recombinant *C. glutamicum* was scaled up to a working volume of 2 L and operated in batch and fed-batch mode. The titers were increased from batch fermentation in CGXII minimal medium with 0.3 g L^{-1} 7-Br-Trp to fed-batch fermentation in HSG complex medium, where up to 1.2 g L^{-1} 7-Br-Trp were obtained. The product isolated from the culture broth was characterized by NMR and LC-MS and shown to be 7-Br-Trp.

2.2.2 Introduction

Brominated tryptophan is typically not found in free form in Nature, but as a biosynthetic precursor in complex structures that for example occur in sponges and lower marine invertebrates (Bittner et al., 2007). The brominated molecules often exhibit pharmaceutical and biological activities. For example, TMC-95A which derives from 7-bromo-L-tryptophan (7-Br-Trp) is biologically active against the chymotrypsin-like, trypsin-like, and peptidylglutamyl-peptide-hydrolyzing activities of the 20S proteasome of eukaryotic cells (Koguchi et al., 2000). Protease inhibitors may be promising candidates for tumor and inflammation therapies (Adams, 2004; Vergnolle, 2016). Free unprotected halotryptophans including 7-Br-Trp and 7-chloro-L-tryptophan (7-Cl-Trp) can serve as substrates for Pd-catalyzed cross-coupling reactions (Willemse et al., 2017) for example in the Suzuki-Miyaura cross-coupling in order to attach an aryl, heteroaryl or alkenyl substituent to the indole ring (Roy et al., 2008). For this reaction, 7-Br-Trp is preferred because it is more reactive than 7-Cl-Trp (Corr et al., 2017). In addition, 7-Br-Trp can also be used in other transition metal-catalyzed cross couplings such as the Mizoroki-Heck reaction (Gruß et al., 2019) giving fluorescent styryl-tryptophans or the Sonogashira cross-coupling reaction (Sonogashira, 2002) to generate compounds such as the new-to-nature bromo-cystargamide or to selectively modify bromo-tryptophan residues as a component of a tripeptide (Corr et al., 2017). 7-Cl-Trp is not useful for the Sonogashira cross coupling reaction since it is too unreactive (Corr et al., 2017). Furthermore, 7-Br-Trp can easily be converted to

7-bromoindole, which may give rise to many indole derivates including the MOM-protected 7-bromoisatin, which is the precursor of the antimitotic agent diazonamide A (Nicolaou et al., 2002; Wang et al., 2007; Bartoli et al., 2014). Halogenation of L-tryptophan (Trp) involves two enzymes of the *reb* operon of *Lechevalieria aerocolonigenes*, the FAD-dependent halogenase RebH and the NADH-dependent flavin reductase RebF required for NADH-dependent redox cofactor regeneration (Nishizawa et al., 2005). The halogenase RebH from *L. aerocolonigenes* chlorinates Trp to 7-Cl-Trp, the precursor of rebeccamycin. While this enzyme also accepts bromide, it prefers chloride over bromide (Yeh et al., 2005). Purified cross-linked enzymes RebH, RebF, and an alcohol dehydrogenase to regenerate NADH by oxidation of isopropanol have successfully been applied to the enzymatic bromination of Trp at the gram-scale (Frese and Sewald, 2015; Schnepel and Sewald, 2017). Fermentative production of 7-Cl-Trp has recently been established using recombinant *Corynebacterium glutamicum* (Veldmann et al., 2019).

Fermentation processes with *C. glutamicum* that serves as a work horse for the biotechnological production of different amino acids are scalable and in the case of L-lysine and L-glutamate applied at the million-ton scale (Wendisch, 2019). Fermentative processes unlike chemical synthesis routes do not require environmentally hazardous compounds (e.g., elemental chlorine or bromine) or protecting / activating groups because of the high stereo- and regioselectivities of the enzymes involved. Biotransformations using purified enzymes may suffer from low stability and low activity (e.g., of halogenases), especially under non-native reaction conditions in the presence of high substrate concentrations (Latham et al., 2017). Fermentative processes start from sugars and the biocatalyst is (re)generated during growth. Fermentative processes are excellent for synthesis if export of the product out of the cell is efficient and neither substrates nor products nor intermediates inhibit cellular metabolism.

C. glutamicum typically shows higher tolerance to many substances including organic acids, furan, and phenolic inhibitors present in lignocellulose hydrolysates (Sakai et al., 2007). Adaptive laboratory evolution led to increased tolerance to methanol (Leßmeier and Wendisch, 2015) or lignocellulose derived inhibitors (Wang et al., 2018). Thus, *C. glutamicum* was engineered for production of carboxylic acids such as pyruvate

(Wieschalka et al., 2012) and succinate (Litsanov et al., 2012), oxoacids such as 2-ketoisovalerate (Krause et al., 2010) and 2-ketoisocaproate (Bückle-Vallant et al., 2014), alcohols such as ethanol (Inui et al., 2004a), isobutanol (Blombach et al., 2011) and *n*-propanol (Siebert and Wendisch, 2015), polymers such as polyhydroxyalkanoate (Ma et al., 2018). As industrial amino acid producer *C. glutamicum* is ideal for fermentative production of various other nitrogenous compounds such as the cyclic amino acid pipecolic acid (Pérez-García et al., 2016), the ω-amino acids γ-aminobutyrate (Kim et al., 2013; Jorge et al., 2016; Pérez-García et al., 2016) and 5-aminovalerate (Rohles et al., 2016; Jorge et al., 2017), the diamines putrescine (Schneider and Wendisch, 2010) and cadaverine (Tateno et al., 2009; Kim et al., 2018) and alkylated and hydroxylated amino acids such as *N*-methylalanine (Mindt et al., 2018) and 5-hydroxy-isoleucine (Wendisch, 2019). Noteworthy, several excellent *C. glutamicum* producer strains have been developed for production of muconic acid (Becker et al., 2018), phenylpropanoids (Kallscheuer and Marienhagen, 2018) *para*-hydroxybenzoic acid (Purwanto et al., 2018) and protocatechuate (Wendisch et al., 2016; Lee and Wendisch, 2017).

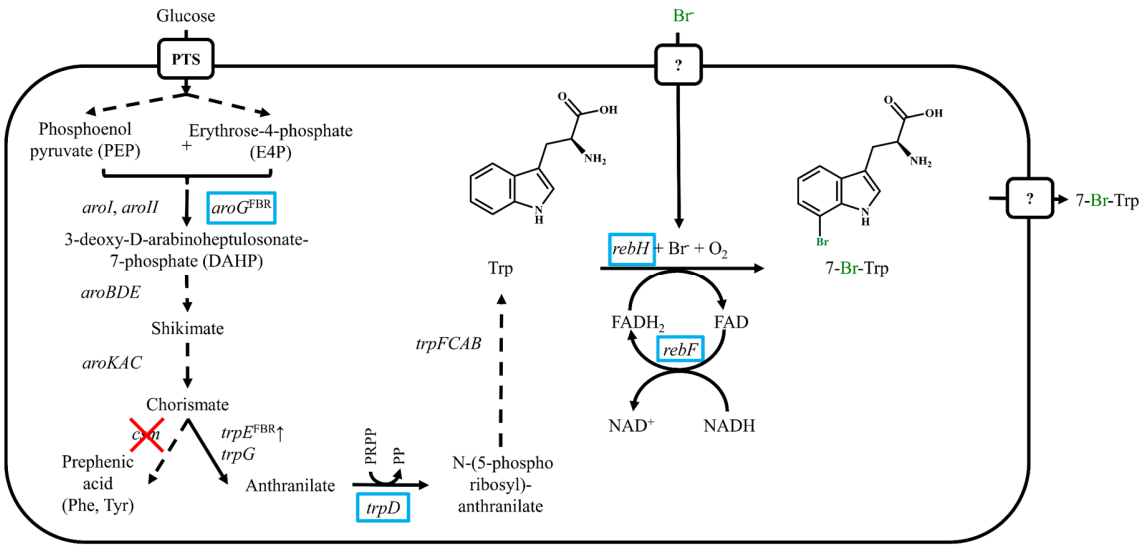

Fig. 2.2.1: Schematic representation of metabolic engineered *C. glutamicum* overproducing Trp and 7-Br-Trp. Genes names are shown next to reaction represented by the arrows. Dashed arrows show several reactions. Heterologously expressed genes are marked by blue boxes, endogenously overexpressed genes are marked by ↑ and deleted genes are showed by red crosses. FBR: feedback resistant.

Accordingly, the Trp overproducing strain Tp679 (Purwanto et al., 2018) served as excellent base strain for halogenation of Trp (Veldmann et al., 2019). In *C. glutamicum* wildtype *trpE* encoding a feedback resistant anthranilate synthase component 1 from *C. glutamicum* and *trpD* encoding an anthranilate phosphoribosyltransferase from *E. coli* were overexpressed to channel the flux from chorismate to Trp. The chorismate mutase *csm* was deleted to prevent the formation of the by-products L-phenylalanine and L-tyrosine. The precursor supply was optimized with the overexpression of *aroG* encoding a feedback resistant 3-deoxy-D-arabinoheptulosonate-7-phosphate synthase from *E. coli* (Fig. 2.2.1). The production of 7-Cl-Trp had already been established with the Trp producing *C. glutamicum* strain overexpressing *rebH* and *rebF*. The strain produced about 0.1 g L^{-1} of 7-Cl-Trp (Veldmann et al., 2019). However, bromination of Trp *in vivo* has not yet been described as basis of a fermentative process leading 7-Br-Trp or other brominated tryptophans. Here, we describe the production of 7-Br-Trp with the above described Trp overproducing *C. glutamicum* strain expressing *rebH* and *rebF* in media with low chloride, but high bromide concentrations. The process was upscaled in bioreactors with a volume of 2 L and 7-Br-Trp was isolated and characterized by NMR and MS.

2.2.3 Material and Methods

2.2.3.1 Bacterial strains and growth conditions

Bacterial strains and plasmids used in this study are listed in Table 2.2.1. *Escherichia coli* DH5α (Hanahan, 1983) was used for cloning the plasmid constructs. *E. coli* and *C. glutamicum* were regularly grown in lysogeny broth medium (LB medium) in 500 mL baffled flasks at 120 rpm at 37 °C or 30 °C, respectively. For growth and production experiments *C. glutamicum* was inoculated in CGXII minimal medium (Eggeling and Bott, 2005) in 500 mL or 100 mL baffled flasks (filling volume 10%) to an optical density (OD_{600}) of 1 and incubated at 120 rpm. Growth was monitored by measuring the optical density at 600 nm using a V-1200 spectrophotometer (VWR, Radnor, PA, USA). For toxicity test *C. glutamicum* was grown in the BioLector® (M2P Labs) in CGXII medium supplemented with the substance to be tested. To produce 7-Br-Trp, CGXII minimal medium or HSG rich medium (40.0 g L^{-1} glucose, 13.5 g L^{-1} soy peptone, 7 g L^{-1} yeast extract, 0.01 g L^{-1} NaCl, 2.3 g L^{-1} K_2HPO_4, 1.5 g L^{-1} KH_2PO_4, 0.249 g L^{-1} $MgSO_4 \times H_2O$) were used and supplemented with 50 mM NaBr. Strains derived from Tp679 were supplemented additionally with 1.37 mM L-tyrosine and 1.5 mM L-phenylalanine in minimal medium.

Table 2.2.1: Strains and plasmids used in this work

Strains and plasmids	Description	Source
Strains		
WT	*C. glutamicum* wild type, ATCC 13032	ATCC
Tp679 (pCES208-*trpD*)	Δ*csm* Δ*trpL*::P_{ilvCM1}-*trpE*^{FBR} Δ*vdh*::P_{ilvCM1}-*aroG*^{FBR} with pCES208-*trpD*	(Purwanto et al., 2018)
HalT2	Tp679 (pCES208-*trpD*) (pEKEx3-optimRBS-*rebH-rebF*)	(Veldmann et al., 2019)

Strains and plasmids	Description	Source
Plasmids		
(pCES208-*trpD*)	Kan^R, pCES208 overexpressing *trpD* from *E. coli* with P_{ilvCM1}	(Purwanto et al., 2018)
(pEKEx3-optimRBS-*rebH*-*rebF*)	Spec^R, pEKEx3 overexpressing *rebH*, *rebF* from *L. aerocolonigenes* with optimized RBS for *rebH*	(Veldmann et al., 2019)

If necessary, the growth medium was supplemented with kanamycin (25 µg mL^{-1}) and/or spectinomycin (100 µg mL^{-1}). Isopropyl-β-D-1-thiogalactopyranoside (IPTG) (1 mM) was added to induce the gene expression from the vector pEKEx3 (Stansen et al., 2005).

2.2.3.2 Determination of the specific activity of the anthranilate phosphoribosyltransferase TrpD

The anthranilate phosphoribosyltransferase overproducing strain Tp679 (pCES208-*trpD*) was inoculated from an overnight culture and was cultivated for 24 h in LB medium at 30 °C with 120 rpm before cells were centrifuged for 10 min at 4 °C and 4000 rpm and stored at -20 °C. After resuspension in 100 mM Tricine buffer (pH 7.0), the cells were sonicated for 9 min at 55% amplitude and 0.5 cycles on ice in the UP200S Ultrasonic Processor from Hielscher Ultrasound Technology. The supernatant obtained after centrifugation (60 min, 4°C, 16400 rpm) was used as crude extract for the enzyme assay. The activity was assayed fluorometrically by monitoring the decrease of anthranilate (Ant) at room temperature. The reaction mixture with a final volume of 1 mL contained 100 mM Tricine buffer (pH 7.0), 15 µM Ant, 0.3 mM PRPP, 10 mM $MgCl_2$, and the crude extract and was filled in a quartz glass cuvette (Hellma Analytics, High Precision cell, Light Path 10 × 4 mm). Ant was detected by fluorescence at 325 nm excitation and 400 nm emission wavelength with the Shimadzu Spectrofluorophotometer RF-5301PC. Protein concentrations were determined by

the Bradford method (Bradford, 1976) with bovine serum albumin as reference. Means and errors from triplicates were calculated.

2.2.3.3 Bioreactor cultures operated in batch and fed-batch mode

A 3.7 L KLF Bioengineering AG stirred tank reactor was used for the production of 7.-Br-Trp. The fermentation was performed at pH 7.0, 30 °C, and an aeration rate of 2 norm liter (NL) min^{-1}. pH was controlled by automatic addition of phosphoric acid (10% (w/w)) and ammonium hydroxide (25% w/w)). Struktol®J647 (Schill and Seilenbacher, Boeblingen, Germany) serves as antifoam agent and was also added automatically. Samples were taken automatically every 2 h and cooled to 4 °C until analysis.

For the batch fermentations the relative dissolved oxygen saturation (rDOS) of 15, 30, and 60%, respectively was controlled by enhancing the stirrer speed gradually in steps of 2%. Two liters CGXII without MOPS but with 50 mM NaBr, 1.37 mM L-tyrosine, 1.5 mM L-phenylalanine and 1 mM IPTG (added at timepoint 0 h) was used as culture medium.

For the fed-batch fermentation the initial volume was 2 L and a constant overpressure of 0.2 bar was adjusted. Due to the new findings (see Fig. 2.2.6) the culture medium was changed to HSG rich medium supplemented with 50 mM NaBr and 1 mM IPTG (added at timepoint 0 h). The feeding medium contained 150 g L^{-1} ammonium sulfate, 400 g L^{-1} glucose, 5.14 g L^{-1} NaBr, 0.25 g L^{-1} L-tyrosine, and 0.25 g L^{-1} L-phenylalanine. Automatic control of the stirrer speed kept the rDOS at 30%. The feeding started automatically when rDOS exceeds 60% and stops when rDOS felt again under the set-point. Here, a pH of 7.0 was established and controlled by automatic addition of phosphoric acid (10% (w/w)) and potassium hydroxide (4 M). Instead of using ammonium hydroxide as alkali to avoid. nitrogen limitation in batch cultures, potassium hydroxide was used in the fed-batch fermentation, since the HSG complex medium is nitrogen rich and, hence, a nitrogen limitation was excluded.

The titer and yield were calculated to the initial volume.

2.2.3.4 Analytical procedures

For the quantification of the extracellular Trp, 7-Br-Trp, and anthranilate (Ant) a high-pressure liquid chromatography (HPLC) system was used (1200 series, Agilent Technologies Deutschland GmbH, Böblingen, Germany). The supernatants of the cell culture were collected by centrifugation (14680 rpm, 20 min, RT) and further used for analysis. For detection of Ant, Trp, and the derivatives, samples were reacted with *ortho*-phthaldialdehyde (OPA) (Schneider and Wendisch, 2010). The amino acid separation was performed by a precolumn (LiChrospher 100 RP18 EC-5 µ (40mm×4 mm), CS-Chromatographie Service GmbH, Langerwehe, Germany) and a column (Li-Chrospher 100 RP18 EC-5 µ (125 mm×4 mm), CS Chromatographie Service GmbH). The detection was carried out with a fluorescence detector (FLD G1321 A, 1200 series, Agilent Technologies) with the excitation and emission wavelengths of 230 nm and 450 nm, respectively. The quantification of carbohydrates and organic acids was done using a column for organic acids (300 × 8 mm, 10 mm particle size, 25 Å pore diameter, CS Chromatographie Service GmbH) and detected by a refractive index detector (RID G1362A, 1200 series, Agilent Technologies) and a diode array detector (DAD G1315B, 1200 series, Agilent Technologies) (Schneider et al., 2011).

2.2.3.5 Analytical RP-HPLC and RP-HPLC-MS

Analytical HPLC was performed on a Shimadzu NexeraXR 20A System with autosampler, degasser, column oven, diode array detector, and a Phenomex Luna C18 column (2.9 µm, 50 × 2.1 mm) with a gradient (in 5.5 min from 5% B to 95% B, 0.5 min 95% B and back to 5 % B in 3 min, total run time 9 min) at a flow rate of 650 µL min^{-1} and column oven temperature of 40 °C. HPLC solvent A consists of 99.9% water and 0.1 % TFA, solvent B of 99.9 % acetonitrile and 0.1 % TFA.

Analytical LC-MS was performed on an Agilent 6220 TOF-MS with a Dual ESI-source, 1200 HPLC system with autosampler, degasser, binary pump, column oven, diode array detector, and a Hypersil Gold C18 column (1.9 µm, 50 × 2.1 mm) with a gradient (in 11 min from 0% B to 98% B, back to 0% B in 0.5 min, total run time 15 min) at a flow rate of 300 µL min^{-1} and column oven temperature of 40 °C. HPLC solvent A consisted of 94.9% water, 5 % acetonitrile, and 0.1% formic acid, solvent B of 5% water, 94.9% acetonitrile and 0.1%

formic acid. ESI mass spectra were recorded after sample injection via 1200 HPLC system in extended dynamic range mode equipped with a Dual-ESI source, operating with a spray voltage of 2.5 kV.

2.2.3.6 NMR spectroscopy

NMR spectra were recorded on a Bruker Avance III 500 HD (^{1}H: 500 MHz, ^{13}C: 126 MHz, ^{19}F: 471 MHz). Chemical shifts δ [ppm] are reported relative to residual solvent signal (DMSO-d_6, ^{1}H: 2.50 ppm, ^{13}C: 39.5 ppm). 2D spectra (COSY, HMQC, HMBC) spectra were used for signal assignment.

2.2.3.7 High-resolution MS

ESI mass spectra were recorded using an Agilent 6220 time-of-flight mass spectrometer (Agilent Technologies, Santa Clara, CA, USA) in extended dynamic range mode equipped with a Dual-ESI source, operating with a spray voltage of 2.5 kV. Nitrogen served both as the nebulizer gas and the dry gas. Nitrogen was generated by a nitrogen generator NGM 11. Samples are introduced with a 1200 HPLC system consisting of an autosampler, degasser, binary pump, column oven and diode array detector (Agilent Technologies, Santa Clara, CA, USA) using a C18 Hypersil Gold column (length: 50 mm, diameter: 2.1 mm, particle size: 1,9 µm) with a short isocratic flow (60% B for 5 min) at a flow rate of 250 µL min^{-1} and column oven temperature of 40 °C. HPLC solvent A consists of 94.9% water, 5% acetonitrile and 0.1% formic acid, solvent B of 5% water, 94.9% acetonitrile and 0.1 % formic acid. The mass axis was externally calibrated with ESI-L Tuning Mix (Agilent Technologies, Santa Clara, CA, USA) as calibration standard. The mass spectra are recorded in both profile and centroid mode with the MassHunter Workstation Acquisition B.04.00 software (Agilent Technologies, Santa Clara, CA, USA). MassHunter Qualitative Analysis B.07.00 software (Agilent Technologies, Santa Clara, CA, USA) was used for processing and averaging of several single spectra.

2.2.3.8 Reversed-Phase column chromatography (GP1)

Automated column chromatography was performed on a Büchi Reveleris X2 with a binary pump and ELSD Detector using a Biotage Snap Ultra C18 column with a gradient (4 min at 5% B, up to 25% B in 14 min, in 1 min up to 100% B for 2 min and flushing with 80% B for 5 min, total run time 27 min) at a flow rate of 30 mL min^{-1}. Solvent A consisted of 99.9% water and 0.1% TFA, solvent B of 99.9% acetonitrile and 0.1% TFA.

2.2.3.9 Isolation and purification of 7-bromo-L-tryptophan from HSG rich medium

7-Br-Trp was isolated from 30 mL HSG rich medium (3 × 10 mL) (see chapter growth conditions) by an automated reversed phase column chromatography. The crude medium was centrifuged (10000 rpm, 4 °C, 30 min) and filtrated over a short plug of celite. The crude filtrate was loaded on a 12 g C18-column and purified according to GP1. The TFA salt of 7-Br-Trp was isolated as a colourless solid (14.3 mg, 36 µmol). RP-column chromatography: t_R = 11.5 min; Anal. RP-HPLC: t_R = 3.3 min; LC-MS: t_R = 5.1 min; ^{1}H NMR (500 MHz, DMSO-d_6) δ [ppm] = 11.28 (d, ^3J = 2.7 Hz, 1H, indole-N**H**), 8.16 (brs, 3H, N$\mathbf{H}_3^+$), 7.58 (d, ^3J = 7.9 Hz, 1H, C4-**H**), 7.32 (d, ^3J = 7.5 Hz, 1H, C6-**H**), 7.30 (d, ^3J = 2.7 Hz, 1H, C2-**H**), 6.97 (dd, ^3J = 7.8 Hz, ^3J = 7.8 Hz, 1H, C5-**H**), 4.15 (dd, ^3J = 7.1 Hz, ^3J = 6.2 Hz, 1H, Cα-**H**), 3.27 (dd, ^2J = 15.0 Hz, ^3J = 5.7 Hz, 1H, Cβ-**H**), 3.22 (dd, ^2J = 14.8 Hz, ^3J = 6.9 Hz, 1H, Cβ-**H**); low res. MS (ESI): found [*m*/*z*] = 265.9 [M(^{79}Br)-NH_2]$^+$, 267.9 [M(^{81}Br)-NH_2]$^+$, 283.0 [M(^{79}Br)+H]$^+$, 285.0 [M(^{81}Br)+H]$^+$; calcd. [*m*/*z*] = 265.9 [M(^{79}Br)-NH_2]$^+$, 267.9 [M(^{81}Br)-NH_2]$^+$, 283.0 [M(^{79}Br)+H]$^+$, 285.0 [M(^{81}Br)+H]$^+$.

2.2.4 Results

2.2.4.1 Production of 7-bromo-L-tryptophan in flasks culture

Fermentative processes are ideal if substrates, intermediates, and products do not inhibit growth and production. The effect of the substrate NaBr and the product 7-Br-Trp on growth of *C. glutamicum* was assessed when various concentrations of these compounds were added upon inoculation of *C. glutamicum* wild type to CGXII minimal medium with 40 g L^{-1} glucose. NaBr concentrations (0 - 500 mM) had a negligible effect on growth and it was estimated by extrapolation that the growth rate would be reduced to 50% at about 1.2 M NaBr (Fig. 2.2.2 A). Therefore, the use of NaBr as a substrate was presumed to be possible. By contrast, already low concentrations of the target product 7-Br-Trp inhibited growth in the BioLector® (M2P Labs). The half maximal specific growth rate of *C. glutamicum* was reached already at a concentration of about 0.32 mM or 0.091 g L^{-1} 7-Br-Trp (Fig. 2.2.2 B). This inhibition is threefold lower than previously observed with 7-Cl-Trp (K_i of about 0.1 mM or 0.024 g L^{-1}; (Veldmann et al., 2019).

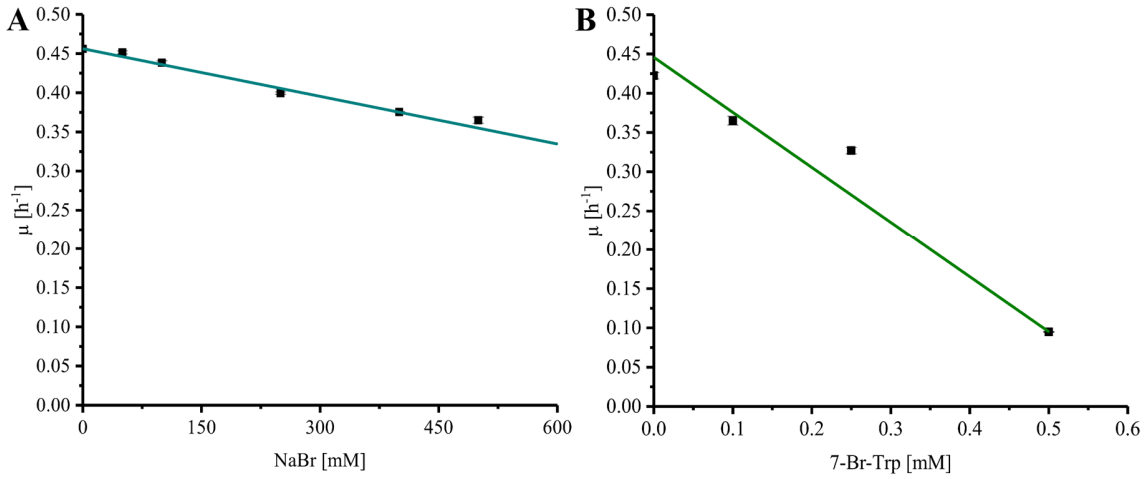

Fig. 2.2.2: Response of *C. glutamicum* wild type to externally added NaBr (A) and 7-Br-Trp (B). To determine the K_i for NaBr and 7-Br-Trp *C. glutamicum* wildtype was grown in CGXII minimal medium with 40 g L^{-1} glucose and different concentration of the substances to be tested. A liner regression was done to determine the half maximal specific growth rate with the substances to be tested. **A:** NaBr concentrations between 0 and 500 mM were tested with *C. glutamicum*. **B:** 7-Br-Trp concentrations between 0 and 0.5 mM were tested.

We hypothesize that the difference is due to the hydration shell of chlorine substituents being smaller than that of a bromine substituent. Accordingly, we speculate that due to its smaller size 7-Cl-Trp can enter catalytic active centres and/or allosteric sites of enzymes easier than 7-Br-Trp and, thus, inhibitory effects are expected to be more pronounced. This may explain why the inhibitory effect of 7-Cl-Trp exceeds that of 7-Br-Trp.

Since it is known that halogenated Ant competitively inhibits Ant converting anthranilate phosphoribosyltransferase TrpD (Lesic et al., 2007), it was tested whether 7-Br-Trp inhibits anthranilate phosphoribosyltransferase in crude extracts of *C. glutamicum* Tp679 (pCES208-*trpD*). This strain possesses endogenous *trpD* on its chromosome and expresses *E. coli trpD* from a plasmid. Crude extracts of *C. glutamicum* Tp679 (pCES208-*trpD*) grown in LB rich media were assayed for TrpD activity in the presence of different concentrations of either 7-Br-Trp or 7-Cl-Trp (Fig. 2.2.3). The specific activity of anthranilate phosphoribosyltransferase was reduced to about one third by either 0.15 mM 7-Br-Trp or by 0.05 mM 7-Cl-Trp (Fig. 2.2.3). Thus, inhibition by 7-Cl-Trp was more pronounced than inhibition by 7-Br-Trp, which showed a K_i value of about 0.03 g L^{-1}. At least in part, the growth inhibition by 7-Br-Trp (Fig. 2.2.2 B) may be due to inhibition of anthranilate phosphoribosyltransferase by 7-Br-Trp (Fig. 2.2.3). Since 7-Br-Trp exerts a lower inhibitory effect as compared to 7-Cl-Trp and since the latter could be produced to a titer of 0.108 g L^{-1}, i.e. five times as high as K_i (Veldmann et al., 2019), it is expected that *C. glutamicum* likely produces 7-Br-Trp only to relatively low concentrations, as well.

For the fermentative production of 7-Br-Trp the *C. glutamicum* strain HalT2 was used. This strain was derived from the Trp overproducing strain Tp679 (pCES208-*trpD*), which overexpresses additionally genes encoding FAD-dependent halogenase RebH and NADH-dependent flavin reductase RebF from the expression vector pEKEx3 (Veldmann et al., 2019). In our previous study, we have tried to optimize RebF and RebH gene expression. On the one hand, a more active promoter helped increase RebH and RebF activities, on the other hand, production could be improved as consequence of optimizing the ribosome binding site [and thus, translation initiation efficiency;(Veldmann et al., 2019)]. Bioinformatics analysis revealed that the codon usage of RebH fits to the codon usage of

C. glutamicum and hence was not further optimized. For RebF the codon usage fits to *C. glutamicum* except one triplet. The ribosome binding site was not optimized for RebF.

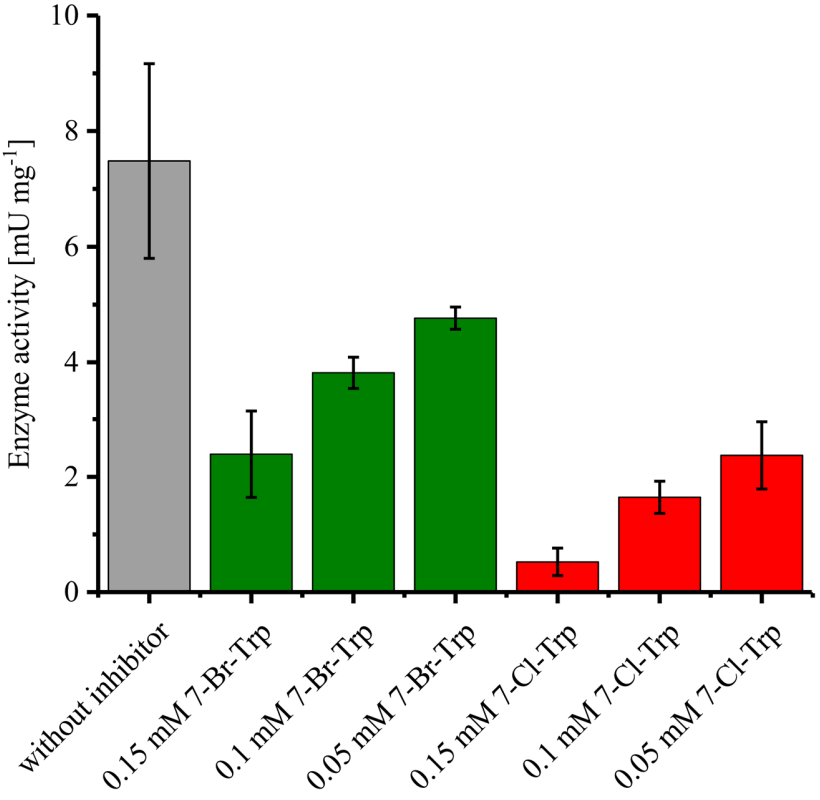

Fig. 2.2.3: Specific activities of anthranilate phosphoribosyltransferase TrpD in the presence or absence of either 7-Br-Trp or 7-Cl-Trp. Crude extracts of *C. glutamicum* Tp679 (pCES208-*trpD*) grown in LB rich media were assayed for TrpD activity in the presence of different concentrations of either 7-Br-Trp or 7-Cl-Trp. Means and standard deviations of triplicates are shown.

HalT2 was inoculated in CGXII minimal medium with 40 g L^{-1} glucose and 50 mM NaBr in 500 mL baffled flasks (50 mL culture) to an OD_{600} of 1. At inoculation, 1 mM IPTG was added. The culture showed a specific growth rate 0.12 ± 0.01 h^{-1}. After 72 h 0.25 ± 0.01 g L^{-1} 7-Br-Trp, 0.81 ± 0.02 g L^{-1} Trp and 1.69 ± 0.03 g L^{-1} Ant were measured (Fig. 2.2.4). When the same strain was inoculated in 500 mL without baffles the specific growth rate was 0.11 ± 0.01 h^{-1} and the production of 7-Br-Trp increased by 38% to a titer of 0.34 ± 0.02 g L^{-1}. Production of Trp was decreased by 34% to 0.54 ± 0.02 g L^{-1}, but production of Ant increased to 1.91 ± 0.03 g L^{-1}. Using 100 mL flasks with 10 mL culture was beneficial for

production of 7-Br-Trp by *C. glutamicum* HalT2 as in baffled flasks 0.48 ± 0.03 g L^{-1} 7-Br-Trp were produced after 72 h and 0.81 ± 0.01 g L^{-1} Trp and 2.82 ± 0.06 g L^{-1} Ant accumulated. In 100 mL flasks without baffles 0.49 ± 0.02 g L^{-1} 7-Br-Trp were produced after 72 h and 0.96 ± 0.03 g L^{-1} Trp and 3.45 ± 0.13 g L^{-1} Ant accumulated (Fig. 2.2.4). With the assumption that the oxygen supply is lower in the 100 mL than in the 500 mL flasks, the production was increased with less oxygen supply. The specific growth rate was lower in 100 mL flasks with baffles (0.09 ± 0.01 h^{-1} as compared to 0.13 ± 0.01 h^{-1}). These results were unexpected since oxygen supply in 500 mL baffled flasks is considered higher than in 100 mL unbaffled flasks we expected higher 7-Br-Trp in 500 mL baffled flasks. Halogenase RebH requires $FADH_2$ as co-factor, Trp, molecular oxygen and a halide salt as substrates. RebH regioselectively chlorinates or brominates Trp at the 7-position. $FADH_2$ is regenerated by RebF, which reduces FAD to $FADH_2$ in an NADH-dependent manner. NADH is provided by cellular metabolism (oxidation of glucose). RebH and RebF derive from the host organism *Lechevalieria aerocolonigenes* which has a growth optimum at 28 °C (Parte, 2012), which fits well with the optimal growth temperature of *C. glutamicum* of 30 °C. Nonetheless, the highest 7-Br-Trp titer observed (about 0.49 g L^{-1}; Fig. 2.2.4) exceeded the K_i value (about 0.09 g L^{-1}; Fig. 2.2.2 B) about five-fold.

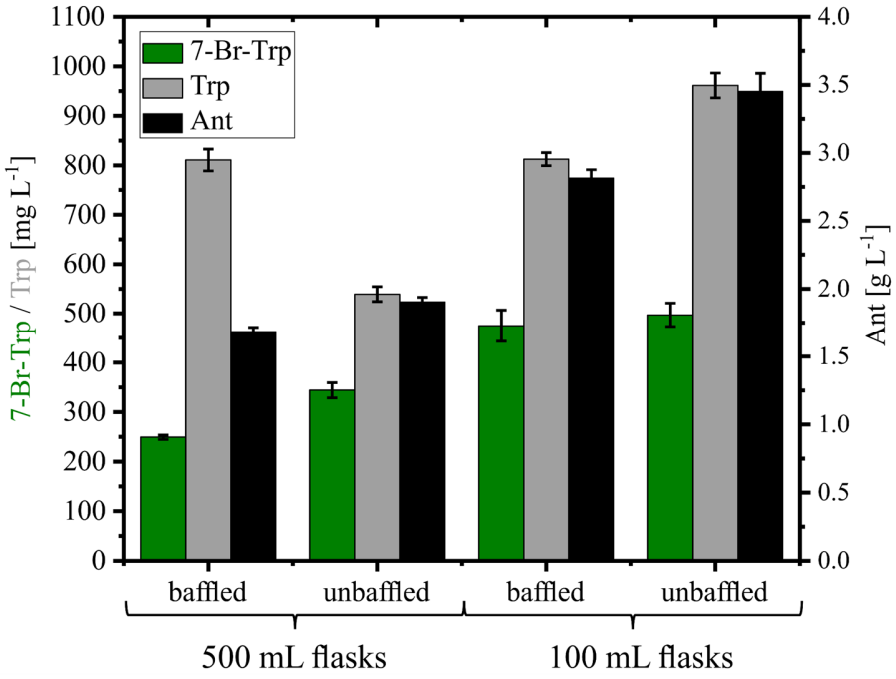

Fig. 2.2.4: Production of 7-Br-Trp, Trp and Ant by *C. glutamicum* HalT2 under different shake flask conditions. HalT2 was grown in CGXII with 40 g L^{-1} glucose after 72 h were measured the titers of 7-Br-Trp, Trp and Ant. The filling volume was 10% of the flasks volume. Means and standard deviations of three replicate cultivations are shown.

2.2.4.2 Batch production of 7-bromo-L-tryptophan in a bioreactor

To scale up the fermentation process and to test the influence of pH control, optimal stirring and controlled oxygen supply, strain HalT2 was cultivated in a 3.7 L baffled bioreactor with a working volume of 2 L with three different rDOSs (rDOS = 15%, 30%, and 60%). Whereas the maximal specific growth rate was comparable and in a range between 0.07 and 0.08 h^{-1}, *C. glutamicum* HalT2 grew to a higher biomass concentration at rDOS of 15% (OD_{600} of 27; Fig. 2.2.5 C) than with rDOS at either 30 or 60% (OD_{600} of 11 and 12, respectively; Fig. 2.2.5 A and B). Glucose was utilized completely (with the exception of 3.6 g L^{-1} glucose remaining in the rDOS 60% bioreactor condition). Lactate accumulated transiently peaking at 32 h, 28 h and 16 h with maximal concentrations of 3.8, 3.8 and 0.5 g L^{-1} lactate for the bioreactors

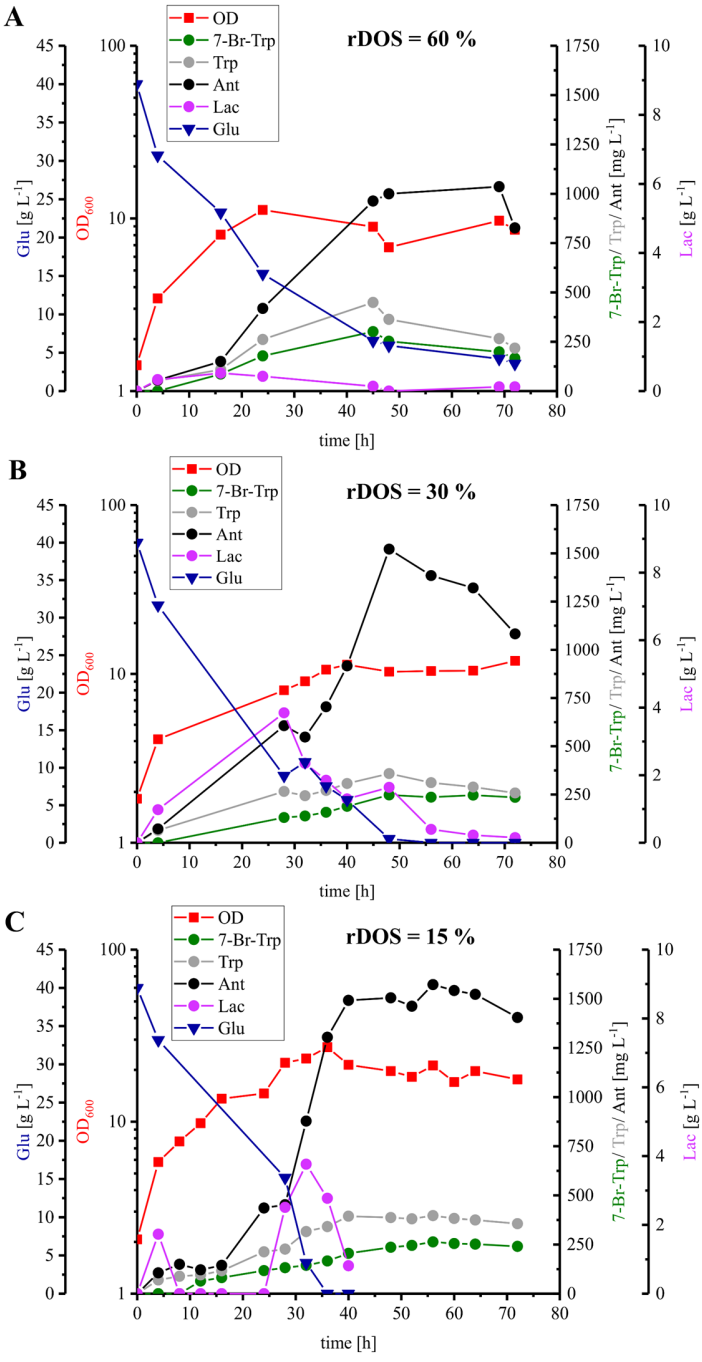

Fig. 2.2.5: Batch fermentation of 7-Br-Trp by *C. glutamicum* HalT2 with three different rDOS. The data given include the glucose consumption [blue triangle], the OD_{600} [red squares], the production of 7-Br-Trp [green circles], Trp [grey circles], Ant [black cirles] and Lac [light purple circles]. The initial culture volume was 2 L. **A:** Batch fermentation with a rDOS set-point of 60%. **B:** Batch fermentation with a rDOS set-point of 30%. **C:** Batch fermentation with a rDOS set-point of 15%.

operated at 15%, 30%, and 60%, respectively (Fig. 2.2.5). The byproducts Trp and Ant accumulated to higher concentrations than 7-Br-Trp. Maximal 7-Br-Trp titers increased slightly with decreasing rDOS, i.e. 0.26, 0.26 and 0.30 g L^{-1} 7-Br-Trp for the bioreactors operated at 15%, 30%, and 60%, respectively (Fig. 2.2.5). The corresponding yields on glucose were 6.6, 6.6, and 7.5 mg g^{-1}. The yields on biomass differed to a larger extent since higher biomass concentrations were observed at low rDOS. At 15% rDOS, for example, an OD_{600} 21 (corresponding to 7.4 gCDW L^{-1}) and a 7-Br-Trp titer of 0.26 g L^{-1} were observed at 56 h, which is equivalent to a 7-Br-Trp yield on biomass of 36 mg $(gCDW)^{-1}$. At 30% rDOS, the Br-Trp yield on biomass was almost two fold higher (74 mg $(gCDW)^{-1}$) and it was almost three fold higher at 60% rDOS (95 mg $(gCDW)^{-1}$). This may indicate that less cells are required for 7-Br-Trp production at high rDOS and/or that growth proceeds to higher biomass concentrations at low rDOS.

2.2.4.3 Fed-batch production of 7-bromo-L-tryptophan in a bioreactor

Stirred tank bioreactor cultivations operated in batch mode yielded lower titers (0.26 to 0.30 g L^{-1}; Fig. 2.2.5) than shake flask cultivation (up to about 0.49 g L^{-1}; Fig. 2.2.4). Under both conditions CGXII glucose minimal medium was used. Since fermentations are often performed in media containing complex sources such as yeast extract and/or protein hydrolysates, production of 7-Br-Trp by *C. glutamicum* HalT2 was compared in 100 mL baffled flasks with either CGXII glucose minimal medium or HSG rich medium containing yeast extract and soy peptone. Growth in the HSG rich medium was faster (a specific growth rate of 0.39 ± 0.02 h^{-1} as compared to 0.19 ± 0.01 h^{-1} in CGXII minimal medium). Within 24 h 0.36 ± 0.04 g L^{-1} 7-Br-Trp were produced in HSG rich medium, but only 0.10 ± 0.01 g L^{-1} 7-Br-Trp in the minimal medium (Fig. 2.2.6). Moreover, the 7-Br-Trp yield on biomass in HSG rich medium [39 ± 5 mg $g(CDW)^{-1}$] was higher than in CGXII minimal medium [6 ± 1 mg $g(CDW)^{-1}$]. Notably, neither Trp nor Ant accumulated as by-products in HSG rich medium, whereas 0.26 ± 0.01 g L^{-1} Trp and 1.88 ± 0.05 g L^{-1} Ant were produced in CGXII minimal medium (Fig. 2.2.6).

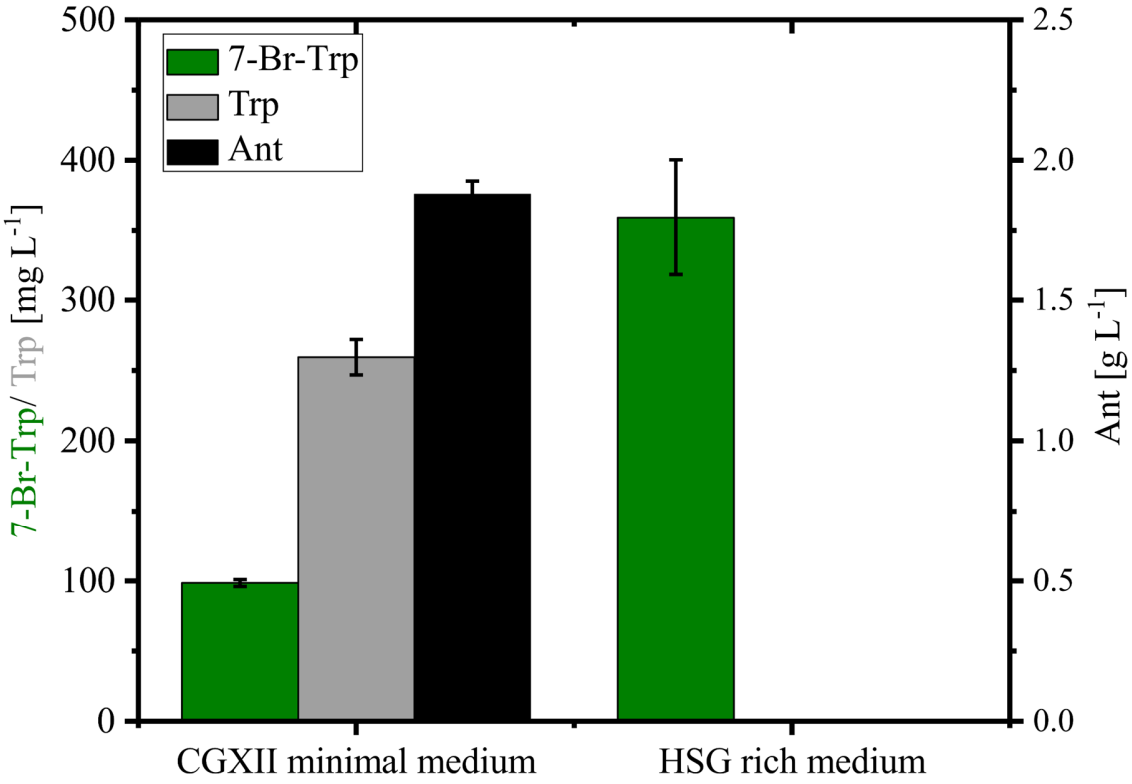

Fig. 2.2.6: Production of 7-Br-Trp by *C. glutamicum* HalT2 in different media. HalT2 was grown in CGXII minimal medium and HSG rich medium with 40 g L^{-1} glucose. The strain was cultivated in 100 mL flasks with 10% filling volume. After 24 h were determined the production of 7-Br-Trp, Trp and Ant. Means and standard deviations of three replicate cultivations are shown.

The product formed by *C. glutamicum* HalT2 in 30 mL HSG rich medium (3 × 10 mL) was isolated and purified in a single step by an automated reversed phase column chromatography. In total 14.3 mg (36 µmol) of 7-Br-Trp as a TFA salt were isolated. The product was identified as 7-Br-Trp by NMR studies. The purity (>95 %) was verified by both NMR (Fig. 2.2.7 A) and LC-MS (Fig. 2.2.7 B) experiments.

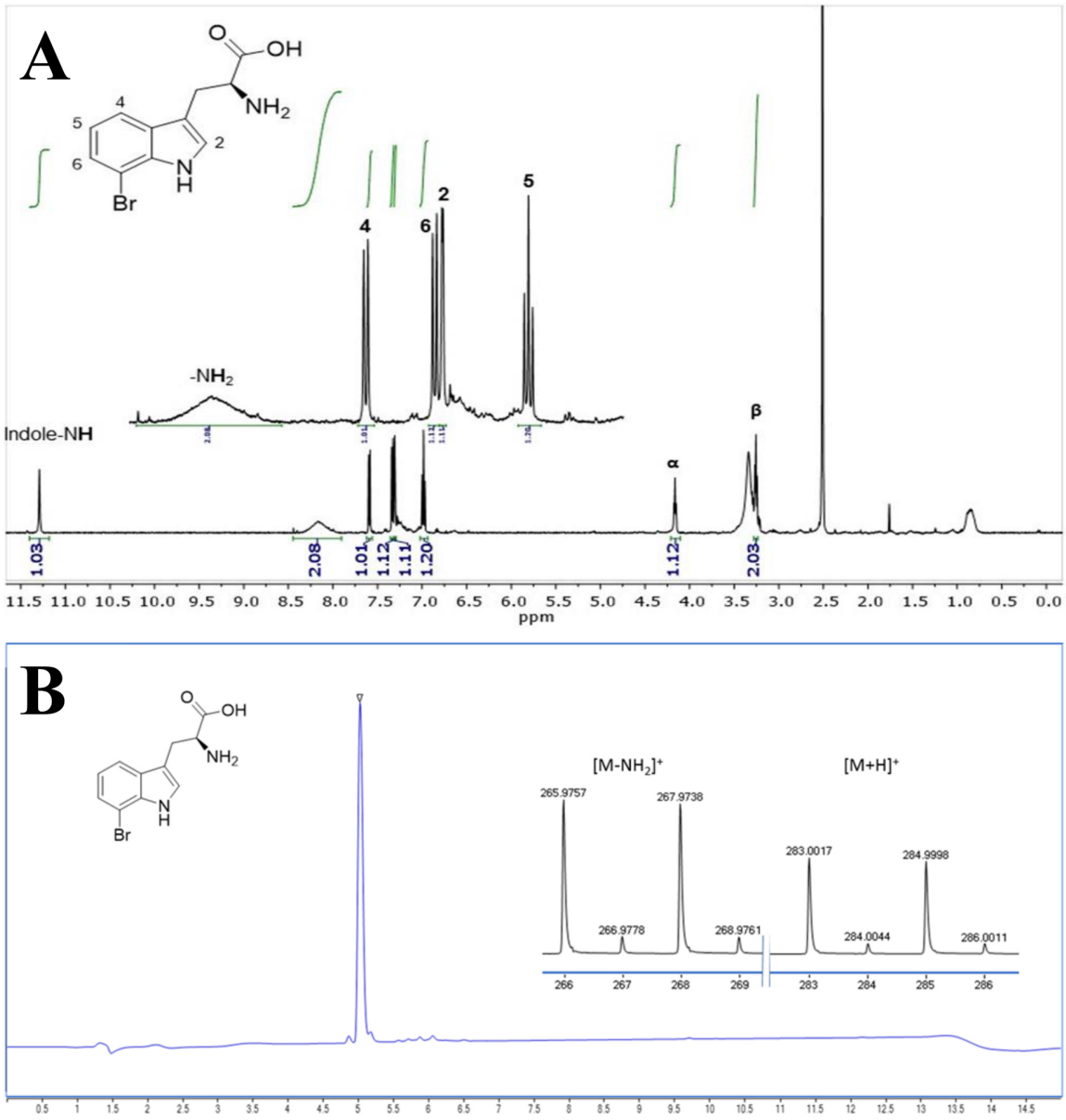

Fig. 2.2.7: Analysis of 7-Br-Trp isolated from HSG medium by (A) ^{1}H NMR (500 MHz, 298 K, DMSO-d_6) and by (B) RP-HPLC-MS analysis. The ionization was performed with a Dual-ESI with a voltage of 2.5 kV leading to an expected deamination during the ionization process. The characteristic isotopic pattern of a single brominated species is clearly observable.

Taken together, HSG rich medium was chosen for fed-batch fermentation because the production occurred faster and the precursors Trp and Ant did not accumulate as by-products and the specific growth rate in rich medium was two-fold higher than in CGXII medium as

mentioned above (0.39 h^{-1} for HSG medium vs. 0.19 h^{-1} for CGXII medium). In figure 2.2.6 the concentrations of Trp, Ant, and 7-Br-Trp after 24 h of cultivation in shake flasks are given. Most likely, in contrast to CGXII medium product formation was finished at this time point using rich medium. This was also confirmed by figure 2.2.5, because 7-Br-Trp formation was not finished after 24 h of cultivation, irrespective of whether rDOS level was used. At 30% rDOS, the highest 7-Br-Trp yield on biomass of 74 mg $(gCDW)^{-1}$ was reached as mentioned above. Therefore, the same set point was used for fed-batch fermentation. *C. glutamicum* HalT2 was used for the fed-batch fermentation to inoculate 2 L HSG rich medium containing 40 g L^{-1} glucose to an initial OD600 of 1.8 (Fig. 2.2.8). The maximal specific growth rate was 0.32 h^{-1}. A total feed of 975 mL was added in the whole process. Four major phases of the fed-batch fermentation could be distinguished. In the first (batch) phase *C. glutamicum* HalT2 grew to an OD_{600} of 37.3 within 18h. Lactate accumulated transiently peaking at 7.0 g L^{-1} after 10 h. At 18h, titers of 0.19 g L^{-1} 7-Br-Trp and 0.1 g L^{-1} Trp were observed. In the next phase (until 30 h when exponential feeding started), 7-Br-Trp was produced to a titer of 0.30 g L^{-1} with a yield on biomass of 0.7 mg $(gCDW)^{-1}$ and a volumetric productivity of 10 mg L^{-1} h^{-1}. Neither Trp nor Ant accumulated during this phase. The third phase is characterized by an exponential increase of the feed volume (at 50 h about 293 mL feed had been added and the OD_{600} reached 62), while the 7-Br-Trp concentration increased linearly to 0.66 g L^{-1}. During this phase the volumetric productivity was 18 mg g^{-1} h^{-1} and the specific productivity was 1 mg $gCDW^{-1}$ h^{-1}. While Trp accumulated to a titer of 0.17 g L^{-1}, Ant was not produced in the third phase. In the last phase that started at 50 h, the residual feed (682 mL) was added until 55 h. The 7-Br-Trp and Trp titers increased in parallel to 1.2 g L^{-1} and about 0.25 g L^{-1}. Only in this last phase, Ant accumulated with Ant titers fluctuating around 0.5 g L^{-1} from 57 h to 72 h (Fig. 2.2.8).

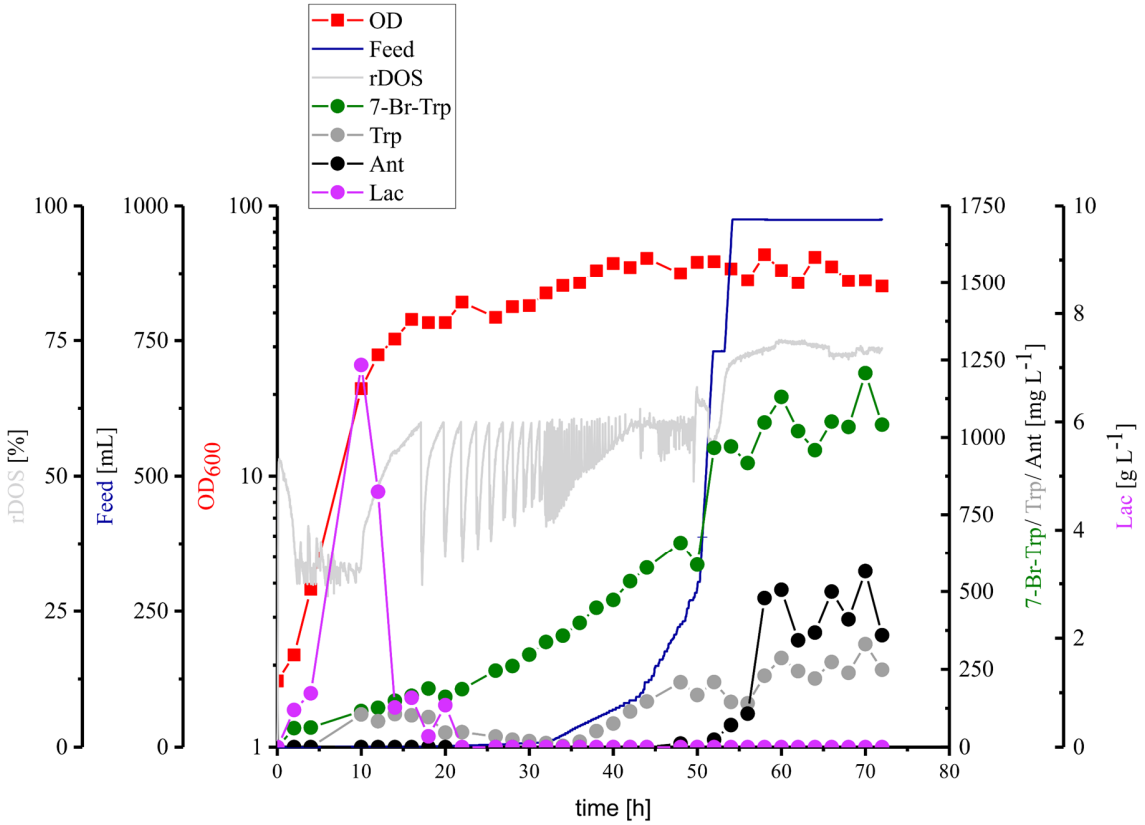

Fig. 2.2.8: Fed-batch fermentation of 7-Br-Trp by *C. glutamicum* HalT2. The data given include rDOS [%] [light grey], the feed [blue], OD_{600} [red squares], 7-Br-Trp [green circles], Trp [grey circles], Ant [black circles] and Lac [light purple circles]. The initial volume was 2 L and 975 mL feed was added. The titer was calculated to the initial volume.

2.2.5 Discussion

Heterologous expression of the genes *rebH* for FAD-dependent halogenase and *rebF* for NADH-dependent flavin reductase from the *reb* cluster of *L. aerocolonigenes* to enable regioselective chlorination of Trp at the 7 position (Nishizawa et al., 2005) in a Trp overproducing *C. glutamicum* strain (Purwanto et al., 2018) provided the basis for the development of fermentative processes for chlorination (Veldmann et al., 2019) and bromination of Trp (this study). Production of 7-Br-Trp by the engineered *C. glutamicum* strain was possible in glucose minimal media supplemented with sodium bromide.

C. glutamicum belongs to the group of bacteria that require chloride for growth at high (sodium) salt concentrations since growth was inhibited in the presence of high concentrations of sodium sulfate and sodium gluconate, but not of sodium chloride (Roeßler et al., 2003). It was postulated that chloride may enhance excretion of cytotoxic sodium ions by salt-induced Na^+/H^+ antiporters and/or simultaneous export of these anions via the ClC-type sodium channels as observed for *E. coli* (Iyer et al., 2002). The finding reported here that *C. glutamicum* can withstand high sodium bromide concentrations (K_i of about 1.2 M; Fig. 2.2.2 A) indicates that bromide may substitute for chloride to sustain growth of *C. glutamicum* at high sodium salt concentrations.

The engineered *C. glutamicum* strain produced 7-Br-Trp to higher titers (1.2 g L^{-1}, Fig. 2.2.8) than 7-Cl-Trp (0.1 g L^{-1}; (Veldmann et al., 2019). This was surprising since pure RebH prefers chlorination (k_{cat} of 1.4 min^{-1}) over bromination (k_{cat} of 0.4 min^{-1}) (Yeh et al., 2005). Unlike in enzyme catalysis with pure RebH (Yeh et al., 2005; Payne et al., 2013), chloride could not be completely replaced by bromide since chloride is required for growth of *C. glutamicum* (s. above). However, at a low chloride concentration in the growth medium a high bromide salt supply (277 fold excess) allowed for bromination by the engineered *C. glutamicum* strain *in vivo*. The purified product of this fermentative process was shown to be 7-Br-Trp without detectable contamination by 7-Cl-Trp (Fig. 2.2.7). Brominated natural products and intermediates are found predominantly in marine environments as ocean water contains a relatively high bromide ion concentration (Gribble, 1996). Moreover, halogenases which prefer bromination are more abundant in marine habitats, those preferring chlorination are encountered more often in terrestrial habitats (Van Peè, 2001). Thus, future process

improvement may make use of halogenases preferring bromination over chlorination such as BrvH from *Brevundimonas* BAL3 (Neubauer et al., 2018) or three halogenases from *Xanthomonas campestris* pv. campestris strain B10046 (Ismail et al., 2019).

FAD-dependent halogenases require molecular oxygen (Bitto et al., 2008). In the reaction catalyzed by RebH, $FADH_2$ binds to the FAD binding pocket of the RebH and reacts with molecular oxygen to flavin hydroperoxide (Andorfer et al., 2016). Flavin peroxide in turn oxidizes the halide anion (X^-, X = Cl, Br) to hypohalous acid (HOX), which is channeled to the active active tryptophan binding pocket. The role of the conserved lysine residue K79 in giving a haloamine intermediate (Yeh et al., 2007) is still under debate (Flecks et al., 2008). The hypohalous acid effects the regioselective electrophilic aromatic substitution of Trp resulting in halogenation at the C7 position (Andorfer et al., 2016). Thus, the supply of molecular oxygen to RebH within the *C. glutamicum* cell may be a bottleneck for halogenation of Trp. Since, of course, the *C. glutamicum* cell requires oxygen for respiration, the response to increased molecular oxygen supply during growth-coupled fermentative production of 7-Br-Trp may be complex. Production of 7-Br-Trp was found to be higher under low oxygen supply in shake flask (although these are relatively ill-defined) or comparable under controlled conditions in bioreactor fermentations with rDOS of 15, 30 and 60% (Fig. 2.2.4, Fig. 2.2.5). For different microorganisms the Monod constants for oxygen are in a range between $3.0 \cdot 10^{-4}$ mg L^{-1} and 0.1 mg L^{-1} (Longmuir, 1954) Therefore, cell growth was not notably affected by oxygen supply even at a rDOS level of 15%. Surprisingly, biomass formation was declined with increasing rDOS set points as shown by the courses of OD_{600} and glucose in figure 2.2.5. While glucose was depleted after 35 h for rDOS of 15% and 48 h for rDOS of 30%, respectively, nearly 4 g L^{-1} glucose remained at the end of cultivation (73 h) at a rDOS level of 60% also indicating a reduced biomass formation. However, halogenation by RebH-RebF requires molecular oxygen. Obviously, a better oxygen supply improves RebH-RebF activity, which counteracts biomass formation (see also max. OD_{600} values as given above). This conclusion is supported by lower specific growth rates during stirred tank reactor cultivation (see above) in contrast to shake flask cultivation (see above), despite a poorer oxygen input in the latter case. In addition, halogenation by RebH-RebF requires both molecular oxygen and NADH at the same time. This is difficult to

achieve in fast growing cells as NADH is oxidized by the respiratory chain using molecular oxygen to generate a trans-membrane pH gradient and subsequently ATP. Moreover, if the oxygen supply is too high flavin reductase RebF oxidizes $FADH_2$ with molecular oxygen to yield H_2O_2. This is commonly observed for flavin-dependent enzymes like monooxygenases and halogenases ("oxygen dilemma"; (Ismail et al., 2019)). Thus, all reactions in *C. glutamicum* requiring $FADH_2$ (e.g. *p*-hydroxybenzoate hydroxylase (Kwon et al., 2007) or flavin-dependent thymidylate synthase; (Kan et al., 2010)) or containing this flavin bound to the enzyme [e.g. membrane-associated malate dehydrogenase (acceptor) (EC 1.1.99.16); (Molenaar et al., 1998)] may be compromised at high oxygen levels in the presence of flavin reductase RebF. Thus, an aeration protocol ensuring optimal supply of oxygen for growth on the one hand and for RebH catalyzed bromination on the other hand remains to be developed. Another optimization step for the fermentative production of 7-Br-Trp, would be the reduction of by-products, like L-lactate. *C. glutamicum* produces L-lactate from pyruvate via the NAD-dependent L-lactate dehydrogenase (encoded by *ldhA*) (Inui et al., 2004b) and is able to utilize the L-lactate as carbon source via the lactate dehydrogenase (encoded by *lldD*) (Stansen et al., 2005). Transient L-lactate accumulation (formed by LdhA and subsequently utilize by LldD) is often observed when glucose uptake is higher than oxygen uptake. Once the glucose uptake rate ceases, L-lactate is re-utilized. Transcription of *ldhA* is regulated by transcriptional regulator SugR (Engels et al., 2008; Toyoda et al., 2009). Under oxygen limitation glucose uptake exceeds oxygen uptake and L-lactate is produced by LdhA to regenerate NAD^+ (Engels et al., 2008). Accordingly, transient L-lactate was more pronounced with low (rDOS of 15%, 30% and fed-batch) as compared to high oxygen supply (rDOS of 60%). We have discussed these facts along with a strategy to avoid transient lactate formation, i.e., by deletion of *ldhA* as has been shown before (Inui et al., 2004b).

Inhibition by halogenated Trp appeared to be the major bottleneck to achieve high product titers. Growth as well as anthranilate phosphoribosyltransferase activity in crude extracts from *C. glutamicum* Tp679 (pCES208-*trpD*) were inhibited by 7-Br-Trp and 7-Cl-Trp (Fig. 2.2.3 and (Veldmann et al., 2019)). When comparing growth and 7-Br-Trp production in CGXII and HSG media, the latter of which is a complex medium and contains about 0.5 mM Trp (data not shown), the specific growth rate in rich medium was two-fold higher than in

CGXII medium (0.39 h^{-1} for HSG medium vs. 0.19 h^{-1} for CGXII medium, s. results section). Thus, addition of Trp may alleviate the growth inhibition as consequence of TrpD inhibition. Previously, O'Gara & Dunican (O'Gara and Dunican, 1995) have shown that purified anthranilate phosphoribosyltransferase TrpD from *C. glutamicum* is inhibited by Trp (K_i of 0.83 mM) and by 5-methyl-L-tryptophan (K_i of 0.32 mM). In this study, anthranilate phosphoribosyltransferase activity in crude extracts was shown to be inhibited by 7-Br-Trp (K_i of about 0.1 mM) and by 7-Cl-Trp (K_i of about 0.06 mM). It should be noted that besides endogenous *trpD* on the *C. glutamicum* chromosome *E. coli trpD* was expressed from a plasmid. TrpD from *E. coli* is insensitive to Trp in the absence of *E. coli* TrpE (Ito and Yanofsky, 1969). Feedback resistant TrpD has been isolated from *C. glutamicum,* which was isolated from a tyrosine and phenylalanine double auxotrophic strain due to its resistance to analogs of Trp, tyrosine, phenylalanine and 5-methyl-L-tryptophan. Feedback resistant TrpD from this *C. glutamicum* strain was shown to confer resistance to 5-methyl-L-tryptophan and 6-fluoro-L-tryptophan on *E. coli* (Herry and Dunican, 1993*)*. Resistance to Trp derivatives with modifications at the 7 position of Trp such as 7-Br-Trp or 7-Cl-Trp has not been determined, thus, it cannot be inferred that the feedback resistant TrpD from *C. glutamicum* ATCC 21850 would alleviate the inhibition of *C. glutamicum* growth and/or TrpD activity by 7-Br-Trp and 7-Cl-Trp. Likely, other TrpD variants either from *C. glutamicum* or from *E. coli* have to be isolated after mutation and screening or by rational enzyme engineering. Alternatively, process intensification may involve fermentation strategies including *in situ* product removal (ISPR) to maintain sub-threshold concentrations of 7-Br-Trp as has been shown for L-phenylalanine separation and concentration by reactive-extraction with liquid-liquid centrifuges in a fed-batch fermentation process with recombinant *E. coli* (Rüffer et al., 2004).

Halogenated amino acids such as 7-Br-Trp are relevant for peptide synthesis, since they can be converted further by Pd-catalyzed cross coupling and nucleophilic substitution reactions (Diederich and Stang, 2008). Various halogenated forms of tryptophan and its derivatives may have potential in the synthesis of serotonin and melatonin agonists or antagonists (Frese et al., 2014). As shown here, based on the insight from enzyme catalysis using pure RebH, crude RebH preparations or CLEAs containing RebH, a fermentative process based on RebH

was developed and adjusted to yield either 7-Cl-Trp or 7-Br-Trp by *C. glutamicum in vivo*. Since halogenases such as RebH, PrnA or BrvH differ in their substrate spectra and regioselectivities, the fermentative approach holds the potential to be extended for various halogenation processes starting from glucose and halide salts *in vivo* provided that the halogenated products do not interfere with vital cellular functions and can be exported out of the cell efficiently.

2.2.6 References

Adams, J. (2004). Proteasome inhibitors in cancer therapy, in Cancer Chemoprevention. Springer. 635-642.

Andorfer, M.C., Park, H.J., Vergara-Coll, J., and Lewis, J.C. (2016). Directed evolution of RebH for catalyst-controlled halogenation of indole C–H bonds. Chem. Sci. 7**,** 3720-3729. doi:10.1039/C5SC04680G.

Bartoli, G., Dalpozzo, R., and Nardi, M. (2014). Applications of Bartoli indole synthesis. Chem. Soc. Rev. 43**,** 4728-4750. doi:10.1039/b000000x

Becker, J., Kuhl, M., Kohlstedt, M., Starck, S., and Wittmann, C. (2018). Metabolic engineering of *Corynebacterium glutamicum* for the production of *cis*, *cis*-muconic acid from lignin. Microb. Cell. Fact. 17**,** 115. doi:10.1186/s12934-018-0963-2.

Bittner, S., Scherzer, R., and Harlev, E. (2007). The five bromotryptophans. Amino acids. 33**,** 19-42. doi:10.1007/s00726-006-0441-8.

Bitto, E., Huang, Y., Bingman, C.A., Singh, S., Thorson, J.S., and Phillips, G.N. (2008). The structure of flavin-dependent tryptophan 7-halogenase RebH. Proteins: Struct., Funct., Bioinf. 70**,** 289-293. doi:10.1002/prot.21627.

Blombach, B., Riester, T., Wieschalka, S., Ziert, C., Youn, J.-W., Wendisch, V.F., et al. (2011). *Corynebacterium glutamicum* tailored for efficient isobutanol production. Appl. Environ. Microbiol. 77**,** 3300-3310. doi:10.1128/AEM.02972-10.

Bradford, M.M. (1976). A rapid and sensitive method for the quantitation of microgram quantities of protein utilizing the principle of protein-dye binding. Anal. Biochem. 72**,** 248-254. doi:10.1016/0003-2697(76)90527-3.

Bückle-Vallant, V., Krause, F.S., Messerschmidt, S., and Eikmanns, B.J. (2014). Metabolic engineering of *Corynebacterium glutamicum* for 2-ketoisocaproate production. Appl. Microbiol. Biotechnol. 98**,** 297-311. doi:10.1007/s00253-013-5310-2.

Corr, M.J., Sharma, S.V., Pubill-Ulldemolins, C., Bown, R.T., Poirot, P., Smith, D.R.M., et al. (2017). Sonogashira diversification of unprotected halotryptophans, halotryptophan containing tripeptides; and generation of a new to nature bromo-natural product and its diversification in water. Chem. Sci. 8**,** 2039-2046. doi:10.1039/C6SC04423A.

Diederich, F., and Stang, P.J. (2008). Metal-Catalyzed Cross-Coupling Reactions. Wiley. doi:DOI:10.1002/9783527619535.

Eggeling, L., and Bott, M. (2005). Handbook of *Corynebacterium glutamicum.* CRC press.

Engels, V., Lindner, S.N., and Wendisch, V.F. (2008). The global repressor SugR controls expression of genes of glycolysis and of the L-lactate dehydrogenase LdhA in *Corynebacterium glutamicum*. J. Bacteriol. 190**,** 8033-8044. doi:10.1128/JB.00705-08.

Flecks, S., Patallo, E.P., Zhu, X., Ernyei, A.J., Seifert, G., Schneider, A., et al. (2008). New insights into the mechanism of enzymatic chlorination of tryptophan. Angew Chem Int Ed Engl. 47**,** 9533-9536. doi:10.1002/anie.200802466.

Frese, M., Guzowska, P.H., Voss, H., and Sewald, N. (2014). Regioselective Enzymatic Halogenation of Substituted Tryptophan Derivatives using the FAD-Dependent Halogenase RebH. ChemCatChem. 6**,** 1270-1276. doi:10.1002/cctc.201301090.

Frese, M., and Sewald, N. (2015). Enzymatic Halogenation of Tryptophan on a Gram Scale. Angew. Chem. Int. Ed. 54**,** 298-301. doi:10.1002/anie.201408561.

Gribble, G.W. (1996). Naturally occuring organohalogen compounds—a comprehensive survery, in Progress in the chemistry of organic natural products. Springer. 1-423.

Gruß, H., Belu, C., Bernhard, L.M., Merschel, A., and Sewald, N. (2019). Fluorogenic Diversification of Unprotected Bromotryptophan by Aqueous Mizoroki–Heck Cross-Coupling. Chem. Eur. J. 25**,** 5880-5883. doi:10.1002/chem.201900437.

Hanahan, D. (1983). Studies on transformation of *Escherichia coli* with plasmids. J. Mol. Biol. 166**,** 557-580. doi:10.1016/S0022-2836(83)80284-8.

Herry, D.M., and Dunican, L.K. (1993). Cloning of the *trp* gene cluster from a tryptophan-hyperproducing strain of *Corynebacterium glutamicum*: identification of a mutation in the *trp* leader sequence. Appl. Environ. Microbiol. 59**,** 791-799.

Inui, M., Kawaguchi, H., Murakami, S., Vertès, A.A., and Yukawa, H. (2004a). Metabolic engineering of *Corynebacterium glutamicum* for fuel ethanol production under oxygen-deprivation conditions. J. Mol. Microbiol. Biotechnol. 8**,** 243-254. doi:10.1159/000086705.

Inui, M., Murakami, S., Okino, S., Kawaguchi, H., Vertès, A.A., and Yukawa, H. (2004b). Metabolic analysis of *Corynebacterium glutamicum* during lactate and succinate productions under oxygen deprivation conditions. J. Mol. Microbiol. Biotechnol. 7**,** 182. doi:10.1159/000079827.

Ismail, M., Frese, M., Patschkowski, T., Ortseifen, V., Niehaus, K., and Sewald, N. (2019). Flavin-Dependent Halogenases from *Xanthomonas campestris* pv. campestris B100 Prefer Bromination over Chlorination. Adv. Synth. Catal. doi:10.1002/adsc.201801591.

Ito, J., and Yanofsky, C. (1969). Anthranilate synthetase, an enzyme specified by the tryptophan operon of *Escherichia coli*: Comparative studies on the complex and the subunits. J. Bacteriol. 97**,** 734-742.

Iyer, R., Iverson, T.M., Accardi, A., and Miller, C. (2002). A biological role for prokaryotic ClC chloride channels. Nature. 419**,** 715. doi:10.1038/nature01000.

Jorge, J.M.P., Leggewie, C., and Wendisch, V.F. (2016). A new metabolic route for the production of gamma-aminobutyric acid by *Corynebacterium glutamicum* from glucose. Amino acids. 48**,** 2519-2531. doi:10.1007/s00726-016-2272-6.

Jorge, J.M.P., Pérez-García, F., and Wendisch, V.F. (2017). A new metabolic route for the fermentative production of 5-aminovalerate from glucose and alternative carbon sources. Bioresour. Technol. 245**,** 1701-1709. doi:10.1016/j.biortech.2017.04.108.

Kallscheuer, N., and Marienhagen, J. (2018). *Corynebacterium glutamicum* as platform for the production of hydroxybenzoic acids. Microb. Cell. Fact. 17**,** 70. doi:10.1186/s12934-018-0923-x.

Kan, S.-C., Liu, J.-S., Hu, H.-Y., Chang, C.-M., Lin, W.-D., Wang, W.-C., et al. (2010). Biochemical characterization of two thymidylate synthases in *Corynebacterium glutamicum* NCHU 87078. Biochim. Biophys. Acta (BBA)-Proteins and Proteomics 1804**,** 1751-1759. doi:10.1016/j.bbapap.2010.05.006.

Kim, H.T., Baritugo, K.-A., Oh, Y.H., Hyun, S.M., Khang, T.U., Kang, K.H., et al. (2018). Metabolic engineering of *Corynebacterium glutamicum* for the high-level production of cadaverine that can be used for the synthesis of biopolyamide 510. ACS Sustain. Chem. Eng. 6**,** 5296-5305. doi:10.1021/acssuschemeng.8b00009.

Kim, J.Y., Lee, Y.A., Wittmann, C., and Park, J.B. (2013). Production of non-proteinogenic amino acids from α-keto acid precursors with recombinant *Corynebacterium glutamicum*. Biotechnol. Bioeng. 110**,** 2846-2855. doi:10.1002/bit.24962.

Koguchi, Y., Kohno, J., Nishio, M., Takahashi, K., Okuda, T., Ohnuki, T., et al. (2000). TMC-95A, B, C, and D, novel proteasome inhibitors produced by *Apiospora montagnei* Sacc. TC 1093. J. Antibiot. 53**,** 105-109. doi:10.7164/antibiotics.53.105.

Krause, F.S., Blombach, B., and Eikmanns, B.J. (2010). Metabolic engineering of *Corynebacterium glutamicum* for 2-ketoisovalerate production. Appl. Environ. Microbiol. 76**,** 8053-8061. doi:10.1128/AEM.01710-10.

Kwon, S.Y., Kang, B.S., Kim, G.H., and Kim, K.J. (2007). Expression, purification, crystallization and initial crystallographic characterization of the p-hydroxybenzoate hydroxylase from *Corynebacterium glutamicum*. Acta Cryst. Section F: Structural Biology and Crystallization Communications 63**,** 944-946. doi:10.1107/S1744309107046386.

Latham, J., Brandenburger, E., Shepherd, S.A., Menon, B.R.K., and Micklefield, J. (2017). Development of halogenase enzymes for use in synthesis. Chem. Rev. 118**,** 232-269. doi:10.1021/acs.chemrev.7b00032.

Lee, J.-H., and Wendisch, V.F. (2017). Biotechnological production of aromatic compounds of the extended shikimate pathway from renewable biomass. J. Biotechnol. 257**,** 211-221. doi:10.1016/j.jbiotec.2016.11.016.

Lesic, B., Lépine, F., Déziel, E., Zhang, J., Zhang, Q., Padfield, K., et al. (2007). Inhibitors of pathogen intercellular signals as selective anti-infective compounds. PLoS Pathog. 3**,** e126. doi:10.1371/journal.ppat.0030126.

Leßmeier, L., and Wendisch, V.F. (2015). Identification of two mutations increasing the methanol tolerance of *Corynebacterium glutamicum*. BMC Microbiol. 15**,** 216. doi:10.1186/s12866-015-0558-6.

Litsanov, B., Kabus, A., Brocker, M., and Bott, M. (2012). Efficient aerobic succinate production from glucose in minimal medium with *Corynebacterium glutamicum*. Microb Biotechnol. 5**,** 116-128. doi:10.1111/j.1751-7915.2011.00310.x.

Longmuir, I.S. (1954). Respiration rate of bacteria as a function of oxygen concentration. Biochem. J. 57**,** 81. doi:10.1042/bj0570081.

Ma, W., Wang, J., Li, Y., Yin, L., and Wang, X. (2018). Poly (3-hydroxybutyrate-co-3-hydroxyvalerate) co-produced with L-isoleucine in *Corynebacterium glutamicum* WM001. Microb. Cell. Fact. 17**,** 93. doi:10.1186/s12934-018-0942-7.

Mindt, M., Risse, J.M., Gruß, H., Sewald, N., Eikmanns, B.J., and Wendisch, V.F. (2018). One-step process for production of *N*-methylated amino acids from sugars and methylamine using recombinant *Corynebacterium glutamicum* as biocatalyst. Sci. Rep. 8**,** 12895. doi:10.1038/s41598-018-31309-5.

Molenaar, D., van der Rest, M.E., and Petrović, S. (1998). Biochemical and genetic characterization of the membrane-associated malate dehydrogenase (acceptor) from *Corynebacterium glutamicum*. Eur. J. Biochem. 254**,** 395-403. doi:10.1046/j.1432-1327.1998.2540395.x.

Neubauer, P.R., Widmann, C., Wibberg, D., Schröder, L., Frese, M., Kottke, T., et al. (2018). A flavin-dependent halogenase from metagenomic analysis prefers bromination over chlorination. PloS One 13**,** e0196797. doi:10.1371/journal.pone.0196797.

Nicolaou, K.C., Bella, M., Chen, D.Y.K., Huang, X., Ling, T., and Snyder, S.A. (2002). Total synthesis of diazonamide A. Angew. Chem. Int. Ed. 41**,** 3495-3499. doi:10.1002/1521-3773(20020916)41:18<3495::AID-ANIE3495>3.0.CO;2-7.

Nishizawa, T., Aldrich, C.C., and Sherman, D.H. (2005). Molecular analysis of the rebeccamycin L-amino acid oxidase from *Lechevalieria aerocolonigenes* ATCC 39243. J. Bacteriol. 187**,** 2084-2092. doi:10.1128/JB.187.6.2084-2092.2005.

O'Gara, J.P., and Dunican, L.K. (1995). Mutations in the *trpD* gene of *Corynebacterium glutamicum* confer 5-methyltryptophan resistance by encoding a feedback-resistant anthranilate phosphoribosyltransferase. Appl. Environ. Microbiol. 61**,** 4477-4479.

Parte, A. (2012). Bergey's manual of systematic bacteriology: Volume 5: The actinobacteria. Springer Science & Business Media.

Payne, J.T., Andorfer, M.C., and Lewis, J.C. (2013). Regioselective Arene Halogenation using the FAD-Dependent Halogenase RebH. Angew. Chem. 125**,** 5379-5382. doi:10.1002/anie.201300762.

Pérez-García, F., Peters-Wendisch, P., and Wendisch, V.F. (2016). Engineering *Corynebacterium glutamicum* for fast production of L-lysine and L-pipecolic acid. Appl. Microbiol. Biotechnol. 100**,** 8075-8090. doi:10.1007/s00253-016-7682-6.

Purwanto, H.S., Kang, M.-S., Ferrer, L., Han, S.-S., Lee, J.-Y., Kim, H.-S., et al. (2018). Rational engineering of the shikimate and related pathways in *Corynebacterium glutamicum* for 4-hydroxybenzoate production. J. Biotechnol. doi:10.1016/j.jbiotec.2018.07.016.

Roeßler, M., Sewald, X., and Müller, V. (2003). Chloride dependence of growth in bacteria. FEMS Microbiol. Lett. 225**,** 161-165. doi:10.1016/S0378-1097(03)00509-3.

Rohles, C.M., Gießelmann, G., Kohlstedt, M., Wittmann, C., and Becker, J. (2016). Systems metabolic engineering of *Corynebacterium glutamicum* for the production of the carbon-5 platform chemicals 5-aminovalerate and glutarate. Microb. Cell. Fact. 15**,** 154. doi:10.1186/s12934-016-0553-0.

Roy, A.D., Goss, R.J.M., Wagner, G.K., and Winn, M. (2008). Development of fluorescent aryltryptophans by Pd mediated cross-coupling of unprotected halotryptophans in water. Chem. Commun.**,** 4831-4833. doi:10.1039/B807512C.

Rüffer, N., Heidersdorf, U., Kretzers, I., Sprenger, G.A., Raeven, L., and Takors, R. (2004). Fully integrated L-phenylalanine separation and concentration using reactive-extraction with liquid-liquid centrifuges in a fed-batch process with *E. coli*. Bioprocess Biosyst. Eng. 26**,** 239-248. doi:10.1007/s00449-004-0354-4.

Sakai, S., Tsuchida, Y., Okino, S., Ichihashi, O., Kawaguchi, H., Watanabe, T., et al. (2007). Effect of lignocellulose-derived inhibitors on growth of and ethanol production by growth-arrested *Corynebacterium glutamicum* R. Appl. Environ. Microbiol. 73**,** 2349-2353. doi:10.1128/AEM.02880-06.

Schneider, J., Niermann, K., and Wendisch, V.F. (2011). Production of the amino acids L-glutamate, L-lysine, L-ornithine and L-arginine from arabinose by recombinant *Corynebacterium glutamicum*. J. Biotechnol. 154**,** 191-198. doi:10.1016/j.jbiotec.2010.07.009.

Schneider, J., and Wendisch, V.F. (2010). Putrescine production by engineered *Corynebacterium glutamicum*. Appl. Microbiol. Biotechnol. 88**,** 859-868. doi:10.1007/s00253-010-2778-x.

Schnepel, C., and Sewald, N. (2017). Enzymatic Halogenation: A Timely Strategy for Regioselective C− H Activation. Chem. Eur. J. 23**,** 12064-12086. doi:10.1002/chem.201701209

Siebert, D., and Wendisch, V.F. (2015). Metabolic pathway engineering for production of 1, 2-propanediol and 1-propanol by *Corynebacterium glutamicum*. Biotechnol. Biofuels 8**,** 91. doi:10.1186/s13068-015-0269-0.

Sonogashira, K. (2002). Development of Pd–Cu catalyzed cross-coupling of terminal acetylenes with sp^2-carbon halides. J. Organomet. Chem. 653**,** 46-49. doi:10.1016/S0022-328X(02)01158-0.

Stansen, C., Uy, D., Delaunay, S., Eggeling, L., Goergen, J.-L., and Wendisch, V.F. (2005). Characterization of a *Corynebacterium glutamicum* lactate utilization operon induced during temperature-triggered glutamate production. Appl. Environ. Microbiol. 71**,** 5920-5928. doi:10.1128/AEM.71.10.5920-5928.2005.

Tateno, T., Okada, Y., Tsuchidate, T., Tanaka, T., Fukuda, H., and Kondo, A. (2009). Direct production of cadaverine from soluble starch using *Corynebacterium glutamicum* coexpressing α-amylase and lysine decarboxylase. Appl. Microbiol. Biotechnol. 82**,** 115. doi:10.1007/s00253-008-1751-4.

Toyoda, K., Teramoto, H., Inui, M., and Yukawa, H. (2009). The *ldhA* gene, encoding fermentative L-lactate dehydrogenase of *Corynebacterium glutamicum*, is under the control of positive feedback regulation mediated by LldR. J. Bacteriol. 191**,** 4251-4258. doi:10.1128/JB.00303-09.

Van Peè, K.-H. (2001). Microbial biosynthesis of halometabolites. Arch. Microbiol. 175**,** 250-258.

Veldmann, K.H., Minges, H., Sewald, N., Lee, J.-H., and Wendisch, V.F. (2019). Metabolic engineering of *Corynebacterium glutamicum* for the fermentative production of halogenated tryptophan. J. Biotechnol. 291**,** 7-16. doi:10.1016/j.jbiotec.2018.12.008.

Vergnolle, N. (2016). Protease inhibition as new therapeutic strategy for GI diseases. Gut. 65**,** 1215-1224. doi:10.1136/gutjnl-2015-309147.

Wang, G., Shang, L., Burgett, A.W.G., Harran, P.G., and Wang, X. (2007). Diazonamide toxins reveal an unexpected function for ornithine δ-amino transferase in mitotic cell division. Proc. Natl. Acad. Sci. 104**,** 2068-2073. doi:10.1073/pnas.0610832104.

Wang, X., Khushk, I., Xiao, Y., Gao, Q., and Bao, J. (2018). Tolerance improvement of *Corynebacterium glutamicum* on lignocellulose derived inhibitors by adaptive evolution. Appl. Microbiol. Biotechnol. 102**,** 377-388. doi:10.1007/s00253-017-8627-4.

Wendisch, V.F. (2019). Metabolic engineering advances and prospects for amino acid production. Metab. Eng. doi:10.1016/j.ymben.2019.03.008.

Wendisch, V.F., Jorge, J.M.P., Pérez-García, F., and Sgobba, E. (2016). Updates on industrial production of amino acids using *Corynebacterium glutamicum*. World J. Microbiol. Biotechnol. 32**,** 1-10. doi:10.1007/s11274-016-2060-1.

Wieschalka, S., Blombach, B., and Eikmanns, B.J. (2012). Engineering *Corynebacterium glutamicum* for the production of pyruvate. Appl. Microbiol. Biotechnol. 94**,** 449-459. doi:10.1007/s00253-011-3843-9.

Willemse, T., Schepens, W., Vlijmen, H., Maes, B., and Ballet, S. (2017). The Suzuki–Miyaura Cross-Coupling as a Versatile Tool for Peptide Diversification and Cyclization. Catalysts 7**,** 74. doi:10.3390/catal7030074.

Yeh, E., Blasiak, L.C., Koglin, A., Drennan, C.L., and Walsh, C.T. (2007). Chlorination by a Long-Lived Intermediate in the Mechanism of Flavin-Dependent Halogenases. Biochem. 46**,** 1284-1292. doi:10.1021/bi0621213.

Yeh, E., Garneau, S., and Walsh, C.T. (2005). Robust in vitro activity of RebF and RebH, a two-component reductase/halogenase, generating 7-chlorotryptophan during rebeccamycin biosynthesis. Proc. Natl. Acad. Sci. U. S. A. 102**,** 3960-3965. doi:10.1073/pnas.0500755102.

2.3 Fermentative production of halogenated L-tryptophan by recombinant *Corynebacterium glutamicum* using feedback resistant anthranilate phosphoribosyltransferases

Kareen H. Veldmann[a], Jin-Ho Lee[b], Volker F. Wendisch[a]

[a] Genetics of Prokaryotes, Faculty of Biology & CeBiTec, Bielefeld University, Universitätsstr. 25, 33615 Bielefeld, Germany

[b] Major in Food Science & Biotechnology, School of Food Biotechnology & Nutrition, BB21+, Kyungsung University, 309, Suyeong-ro, Nam-gu, Busan 48434, Republic of Korea

2.3.1 Abstract

Halogenated amino acids, like 7-chloro-L-tryptophan (7-Cl-Trp) and 7-bromo-L-tryptophan (7-Br-Trp), are important building blocks of bioactive compounds, like the antitumor antibiotic rebeccamycin or the 20S-proteasome inhibitor TMC-95A. They have various applications in the pharmaceutical, chemical and agrochemical industries. The chemical halogenation process is characterized as hazardous and highly toxic. In our previous study, we established an environmental friendly bacterial fermentation process for the production of 7-Cl-Trp and 7-Br-Trp with *Corynebacterium glutamicum*. But the production was limited because the anthranilate phosphoribosyltransferase (TrpD) the second enzyme in L-tryptophan (Trp) biosynthesis was feedback inhibited by halogenated Trp. TrpD catalyzes the transfer of the phosphoribosyl group of 5-phospho-α-D-ribose 1-diphosphate to anthranilate (Ant) to yield *N*-(5-phospho-β-D-ribosyl)-anthranilate. Hence, due to the inhibition Ant accumulates and the production of Trp was decreased. To prevent the accumulation of Ant, six TrpDs were investigated regarding their resistance towards Trp and its halogenated derivatives. Integration of the TrpDs into an Ant overproducing *C. glutamicum* strain resulted in complete conversion of Ant by four TrpDs. Additionally, the TrpDs were overexpressed in an Ant overproducing *C. glutamicum* strain overexpressing

the genes for the FAD-dependent halogenase RebH and NADH-dependent flavin reductase RebF which are responsible for the halogenation of Trp. During the fermentative production of halogenated Trp derivatives, four strains completely converted the Ant, although 0.3 g L^{-1} 7 Cl-Trp or 0.5 g L^{-1} 7-Br-Trp were present. Hence, the TrpDs of *E. coli*, *E. coli* mutant (S319T), *Bacillus subtilis* and *Bacillus subtilis* subsp. *spizizenii* show higher resistance to Trp and the halogenated derivatives.

2.3.2 Introduction

Halogenated compounds, like 7-chloro-L-tryptophan (7-Cl-Trp) and 7-bromo-L-tryptophan (7-Br-Trp), are important intermediates in the pharmaceutical, chemical and agrochemical industries (Diederich and Stang, 2008). More than 5000 naturally occurring halogenated compounds are known, like the antitumor antibiotic rebeccamycin and 20S-proteasome inhibitor TMC-95 (Koguchi et al., 2000; Onaka et al., 2003; Nishizawa et al., 2005; Gribble, 2012). 7-Cl-Trp and 7-Br-Trp are the precursors of rebeccamycin and TMC-95. For the synthesis of halogenated L-tryptophan the FAD-dependent halogenase RebH and the NADH-dependent flavin reductase RebF from *Lechevalieria aerocolonigenes* are required (Nishizawa et al., 2005; Yeh et al., 2005). By cross-linked enzyme aggregates containing RebH, RebF, and an alcohol dehydrogenase the halogenation of L-tryptophan (Trp) in gram-scale was established (Frese and Sewald, 2015). In our previous study, fermentative production of 7-Cl-Trp and 7-Br-Trp by metabolically engineered *Corynebacterium glutamicum* was established yet production was limited by product inhibition of the anthranilate phosphoribosyltransferase (TrpD, [EC:2.4.2.18]) an enzyme of the Trp biosynthesis (Veldmann et al., 2019a; Veldmann et al., 2019b).

The biosynthesis of Trp consists of two consecutively connected pathways: the shikimate pathway and the Trp pathway. In both pathways, genes are feedback regulated to prohibit the overproduction of the products (Fig 2.3.1 A). The feedback regulation of the Trp biosynthesis pathway has been investigated in the last decades (Hagino and Nakayama, 1975b; O'Gara and Dunican, 1995). Product feedback inhibition was observed for the anthranilate synthase

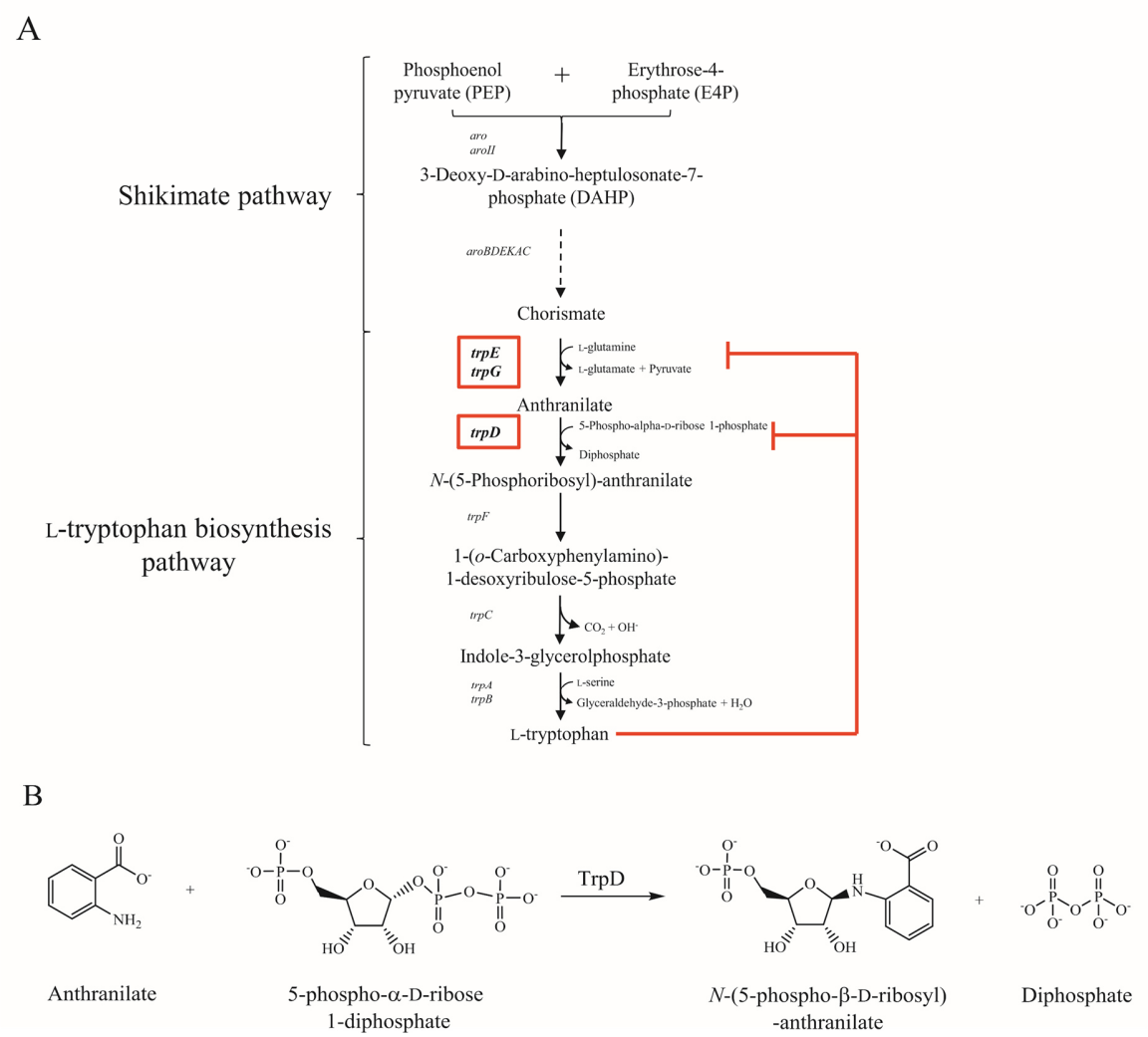

Figure 2.3.1: Schematic overview of the Trp biosynthesis of *C. glutamicum* and the TrpD reaction. A: The Trp biosynthesis consists of the shikimate and the Trp pathway. The enzymes TrpE, TrpG, and TrpD are feedback inhibited by Trp (red lines). **B:** The TrpD transfers the phosphoribosyl group of the 5-phospho-α-D-ribose 1-diphosphate (PRPP) to Ant and built *N*-(5-phospho-β-D-ribosyl)-anthranilate and diphosphate. Abbreviations: 3-deoxy-D-arabino-heptulosonate 7-phosphate synthase (encoded by *aro*, *aroII*), 3-dehydroquinate synthase (encoded by *aroB*), 3-dehydroquinate dehydratase (encoded by *aro*D), NADPH-dependent shikimate dehydrogenase (encoded by *aro*E), shikimate kinase (encoded by *aroK*), 5-enolpyruvylshikimate 3-phosphate synthase (encoded by *aro*A), chorismate synthase (encoded by *aroC*), anthranilate synthase (encoded by *trpE, trpG*), anthranilate phosphoribosyltransferase (encoded by *trpD*), phosphoribosyl anthranilate isomerase (encoded by *trpF*), indole-3-glycerol phosphate synthase (encoded by *trpC*), tryptophan synthase (encoded by *trpA, trpB*). Dashed lines symbolize several enzymatic steps.

component I and II [EC:4.1.3.27] (encoded by *trpE* and *trpG*) and for TrpD. The first step in the Trp biosynthesis is catalyzed by TrpE and TrpG, which convert chorismate and L-glutamine to anthranilate (Ant), L-glutamate, and pyruvate (Tamir and Srinivasan, 1970). The second enzyme TrpD catalyzes the second step of the Trp biosynthesis and transfers a phosphoribosyl group to Ant to build *N*-(5-phospho-β-D-ribosyl)-anthranilate (Lambrecht and Downs, 2012) (Fig. 2.3.1 B). In some microorganisms, like *E. coli* the TrpE, TrpG, and TrpD are arranged in a protein complex. In this complex, only the TrpE is inhibited, however, this has an inhibitory effect on the whole complex (Ito and Yanofsky, 1969). When the TrpD of *E. coli* arises alone (without TrpE and TrpG) activity was observed and additionally lower inhibition by Trp was revealed (Ito and Yanofsky, 1969). But not only Trp inhibits TrpD, the substrate Ant, 3-hydroxyanthranilate or 5-methylantranilate can inhibit the enzyme likewise (Bode and Birnbaum, 1978; O'Gara and Dunican, 1995).

Moreover, in our previous study, we observed inhibition of TrpD by other compounds, like the halogenated Trp derivatives, 7-Cl-Trp, and 7-Br-Trp (Veldmann et al., 2019a; Veldmann et al., 2019b). This inhibitory effect of TrpD from *E. coli* could be observed *in vitro* as well as *in vivo*. Hence, a TrpD resistant to Trp and its derivatives was needed to ensure the complete conversion of Ant and enhance the precursor supply for the halogenation of Trp. Analysis of Trp producing strains or strains with higher resistance for Trp and its derivatives revealed higher resistance of the Trp proteins to these substances. In the 5-fluoro-tryptophan resistant *Bacillus subtilis* mutant strain FT-39 the TrpE showed a 280-fold higher activity compared to the enzyme from the *Bacillus subtilis* wildtype strain Tr-44, which is not resistant to 5-fluoro-tryptophan (Shiio et al., 1973). Additionally, the resistant *B. subtilis* FT-39 showed the highest Trp production of 2 g L^{-1}. A similar effect was observed for a 5-fluoro-tryptophan resistant *C. glutamicum* mutant strain, in which the specific enzyme activity of the TrpE and TrpD was increased 29-fold and 23-fold, respectively, compared to the parental strain (Matsui et al., 1987). The difference in the *trp* operon sequence consisted of one base-pair exchanges in the *trpE* coding sequence and one in the attenuator sequence of the *trp* operon. The 5-fluoro-tryptophan resistance could be transferred to another *E. coli* strain by integration of the mutated *trpE* gene from *C. glutamicum* (Matsui et al., 1987). Furthermore, it was shown, that the TrpD of a 5-methyl-tryptophan resistant *C. glutamicum*

ATCC 21850 was less feedback inhibited by Trp and 5-methyl-tryptophan (O'Gara and Dunican, 1995).

Here, we tested different TrpDs regarding their resistance to Trp, 7-Cl-Trp, and 7-Br-Trp. Mutations, deriving from Trp derivative resistant *C. glutamicum* strains, were transferred to the TrpDs of *C. glutamicum* ATCC 13032 and *E. coli* K-12. The crystal structure of the mutated and the wildtype TrpDs with ligand were predicted (Coach-D, Phyre 2). The conversion of Ant was proven in a Trp, 7-Cl-Trp and 7-Br-Trp production experiment in *C. glutamicum*.

For this approach, we choose the Ant overproducing *C. glutamicum* strain Tp679 (Purwanto et al., 2018). To increase the Ant production genetic modifications were performed: a feedback resistant 3-deoxy-D-arabino-heptulosonate 7-phosphate synthase gene (*aroG*) from *E. coli* was overexpressed to optimize the precursor supply. Further, to prevent the by-product formation of the aromatic amino acids L-phenylalanine and L-tyrosine the chorismate mutase encoded by *csm* was deleted. The feedback resistant *trpE* encoding the anthranilate synthase component I from *C. glutamicum* was overexpressed to channel the flux to Ant. To enable the production of halogenated Trp the genes for the FAD-dependent halogenase RebH and the NADH dependent flavin reductase RebH from *L. aerocolonigenes* were overexpressed in *C. glutamicum*.

2.3.3 Material and Methods

2.3.3.1 Bacterial strains and growth conditions

Bacterial strains and plasmids used in this study are listed in Table 2.3.1. *Escherichia coli* DH5α (Hanahan, 1983) was used for cloning the plasmid constructs. *E. coli* and *C. glutamicum* were regularly grown in lysogeny broth (LB) in 500 mL baffled flasks at 120 rpm at 37 °C or 30 °C, respectively. For growth and production experiments *C. glutamicum* was inoculated in CGXII minimal medium (Eggeling and Bott, 2005) in 100 mL (filling volume 10%) to an optical density (OD_{600}) of 1 and incubated at 120 rpm. Growth was monitored by measuring the optical density at 600 nm using a V-1200 spectrophotometer (VWR, Radnor, PA, USA). To produce 7-Br-Trp, 7-Cl-Trp, and Trp, CGXII minimal medium supplemented with 50 mM NaBr or 50 mM $CaCl_2$ was used. Strains derived from Tp679 were supplemented additionally with 1.37 mM L-tyrosine and 1.5 mM L-phenylalanine in minimal medium. If necessary, the growth medium was supplemented with spectinomycin (100 µg mL^{-1}) and/or tetracycline (5 µg mL^{-1}). Isopropyl-β-D-1-thiogalactopyranoside (IPTG) (1 mM) was added to induce the gene expression from the vectors pECXT99A (Kirchner and Tauch, 2003) or pEKEx3 (Stansen et al., 2005).

Table 2.3.1: List of strains and plasmids used in this work.

Strains and plasmids	Description	Source
Strains		
Tp679	*C. glutamicum* ATCC 13032 wild type *Δcsm* Δ*trpL*::P_{ilvCM1}*trpE*^{fbr} Δ*vdh*::P_{ilvC}*aroG*^{fbr}	(Purwanto et al., 2018)
Tp679 (pEKEx3-optimRBS-*rebH-rebF*)	Tp679 carrying pEKEx3-optimRBS-*rebH-rebF*	This work
Tp679 (pEKEx3)	Tp679 carrying pEKEx3	This work
Tp679 (pEKEx) (pECXT99A)	Tp679 carrying pEKEx3 and pEXCT999A	This work
Tp679 (pCES208-*trpD*)	Tp679 carrying pCES208-*trpD*	(Purwanto et al., 2018)

Strains and plasmids	Description	Source
TrpCg	Tp679 (pEKEx3) carrying (pECXT99A-optimRBS-*trpD-Cg*)	This work
TrpCgm	Tp679 (pEKEx3) carrying (pECXT99A-optimRBS-*trpD-Cg*-mut)	This work
TrpEc	Tp679 (pEKEx3) carrying (pECXT99A-optimRBS-*trpD-Ec*)	This work
TrpEcm	Tp679 (pEKEx3) carrying (pECXT99A-optimRBS-*trpD-Ec*-mut)	This work
TrpBs	Tp679 (pEKEx3) carrying (pECXT99A-optimRBS-*trpD-Bs*)	This work
TrpSp	Tp679 (pEKEx3) carrying (pECXT99A-optimRBS-*trpD-spizi*)	This work
HalTCg	Tp679 (pEKEx3-optimRBS-*rebH-rebF*) carrying (pECXT99A-optimRBS-*trpD-Cg*)	This work
HalTCgm	Tp679 (pEKEx3-optimRBS-*rebH-rebF*) carrying (pECXT99A-optimRBS-*trpD-Cg*-mut)	This work
HalTEc	Tp679 (pEKEx3-optimRBS-*rebH-rebF*) carrying (pECXT99A-optimRBS-*trpD-Ec*)	This work
HalTEcm	Tp679 (pEKEx3-optimRBS-*rebH-rebF*) carrying (pECXT99A-optimRBS-*trpD-Ec*-mut)	This work
HalTBs	Tp679 (pEKEx3-optimRBS-*rebH-rebF*) carrying (pECXT99A-optimRBS-*trpD*-Bs)	This work
HalTSp	Tp679 (pEKEx3-optimRBS-*rebH-rebF*) carrying (pECXT99A-optimRBS-*trpD-spizi*)	This work
Plasmids		
pEKEx3	$Spec^R$, *C. glutamicum*/*E. coli* shuttle vector (Ptac, *lacI*, pBL1 $OriV_{C.g.}$)	(Stansen et al., 2005)

Strains and plasmids	Description	Source
pECTX99A	Tet^R, *C. glutamicum*/ *E. coli* shuttle vector (Ptrc, *lacI*, pGA1, $OriV_{Cg}$)	(Kirchner and Tauch, 2003)
pCES208-trpD	KanR, pCES208 overexpressing *trpD* from *E. coli* with PilvC-M1	(Purwanto et al., 2018)
pEKEx3-optimRBS-*rebH-rebF*	$Spec^R$, pEKEx3 overexpressing *rebH*, *rebF* from *L. aerocolonigenes* with optimized RBS for *rebH*	(Veldmann et al., 2019b)
pECXT99A-optimRBS-*trpD-Cg*	Tet^R, pECXT99A overexpressing *trpD* from *C. glutamicum* with optimized RBS for *trpD*	This work
pECXT99A-optimRBS-*trpD-Cg*-mut	Tet^R, pECXT99A overexpressing $trpD_{V11A, A125T, D138A, S149F, A162E}$ from *C. glutamicum* ATCC 13032 with optimized RBS for *trpD*	This work
pECXT99A-optimRBS-*trpD-Ec*	Tet^R, pECXT99A overexpressing *trpD* from *E. coli* K-12 with optimized RBS for *trpD*	This work
pECXT99A-optimRBS-*trpD-Ec*-mut	Tet^R, pECXT99A overexpressing $trpD_{S319T}$ from *E. coli* K-12 with optimized RBS for *trpD*	This work
pECXT99A-optimRBS-*trpD-Bs*	Tet^R, pECXT99A overexpressing *trpD* from *B. subtilis* 168 optimized RBS for *trpD*	This work
pECXT99A-optimRBS-*trpD-spizi*	Tet^R, pECXT99A overexpressing *trpD* from B. *subtilis* subsp. *spizizenii* with optimized RBS for *trpD*	This work

2.3.3.2 Molecular genetic technique and strain construction

For cloning, *E. coli* was used as host organism. *E. coli* was transformed by heat shock (Sambrook et al., 1989) and *C. glutamicum* with electroporation at 2.5 kV, 200 Ω and 25 µF (Eggeling and Bott, 2005). All used primers are listed in Table 2.3.2. The forward primers *trpD*-1-*Cg*, *trpD*-1-*Ec*, *trpD-Bs*, and *trpD-spizi* harbor the ribosome binding site (RBS)

sequence. The primer pair *trpD*-1-*Cg*-fwd/ *trpD*-3-*Cg*-rv were used for the amplification of *trpD* from *C. glutamicum* ATCC 13032. To amplify the *trpD* $^{V11A, A125T, D138A, S149F, A162E}$ the gene was split into three parts. The second part with the mutation V111A, A125T, D138A, S149F, A162E was synthetic synthesized (from T97 to L173) at Eurofins. This part was amplified with the primer pair *trpD*-2-*Cg*-fwd/*trpD*-2-*Cg*-rv. The first part (M1 to T96) was amplified with the primers *trpD*-1-*Cg*-fwd/*trpD*-1-*Cg*-rv and the third part (K174 to the stop codon) with the primers *trpD*-3-*Cg*-fwd/*trpD*-3-*Cg*-rv. With the primer pair *trpD*-1-*Ec*-fwd and *trpD*-2-*Ec*-rv, the *trpD* from *E. coli* was amplified. To introduce the mutation S319T in the *trpD* of *E. coli* the gene was split into two parts. The first part was amplified with the primers *trpD*-1-*Ec*-fwd/ *trpD*-1-*Ec*-rv whereat the reverse primer included the base pairs exchange. The second part was amplified with the primer pair *trpD*-2-*Ec*-fwd/ *trpD*-2-*Ec*-rv (the base pairs exchange was included in the *trpD*-2-*Ec*-fwd). To amplify the *trpD* from *B. subtilis* 168 (DSM 402) the primers *trpD-Bs*-fwd/ *trpD-Bs*-rv were used. The gene *trpD* from *B. subtilis* subsp. *spizizenii* (DSM 347) was amplified with the primer pair *trpD-spizi*-fwd/*trpD-spizi*-rv. The *trpD* genes (consisting of 1, 2 or 3 parts) were cloned in the vector pECXT99A restricted with BamHI via Gibson assembly (Gibson et al., 2009). The developed plasmids were pECXT99A-optimRBS-*trpD-Cg*, pECXT99A-optimRBS-*trpD-Cg*-mut, pECXT99A-optimRBS-*trpD-Ec*, pECXT99A-optimRBS-*trpD-Ec*-mut, pECXT99A-optimRBS-*trpD-Bs* and pECXT99A-optimRBS-*trpD-spizi* and were transformed in *C. glutamicum*.

Table 2.3.2: List of primers used in this work

Name	Sequence
trpD-1-*Cg*-fwd	CATGGAATTCGAGCTCGGTACCCGGGTTTAACGTATTATTAAA AGGAGGTATTTTTATGACTTCTCCAGCAACACTG
trpD-1-*Cg*-rv	GGATGCTGCGATCAGGGATGCGCCGGTGGTGATGTTGATGGT GTTGGCAC
trpD-2-*Cg*-fwd	GGTGCCAACACCATCAACATCACCACCGGCGCATCCCTGATC GCAGCATC

Name	Sequence
trpD-2-*Cg*-rv	AGCGTGTTGAAGATGGTGGGGAATTTCAGCGCCTGGCGAACC GGCTGCAC
trpD-3-*Cg*-fwd	GTGCAGCCGGTTCGCCAGGCGCTGAAATTCCCCACCATCTTCA ACACGCT
trpD-3-*Cg*-rv	GCCTGCAGGTCGACTCTAGAGGATCCTAGTCATTGGAAGACT CCTTTTC
trpD-1-*Ec*-fwd	CATGGAATTCGAGCTCGGTACCCGGGGAAAGGAGGCCCTTCA GATGGCTGACATTCTGCTGCTCG
trpD-1-*Ec*-rv	CCGCCAGCAGATCGGTCGAACCAGATTTAC
trpD-2-*Ec*-fwd	AGCGTCTCCAGTAAATCTGGTTCGACCGATCTGCTGGCGGCGT TCGGTAT
trpD-2-*Ec*-rv	GCCTGCAGGTCGACTCTAGAGGATCTTACCCTCGTGCCGCCAG TGCGGTG
trpD-Bs-fwd	TCGAGCTCGGTACCCGGGCAGCTACAGGTTCTAATCAGATAT ATATTATTAAAGGAGGTTTTTTATGAACAGATTTCTAC
trpD-Bs-rv	GCCTGCAGGTCGACTCTAGAGGATCTCAAGCATAGATCTCTTC CTC
trpD-spizi-fwd	CATGGAATTCGAGCTCGGTACCCGGGTATTAATTAAAATATA GCGGAGGAGGTTTTTTATGAACAAATTTCTACAATTG
trpD-spizi-rv	GCCTGCAGGTCGACTCTAGAGGATCTCAAGCATAGATCTCTTC CTCTTTC

2.3.3.3 Cultivation and disruption of anthranilate phosphoribosyltransferase overproducing *C. glutamicum* strains

TrpD overexpressing *C. glutamicum* strains were inoculated in 50 mL LB from an overnight culture. Expression of *trpD* gene was induced by 1 mM IPTG and the cells were grown for 24 h at 30 °C at 120 rpm before the cells were spun down and stored at -20 °C. To disrupt the cells the pellet was resuspended in TN-buffer (pH 6.3) and sonicated for 9 min 55%

amplitude and 0.5 cycles on ice in the UP200S Ultrasonic Processor from Hielscher Ultrasound Technology. The supernatant after centrifugation (60 min, 4°C, 16400 rpm) was used as crude extract for a 10% sodium dodecyl sulfate-polyacrylamide gel electrophoresis (SDS-PAGE).

2.3.3.4 Analytic procedure

For the quantification of the extracellular Trp, 7-Br-Trp, 7-Cl-Trp, and Ant, a high-pressure liquid chromatography (HPLC) system was used (1200 series, Agilent Technologies Deutschland GmbH, Böblingen, Germany). The supernatants of the cell culture were collected by centrifugation (14680 rpm, 20 min, RT) and further used for analysis. For detection of Ant, Trp, and the derivatives, samples were reacted with *ortho*-phthaldialdehyde (OPA) (Schneider and Wendisch, 2010). The amino acid separation was performed by a precolumn (LiChrospher 100 RP18 EC-5 µ (40mm×4 mm), CS-Chromatographie Service GmbH, Langerwehe, Germany) and a column (Li-Chrospher 100 RP18 EC-5 µ (125 mm×4 mm), CS Chromatographie Service GmbH). The detection was carried out with a fluorescence detector (FLD G1321 A, 1200 series, Agilent Technologies) with the excitation and emission wavelengths of 230 nm and 450 nm, respectively.

2.3.4 Results and Discussion

2.3.4.1 Identification of feedback resistant anthranilate phosphoribosyltransferases

In our previous studies (Veldmann et al., 2019a; Veldmann et al., 2019b), we observed an incomplete conversion of Ant in the production of halogenated Trp by *C. glutamicum*. Additionally, in the enzymatic assay of the enzyme TrpD, which convert Ant to *N*-(5-phosphoribosyl)-anthranilate, inhibition of the enzyme was observed, when 7-Cl-Trp or 7-Br-Trp was added to the reaction. To overcome this inhibition different TrpDs, from various microorganisms or TrpDs with specific mutations were chosen and tested (Table 2.3.3). Some *B. substilis* strains showed higher resistance to different Trp derivatives, like 5-methyl-tryptophan, 6-fluoro-tryptophan, 4-fluoro-tryptophan, 7-aza-tryptophan or 5-hydroxy-tryptophan (Shiio et al., 1973; Kurahashi et al., 1987a; Kurahashi et al., 1987b). Because of this higher resistance, the TrpDs of *B. subtilis* 168 and the close related *B. subtilis* subsp. *spizizenii* were chosen as promising candidates.

To generate a higher tolerance of the TrpD of *C. glutamicum* ATCC 13032, the wildtype gene was compared to different TrpDs of close related microorganism, which show higher resistance to Trp derivatives. The TrpD of the tryptophan-hyper producing *C. glutamicum* ATCC 21850 indicates a higher resistance to the Trp derivative 5-methyl-tryptophan (O'Gara and Dunican, 1995). In comparison to the wildtype gene of *C. glutamicum* ATCC 13032, it owns two amino acid exchanges, at position 149 instead of serine phenylalanine is encoded and at position 162 a glutamic acid is encoded instead of an alanine (O'Gara and Dunican, 1995). A second close related microorganism is *C. glutamicum* ATCC 13869 (DSM 1412), which is resistant to 5-fluoro-tryptophan. In comparison to the TrpD of ATCC 13032 two amino acid exchanges exist, the alanine 125 is a threonine and the aspartic acid 138 is an alanine (O'Gara and Dunican, 1995). The last amino acid exchange was found in comparison to the 5-fluoro-tryptophan resistant and Trp producing *C. glutamicum* strain ATCC 14067 (Shiio et al., 1982; Sugimoto and Shiio, 1982). Here, the valine 111 was traded for alanine. All these 5 mutations were introduced in the *trpD* gene of ATCC 13032 to generate the mutant *trpD*$_{\text{V111A, A125T, D138A, S149F, A162E}}$ (*trpD-Cg*-mut) (Table 2.3.3). In figure 2.3.2 A and B the crystal structures of TrpD-*Cg* and Trp-*Cg*-mut are shown. Two of the mutations are close

to the Ant binding pocket, the three other mutations are located at the surface. The last two TrpD enzymes are the TrpD wildtype form from *E. coli* and a mutated version. Through multiple sequence alignment between the TrpDs of *E. coli*, *C. glutamicum*, *B. subtilis* and *B. subtilis* subsp. *spizizenii* one conserved region (KHGNRSVSSKSGSSDLL) was figured out in all TrpDs. At position 319 (underlined) in *E. coli* a serine is encoded, wherein the other species an alanine is present. At the same position a threonine is located in the 5-fluoro-tryptophan resistant *C. glutamicum* strain ATCC 13869 (O'Gara and Dunican, 1995). Because the resistance of the TrpD-*Ec* should be increased against halogenated Trp, the serine was also exchanged by a threonine (S319T; TrpD-*Ec*-mut) (Table 2.3.3). The same amino acid mutation was introduced in TrpD-*Cg*-mut (A125T).

Table 2.3.3: Overview of the identified feedback resistant TrpDs.

Identified feedback resistant TrpDs	**Description**
TrpD-*Cg*	Wildtype TrpD from *C. glutamicum*
TrpD-*Cg*-mut	Wildtype TrpD from *C. glutamicum* with the following mutations: V111A, A125T, D138A, S149F, A162E
TrpD-*Ec*	Wildtype TrpD from *E. coli* K-12
TrpD-*Ec*-mut	Wildtype TrpD from *E. coli* K-12 with the following mutation: S319T
TrpD-*Bs*	Wildtype TrpD from *B. subtilis* 168
TrpD-*spizi*	Wildtype TrpD from *B. subtilis* subsp. *spizizenii*

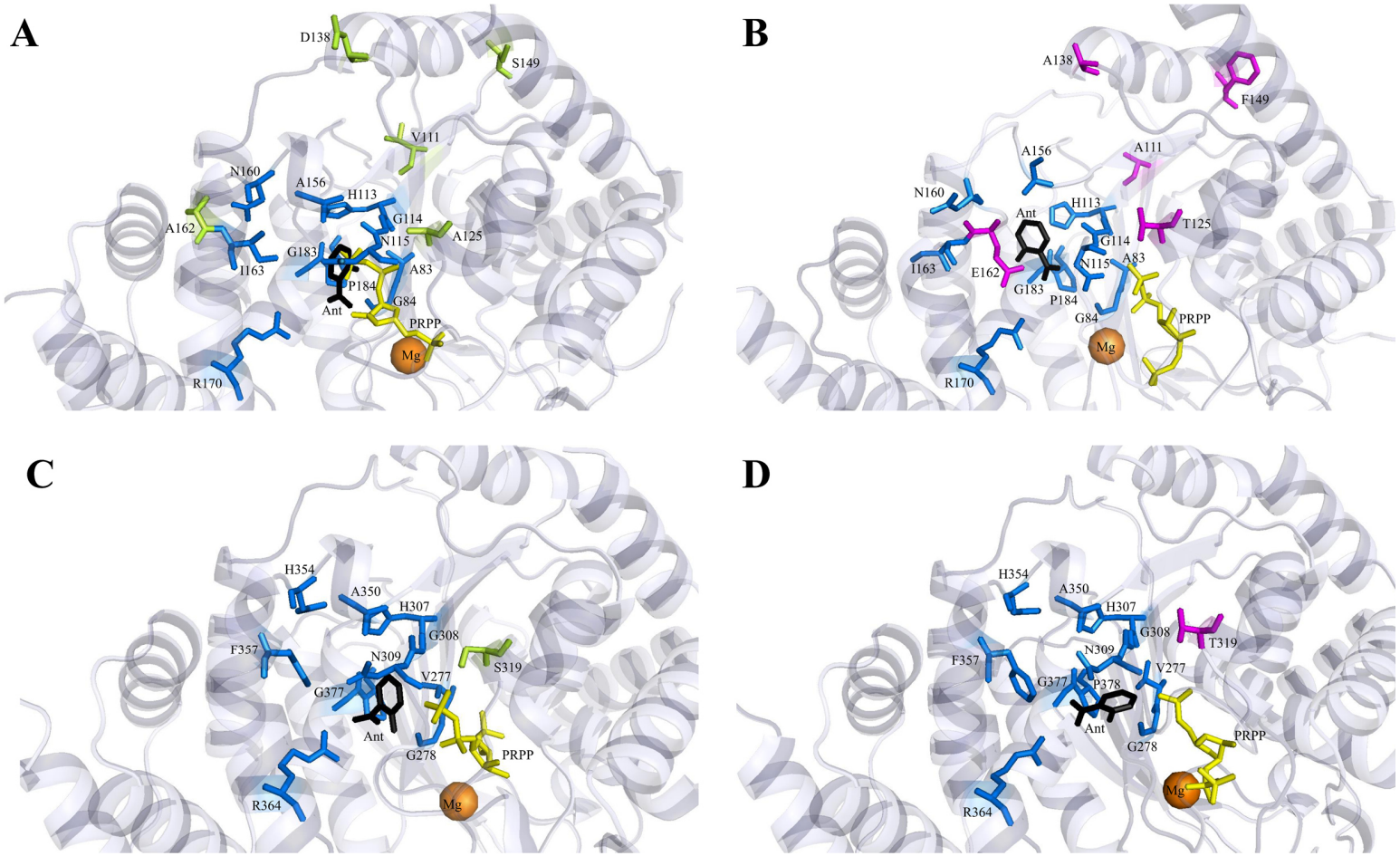

Figure 2.3.2: Crystal structure of TrpD-*Cg* and TrpD-*Ec* and the mutants. The blue amino acid sticks show the Ant binding pocket. The bright green sticks (A and C) show the original amino acids of both TrpDs. The magenta sticks show the mutated amino acids (B and D) of the enzymes. **A**: TrpD-*Cg* **B**: TrpD-*Cg*-mut **C**: TrpD-*Ec* **D**: TrpD-*Ec*-mut. The PDB file was created by Phyre[2] (Protein Homology/analogY Recognition Engine V 2.0).

2.3.4.2 Overexpression of different *trpD*s

Six *trpD*s were overexpressed from the pECXT99A vector in the Ant producing *C. glutamicum* strain Tp679 (pEKEx3). Two *trpD*s derived from *C. glutamicum*: $trpD_{Cg\text{-wildtype}}$ and $trpD_{V11A,\ A125T,\ D138A,\ S149F,\ A162E}$. Two further *trpD*s arise from *E. coli*: $trpD_{Ec\text{-wildtype}}$ and $trpD_{S319T}$. The last two *trpD*s derive from *B. subtilis* 168 (DSM 402) and *B. subtilis* subsp. *spizizenii* (DSM 347). The resulting strains TrpCg, TrpDCgm, TrpEc, TrpEcm, TrpBs, and TrpSp were inoculated in LB supplemented with 1 mM IPTG for induction of gene expression. After 24 h the cells were harvested and used for crude extract preparation. 10 µg of the crude extract was load on acrylamide gel. The separation of the proteins on the acylamide gel revealed an additional band in all crude extracts with the expected size of the respective TrpD: both TrpDs from *C. glutamicum* had a size of ~ 37 kDa, the TrpDs from *E. coli* ~ 57 kDa and both of *B. subtilis* and *B. subtilis* subsp. *spizizenii* had a size of ~ 36 kDa (Fig. 2.3.3).

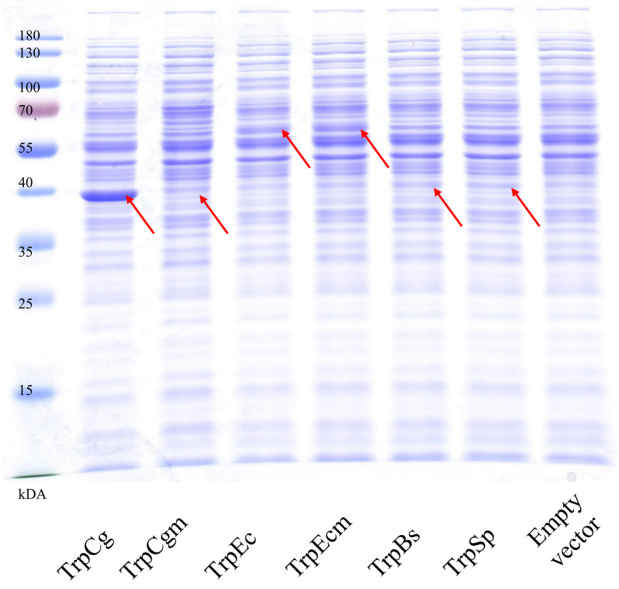

Figure 2.3.3: 12.5% Acrylamide gel of the crude extracts of *C. glutamicum* strains expressing the different *trpD*s. The strains were grown in LB with 1 mM IPTG for 24 h. The strains derived from Tp679 (pEKEx3) and carried an additional plasmid for the overexpression of the various *trpD*s: pECXT99A-optimRBS-*trpD-Cg* (line 1), pECXT99A-optimRBS-*trpD-Cg*-mut (line 2), pECXT99A-optimRBS-*trpD-Ec* (line 3), pECXT99A-optimRBS-*trpD-Ec*-mut (line 4), pECXT99A-optimRBS-*trpD-Bs* (line 5), pECXT99A-optimRBS-*trpD-spizi* (line 6) and pECXT99A (line 7). The additional band of the TrpDs is marked with a red arrow. Ladder: PageRuler Prestained Protein Ladder from ThermoFisher.

2.3.4.3 Fermentive production of L-tryptophan, 7-chloro-L-tryptophan, and 7-bromo-L-tryptophan using various anthranilate phosphoribosyltransferase

In order to test the Trp resistance of the chosen TrpDs *in vivo*, the genes were introduced into several production strains. For the production of Trp, the *C. glutamicum* strain Tp679 (pEKEx3) overexpressing only the *trpD*s was used (Trp-strains). Additionally, to obtain 7-Cl-Trp or 7-Br-Trp the genes encoding for the FAD-dependent halogenase RebH and the NADH dependent flavin reductase RebF from *L. aerocolonigenes* were overexpressed from pEKEx3 (Hal-strains) in the Trp-strains (Veldmann et al., 2019b). As control the Ant overproducing strain Tp679 with the empty vectors pEKEx3 and pECT99A was used. First, the influence of Trp towards TrpDs was tested by fermentative production of Trp (Fig. 2.3.4). All strains showed a similar growth rate (Supplementary data table 2.3.1). The control strain showed a production of 0.04 ± 0.00 g L^{-1} Trp, however, an incomplete conversion of the precursor Ant (1.8 ± 0.06 g L^{-1}) was observed as well. The accumulation of Ant was reduced in the TrpCgm strain expressing the mutated *trpD* compared to TrpCg overexpressing the wildtype *trpD* from *C. glutamicum*. Consequently, TrpDCgm is less inhibited by Trp, because it produced 8 times more Trp then TrpCg. The strains TprDEc and TrpDEcm overexpressing either the wildtype or the mutant of *trpD* from *E. coli* showed a complete conversion of Ant. They produced 1.96 ± 0.07 g L^{-1} (TrpDEc) and 1.88 ± 0.06 g L^{-1} (TrpDEcm) Trp. Expression of the *trpD*s from *B. subtilis* and *B. subitlis* subsp. *spizizenii* resulted in full conversion of Ant and in a production of about 2 g L^{-1} Trp (Supplementary data Table 2.3.1).

In the next step, we wanted to investigate the influence of TrpD and its mutants regarding the fermentative production of the halogenated Trp derivative 7-Cl-Trp (Fig. 2.3.4). The strains Tp679 (pEKEx3-optimRBS-*rebH-rebF*) overexpressing the different *trpD*s were used for this approach. All strains showed a similar growth rate (Supplementary data table 2.3.1.). HalCgm produced 1.5 times more Trp, 1.6 times less Ant and almost the same amount of 7-Cl-Trp about 280 mg L^{-1} compared to HalCg (Fig. 2.3.4). Hence, no complete conversion of Ant took place. But it could be observed, that HalCg is more inhibited by Trp and 7-Cl-Trp then HalCgm. Production titers of HalEc, HalEcm, HalBs, and HalSp were similar to about 300 mg L^{-1} 7-Cl-Trp and about 3 g L^{-1} Trp. Although all four strains produced

7-Cl-Trp, there was no accumulation of Ant, indicating that the strains show a higher resistance to the inhibition by 7-Cl-Trp.

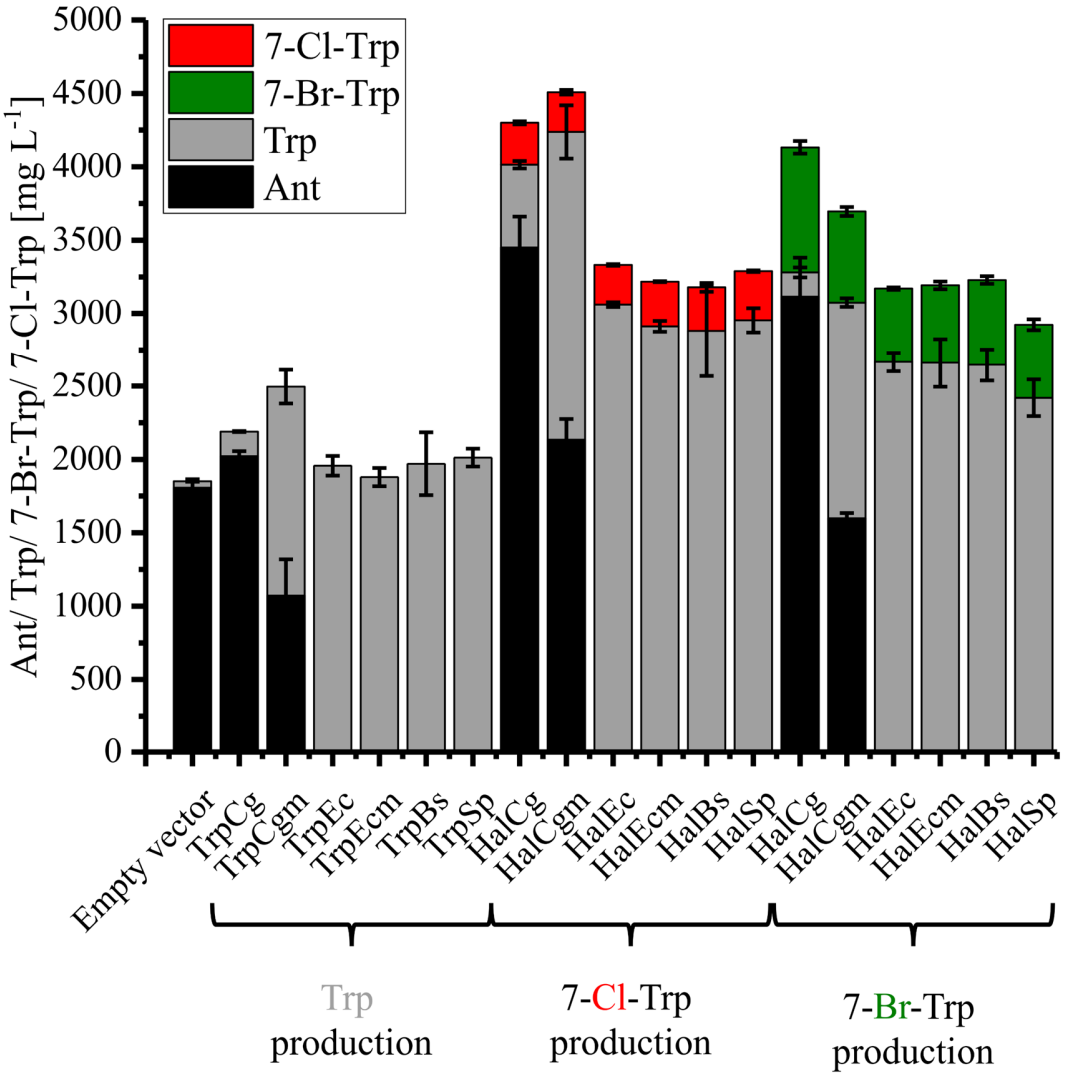

Figure 2.3.4: Production of Ant, Trp, 7-Cl-Trp, and 7-Br-Trp by overexpressing different *trpD*s in either the Ant overproducing *C. glutamicum* strain Tp679 (pEKEx3) or in the Trp halogenating *C. glutamicum* strainTp679 (pEKEx3-optimRBS-*rebH-rebF*). For the production of Trp the various *trpD*s of *C. glutamicum* (TrpCg [wildtype]/ TrpCgm [mutant]), *E. coli* (TrpEc [wildtype]/ TrpEcm [mutant]), *B. subtilis* (TrpBs) and *B. subtilis* subsp. *spizizenii* (TrpSp) were overexpressed in the Ant overproducing *C. glutamicum* strain Tp679 (pEKEx3). For the production of halogenated Trp the different *trpD*s were overexpressed in the Trp halogenating *C. glutamicum* strain Tp679 (pEKEx3-optimRBS-*rebH-rebF)*. The resulting strains are: *C. glutamicum* (HalCg [wildtype]/ HalCgm [mutant]), *E. coli* (HalEc [wildtype]/ HalEcm [mutant]), *B. subtilis* (HalBs) and *B. subtilis* subsp. *spizizenii* (HalSp). For the production of 7-Cl-Trp or 7-Br-Trp, 50 mM $CaCl_2$ or 50 NaBr were added, respectively. Means and standard deviations of three replicate cultivations are shown.

In the third fermentative production process, 7-Br-Trp production was analyzed and similar results compared to the 7-Cl-Trp production could be observed (Fig. 2.3.4). Ant accumulation could only be detected for the strains HalCg and HalCgm. However, HalCg and HalCgm had the highest production titers of 7-Br-Trp with 852.2 ± 42.9 mg L^{-1} and 621.1 ± 30.8 mg L^{-1}, respectively. Though both accumulated Ant whereat HalCg produced 1.9-times more Ant and 7.7-times less Trp then HalCgm. Hence, HalCgm showed higher resistance to the inhibitors Trp and 7-Br-Trp. The growth rates of all six strains were about 0.08 h^{-1} (Supplementary data table 2.3.1). HalEc, HalEcm, HalBs, and HalSp produced almost the same amount of Trp and 7-Br-Trp: about 2.6 g L^{-1} Trp and 530 mg L^{-1} 7-Br-Trp (Fig. 2.3.4; Supplementary data Table 2.3.1). Thus, these strains have a higher tolerance for Trp and 7-Br-Trp compared to HalCg and HalCgm since no Ant accumulation was detected. All in all, was the production of 7-Cl-Trp and 7-Br-Trp in shake flasks increased by the overexpression of the chosen *trpD*s.

The higher resistance of the TrpDs of the strains HalEc, HalEcm, HalBs, and HalSp can be the result of different factors. For the overexpression of the *trpD*s, another expression system was used compared to the strains of the previous study (Veldmann et al., 2019a; Veldmann et al., 2019b). Here, the IPTG-inducible vector pECXT99A (Kirchner and Tauch, 2003) and an optimized RBS were used. In the previous study *trpD* from *E. coli* was overexpressed from the vector pCES208 harboring the constitutive promoter $P_{ilvC\text{-}M1}$ (Lee, 2014; Veldmann et al., 2019b). The efficient overexpression was visible on the acrylamide gel (Fig. 2.3.2). The *trpD* from pCES208-$P_{ilvC\text{-}M1}$ was not detectable on the acrylamide gel (data not shown). Further, it could be observed, that the five mutations in the TrpD from *C. glutamicum* had a positive effect. In the predicted crystal structure it is shown, that two mutations are located near to the binding pocket of the Ant and the others are partly located at the protein surface. It remains still unknown if the inhibitory molecule either competes with Ant or the co-factor 5-phospho-α-D-ribose 1-diphosphate (PRPP) in the active site or if a non-competitive inhibition takes place. Therefore, each mutation has to be investigated on its own and in combination to figure out at which area the inhibition takes place. Additionally, TrpDs from other resistant *C. glutamicum* strains could be analyzed regarding the localization of its mutations to curtail the binding area of the inhibitor. For example, the *C. glutamicum* strain

4MT-11 shows resistance to the Trp analogs 5-methyl-tryptophan, tryptophanhydroxamate, 6-fluoro-tryptophan, and 4-methyl-tryptophan and further mutants derived from 4MT-11 are resistant to the L-phenylalanine and L-tyrosine analogs *p*-fluorophenylalanine, *p*-amino-phenylalanine, tyrosinehydroxamate, and phenylalaninehydroxate (Hagino and Nakayama, 1975a). Further, the enzyme could be analyzed by determination of the type of inhibitor, therefore different prediction methods are known. For example, Lai and co-workers determined the type of inhibition via the calculation of the percent of inhibition changes with various inhibitor concentrations (Lai and Wu, 2003) while F. Tholander predicted the kind of inhibition via comparative analysis of uninhibited versus inhibited reactions (Tholander, 2012). Hence, some binding sites could be excluded. Additionally, via 3D-structure designing programs, crystal structures and docking analysis the binding area of the inhibitor could be predicted (Eleftheriou et al., 2015). Taken all these methods together, the binding site of Trp, 7-Cl-Trp, and 7-Br-Trp should be determined and analyzed to create feedback resistance mutants. The mutation in the TrpD of *E. coli* had no effect in relation to the resistance because no difference to the wildtype TrpD of *E. coli* could be observed. The TrpD of *B. subtilis* and *B. subtilis* subsp. *spizizenii* were resistant to Trp, 7-Cl-Trp, and 7-Br-Trp. This reflects the potential of enzymes of *Bacillus* species. *Bacillus* enzymes are known to have poly-extreme tolerance; hence, they are still functional under extreme temperature, pH and presence of inhibitors (Joshi and Satyanarayana, 2013; Baweja et al., 2016; Singh and Bajaj, 2017). Another TrpD with a high potential to tolerate halogenated Trp is the enzyme from the *B. subtilis* strain AJ 11982 (Kurahashi et al., 1987a), which produces 13.6 g L^{-1} Trp and is resistant to several inhibitors (azaserine, 6-diazo-5-oxo-l-norleucine, cinnamate, 5-fluoro-tryptophan, indolmycin, 4-fluoro-tryptophan, and 7-aza-tryptophan). Despite the addition of the inhibitor the production of Trp is high (Kurahashi et al., 1987a), which leads to the conclusion, that the enzymes of the *trp* operon, including *trpD*, are resistant to this inhibitors.

It was observed, that the production of Ant and Trp was higher in the production strains performing the halogenation. The same effect was observed before in the previous studies, with higher production of halogenated Trp the amount of the precursors increased (Veldmann et al., 2019a; Veldmann et al., 2019b). Hence, the higher production of Ant and Trp has to

be related to the production of halogenated Trp. It may be that the production of halogenated triggers a pull effect towards the production of Trp. But until now, it is not known if this effect is caused by the overexpression of *rebH* and *rebF* or by the production of halogenated Trp.

2.3.5 Conclusion

In the fermentative production of Trp, 7-Cl-Trp, and 7-Br-Trp by an Ant overproducing *C. glutamicum* strain overexpressing different *trpD*s, the conversion of the entire Ant was observed in four cases. Hence, the TrpDs of *E. coli*, *E. coli* with a mutation, *B*. *subtilis* and *B*. *subitlis* subsp. *Spizizenii* were not feedback inhibited by Trp, 7-Cl-Trp, and 7-Br-Trp during the production. Thus, the production of 7-Cl-Trp and 7-Br-Trp were increased in shake flask culture.

2.3.6 Reference

Baweja, M., Tiwari, R., Singh, P.K., Nain, L., and Shukla, P. (2016). An alkaline protease from *Bacillus pumilus* MP 27: functional analysis of its binding model toward its applications as detergent additive. Front. Microbiol. 7**,** 1195. doi:10.3389/fmicb.2016.01195.

Bode, R., and Birnbaum, D. (1978). Enzymes of the aromatic amino acid biosynthesis in *Hansenula henricii*: anthranilate phosphoribosylpyrophosphate-phosphoribosyltransferase (EC 2.4. 2.18). Zeitschrift fur allgemeine Mikrobiologie 18**,** 559.

Bolten, C.J., Kiefer, P., Letisse, F., Portais, J.-C., and Wittmann, C. (2007). Sampling for Metabolome Analysis of Microorganisms. Anal. Chem. 79**,** 3843-3849. doi:10.1021/ac0623888.

Diederich, F., and Stang, P.J. (2008). Metal-Catalyzed Cross-Coupling Reactions. Wiley. doi:DOI:10.1002/9783527619535.

Eggeling, L., and Bott, M. (2005). Handbook of *Corynebacterium glutamicum.* CRC press.

Eleftheriou, P., Petrou, A., Geronikaki, A., Liaras, K., Dirnali, S., and Anna, M. (2015). Prediction of enzyme inhibition and mode of inhibitory action based on calculation of distances between hydrogen bond donor/acceptor groups of the molecule and docking analysis: An application on the discovery of novel effective PTP1B inhibitors. SAR QSAR Environ. Res. 26**,** 557-576. doi:10.1080/1062936X.2015.1074939.

Frese, M., and Sewald, N. (2015). Enzymatic Halogenation of Tryptophan on a Gram Scale. Angew. Chem. Int. Ed. 54**,** 298-301. doi:10.1002/anie.201408561.

Gibson, D.G., Young, L., Chuang, R.-Y., Venter, J.C., Hutchison Iii, C.A., and Smith, H.O. (2009). Enzymatic assembly of DNA molecules up to several hundred kilobases. Nat. Methods 6**,** 343. doi:10.1038/nmeth.1318.

Gribble, G.W. (2012). Occurrence of halogenated alkaloids, in The Alkaloids: Chemistry and Biology. Elsevier. 1-165.

Hagino, H., and Nakayama, K. (1975a). L-Tryptophan production by analog-resistant mutants derived from a phenylalanine and tyrosine double auxotroph of *Corynebacterium glutamicum*. Agric. Biol. Chem. 39**,** 343-349. doi:10.1080/00021369.1975.10861621.

Hagino, H., and Nakayama, K. (1975b). Regulatory properties of anthranilate synthetase from *Corynebacterium glutamicum*. Agric. Biol. Chem. 39**,** 323-330. doi:10.1080/00021369.1975.10861619.

Hanahan, D. (1983). Studies on transformation of *Escherichia coli* with plasmids. J. Mol. Biol. 166**,** 557-580. doi:10.1016/S0022-2836(83)80284-8.

Ito, J., and Yanofsky, C. (1969). Anthranilate synthetase, an enzyme specified by the tryptophan operon of *Escherichia coli*: Comparative studies on the complex and the subunits. J. Bacteriol. 97**,** 734-742.

Joshi, S., and Satyanarayana, T. (2013). Characteristics and applications of a recombinant alkaline serine protease from a novel bacterium *Bacillus lehensis*. Bioresour. Technol. 131**,** 76-85. doi:10.1016/j.biortech.2012.12.124.

Kirchner, O., and Tauch, A. (2003). Tools for genetic engineering in the amino acid-producing bacterium *Corynebacterium glutamicum*. J. Biotechnol. 104**,** 287-299. doi:10.1016/S0168-1656(03)00148-2.

Koguchi, Y., Kohno, J., Nishio, M., Takahashi, K., Okuda, T., Ohnuki, T., et al. (2000). TMC-95A, B, C, and D, novel proteasome inhibitors produced by *Apiospora montagnei* Sacc. TC 1093. J. Antibiot. 53**,** 105-109. doi:10.7164/antibiotics.53.105.

Kurahashi, O., Noda-Watanabe, M., Toride, Y., Takenouchi, T., Akashi, K., Morinaga, Y., et al. (1987a). Production of L-tryptophan by azaserine-, 6-diazo-5-oxo-L-norleucine- and cinnamate-resistant mutants of *Bacillus subtilis* K. Agric. Biol. Chem. 51**,** 1791-1797. doi:10.1080/00021369.1987.10868316.

Kurahashi, O., Yokozeki, K., Nakamori, S., Yamanaka, S., and Enei, H. (1987b). Production of L-tryptophan by 5-fluorotryptophan and indolmycin resistant mutants of *Bacillus subtilis* K. Agric. Biol. Chem. 51**,** 231-235. doi:10.1080/00021369.1987.10868006.

Lai, C.-J., and Wu, J.C. (2003). A simple kinetic method for rapid mechanistic analysis of reversible enzyme inhibitors. Assay Drug Dev. Technol. 1**,** 527-535. doi:10.1089/154065803322302781.

Lambrecht, J.A., and Downs, D.M. (2012). Anthranilate phosphoribosyl transferase (TrpD) generates phosphoribosylamine for thiamine synthesis from enamines and phosphoribosyl pyrophosphate. ACS Chem. Biol. 8**,** 242-248. doi:10.1021/cb300364k.

Lee, J. (2014). Development and characterization of expression vectors for *Corynebacterium glutamicum*. J Microbiol Biotechnol 24**,** 70-79. doi:10.4014/jmb.1310.10032.

Matsui, K., Miwa, K., and Sano, K. (1987). Two single-base-pair substitutions causing desensitization to tryptophan feedback inhibition of anthranilate synthase and enhanced expression of tryptophan genes of *Brevibacterium lactofermentum*. J. Bacteriol. 169**,** 5330-5332.

Nishizawa, T., Aldrich, C.C., and Sherman, D.H. (2005). Molecular analysis of the rebeccamycin L-amino acid oxidase from *Lechevalieria aerocolonigenes* ATCC 39243. J. Bacteriol. 187**,** 2084-2092. doi:10.1128/JB.187.6.2084-2092.2005.

O'Gara, J.P., and Dunican, L.K. (1995). Mutations in the *trpD* gene of *Corynebacterium glutamicum* confer 5-methyltryptophan resistance by encoding a feedback-resistant anthranilate phosphoribosyltransferase. Appl. Environ. Microbiol. 61**,** 4477-4479.

Onaka, H., Taniguchi, S.-i., Igarashi, Y., and Furumai, T. (2003). Characterization of the biosynthetic gene cluster of rebeccamycin from *Lechevalieria aerocolonigenes* ATCC 39243. Biosci. Biotechnol. Biochem. 67**,** 127-138. doi:10.1271/bbb.67.127.

Purwanto, H.S., Kang, M.-S., Ferrer, L., Han, S.-S., Lee, J.-Y., Kim, H.-S., et al. (2018). Rational engineering of the shikimate and related pathways in *Corynebacterium glutamicum* for 4-hydroxybenzoate production. J. Biotechnol. doi:10.1016/j.jbiotec.2018.07.016.

Sambrook, Joseph, Fritsch, E. F. (Edward F.), Maniatis, Tom, et al. (1989). Molecular cloning : a laboratory manual. New York : Cold Spring Harbor Laboratory Press 2nd ed.

Schneider, J., and Wendisch, V.F. (2010). Putrescine production by engineered *Corynebacterium glutamicum*. Appl. Microbiol. Biotechnol. 88**,** 859-868. doi:10.1007/s00253-010-2778-x.

Shiio, I., Ishii, K., and Yokozeki, K. (1973). Production of L-tryptophan by 5-fluorotryptophan resistant mutants of *Bacillus subtilis*. Agric. Biol. Chem. 37**,** 1991-2000. doi:10.1080/00021369.1973.10860955.

Shiio, I., Sugimoto, S.-i., and Kawamura, K. (1982). Production of L-Tryptophan by Azaserine-resistant Mutants of *Brevibacterium flavum*. Agric. Biol. Chem. 46**,** 1849-1854. doi:10.1080/00021369.1982.10865346.

Singh, S., and Bajaj, B.K. (2017). Potential application spectrum of microbial proteases for clean and green industrial production. Energy, Ecology and Environment 2**,** 370-386. doi:10.1007/s40974-017-0076-5.

Stansen, C., Uy, D., Delaunay, S., Eggeling, L., Goergen, J.-L., and Wendisch, V.F. (2005). Characterization of a *Corynebacterium glutamicum* lactate utilization operon induced during temperature-triggered glutamate production. Appl. Environ. Microbiol. 71**,** 5920-5928. doi:10.1128/AEM.71.10.5920-5928.2005.

Sugimoto, S.-i., and Shiio, I. (1982). Tryptophan synthase and production of L-tryptophan in regulatory mutants. Agric. Biol. Chem. 46**,** 2711-2718. doi:10.1080/00021369.1982.10865516.

Tamir, H., and Srinivasan, P.R. (1970). Studies of the mechanism of anthranilate synthase reaction. Proc. Natl. Acad. Sci. 66**,** 547-551. doi:10.1073/pnas.66.2.547.

Tholander, F. (2012). Improved inhibitor screening experiments by comparative analysis of simulated enzyme progress curves. PloS One 7**,** e46764. doi:10.1371/journal.pone.0046764.

Veldmann, K.H., Dachwitz, S., Risse, J.M., Lee, J.-H., Sewald, N., and Wendisch, V.F. (2019a). Bromination of L-tryptophan in a fermentative process with *Corynebacterium glutamicum*. Front. bioeng. biotechnol. 7**,** 219. doi:10.3389/fbioe.2019.00219.

Veldmann, K.H., Minges, H., Sewald, N., Lee, J.-H., and Wendisch, V.F. (2019b). Metabolic engineering of *Corynebacterium glutamicum* for the fermentative production of halogenated tryptophan. J. Biotechnol. 291**,** 7-16. doi:10.1016/j.jbiotec.2018.12.008.

Yeh, E., Garneau, S., and Walsh, C.T. (2005). Robust in vitro activity of RebF and RebH, a two-component reductase/halogenase, generating 7-chlorotryptophan during rebeccamycin biosynthesis. Proc. Natl. Acad. Sci. U. S. A. 102**,** 3960-3965. doi:10.1073/pnas.0500755102.

2.3.7 Supplementary data

Table 2.3.1: Growth rates, biomass, production yields of Ant, Trp, 7-Cl-Trp, and 7-Br-Trp of *C. glutamicum*. For the production of 7-Cl-Trp 50 mM $CaCl_2$ was added. For the production of 7-Br-Trp 50 mM NaBr was added.

	Strain	Growth rate [h^{-1}]	Biomass [g L(CDW)$^{-1}$]	Ant yield [mg g(CDW)$^{-1}$]	Trp yield [mg g(CDW)$^{-1}$]	7-Cl-Trp yield [mg g(CDW)$^{-1}$]	7-Br-Trp yield [mg g(CDW)$^{-1}$]
Trp production	Empty vector	0.08 ± 0.00	7.3 ± 0.3	248 ± 3	6 ± 0	0	0
	TrpCg	0.10 ± 0.00	7.8 ± 0.3	258 ± 15	21 ± 1	0	0
	TrpCgm	0.10 ± 0.02	6.8 ± 0.1	158 ± 36	209 ± 16	0	0
	TrpEc	0.07 ± 0.01	7.2 ± 0.0	0	270 ± 8	0	0
	TrpEcm	0.08 ± 0.00	7.6 ± 0.5	0	248 ± 9	0	0
	TrpBs	0.07 ± 0.01	7.3 ± 0.1	0	269 ± 29	0	0
	TrpSp	0.08 ± 0.01	7.1 ± 0.2	0	282 ± 16	0	0
7-Cl-Trp production	HalCg	0.12 ± 0.01	7.5 ± 0.8	462 ± 30	76 ± 11	38 ± 5	0
	HalCgm	0.12 ± 0.01	6.7 ± 0.6	319 ± 33	312 ± 6	40 ± 4	0
	HalEc	0.12 ± 0.00	7.1 ± 0.2	0	432 ± 16	38 ± 1	0
	HalEcm	0.15 ± 0.00	6.9 ± 0.5	0	427 ± 23	45 ± 3	0
	HalBs	0.12 ± 0.01	6.3 ± 0.3	0	459 ± 68	47 ± 17	0
	HalSp	0.13 ± 0.00	6.0 ± 0.1	0	495 ± 13	56 ± 1	0
7-Br-Trp production	HalCg	0.08 ± 0.00	7.3 ± 0.8	434 ± 63	23 ± 4	0	119 ± 18
	HalCgm	0.08 ± 0.01	7.6 ± 0.2	210 ± 9	194 ± 6	0	82 ± 7
	HalEc	0.08 ± 0.01	7.4 ± 1.7	0	378 ± 90	0	72 ± 19
	HalEcm	0.11 ± 0.01	9.7 ± 0.1	0	273 ± 19	0	55 ± 3
	HalBs	0.09 ± 0.00	8.4 ± 0.3	0	317 ± 19	0	70 ± 4
	HalSp	0.07 ± 0.01	7.6 ± 0.4	0	321 ± 33	0	67 ± 7

Means and standard deviations obtained from triplicate shake flask cultivations in CGXII minimal medium after 72 h are given. Product yields are normalized to the biomass. The biomass concentration was determined according to the correlation CDW = 0.353 OD (Bolten et al., 2007).

2.4 Fermentative production of indole with *Corynebacterium glutamicum* overexpressing different tryptophanases

Kareen H. Veldmann[a#], Anastasia Kerbs[a#], Christian Schnepel[b], Norbert Sewald[b], Jin-ho Lee[c], Volker F. Wendisch[a]

[a] Genetics of Prokaryotes, Faculty of Biology & CeBiTec, Bielefeld University, Universitätsstr. 25, 33615 Bielefeld, Germany

[b] Organic Chemistry III, Faculty of Chemistry & CeBiTec, Bielefeld University, Universitätsstr. 25, 33615 Bielefeld, Germany

[c] Major in Food Science & Biotechnology, School of Food Biotechnology & Nutrition, BB21+, Kyungsung University, 309, Suyeong-ro, Nam-gu, Busan 48434, Republic of Korea

#both authors contributed equally.

2.4.1 Abstract

The aromatic compound indole serves in bacteria as an intracellular signal molecule to control various processes, like the biofilm formation. It has various applications in the pharmaceutical, dye and pigment industries. For large scale production of indole, different synthetic chemical pathways are known, like the Fischer indole synthesis and Bischler indole synthesis. In nature, indole producing microorganisms own a tryptophanase (TnaA), which converts L-tryptophan (Trp) to indole, pyruvate, and ammonia. Until now, this environmentally friendly enzymatical route has not been transferred and used as a new production platform, for example to a fermentative indole production. In this study, the enzyme activities of different heterologous expressed *tnaA*s in *Corynebacterium glutamicum* were tested and the fermentative production of indole was established. In enzyme activity assays, the TnaAs of *Escherichia coli*, *Propionibacterium acnes* and *Proteus vulgaris* showed to be active in *C. glutamicum* with Trp as substrate. Additionally, was shown, that the TnaAs from *E. coli* and *P. vulgaris* have an extended substrate spectrum and accept the Trp derivatives 7-chloro-L-tryptophan and 7-bromo-L-tryptophan. In glucose and ammonium

based fermentative production a final titer of 329 ± 17 mg L^{-1} indole was reached by overexpression of the *tnaA* from *P. vulgaris* in a Trp overproducing *C. glutamicum* strain.

2.4.2 Introduction

Indole is an aromatic compound that serves in bacteria as an intracellular signal and controls different bacterial processes, like plasmid stability, drug resistance and biofilm formation (Lee and Lee, 2010). Indole has a bicyclic structure consisting of a bezene ring and a pyrrol ring (DeRosa, 2006). In daily life, indole has different applications for the production of pharmaceuticals (Dhani et al., 2011; Lalit et al., 2012), antioxidants (Herraiz and Galisteo, 2004), dye and pigments (Barden, 2010) and fragrances (Pybus and Sell, 2007). Indole, in industrial scale, is produced via different chemical synthetic routes, like the Fischer indole synthesis or the Bischler indole synthesis (Fischer and Jourdan, 1883; Bischler, 1892; Taber and Tirunahari, 2011). Almost all of these pathways work with the principle to annulate a five-membered ring to an existing functionalized benzene ring (Inman and Moody, 2013). But often the provisioning and availability of the precursor for the synthesis are limited and complex because of the limited accessibility (Inman and Moody, 2013). In nature, indole is produced by different Gram-positive and Gram-negative bacteria, and plants. In bacteria, indole is produced by the tryptophanase (TnaA; EC 4.1.99.1) (Lee and Lee, 2010), which converts reversible L-tryptophan (Trp) to indole, pyruvate, and ammonia consuming the co-factor pyridoxal 5′-phosphate (PLP) (Newton and Snell, 1965) (Fig. 2.4.1).

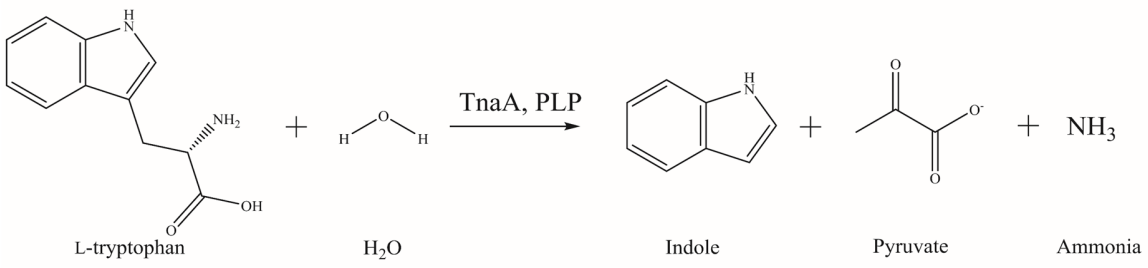

Figure 2.4.1: Schematic reaction of a tryptophanase. The L-tryptophan is converted by the tryptophanase (TnaA) to free indole, pyruvate, and ammonia under the consumption of the co-factor pyridoxal phosphate (PLP).

In plants, the indole-3-glycerol phosphate lyase converts indole-3-glycerol phosphate, an intermediate of the Trp biosynthetic pathway, to free indole (Frey et al., 2000).

Various tryptophanases were already identified. Most of them have a similar molecular weight, subunit structure, and PLP content. But they differ in the amino acid composition (Snell, 1975; Sasaki-Imamura et al., 2010), in the substrate spectrum (Gogoleva et al., 2003; Yoshida et al., 2009; Phillips et al., 2011), in the pH optimum (Watanabe and Snell, 1972; Yoshida et al., 2009) and specific enzymatic activity (Cowell et al., 1973; Zhang and Hong, 2009). A crucial aspect of the indole biosynthesis is the regulation of the tryptophanases since higher concentrations of indole can have a toxic effect on the bacteria (Chant and Summers, 2007). The TnaA of *E. coli* is one of the most studied examples which has different mechanisms to regulate indole production. Intracellularly the TnaA is regulated through the amount of Trp, the expression of *tnaA* is downregulated while the *trp* operon is upregulated when the concentration of Trp is low, as consequence, the indole concentration is low and the Trp concentration is increasing (Yanofsky et al., 1991; Gong and Yanofsky, 2002). With higher concentration of Trp the *tnaA* expression is not repressed and the indole production is increasing yet is not extending the toxic concentration. Additionally, the indole biosynthesis is regulated by environmental factors, like cell population, cell density, carbon source, temperature and pH control (Lee and Lee, 2010).

The biotransformation of added Trp to a process was established a few years ago, however, fermentative production of indole starting from glucose has not been reported (Sasaki-Imamura et al., 2010; Li and Young, 2013).

Since decades, *C. glutamicum* serves as host for the fermentative production of various amino acids, like L-glutamate and L-lysine (Lee and Wendisch, 2017). Further, this bacterium has been engineered for the production of different compounds, like the proteinogenic amino acids L-serine (Peters-Wendisch et al., 2005), L-valine (Blombach et al., 2009; Chen et al., 2015; Mahr et al., 2015), L-leucine and L-isoleucine (Vogt et al., 2014; Vogt et al., 2015), the cyclic amino acid pipecolic acid (Pérez-García et al., 2016), the omega amino acids γ-aminobutyrate (Kim et al., 2013b; Jorge et al., 2016), and ectoine (Becker et al., 2013; Pérez-García et al., 2017), the alkylated amino acid *N*-methylalanine (Mindt et al., 2018) and

the halogenated amino acid 7-Cl-Trp and 7-Br-Trp (Veldmann et al., 2019a; Veldmann et al., 2019b).

Since indole is a derivative of Trp, the Trp overproducing *C. glutamicum* strain Tp679 (pCES208-*trpD*) (Purwanto et al., 2018; Veldmann et al., 2019b) was an ideal host strain for the fermentative production of indole. In order to enable high Trp concentration, the *C. glutamicum* wildtype was modified by following changes. The feedback resistant 3-deoxy-D-arabinoheptulosonate-7-phosphate synthase gene (*aroG*) from *E. coli* was overexpressed to channel the flux to chorismate, the precursor of all aromatic amino acids. To avoid the by-product formation of L-phenylalanine and L-tyrosine the chorismate mutase encoded by *csm* was deleted. Further, the flux from chorismate to Trp was optimized by overexpression of the homologous feedback resistant anthranilate synthase component 1 gene (*trpE)* and the *trpD* the anthranilate phosphoribosyltransferase gene from *E. coli*.

Here, we describe the fermentative production of indole starting with the Trp overproducing *C. glutamicum* strain Tp679 (pCES208-*trpD*). *TnaA*s from *Photobacterium profundum, E. coli, Aeromonas hydrophila, Porphyromonas gingivalis, Propionibacterium acnes,* and *Proteus vulgaris* were heterologously overexpressed in *C. glutamicum*. Their specific enzyme activities with their natural substrate Trp were determined, an extended substrate portfolio was tested, and the fermentative production of indole was established.

2.4.3 Material and Methods

2.4.3.1 Bacterial strains and growth conditions

Bacterial strains and plasmids used in this study are listed in Table 2.4.1. *Escherichia coli* DH5α (Hanahan, 1983) was used for cloning the plasmid constructs. *E. coli* and *C. glutamicum* were regularly grown in lysogeny broth (LB) in 500 mL baffled flasks at 120 rpm at 37 °C or 30 °C, respectively. For growth and production experiments *C. glutamicum* was inoculated in CGXII minimal medium with 40 g L^{-1} glucose (Eggeling and Bott, 2005) in 500 mL (filling volume 10%) to an optical density (OD_{600}) of 1 and incubated at 120 rpm. Growth was monitored by measuring the optical density at 600 nm using a V-1200 spectrophotometer (VWR, Radnor, PA, USA). For tolerance test, *C. glutamicum* was grown in the BioLector® microfermentation system (m2p Labs) in CGXII medium supplemented with indole. To produce indole, CGXII minimal medium was used. Strains derived from Tp679 were supplemented additionally with 1.37 mM L-tyrosine and 1.5 mM L-phenylalanine in minimal medium. When necessary, the growth medium was supplemented with kanamycin (25 μg mL^{-1}) and/or tetracycline (5 μg mL^{-1}). Isopropyl-β-D-1-thiogalactopyranoside (IPTG) (1 mM) was added to induce the gene expression from the vector pECXT99A (Kirchner and Tauch, 2003).

Table 2.4.1: List of strains and plasmids used in this work

Strains and plasmids	Description	Source
Strains		
WT	*C. glutamicum* wild type, ATCC, 13032	ATCC
WT (pECXT99A-*tnaA-Pp*)	WT carrying pECXT99A-*tnaA-Pp*	This work
WT (pECXT99A-*tnaA-Ec*)	WT carrying pECXT99A-*tnaA-Ec*	This work
WT (pECXT99A-*tnaA-Ah*)	WT carrying pECXT99A-*tnaA-Ah*	This work
WT (pECXT99A-*tnaA-Pg*)	WT carrying pECXT99A-*tnaA-Pg*	This work
WT (pECXT99A-*tnaA-Pa*)	WT carrying pECXT99A-*tnaA-Pa*	This work
WT (pECXT99A-*tnaA-Pv*)	WT carrying pECXT99A-*tnaA-Pv*	This work
WT (pECXT99A)	WT carrying pECXT99A	This work

Strains and plasmids	Description	Source
Tp679 (pCES208-*trpD*)	*C. glutamicum* ATCC 13032 wild type *Δcsm* Δ*trpL*::P_{ilvCM1}*trpE*^{fbr} Δ*vdh*::P_{ilvC}*aroG*^{fbr} carrying pCES208-*trpD*	(Purwanto et al., 2018)
IndoPp	Tp679 (pCES208-*trpD*) carrying pECXT99A-*tnaA-Pp*	This work
IndoEc	Tp679 (pCES208-*trpD*) carrying pECXT99A-*tnaA-Ec*	This work
IndoAh	Tp679 (pCES208-*trpD*) carrying pECXT99A-*tnaA-Ah*	This work
IndoPg	Tp679 (pCES208-*trpD*) carrying pECXT99A-*tnaA-Pg*	This work
IndoPa	Tp679 (pCES208-*trpD*) carrying pECXT99A-*tnaA-Pa*	This work
IndoPv	Tp679 (pCES208-*trpD*) carrying pECXT99A-*tnaA-Pv*	This work
IndoEmpty	Tp679 (pCES208-*trpD*) carrying pECXT99A	This work
Plasmids		
pECXT99A	Tet^R, *C. glutamicum*/ *E. coli* shuttle vector (Ptrc, *lacI*, pGA1, $OriV_{Cg}$)	(Kirchner and Tauch, 2003)
(pECXT99A-*tnaA-Pp*)	Tet^R, pECXT99A overexpressing *tnaA* from *P. profundum*	This work
(pECXT99A-*tnaA-Ec*)	Tet^R, pECXT99A overexpressing *tnaA* from *E. coli*	This work
(pECXT99A-*tnaA-Ah*)	Tet^R, pECXT99A overexpressing *tnaA* from *A. hydrophila*	This work
(pECXT99A-*tnaA-Pg*)	Tet^R, pECXT99A overexpressing *tnaA* from *P. gingivalis*	This work

Strains and plasmids	Description	Source
(pECXT99A-*tnaA*-*Pa*)	Tet^R, pECXT99A overexpressing *tnaA* from *P. acnes*	This work
(pECXT99A-*tnaA*-*Pv*)	Tet^R, pECXT99A overexpressing *tnaA* from *P. vulgaris*	This work

2.4.3.2 Molecular genetic technique and strain construction

E. coli was used as host organism for gene cloning. Transformation in *E. coli* was done by heat shock at 42 °C for 90 s with the rubidium chloride method (Hanahan, 1983). *C. glutamicum* was transformed by electroporation at 2.5 kV, 200 Ω and 25 µF (Eggeling and Bott, 2005). All used primers are listed in Table 2.4.2. The forward primers *Pp-tnaA*-1, *Ec-tnaA*-1, *Ah-tnaA*-1, *Pg-tnaA*-1, *Pa-tnaA* and *Pv-tnaA*-1 harbor the artificial ribosome binding site (RBS) sequence (GAAAGGAGGCCCTTCAG). Some genes were amplified in two parts to enable a base pair exchange. The primers *Pp-tnaA*-1-fwd/*Pp-tnaA*-1-rv (part I) and *Pp-tnaA*-2-fwd/*Pp-tnaA*-2-rv (part II) were used for the amplification of *tnaA-Pp* gene from the genomic DNA of *Photobacterium profundum* (DSM 21095). The isoleucine 119 was codon-optimized with the primer *Pp-tnaA*-2-fwd/*Pp-tnaA*-1-rv. The primer pairs *Ec-tnaA*-1-fwd/*Ec-tnaA*-1-rv (part I) and *Ec-tnaA*-2-fwd/*Ec-tnaA*-2-rv (part II) were used to amplify *tnaA-Ec* gene from genomic DNA of *E. coli* K12. The primers *Ec-tnaA*-2-fwd/*Ec-tnaA*-1-rv harbor a base pair exchange to optimize the codon usage of arginine 295 for *C. glutamicum*. The primer pairs *Ah-tnaA*-1-fwd/*Ah-tnaA*-1-rv (part I) and *Ah-tnaA*-2-fwd/*Ah-tnaA*-2-rv (part II) were used to amplify the *tnaA-Ah* gene from the genomic DNA of *Aeromonas hydrophila* (DSM 30187). The two amino acids isoleucine 4 and isoleucine 244 were codon-optimized for *C. glutamicum* with the primers *Ah-tnaA*-1-fwd, *Ah-tnaA*-2-fwd, and *Ah-tnaA*-1-rv which included a base pair exchange compared to the original sequence. The gene *tnaA-Pg* was amplified with the primer pairs *Pg-tnaA*-1-fwd/*Pg-tnaA*-1-rv (part I) and *Pg-tnaA*-2-fwd/*Pg-tnaA*-2-rv (part II) from the genomic DNA of *Porphyromonas gingivalis* (DSM 20709). The isoleucine 167 was codon-optimized for *C. glutamicum* with the primers *Pg-tnaA*-2-fwd/*Pg-tnaA*-1-rv which contain a base pair exchange in comparison to the original sequence. The gene *tnaA-Pa* was

amplified with the primer pair *Pa-tnaA*-fwd and *Pa-tnaA*-rv from the genomic DNA of *Propionibacterium acnes* (DSM 16379). For amplification of the *tnaA-Pv* gene the genomic DNA of *Proteus vulgaris* (DSM 13387) and the primer pairs *Pv-tnaA*-1-fwd/*Pv-tnaA*-1-rv (part I) and *Pv-tnaA*-2-fwd/*Pv-tnaA*-2-rv (part II) were used. For the codon optimization of the arginine 4, isoleucine 284, arginine 289, arginine 457 and arginine 462 for *C. glutamicum* the primer *Pv-tnaA*-1-fwd, *Pv-tnaA*-1-rv, *Pv-tnaA*-2-fwd, and *Pv-tnaA*-2-rv were used. The *tnaA* genes (consisting of one or two parts) were cloned via Gibson assembly (Gibson et al., 2009) in the vector pECXT99A (Kirchner and Tauch, 2003) digested with BamHI. The developed plasmids were pECXT99A-*tnaA-Ec*, pECXT99A-*tnaA-Pg*, pECXT99A-*tnaA-Pp*, pECXT99A-*tnaA-Pv*, pECXT99A-*tnaA-Ah* and pECXT99A-*tnaA-Pa*. The constructed plasmids were used to transform *C. glutamicum* strains.

Table 2.4.2: Primers used in this work.

Name	**Sequence**
Pp-tnaA-1-fwd	CATGGAATTCGAGCTCGGTACCCGGGAAAGGAGGCCCTTCAG ATGGAAAACTTTAAACACTTACC
Pp-tnaA-1-rv	GTCCCTTCTCGATTTCACGT
Pp-tnaA-2-fwd	CGTGAAATCGAGAAGGGACT
Pp-tnaA-2-rv	GCCTGCAGGTCGACTCTAGAGGATCTTAAGCTTCTTCTAGAAT CTGGTT
Ec-tnaA-1-fwd	CATGGAATTCGAGCTCGGTACCCGGGGAAAGGAGGCCCTTCA GATGGAAAACTTTAAACATCTCCCT
Ec-tnaA-1-rv	GCAAAGGGTGCGGCACTCGGTG
Ec-tnaA-2-fwd	CACCGAGTGCCGCACCCTTTGC
Ec-tnaA-2-rv	GCCTGCAGGTCGACTCTAGAGGATCTTAAACTTCTTTAAGTTT GCGGTG
Ah-tnaA-1-fwd	CATGGAATTCGAGCTCGGTACCCGGGGAAAGGAGGCCCTTCA GATGCGTCGTATCCCCGAGCCG
Ah-tnaA-1-rv	TGGCGCACGATCTCCTTGATGCTG
Ah-tnaA-2-fwd	CATCAAGGAGATCGTGCGCCAG

Name	Sequence
Ah-tnaA-2-rv	GCCTGCAGGTCGACTCTAGAGGATCTCAGACCGGCTTGAGCC GCGCG
Pg-tnaA-1-fwd	CATGGAATTCGAGCTCGGTACCCGGGGAAAGGAGGCCCTTCA GATGGAATTACCTTTTTAGAATCC
Pg-tnaA-1-rv	GTCTCTTTCAGGATTTTCTCTA
Pg-tnaA-2-fwd	GTTAGAGAAAATCCTGAAAGAG
Pg-tnaA-2-rv	GCCTGCAGGTCGACTCTAGAGGATCTTACTTGGCTTTTTCCAG CT
Pa-tnaA-fwd	CATGGAATTCGAGCTCGGTACCCGGGGAAAGGAGGCCCTTCA GATGAAGTACATCCCCGAACC
Pa-tnaA-rv	GCCTGCAGGTCGACTCTAGAGGATCTCACCGAATTGGTTCGA GTCG
Pv-tnaA-1-fwd	CATGGAATTCGAGCTCGGTACCCGGGGAAAGGAGGCCCTTCA GATGGCTAAACGCATCGTAGAACCAT
Pv-tnaA-1-rv	GTTGGCGTGCTAACGTGAAGATTTCTTC
Pv-tnaA-2-fwd	CGTGATAATGAAGAAATCTTCACGTTAGCACGCCAACGTTG
Pv-tnaA-2-rv	GCCTGCAGGTCGACTCTAGAGGATCTTATTTGATTGGTTTTAA GCGAGCAGTAAAGTGGCGTAATACAG

2.4.3.3 Colorimetric indole detection

To visualize the production of indole *C. glutamicum* strains containing the overexpressed *tnaA*s were plated on an LB plate containing 0.5 mM L-tryptophan, 1 mM IPTG and 5 µg mg^{-1} tetracycline. The plate was incubated at 30 °C for 24 h. The cells were covered with 1 mL of indole Kovac reagent (*n*-Butanol, Hydrochloric acid, 4-(Dimethylamino)benzaldehyde. A red-violet coloring was visible when indole was produced.

2.4.3.4 Cultivation and disruption of tryptophanase overproducing *C. glutamicum* cells

TnaA overexpressing *C. glutamicum* strains were inoculated in 50 mL LB from an overnight culture. Expression of *tnaA* was induced by 1 mM IPTG and the cells were grown for 24 h at 30 °C at 120 rpm before the cells were harvested and the cell pellet stored at -20 °C for later analysis. To disrupt the cells the pellet was resuspended in 200 mM potassium phosphate buffer (pH 8.3) or 10 mM dipotassium phosphate buffer (pH 7.0) and sonicated for 9 min at an amplitude of 55% and a cycle of 0.5 on ice with the UP200S Ultrasonic Processor from Hielscher Ultrasound Technology. After centrifugation (60 min, 4°C, 16400 rpm), the supernatant was used for the enzymatic assay and for a 10% sodium dodecyl sulfate-polyacrylamide gel electrophoresis (SDS-PAGE).

2.4.3.5 Enzymatic assay for tryptophanase (Colorimetric)

The tryptophanase enzymatic assay was measured colorimetrically by endpoint determination of the formed indole. The measurement was performed in triplicates. The assay was performed with a mixture containing 200 mM potassium phosphate buffer pH 8.3, 0.041 mM pyridoxal 5-phosphate and the crude extract. The samples were incubated at 30 °C for 10 min. The reaction was stopped by addition of 100 µL of trichloroacetic acid (100%). To phase extract the liberated indole 2 mL toluene were added. 200 µL of the toluene-free supernatant was taken and mixed with 5% (w/v) *p*-dimethylaminobenzaldehyde solution (DMAB) and 8.8 mL of 8% hydrochloric acid diluted in 95% ethanol were added. After 10 min of equilibration 1 mL of the solution was used for colorimetric measurement at 540 nm. The indole standards were prepared using the same procedure.

2.4.3.6 Enzymatic assay for tryptophanase with tryptophan derivates

The measurement was performed in triplicates. The formation of 7-bromoindole and 7-chloroindole in the enzyme assay was measured by HPLC. The reaction mixture contained 10 mM dipotassium phosphate buffer (pH 7.0), 0.1 mM pyridoxal-5-phosphate, 1 mM 7-bromo-tryptophan/ 7-chloro-tryptophan, 5% 2-propanol (v/v) and the crude extract. The mixture was incubated at 30 °C and aliquots were taken in regular time intervals. The reaction

was stopped with one volume of methanol and the product formation was measured with HPLC.

2.4.3.7 Analytic procedure

For the quantification of Trp a high-pressure liquid chromatography (HPLC) system was used (1200 series, Agilent Technologies Deutschland GmbH, Böblingen, Germany). The supernatants of the cell culture or enzyme assay were collected by centrifugation (14680 rpm, 20 min, RT) and further used for analysis. For the detection of Trp, the samples were derivatised with *ortho*-phthaldialdehyde (OPA) (Schneider and Wendisch, 2010). The amino acid separation was performed by a precolumn (LiChrospher 100 RP18 EC-5 µ (40 mm × 4 mm), CS-Chromatographie Service GmbH, Langerwehe, Germany) and a column (LiChrospher 100 RP18 EC-5 µ (125 mm × 4 mm), CS Chromatographie Service GmbH). The detection was carried out with a fluorescence detector (FLD G1321 A, 1200 series, Agilent Technologies) with the excitation and emission wavelengths of 230 nm and 450 nm, respectively.

To detect indole the samples were derivatized with 9-fuorenylmethyl chlorocarbonate (Fmoc-Cl) according to published methods (Schneider et al., 2012) with modifications (Jensen and Wendisch, 2013). L-proline was used as an internal standard. The separation was carried out by a reversed-phase HPLC using a pre-column (LiChrospher 100 RP8 EC-5 µ (40 mm × 4.6 mm), CS-Chromatographie Service GmbH, Langerwehe, Germany) and a column (LiChrospher 100 RP8 EC-5µ (125 mm × 4.6 mm), CS Chromatographie Service GmbH). The detection was performed with a fluorescence detector (FLD G1321A, 1200 series, Agilent Technologies) with the excitation and emission wavelength of 263 nm and 310 nm respectively. Analytical HPLC for the quantification of 7-chloro/bromo-L-tryptophan and 7-chloro/bromoindole was performed on a Shimadzu NexeraXR 20A System with autosampler, degasser, column oven, diode array detector, and a Phenomex Luna C18 column (2.9 µm, 50 × 2.1 mm) with a gradient (in 5.5 min from 5% B to 95% B, 0.5 min 95% B and back to 5% B in 3 min, total run time 9 min) at a flow rate of 650 µL min^{-1} and column oven temperature of 40 °C. HPLC solvent A consists of 99.9% water and 0.1% TFA, solvent B of 99.9% acetonitrile and 0.1% TFA.

2.4.4 Results & Discussion

2.4.4.1 Determination of tryptophanase gene expression in *C. glutamicum*

Six different TnaAs from *Photobacterium profundum* (Phillips et al., 2011), *E. coli* (Li and Young, 2013), *Aeromonas hydrophila* (Cowell et al., 1973), *Porphyromonas gingivalis* (Yoshida et al., 2009), *Propionibacterium acnes* (Jakab et al., 1996) *and Proteus vulgaris* (Pioselli et al., 2004) were chosen for the indole production by *C. glutamicum*. They were selected, due to their different temperature optima, specific enzyme activities and substrate spectra. The amino acid sequences of all chosen TnaAs were compared using T-coffee (Supplementary data Fig. 2.4.1) (Notredame et al., 2000; Wallace et al., 2006; Moretti et al., 2007; Tateno et al., 2009; Di Tommaso et al., 2011). They showed a high sequence identity between 95 to 98%.

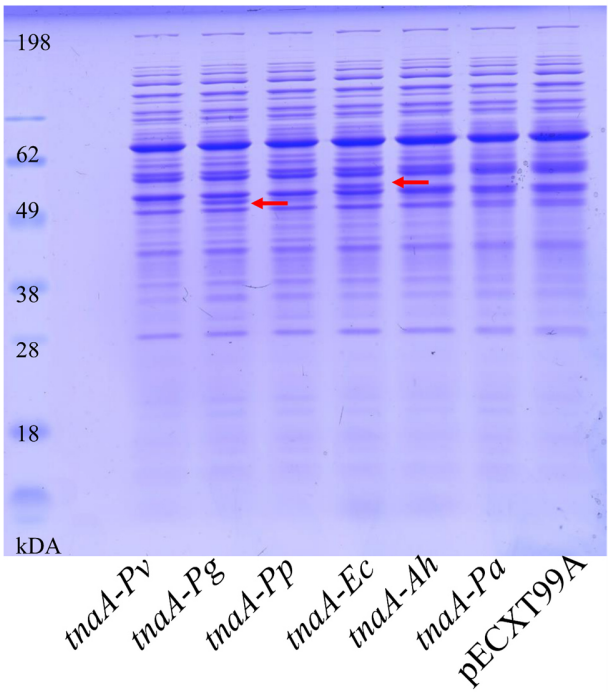

Figure 2.4.2: Acrylamide gel of *C. glutamicum* wildtype overexpressing *tnaAs*. The *tnaAs* were overexpressed from the expression plasmid pECXT99A in *C. glutamicum* wildtype. The strains were cultivated for 24 h in LB with 1 mM IPTG. Line 1: WT (pECXT99A-*tnaA-Pv*); line 2: WT (pECXT99A-*tnaA-Pg*); line 3: WT (pECXT99A-*tnaA-Pp*); line 4: WT (pECXT99A-*tnaA-Ec*); line 5: WT (pECXT99A-*tnaA-Ah*); line 6: WT (pECXT99A-*tnaA-Pa*); line 6: WT (pECXT99A).

To test the expression of the *tnaA*s the expression plasmids were transformed in *C. glutamicum* WT and after growth in LB medium with 1 mM IPTG, the crude extracts were checked in an acrylamide gel. The expression of *tnaA-Pg* and *tnaA-Ec* were approved, since an additional band (TnaA-*Pg*: 52 kDa; TnaA-*Ec*: 53 kDa) compared to the empty vector control was visible (Fig. 2.4.2). Additional bands for the TnaAs TnaA-*Pv* (52 kDa), TnaA-*Pp* (54 kDa), TnaA-*Ah* (51 kDa) and TnaA-*Pa* (51 kDa) were not detectable.

In order to test the indole production a qualitative assay was performed (see chapter 2.4.3.3). The *C. glutamicum* strains wildtype and Tp679 (pCES20-*trpD*) overexpressing the *tnaA*s were grown on an LB-agar plate with 0.5 mM Trp and 1 mM IPTG overnight and were covered with Kovac reagent to visualize produced indole. The *C. glutamicum* wildtype and Tp679 (pCEs208-*trpD*) strains overexpressing *tnaA-Ec*, *tnaA-Pv* and *tnaA-Pg* showed a reddish color thus this TnaAs were active in *C. glutamicum* (Fig. 2.4.3). Additionally, in *C. glutamicum* wildtype the TnaA-*Pa* showed activity (Fig. 2.4.3). The empty vector control did not show a reddish color. To verify the activity of the TnaAs a quantitative enzyme activity assay was performed.

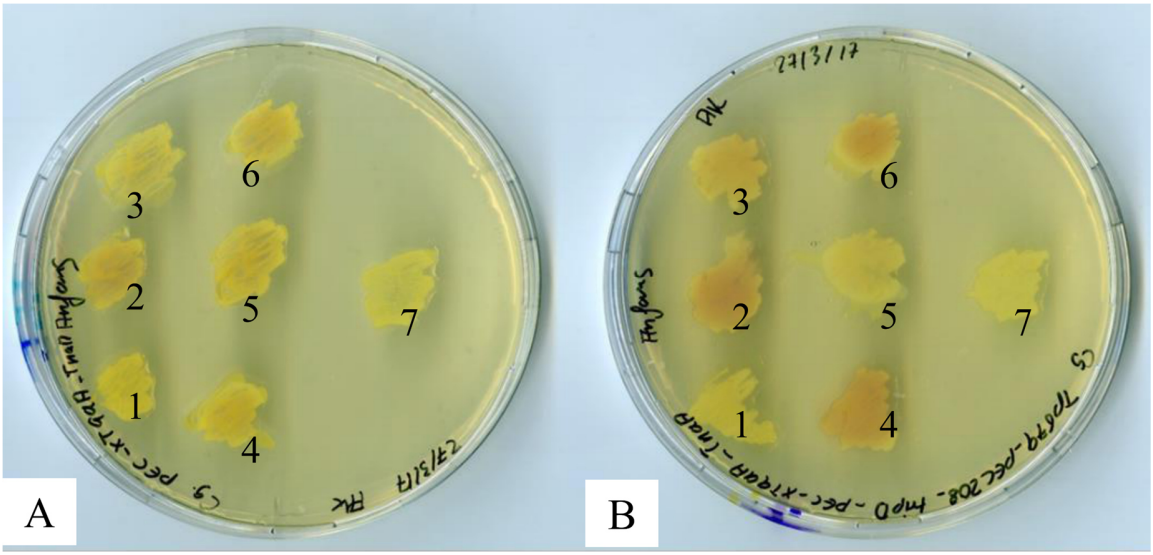

Figure 2.4.3: Qualitative test for indole production by *C. glutamicum* strains overexpressing *tnaAs*. The *tnaAs* overexpressing *C. glutamicum* strains were grown on LB-agar plates with 0.5 mM Trp and 1 mM IPTG and covered with 1 mL Kovac reagent. 1: *tnaA-Pp*; 2: *tnaA-Ec*; 3: *tnaA-Ah*; 4: *tnaA-Pg*; 5: *tnaA-Pa*; 6: *tnaA-Pv*; 7: empty vector. A: *C. glutamicum* wildtype; B: Trp overproducing *C. glutamicum* strain Tp679 (pCES208-*trpD*).

2.4.4.2 Determination of the specific enzyme activity of TnaAs (colorimetric)

Although some TnaAs were neither seen in the acrylamide gel not showed indole production in the qualitative assay, a quantitative colorimetric enzyme assay was performed using crude extracts. The TnaAs TnaA-*Ec*, TnaA-*Pv*, TnaA-*Pa,* and TnaA-*Pp* showed specific enzymatic activity, whereas, for TnaA-*Ah*, TnaA-*Pg* and the empty vector control no activity was observed. This reflects the previous results of the qualitative assay, where the TnaA-*Ec*, TnaA-*Pv,* and TnaA-*Pa* were active as well. However, TnaA-*Pg* which was active in the qualitative assay and an additional band was observed in the acrylamide gel did not exhibit activity in the quantitative colorimetric enzyme assay. For TnaA-*Pp* activity was observed for the first time in the qualitative enzyme assay. TnaA-*Ah* and the empty vector control did not show activity in any test.

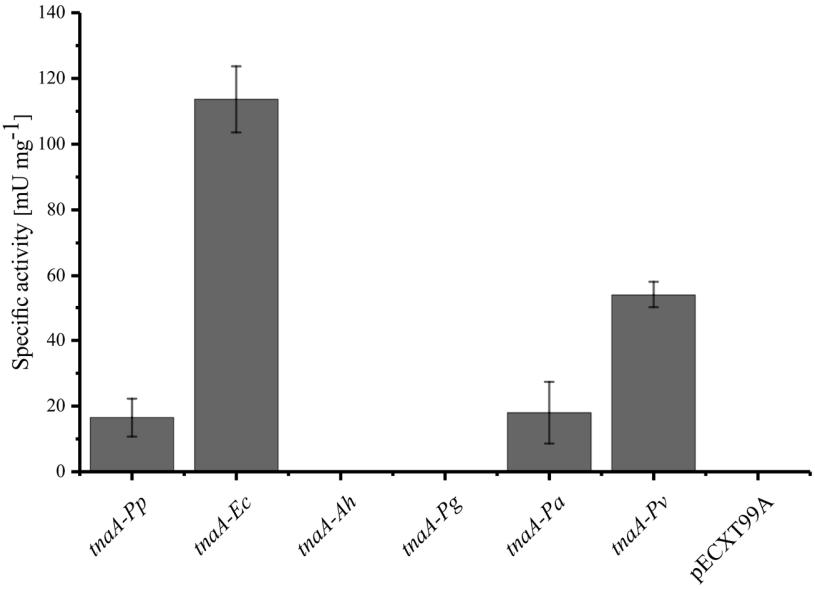

Figure 2.4.4: Specific enzymatic activity of the *tnaA*s overexpressed in *C. glutamicum* wildtype. *C. glutamicum* wildtype carried an expression plasmid overexpressing the *tnaA*s. The strains were grown in LB with 1 mM IPTG. The crude extracts were assayed for TnaA activity in a colorimetric enzyme assay. Means and standard deviations of triplicates are shown.

The highest specific enzymatic activity of 114 ± 10 mU mg^{-1} was measured in the crude extract harboring TnaA-*Ec* (Fig. 2.4.4). The specific activity of 818 ± 37 mU mg^{-1} was reported in the crude extract of *E. coli*, which is 7-times higher compared to this study (Zhang and Hong, 2009). The TnaA-*Pv* had a specific activity of 54 ± 4 mU mg^{-1} in the crude extract

of *C. glutamicum* (Fig. 2.4.4). The specific activity of the enzyme with Trp as substrate is not reported. The enzymes TnaA-*Pa* and TnaA-*Pp* showed in the *C. glutamicum* crude extracts similar specific enzyme activities, of 18 ± 9 mU mg^{-1} and 16 ± 6 mU mg^{-1}, respectively (Fig. 2.4.4). The specific enzymatic activity of the TnaAs of *P. acnes* and *P. profundum* is not reported in crude extract.

Hence, the TnaA-*Ec* and TnaA-*Pa* are promising candidates for the fermentative production of indole, since both showed high activity in the quantitative (strong reddish color) and qualitative assay.

2.4.4.3 Expansion of the substrate spectrum of the tryptophanases

Further, the TnaAs were investigated regarding their substrate spectrum. Here, the active TnaAs from *E. coli*, *P. vulgaris* and *P. acnes* were further analyzed (see chapter 2.4.3.6). To analyze the substrate spectrum the halogenated Trp derivatives 7-chloro-tryptophan (7-Cl-Trp) and 7-bromo-tryptophan (7-Br-Trp) were tested (Figure 2.4.5) since in the previous studies these compounds were produced by *C. glutamicum* (Veldmann et al., 2019a; Veldmann et al., 2019b). Further conversion of 7-Cl-Trp and 7-Br-Trp to 7-chloroindole and 7-bromoindole by overexpression of a *tnaA* in the halogenated Trp producing *C. glutamicum* strain HalT2 could be considered. As control substrate Trp was chosen and as control strain WT (pECXT99A). The substrates were tested in an enzymatic activity assay. With the natural substrate Trp the results of the colorimetric were reflected. TnaA-*Ec* showed the highest conversion of Trp to indole after 30 min, it consumed half of the added Trp. 37.4% Trp was converted to indole by the TnaA-*Pv* and only 23.7% by the TnaA-*Pa*, while the empty vector control (WT (pECXT99A)) showed no activity. In case of the halogenated Trp derivatives the conversion rate dropped dramatically. Only the TnaA-*Ec* and TnaA-*Pv* accepted 7-Cl-Trp and 7-Br-Trp as substrate. In the case of 7-Cl-Trp, the TnaA-*Ec* and TnaA-*Pv* converted 2.4% and 1.6%, respectively, into 7-chloroindole within 48 h. 7-Cl-Trp was not consumed by the TnaA-*Pa* and the empty vector control. The conversion of 7-Br-Trp proceeded faster, already after 60 min the TnaA-*Ec* converted 2.2% and the TnaA-*Pv* 0.95% 7-Br-Trp to 7-bromoindole. TnaA-*Pa* and the empty vector control did not accept 7-Br-Trp as substrate (Fig. 2.4.5).

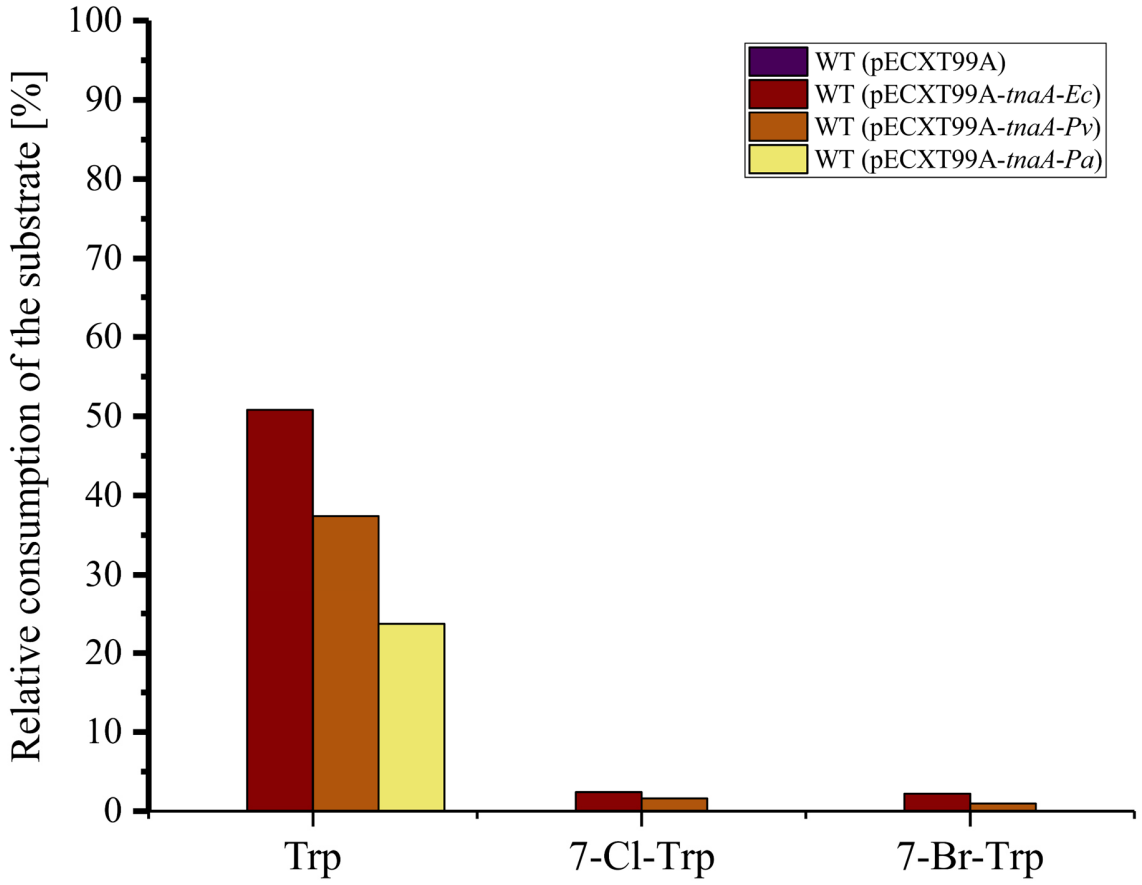

Figure 2.4.5: Enzymatic activity assay of three TnaAs with Trp, 7-Cl-Trp, and 7-Br-Trp as substrate. The crude extract of the strains WT (pECXT99A-*tnaA-Ec*), WT (pECXT99A-*tnaA-Pv*), WT (pECXT99A-*tnaA-Pa*), and WT (pECXT99A) grown in LB with 1 mM IPTG, were tested with 1mM Trp, 7-Cl-Trp or 7-Br-Trp as substrate. The substrate consumption of Trp, 7-Cl-Trp, and 7-Br-Trp was measured after 0.5 h, 48 h, and 1 h, respectively.The substrate consumption was measured with the HPLC.

It was already shown that the TnaA from *P. vulgaris* has a broad substrate spectrum. The wildtype TnaA from *P. vulgaris* accepts different cysteine derivatives beside the natural substrate Trp, like *S*-(*o*-Nitrophenyl)-L-cysteine (SOPC), *S*-methyl-L-cysteine, *S*-ethyl-L-cysteine, and *S*-benzyl-L-cysteine, and the chlorinated L-alanine β-chloro-L-alanine (Kulikova et al., 2006). But the substrate affinity (K_m) for most of the substrates was low, except for L-tryptophan, SOPC, and *S*-benzyl-L-cysteine. This held room for further improvement. By an amino acid replacement of the L-tyrosine 72 to an L-phenylalanine, the active site of the TnaA was rearranged. Hence, the activity of the mutant TnaA Y72F increased 50.000-fold for Trp. Additionally, the K_m for the previously mentioned substrate

decreased by a multiple (Kulikova et al., 2006). This mutation was created to increase the room around the α-carbon atom of the substrate. This may be helpful for 7-Cl-Trp and 7-Br-Trp because the activity and the K_m for Trp have improved a lot and thus the substrate affinity for the halogenated may increase as well. Additionally, the active site could be further improved by a rearrangement of the active site around the indole ring of Trp. By an expansion around this area the space for other Trp derivatives like 5,6-halo-L-tryptophans, methyl-L-tryptophans or hydroxy-L-tryptophans could be created. For the wildtype TnaA from *E. coli* it was shown before that it accepts different Trp derivatives, like 4,5,6,7-methyl-tryptophan and 4,5,6,7-chloro-tryptophan (Snell, 1975). In this study the TnaA from *E. coli* showed the lowest and slowest conversion rate with 7-Cl-Trp, which fits the previously tested *E. coli* TnaA, which has the lowest substrate affinity towards 7-Cl-Trp. Additionally, an *E. coli* TnaA mutant from a Trp auxotroph *E. coli* strain was tested, but no activity with halogenated Trp as substrate was observed (Snell, 1975). Hence, no improvement of this *E. coli* TnaA mutant was achieved. Another promising *E. coli* TnaA mutant was generated and tested by Phillips and co-workers. In this mutant histidine 463 was exchanged by phenylalanine, which is located in the substrate-binding portion of the active site (Phillips et al., 2002). Hence, the high activity and substrate specify towards Trp got lost but the substrate spectrum was extended to the Trp benzimidazole analog β-(Benzimidazol-1-yl)-L-alanine (Harris and Phillips, 2013). Since the activity with the main substrate decreased and the activity increased for Trp analogues, it might be a benefit for other substrates, like halogenated Trp.

2.4.4.4 Fermentative production of indole

The impact of the product indole on growth was tested by adding different concentrations of indole to cultivation. Indole was added at inoculation to *C. glutamicum* wildtype in CGXII minimal medium with 40 g L^{-1} glucose. The half maximal growth rate of *C. glutamicum* was reached with an indole concentration of 4.5 mM (527 mg L^{-1}) (Fig. 2.4.6).

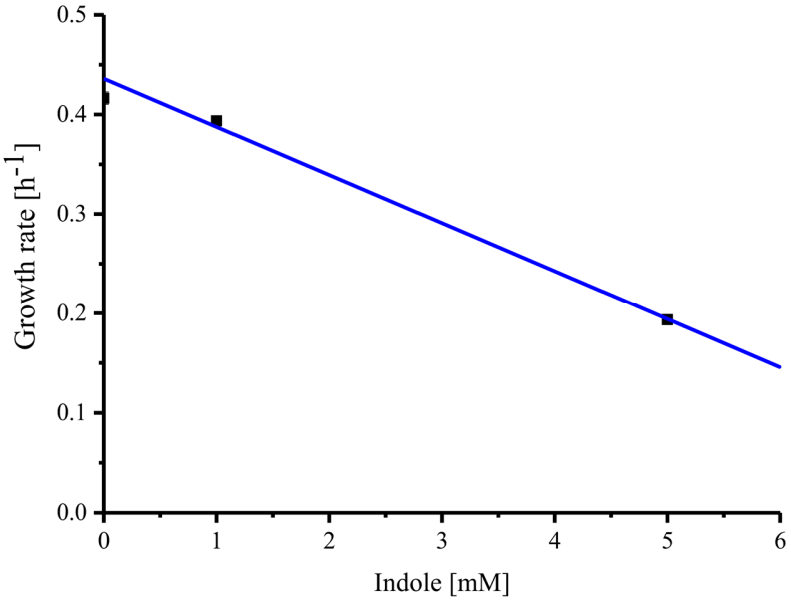

Figure 2.4.6: Response of *C. glutamicum* wildtype to externally added indole. To determine the K_i value for indole *C. glutamicum* wildtype was grown in CGXII supplemented with 40 g L^{-1} glucose and different concentration of indole, between 0 and 5 mM. The half-maximal specific growth rate was determined by linear regression.

In other microorganisms, it is known that indole has a toxic effect in low concentration. The growth of *Pseudomonas putida* KT2440 is already strongly inhibited at a concentration of 2 mM indole, which is caused by the inhibition of cellular energy production and protein folding (Kim et al., 2013a). In *E. coli*, which owns a TnaA, indole is toxic to the microorganism at a concentration of 5 mM (Wang et al., 2001). Indole might cause membrane changes which result in the generation of superoxide (Garbe et al., 2000). An important aspect of indole production in *C. glutamicum* could be the metabolization of indole to further metabolites which would prevent indole accumulation. Some Gram-positive *cocci* are able to utilize indole as sole carbon and energy source via the anthranilate pathway, where indole is degraded via 2,3-dihydroxyindole, *N*-carboxyanthranilic acid to anthranilic acid (Fujioka and Wada, 1968). Other Gram-negative bacteria degrade indole via isatin, *N*-formylanthranilic acid, anthranilic acid, salicylic acid to catechol via the catechol pathway (Sakamoto et al., 1953). So far in *C. glutamicum* is not known a degradation pathway of indole, whereby it is a possible host for indole production.

To enable the fermentative production of indole by *C. glutamicum*, different *tnaA* genes from *E. coli* (IndoEc), *P. gingivalis* (IndoPg), *P. profundum* (IndoPp), *P. vulgaris* (IndoPv), *A. hydrophila* (IndoAh) and *P. acnes* (IndoPa) were overexpressed in the Trp overproducing strain Tp679 (pCES208-*trpD*). The recombinant strains were inoculated in CGXII minimal medium with 40 g L^{-1} glucose and 1 mM IPTG to an OD_{600} of 1. IndoPp and IndoAh grew with a specific growth rate of 0.15 ± 0.00 h^{-1} and 0.12 ± 0.01 h^{-1}, respectively. Both strains produced Trp (IndoPp: 276 ± 89 mg L^{-1}; IndoAh: 399 ± 15 mg L^{-1}), but in case of IndoPp indole was not detectable and IndoAh produced a low amount (Indole: 62 ± 3 mg L^{-1}) (Fig. 2.4.7). This reflects the other experiments where the TnaA-*Pp* showed low activity in the enzymatic assay and the TnaA-*Ah* showed no activity in the other experiments. The strain IndoPg showed a specific growth rate of 0.14 ± 0.01 h^{-1} and produced 278 ± 85 mg L^{-1} Trp and 28 ± 10 mg L^{-1} indole. The low amount of indole production fits to the results of the enzyme assay where the specific enzyme activity of TnaA-*Pg* was not detectable. However, the TnaA-*Ec*, TnaA-*Pv,* and TnaA-*Pa* were positive in all experiments, except the acrylamide gel (TnaA-*Pv*, TnaA-*Pa*). IndoPa and IndoEc grew with a specific growth rate of 0.15 ± 0.01 h^{-1} and 0.11 ± 0.01 h^{-1}, respectively. IndoPa produced 438 ± 10 mg L^{-1} Trp and 165 ± 46 mg L^{-1} indole and IndoEc 342 ± 15 mg L^{-1} Trp and 210 ± 23 mg L^{-1} indole. The highest titer of indole was reached by IndoPv, it produced 329 ± 17 mg L^{-1} indole and 333 ± 9 mg L^{-1} Trp (Fig. 2.4.7). The empty vector control showed no indole production. Until now, a fermentative production process of indole is not shown.

To increase the production of indole, strategies from indole producing microorganisms could be transferred to the recombinant indole producing strains. Most of the complex regulatory processes are triggered by the environment (Lee and Lee, 2010; Han et al., 2011). Hence, some of these triggers may have a direct influence on the TnaA, like antibiotics or trace elements, and consequently change the activity or substrate affinity (Han et al., 2011). Another option to increase the indole production is to enhance the *tnaA* expression. By the exchange of the promoter and the RBS the expression in *C. glutamicum* can be increased (Shi et al., 2018). A limiting step to produce indole may be the regeneration of the co-factor of the TnaA: PLP. For the binding of PLP in the active site of the TnaA the monovalent cations potassium or ammonium are required (Watanabe and Snell, 1972; Rety et al., 2015).

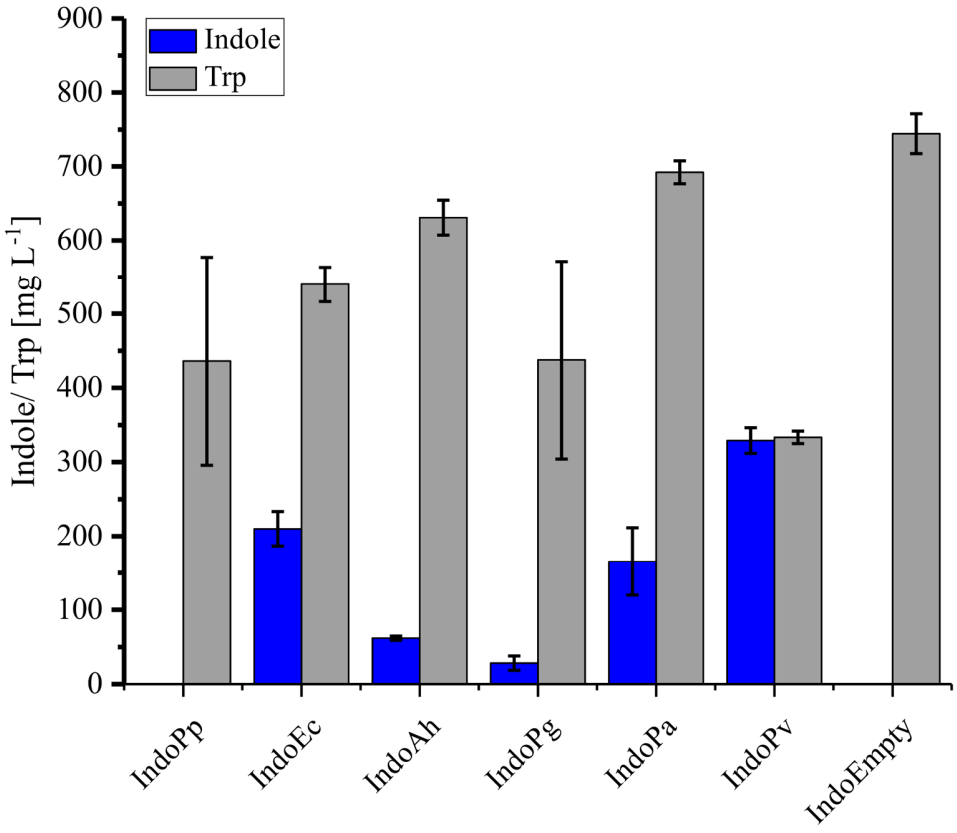

Figure 2.4.7: Production of indole and Trp by *C. glutamicum* Tp679 (pCES208-*trpD*) strains overexpressing the *tnaAs*. The strains were grown in CGXII minimal medium with 40 g L^{-1} glucose. After 72 h the titers of indole and Trp were measured. Means and standard deviations of three replicate cultivations are shown.

In *C. glutamicum* it was shown, that during the production of γ-aminobutyrate (GABA) from xylose an PLP limitation appeared (Baritugo et al., 2018). This resulted, that the PLP-dependent glutamate decarboxylase did not convert glutamate to GABA and glutamate accumulated. The PLP limitation was caused by the utilization of the carbon source xylose. During the utilization xylulose is converted to xylulose 5-phosphate, which requires ATP (Anderson and Wood, 1962). Consequently, the intracellular ATP concentration was to low for the ATP-dependent regeneration of PLP. The limitation was abrogated by the addition of PLP (Baritugo et al., 2018). Hence, an addition or an enhanced regeneration of PLP during the indole production by *C. glutamicum* can enhance the production of indole. One strategy to increase the production of PLP is described by Ma et al., 2015. The ribose 5-phosphate

dependent genes *pdxS* and *pdxT* from *B. subtilis* were overexpressed in cadaverine overexpressing *E. coli* strain (Ma et al., 2015). The intracellular concentration of PLP was increased 2.4-fold to 1144 nmol/g(DCW) and the PLP-dependent production of cadaverine from L-lysine was improved as well. This system could be transferred to *C. glutamicum* for a higher intracellular concentration of PLP.

Another option to improve the indole production is the prevention of product toxicity by indole. It is shown, that adaptive laboratory evolution (ALE) improved the stress response to certain substances (Lee et al., 2013). Hence, a *C. glutamicum* strain improved by ALE towards indole tolerance could have an enhanced indole production. The changes in the developed strain could be analyzed by DNA-sequencing or RNA-Seq. Another approach is the extraction of the indole of the aqueous culture medium in the fermentative production by a two-phase cultivation (aqueous/organic). The aqueous culture medium could be layered with an organic layer such as dodecane or tributyrin in which the produced indole accumulates and thus the product toxicity limitation by indole is prevented (Byrne et al., 2016; Luo et al., 2019). Additionally, could an enhanced export of indole circumvent the product toxicity. Until now the export system of *C. glutamicum* for indole is unknown. In *E. coli* two efflux proteins (encoded by *acrEF*) are known which partially export indole (Kawamura-Sato et al., 1999). Overexpression of *acrEF* in *C. glutamicum* could lead to less product toxicity since more indole is exported extracellularly.

2.4.5 Conclusion

TnaAs from various microorganisms were overexpressed in *C. glutamicum*. Specific enzymatic activity was observed for the TnaA of *E. coli* and *P. vulgaris* for the main substrate Trp and for the Trp derivatives 7-Cl-Trp and 7-Br-Trp. Fermentative production of indole from sugar and ammonium was enabled by the heterologous overexpression of different *tnaA*s in the Trp overproducing *C. glutamicum* strain Tp679 (pCES208-*trpD*). However, production titers were low due to TnaA efficiency.

2.4.6 References

Anderson, R.L., and Wood, W.A. (1962). Purification and properties of L-xylulokinase. J. Biol. Chem. 237**,** 1029-1033.

Barden, T.C. (2010). Indoles: industrial, agricultural and over-the-counter uses, in Heterocyclic Scaffolds II:. Springer. 31-46.

Baritugo, K.-A., Kim, H.T., David, Y., Khang, T.U., Hyun, S.M., Kang, K.H., et al. (2018). Enhanced production of gamma-aminobutyrate (GABA) in recombinant *Corynebacterium glutamicum* strains from empty fruit bunch biosugar solution. Microb. Cell. Fact. 17**,** 129. doi:10.1186/s12934-018-0977-9.

Becker, J., Schäfer, R., Kohlstedt, M., Harder, B.J., Borchert, N.S., Stöveken, N., et al. (2013). Systems metabolic engineering of *Corynebacterium glutamicum* for production of the chemical chaperone ectoine. Microb. Cell. Fact. 12**,** 110. doi:10.1186/1475-2859-12-110.

Bischler, A. (1892). Ueber die entstehung einiger substituirter indole. Berichte der deutschen chemischen Gesellschaft 25**,** 2860-2879. doi:10.1002/cber.189202502123.

Blombach, B., Arndt, A., Auchter, M., and Eikmanns, B.J. (2009). L-Valine production during growth of pyruvate dehydrogenase complex-deficient *Corynebacterium glutamicum* in the presence of ethanol or by inactivation of the transcriptional regulator SugR. Appl. Environ. Microbiol. 75**,** 1197-1200. doi:10.1128/AEM.02351-08.

Byrne, F.P., Jin, S., Paggiola, G., Petchey, T.H.M., Clark, J.H., Farmer, T.J., et al. (2016). Tools and techniques for solvent selection: green solvent selection guides. Sustain. Chem. Process. 4**,** 7. doi:10.1186/s40508-016-0051-z.

Chant, E.L., and Summers, D.K. (2007). Indole signalling contributes to the stable maintenance of *Escherichia coli* multicopy plasmids. Mol. Microbiol. 63**,** 35-43. doi:10.1111/j.1365-2958.2006.05481.x.

Chen, C., Li, Y., Hu, J., Dong, X., and Wang, X. (2015). Metabolic engineering of *Corynebacterium glutamicum* ATCC13869 for L-valine production. Metab. Eng. 29**,** 66-75. doi:10.1016/j.ymben.2015.03.004.

Cowell, J.L., Moser, K., and Demoss, R.D. (1973). Tryptophanase from *Aeromonas liquefaciens*. Purification molecular weight and some chemical, catalytic and immunochemical properties. Biochim. Biophys. Acta (BBA)-Enzymology 315**,** 449-463.

DeRosa, T.F. (2006). Indoles, in Advances in Synthetic Organic Chemistry and Methods Reported in US Patents*,* ed. T.F. DeRosa. (Oxford: Elsevier. 326-336.

Dhani, R., Avinash, A., Salenaagina, S.K., Teja, M.V.S., Masthanaiah, P., Rathnam, P.R., et al. (2011). Indole: The molecule of diverse pharmacological activities. J. Chem. Pharm. Res 3**,** 519-523.

Di Tommaso, P., Moretti, S., Xenarios, I., Orobitg, M., Montanyola, A., Chang, J.-M., et al. (2011). T-Coffee: a web server for the multiple sequence alignment of protein and RNA sequences using structural information and homology extension. Nucleic Acids Res. 39**,** W13-W17. doi:10.1093/nar/gkr245.

Eggeling, L., and Bott, M. (2005). Handbook of *Corynebacterium glutamicum.* CRC press.

Fischer, E., and Jourdan, F. (1883). Ueber die hydrazine der brenztraubensäure. Berichte der deutschen chemischen Gesellschaft 16**,** 2241-2245. doi:10.1002/cber.188301602141.

Frey, M., Stettner, C., Paré, P.W., Schmelz, E.A., Tumlinson, J.H., and Gierl, A. (2000). An herbivore elicitor activates the gene for indole emission in maize. Proc. Natl. Acad. Sci. 97**,** 14801-14806. doi:10.1073/pnas.260499897.

Fujioka, M., and Wada, H. (1968). The bacterial oxidation of indole. Biochim. Biophys. Acta (BBA)-General Subjects 158**,** 70-78. doi:10.1016/0304-4165(68)90073-1.

Garbe, T.R., Kobayashi, M., and Yukawa, H. (2000). Indole-inducible proteins in bacteria suggest membrane and oxidant toxicity. Arch. Microbiol. 173**,** 78-82.

Gibson, D.G., Young, L., Chuang, R.-Y., Venter, J.C., Hutchison Iii, C.A., and Smith, H.O. (2009). Enzymatic assembly of DNA molecules up to several hundred kilobases. Nat. Methods 6**,** 343. doi:10.1038/nmeth.1318.

Gogoleva, O.I., Zakomirdina, L.N., Demidkina, T.V., Phillips, R.S., and Faleev, N.G. (2003). Tryptophanase in aqueous methanol: the solvent effects and a probable mechanism of the hydrophobic control of substrate specificity. Enzyme Microb. Technol. 32**,** 843-850. doi:10.1016/S0141-0229(03)00057-7.

Gong, F., and Yanofsky, C. (2002). Analysis of tryptophanase operon expression in vitro accumulation of TnaC-peptidyl-tRNA in a release factor 2-depleted S-30 extract prevents Rho factor action, simulating induction. J. Biol. Chem. 277**,** 17095-17100. doi:10;277(19):17095-100.

Han, T.H., Lee, J.-H., Cho, M.H., Wood, T.K., and Lee, J. (2011). Environmental factors affecting indole production in *Escherichia coli*. Microbiol. Res. 162**,** 108-116. doi:10.1016/j.resmic.2010.11.005.

Hanahan, D. (1983). Studies on transformation of *Escherichia coli* with plasmids. J. Mol. Biol. 166**,** 557-580. doi:10.1016/S0022-2836(83)80284-8.

Harris, A.P., and Phillips, R.S. (2013). Benzimidazole analogs of L-tryptophan are substrates and inhibitors of tryptophan indole lyase from *Escherichia coli*. FEBS J. 280**,** 1807-1817. doi:10.1111/febs.12205.

Herraiz, T., and Galisteo, J. (2004). Endogenous and dietary indoles: a class of antioxidants and radical scavengers in the ABTS assay. Free Radic. Res. 38**,** 323-331. doi:10.1080/10611860310001648167.

Inman, M., and Moody, C.J. (2013). Indole synthesis–something old, something new. Chem. Sci. 4**,** 29-41. doi:10.1039/C2SC21185H.

Jakab, E., Zbinden, R., Gubler, J., Ruef, C., Von Graevenitz, A., and Krause, M. (1996). Severe infections caused by *Propionibacterium acnes*: an underestimated pathogen in late postoperative infections. Yale J. Biol. Med. 69**,** 477.

Jensen, J.V.K., and Wendisch, V.F. (2013). Ornithine cyclodeaminase-based proline production by *Corynebacterium glutamicum*. Microb. Cell. Fact. 12**,** 63. doi:10.1186/1475-2859-12-63.

Jorge, J.M.P., Leggewie, C., and Wendisch, V.F. (2016). A new metabolic route for the production of gamma-aminobutyric acid by *Corynebacterium glutamicum* from glucose. Amino acids. 48**,** 2519-2531. doi:10.1007/s00726-016-2272-6.

Kawamura-Sato, K., Shibayama, K., Horii, T., Iimuma, Y., Arakawa, Y., and Ohta, M. (1999). Role of multiple efflux pumps in *Escherichia coli* in indole expulsion. FEMS Microbiol. Lett. 179**,** 345-352. doi:10.1111/j.1574-6968.1999.tb08748.x.

Kim, J., Hong, H., Heo, A., and Park, W. (2013a). Indole toxicity involves the inhibition of adenosine triphosphate production and protein folding in *Pseudomonas putida*. FEMS Microbiol. Lett. 343**,** 89-99. doi:10.1111/1574-6968.12135.

Kim, J.Y., Lee, Y.A., Wittmann, C., and Park, J.B. (2013b). Production of non-proteinogenic amino acids from α-keto acid precursors with recombinant *Corynebacterium glutamicum*. Biotechnol. Bioeng. 110**,** 2846-2855. doi:10.1002/bit.24962.

Kirchner, O., and Tauch, A. (2003). Tools for genetic engineering in the amino acid-producing bacterium *Corynebacterium glutamicum*. J. Biotechnol. 104**,** 287-299. doi:10.1016/S0168-1656(03)00148-2.

Kulikova, V.V., Zakomirdina, L.N., Dementieva, I.S., Phillips, R.S., Gollnick, P.D., Demidkina, T.V., et al. (2006). Tryptophanase from *Proteus vulgaris*: the conformational rearrangement in the active site, induced by the mutation of tyrosine 72 to phenylalanine, and its mechanistic consequences. Biochim. Biophys. Acta (BBA)-Proteins and Proteomics 1764**,** 750-757. doi:10.1016/j.bbapap.2005.12.003.

Lalit, K., Shashi, B., and Kamal, J. (2012). The Diverse Pharmacological Importance of Indole Derivatives: A Review. IJRPS 2.

Lee, J.-H., and Lee, J. (2010). Indole as an intercellular signal in microbial communities. FEMS Microbiol. Rev. 34**,** 426-444. doi:10.1111/j.1574-6976.2009.00204.x.

Lee, J.-H., and Wendisch, V.F. (2017). Biotechnological production of aromatic compounds of the extended shikimate pathway from renewable biomass. J. Biotechnol. 257**,** 211-221. doi:10.1016/j.jbiotec.2016.11.016.

Lee, J.-Y., Seo, J., Kim, E.-S., Lee, H.-S., and Kim, P. (2013). Adaptive evolution of *Corynebacterium glutamicum* resistant to oxidative stress and its global gene expression profiling. Biotechnol. Lett. 35**,** 709-717. doi:10.1007/s10529-012-1135-9.

Li, G., and Young, K.D. (2013). Indole production by the tryptophanase TnaA in *Escherichia coli* is determined by the amount of exogenous tryptophan. Microbiology 159**,** 402-410. doi:10.1099/mic.0.064139-0.

Luo, Z.W., Cho, J.S., and Lee, S.Y. (2019). Microbial production of methyl anthranilate, a grape flavor compound. Proc. Natl. Acad. Sci. 116**,** 10749-10756. doi:10.1073/pnas.1903875116.

Ma, W., Cao, W., Zhang, B., Chen, K., Liu, Q., Li, Y., et al. (2015). Engineering a pyridoxal 5'-phosphate supply for cadaverine production by using *Escherichia coli* whole-cell biocatalysis. Sci. Rep. 5**,** 15630. doi:10.1038/srep15630.

Mahr, R., Gätgens, C., Gätgens, J., Polen, T., Kalinowski, J., and Frunzke, J. (2015). Biosensor-driven adaptive laboratory evolution of L-valine production in *Corynebacterium glutamicum*. Metab. Eng. 32**,** 184-194. doi:10.1016/j.ymben.2015.09.017.

Mindt, M., Risse, J.M., Gruß, H., Sewald, N., Eikmanns, B.J., and Wendisch, V.F. (2018). One-step process for production of *N*-methylated amino acids from sugars and methylamine using recombinant *Corynebacterium glutamicum* as biocatalyst. Sci. Rep. 8**,** 12895. doi:10.1038/s41598-018-31309-5.

Moretti, S., Armougom, F., Wallace, I.M., Higgins, D.G., Jongeneel, C.V., and Notredame, C. (2007). The M-Coffee web server: a meta-method for computing multiple sequence alignments by combining alternative alignment methods. Nucleic Acids Res. 35**,** W645-W648. doi:10.1093/nar/gkm333.

Newton, W.A., and Snell, E.E. (1965). Formation and interrelationships of tryptophanase and tryptophan synthetases in *Escherichia coli*. J. Bacteriol. 89**,** 355-364.

Notredame, C., Higgins, D.G., and Heringa, J. (2000). T-Coffee: A novel method for fast and accurate multiple sequence alignment. J. Mol. Biol. 302**,** 205-217. doi:10.1006/jmbi.2000.4042.

Pérez-García, F., Peters-Wendisch, P., and Wendisch, V.F. (2016). Engineering *Corynebacterium glutamicum* for fast production of L-lysine and L-pipecolic acid. Appl. Microbiol. Biotechnol. 100**,** 8075-8090. doi:10.1007/s00253-016-7682-6.

Pérez-García, F., Ziert, C., Risse, J.M., and Wendisch, V.F. (2017). Improved fermentative production of the compatible solute ectoine by *Corynebacterium glutamicum* from glucose and alternative carbon sources. J. Biotechnol. 258**,** 59-68. doi:10.1016/j.jbiotec.2017.04.039.

Peters-Wendisch, P., Stolz, M., Etterich, H., Kennerknecht, N., Sahm, H., and Eggeling, L. (2005). Metabolic engineering of *Corynebacterium glutamicum* for L-serine production. Appl. Environ. Microbiol. 71**,** 7139-7144. doi:10.1128/AEM.71.11.7139-7144.2005.

Phillips, R.S., Ghaffari, R., Dinh, P., Lima, S., and Bartlett, D. (2011). Properties of tryptophan indole-lyase from a piezophilic bacterium, *Photobacterium profundum* SS9. Arch. Biochem. Biophys. 506**,** 35-41. doi:10.1016/j.abb.2010.11.002.

Phillips, R.S., Johnson, N., and Kamath, A.V. (2002). Formation in vitro of hybrid dimers of H463F and Y74F mutant *Escherichia coli* tryptophan indole-lyase rescues activity with L-tryptophan. Biochem. 41**,** 4012-4019. doi:10.1021/bi015838t.

Pioselli, B., Bettati, S., Demidkina, T.V., Zakomirdina, L.N., Phillips, R.S., and Mozzarelli, A. (2004). Tyrosine phenol-lyase and tryptophan indole-lyase encapsulated in wet nanoporous silica gels: Selective stabilization of tertiary conformations. Protein Sci. 13**,** 913-924. doi:10.1110/ps.03492904.

Purwanto, H.S., Kang, M.-S., Ferrer, L., Han, S.-S., Lee, J.-Y., Kim, H.-S., et al. (2018). Rational engineering of the shikimate and related pathways in *Corynebacterium glutamicum* for 4-hydroxybenzoate production. J. Biotechnol. doi:10.1016/j.jbiotec.2018.07.016.

Pybus, D., and Sell, C. (2007). The chemistry of fragrances. Royal Society of Chemistry.

Rety, S., Deschamps, P., and Leulliot, N. (2015). Structure of *Escherichia coli* tryptophanase purified from an alkaline-stressed bacterial culture. Acta Cryst. Section F: Structural Biology Communications 71**,** 1378-1383. doi:10.1107/S2053230X15017549.

Sakamoto, Y., Uchida, M., and Ichihara, K. (1953). The bacterial decomposition of indole. I. Studies on its metabolic pathway by successive adaptation. Med. J. Osaka Univ. 3**,** 477–486.

Sasaki-Imamura, T., Yano, A., and Yoshida, Y. (2010). Production of indole from L-tryptophan and effects of these compounds on biofilm formation by *Fusobacterium nucleatum* ATCC 25586. Appl. Environ. Microbiol. 76**,** 4260-4268. doi:10.1128/AEM.00166-10.

Schneider, J., Eberhardt, D., and Wendisch, V.F. (2012). Improving putrescine production by *Corynebacterium glutamicum* by fine-tuning ornithine transcarbamoylase activity using a plasmid addiction system. Appl. Microbiol. Biotechnol. 95**,** 169-178. doi:10.1007/s00253-012-3956-9.

Schneider, J., and Wendisch, V.F. (2010). Putrescine production by engineered *Corynebacterium glutamicum*. Appl. Microbiol. Biotechnol. 88**,** 859-868. doi:10.1007/s00253-010-2778-x.

Shi, F., Luan, M., and Li, Y. (2018). Ribosomal binding site sequences and promoters for expressing glutamate decarboxylase and producing γ-aminobutyrate in *Corynebacterium glutamicum*. AMB Express 8**,** 61. doi:10.1186/s13568-018-0595-2.

Snell, E.E. (1975). Tryptophanase: structure, catalytic activities, and mechanism of action. Adv. Enzymol. Relat. Areas Mol. Biol 42**,** 287-333.

Taber, D.F., and Tirunahari, P.K. (2011). Indole synthesis: a review and proposed classification. Tetrahedron 67**,** 7195. doi:10.1016/j.tet.2011.06.040.

Tateno, T., Okada, Y., Tsuchidate, T., Tanaka, T., Fukuda, H., and Kondo, A. (2009). Direct production of cadaverine from soluble starch using *Corynebacterium glutamicum* coexpressing α-amylase and lysine decarboxylase. Appl. Microbiol. Biotechnol. 82**,** 115. doi:10.1007/s00253-008-1751-4.

Veldmann, K.H., Dachwitz, S., Risse, J.M., Lee, J.-H., Sewald, N., and Wendisch, V.F. (2019a). Bromination of L-tryptophan in a fermentative process with *Corynebacterium glutamicum*. Front. bioeng. biotechnol. 7**,** 219. doi:10.3389/fbioe.2019.00219.

Veldmann, K.H., Minges, H., Sewald, N., Lee, J.-H., and Wendisch, V.F. (2019b). Metabolic engineering of *Corynebacterium glutamicum* for the fermentative production of halogenated tryptophan. J. Biotechnol. 291**,** 7-16. doi:10.1016/j.jbiotec.2018.12.008.

Vogt, M., Haas, S., Klaffl, S., Polen, T., Eggeling, L., van Ooyen, J., et al. (2014). Pushing product formation to its limit: metabolic engineering of *Corynebacterium glutamicum* for L-leucine overproduction. Metab. Eng. 22**,** 40-52. doi:10.1016/j.ymben.2013.12.001.

Vogt, M., Krumbach, K., Bang, W.-G., van Ooyen, J., Noack, S., Klein, B., et al. (2015). The contest for precursors: channelling L-isoleucine synthesis in *Corynebacterium glutamicum* without byproduct formation. Appl. Microbiol. Biotechnol. 99**,** 791-800. doi:10.1007/s00253-014-6109-5.

Wallace, I.M., O'Sullivan, O., Higgins, D.G., and Notredame, C. (2006). M-Coffee: combining multiple sequence alignment methods with T-Coffee. Nucleic Acids Res. 34**,** 1692-1699. doi:10.1093/nar/gkl091.

Wang, D., Ding, X., and Rather, P.N. (2001). Indole can act as an extracellular signal in *Escherichia coli*. J. Bacteriol. 183**,** 4210-4216. doi:10.1128/JB.183.14.4210-4216.2001.

Watanabe, T., and Snell, E.E. (1972). Reversibility of the tryptophanase reaction: synthesis of tryptophan from indole, pyruvate, and ammonia. Proc. Natl. Acad. Sci. 69**,** 1086-1090.

Yanofsky, C., Horn, V., and Gollnick, P. (1991). Physiological studies of tryptophan transport and tryptophanase operon induction in *Escherichia coli*. J. Bacteriol. 173**,** 6009-6017.

Yoshida, Y., Sasaki, T., Ito, S., Tamura, H., Kunimatsu, K., and Kato, H. (2009). Identification and molecular characterization of tryptophanase encoded by *tnaA* in *Porphyromonas gingivalis*. Microbiology 155**,** 968-978. doi:10.1099/mic.0.024174-0.

Zhang, Y., and Hong, G. (2009). Evidences of Hfq associates with tryptophanase and affects extracellular indole levels. Acta biochim biophys Sin 41, 709-717. doi:10.1093/abbs/gmp059.

2.4.7 Supplementary data

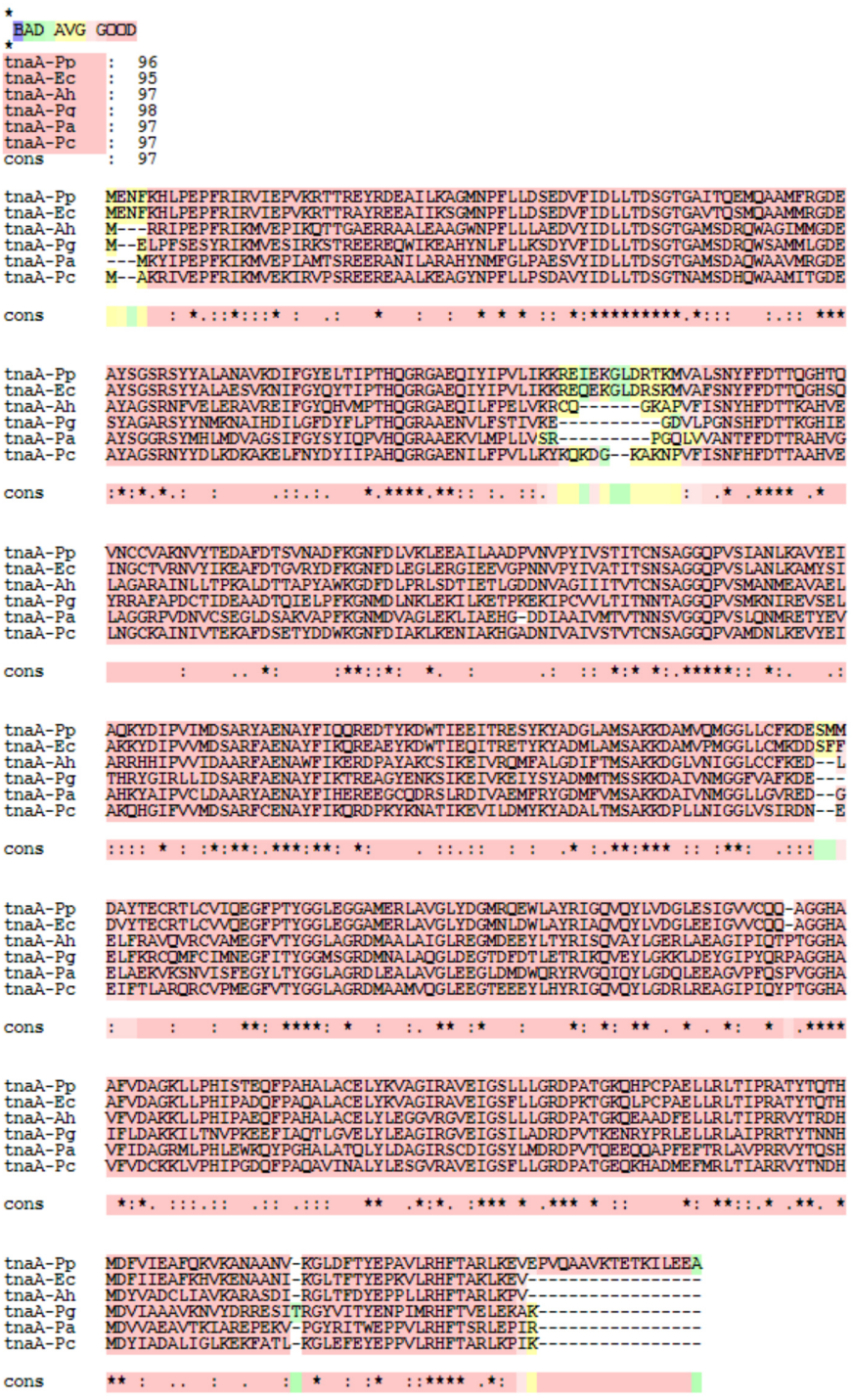

Figure: 2.4.1: Sequence alignment of the six TnaAs. The sequence alignment was done with T-coffee. The TnaAs have a sequence identity of 95 up to 98%. In red a high sequence identity is displayed. With diminishing identity, the color turns from yellow to green and then to blue.

3. Discussion

In this study, the fermentative production of the L-tryptophan (Trp) derivatives 7-chloro-L-tryptophan (7-Cl-Trp), 7-bromo-L-tryptophan (7-Br-Trp) and indole was established. Before a biocatalytic process for the halogenation of Trp with cross-linked enzyme aggregates containing the FAD-dependent halogenase RebH, the NADH-dependent flavin reductase RebF, both deriving from *Lechevalieria aerocolonigenes*, and an alcohol dehydrogenase ADH, has been investigated, but the approach suffers from missing co-factor regeneration systems and costly substrates (Frese and Sewald, 2015). To enable the *de novo* synthesis of halogenated Trp by microbial fermentation RebH and RebF should be integrated in *C. glutamicum*. Fortunately, in previous studies a Trp overproducing *C. glutamicum* strain was constructed (Purwanto et al., 2018) and thus overexpression of *rebH* and *rebF* in this strain facilitated for the first time fermentative production of halogenated Trp from sugar, ammonium and halide salt (see chapter 2.1). First 7-Cl-Trp was produced since chlorine is the preferred ion of RebH (Yeh et al., 2005) and *C. glutamicum* can handle high concentration of chloride salt. To expand this approach bromide ions were used, and it turned out that the bromination of Trp by recombinant *C. glutamicum* was more efficient then the chlorination (see chapter 2.2). This is a great achievement since the bromination occurs rarely in nature and stereoselective bromination is a difficult reaction (Gribble, 1996). Furthermore, it was shown that different tryptophanases (convert Trp to indole) accept 7-Cl-Trp and 7-Br-Trp as substrate (see chapter 2.4). Hence, introduction of a tryptophanase in the halogenating *C. glutamicum* strain could lead to new halogenated products.

3.1 Comparison between the production of halogenated L-tryptophan by chemical synthesis, biocatalysis, biosynthesis in plants, and bacterial fermentation

Halogenated compounds are important precursors of several bioactive compounds, like the well investigated halogenated compounds rebeccamycin and pyrrolnitrin, which both derive from the halogenated Trp derivative 7-Cl-Trp (Kirner et al., 1998; Sánchez et al., 2002). The production of 7-Cl-Trp and the brominated derivative 7-Br-Trp was established by three

different methods: i) the chemical synthesis (Cantillo and Kappe, 2017), ii) synthesis by biocatalysis (Frese et al., 2014; Frese and Sewald, 2015), and iii) biosynthesis in plants by introduction of halogenases (Runguphan et al., 2010; Fräbel et al., 2016). These established methods suffer from using toxins, environmental unfriendliness, missing cofactor recycling system and low space-time yields. To overcome these disadvantages, this study aimed at the fermentative production of halogenated Trp by *C. glutamicum*. In a glucose-based production titer of 0.34 ± 0.52 g L^{-1} 7-Cl-Trp and 1.2 g L^{-1} 7-Br-Trp could be achieved (see chapter 2.2, 2.3).

The halogenation reaction in organic chemistry is carried out using various methods: the free radical halogenation, the halogenation addition reaction, and the electrophilic halogenation. The last method the electrophilic halogenation is used especially for aromatic compounds, such as Trp (Speight, 2017) This method is a complex and hazardous process, including molecular halogens and therefore causing tremendous environmental issues. The handling of molecular chlorine (Cl_2) and bromine (Br_2) is difficult since chlorine is highly reactive and undesirable overreactions occur (Schmittinger et al., 2000). Further bromine is extremely corrosive and toxic as liquid and gas reagent (Zeller, 2001). To prevent the use of molecular chlorine and bromine different halogenating agents are in use (Saikia et al., 2016). One well-known chlorinating agent is sodium hypochlorite, which is used for the disinfection of water by chlorination (Ishaq et al., 2018). In order to optimize the process towards higher environmental friendliness, the following procedures have to be executed: i) the different air streams (acidic streams, reaction gases, and neutral waste streams) in the halogenation process have to be separated, ii) additionally, the waste-water streams have to be purified, which is partially done by biological treatment. But increasing concentrations of halogens results in decreased efficiency of the cleaning process (Speight, 2017). Hence, the production of halogenated compounds by chemical processes is hazardous and highly environmental unfriendly through the arising waste streams. However, an advantage of the chemical halogenation process is the easy purification of the product by a wide range of standard techniques (Elvers, 2014).

The biocatalysis is the second system for the production of halogenated Trp, therefore an enzymatic halogenation system was established (Frese et al., 2014; Frese and Sewald, 2015). For this approach, RebH was mixed with the NADH-dependent flavin reductase PrnF from *Pseudomonas fluorescens* and the alcohol dehydrogenase ADH from *Rhodococcus* sp., which are responsible for the co-factor recycling, and the resulting mixture converted Trp almost quantitatively to 7-Cl-Trp (Frese et al., 2014). To optimize the biocatalysis the enzymes were cross linked in multifunctional cross-linked enzyme aggregates (combiCLEAs). The resulting CLEAs converted after 8 days 1g of Trp to 7-Br-Trp (276 mg L-1) (Frese and Sewald, 2015). Compared to the bacterial fermentation approach the biocatalysis requires the addition of the co-factors, the purified enzyme for the regeneration of the co-factors and the substrate, which made the process costly. Furthermore, in the bacterial fermentation of halogenated Trp only a carbon source, ammonium, and halide salts are needed. Additionally, by metabolic engineering *C. glutamicum* has access to alternative feedstocks as carbon source (Wendisch et al., 2016). In this study, the production of 7-Cl-Trp from the alternative carbon sources xylose, arabinose and glucosamine was established (see chapter 2.1). Consequently, bacterial fermentative production does not compete with food and feed using alternative carbon sources. An advantage of the biocatalysis is the full conversion of the substrate towards the product (for Trp to 7-Cl-Trp and 7-Br-Trp) and a manageable reaction mixture. Thus, a target-oriented isolation of the product is feasible.

The third approach to produce halogenated Trp was carried out with genetically engineered plants. Some plants and algae produce naturally halogenated compounds in small amounts (Gribble, 2004; Cabrita et al., 2010), but in addition, the production of halogenated compounds by heterologously expressed genes was established in plants (Runguphan et al., 2010; Fräbel et al., 2016). For the production of halogenated compounds the medicinal plant *Catharanthus roseus*, a natural producer of monoterpene indole alkaloids, like 19,20-dihydroakuammicine, ajmalicine, tabersonine and catharanthine, was chosen (O'Connor and Maresh, 2006). The natural metabolic pathway of these alkaloids starts with Trp, which is decarboxylated to L-tryptamine (De Luca et al., 1989). This is converted to

secologanin and further to strictosidine the precursor of several alkaloids in *C. roseus* (Runguphan et al., 2010). In biotransformation it was pretested if the *C. roseus* enzymes accept halogenated compounds, therefore *C. roseus* was supplemented with different halogenated tryptamine derivatives which resulted in the formation of the corresponding halogenated alkaloids (McCoy and O'Connor, 2006). Hence, *C. roseus* accepted and could handle halogenated compounds. Runguphan and co-workers used this knowledge for the biosynthesis of halogenated compounds in *C. roseus* hairy roots (Runguphan et al., 2010). By overexpression of *rebH* (Yeh et al., 2005) or of the gene for the FAD-dependent halogenases PyrH from *Streptomyces rugosporus* (Zehner et al., 2005) with *rebF* (Yeh et al., 2005) from a constitutive promoter, *C. roseus* hairy roots produced 50 ± 12 µg per gram of fresh root weight 7-Cl-Trp and 9 ± 1 µg per gram of fresh root weight 5-chloro-tryptophan, respectively (Runguphan et al., 2010) (Table 3.1). But most of the halogenated Trp was directly converted further to 5 or 7-chloro-tryptamine and later on to the chlorinated alkaloids, 12-chloro-19,20-dihydroakuammicine (7-Cl-Trp derivative) and 10-chloroajmalicine (5-chloro-typtophan derivative) (Runguphan et al., 2010). By addition of potassium bromide to the hairy roots in a low-chloride solid medium bromination worked out with RebH and RebF and 12-bromo-19,20-dihydroakuammicine was produced (Runguphan et al., 2010). Several advantages and disadvantages occur with the production of halogenated Trp in plants such as production titer, time and product purification. In the bacterial fermentative production of this study 56 ± 1 mg per gram cell dry weight 7-Cl-Trp were produced (see chapter 2.3). Hence, the product concentration of halogenated Trp produced by *C. glutamicum* exceeds the concentration of *C. roseus* by a multiple. Furthermore, the production process of *C. roseus* starting from transformation of the seedlings until the analyzation of the products from the hairy roots takes around eight weeks (Hughes et al., 2002). In comparison the production time of 7-Cl-Trp with *C. glutamicum* is shorter with around six days (starting from transformation until analyzation) (see chapter 2.1, 2.2 and 2.3). Additionally, the isolation of the alkaloids from plants is complex since the products are not exported and the whole alkaloid spectrum is isolated (Runguphan et al., 2010). To prevent the isolation of the non-halogenated alkaloids a Pd-catalyzed Suzuki-Miyaura cross-coupling reaction (Roy et al., 2008) with six different aryl and

heteroaryl boronic acid substrates were performed (Runguphan and O'Connor, 2013). Since only the halogenated alkaloids interfere in the cross-coupling reaction, the plant crude extract was used. After the reaction, the product was purified by a reverse phase HPLC. Hence, the alkaloid analog 12-chloro-19,20-dihydroakuammicine was isolated in milligram scale from 16 g of hairy roots (Runguphan and O'Connor, 2013). The isolation and purification of 7-Br-Trp produced in the bacterial fermentation is easier because it worked without an additional reaction and the product is exported to the culture medium (see chapter 2.2). Thus, the supernatant of the culture medium was filtrated over a short plug of celite. The filtrate was purified by an automated reversed phase column chromatography. The purified 7-Br-Trp was available as trifluoroacetic acid salt (TFA). Already 14 mg were isolated from 30 mL culture supernatant. In comparison to the biocatalysis is the purification and isolation of the products from plants and bacterial fermentation more complex since the products occur in mixture of several compounds, including the product, intermediates and precursors (see above).

The further conversion of 5-chloro-tryptophan or 7-Cl-Trp to alkaloids is both an advantage and a disadvantage of the plant production. On the one hand, special and complex halogenated alkaloids are produced without additional effort, since the enzymes, which are encoded endogenous by *C. roseus*, accept the halogenated Trp as substrate (Runguphan et al., 2010). On the other hand, production of pure 5-chloro-tryptophan or 7-Cl-Trp is unfeasible as long the product is used for the production of alkaloids. Only the deletion of the Trp decarboxylase, which degrades Trp to tryptamine, would facilitate the production of 5-chloro-tryptophan or 7-Cl-Trp (Goddijn et al., 1994).

In another plant, *Nicotiana benthamiana* the genes for the FAD-dependent halogenases SttH from *Streptomyces toxytricini* (Zeng and Zhan, 2011) and for RebH were overexpressed in the chloroplast (Fräbel et al., 2016). Four weeks old plants were transformed via *Agrobacterium*-mediated gene transfer (Dandekar and Fisk, 2005). After four to six days 77.8 ± 16.6 µg per gram fresh weight 7-Cl-Trp and 70.3 ± 13.0 µg per gram fresh weight 6-chloro-tryptophan were produced. By infiltration with potassium bromide the plants produced 81.5 ± 2.9 µg per gram fresh weight 7-Br-Trp and 42.1 ± 21.4 µg per gram fresh weight 6-bromo-tryptophan (Table 3.1) (Fräbel et al., 2016). *C. glutamicum* HalT2 produced

after 70 h 65 mg per gram cell dry weight 7-Br-Trp (see chapter 2.2). Hence, bacterial fermentative production is more time-efficient and the product concentration of halogenated Trp exceeds the production of the plant by a multiple. Two advantages in the production of halogenated Trp with *N. benthamiana* were observed compared to the production with *C. roseus* or *C. glutamicum*. In contrast to *C. roseus, N. benthamiana* accumulates the halogenated Trp, instead of converting it further into derivatives, whereby isolation of halogenated Trp is possible. The second advantage of the production with *N. benthamiana* is the disuse of the co-enzyme RebF because the same amount of halogenated Trp is produced in the chloroplast with or without the flavin reductase. Fräbel and co-workers proposed that the $FADH_2$ regeneration is carried out by reductases or other proteins involved in the electron transfer of the photosystem. Additionally, FAD and $FADH_2$ are diffusible in the organelles supplying the required co-factor (Fräbel et al., 2016). To achieve new-to-nature halogenated Trp derivatives further genes were overexpressed in the *N. benthamiana* strain. Production of halogenated tryptamine was accomplished by overexpression of the Trp decarboxylase gene from *C. roseus*. By overexpression of the genes for the tryptophanase from *E. coli*, the human cytochrome P450 monooxygenase mutant 2A6, and the endogenous glucosyltransferase, in the 5,6 or 7-Cl-Trp producing *N. benthamiana*, 0.93 ± 0.089 mg per gram cell dry weight 5-chlorindican, 0.31 ± 0.017 mg per gram cell dry weight 7-chlorindican and 0.10 ± 0.016 mg per gram cell dry weight 6-chlorindican were produced (Fräbel et al., 2018). The production of these new-to-nature products could be transferred to the halogenated Trp producing *C. glutamicum* strain. To facilitate this approach, the coupling of the enzymes has to be adjusted due to their activity and the conversion step in the pathway. The overexpression could be regulated by different expression systems, for example, with constitutive expression vectors (Henke et al., 2016a; Jia et al., 2018), IPTG or tertracyline inducible vectors (Kirchner and Tauch, 2003; Stansen et al., 2005; Lausberg et al., 2012) or by light-inducible vectors using photocaged IPTG (Binder et al., 2016). All in all is the fermentative production a promising alternative for the production of halogenated Trp since the process requires only sugar or other alternative carbon sources, ammonium and halide salts for the production of 7-Cl-Trp and 7-Br-Trp, it has his own co-factor regeneration system and the isolation and purification of the product is simple.

Table 3.1: Summery of production processes of halogenated Trp by biocatalysis, biosynthesis in plants and bacterial fermentation. Values for the production of halogenated Trp by chemical synthesis are unknown.

Production system/ production organism	Product	Production	Production time	References
Biocatalysis	7-chloro-tryptophan	58 mg L^{-1}	60 min	(Frese et al., 2014)
	7-bromo-tryptophan	276 mg L^{-1}	8 days	(Frese and Sewald, 2015)
Plant production/ *C. roseus*	7-chloro-tryptophan	50 ± 12 µg per gram of fresh root weight	8 weeks (transformation to product isolation)	(Runguphan et al., 2010)
	5-chloro-tryptophan	9 ± 1 µg per gram of fresh root weight	8 weeks (transformation to product isolation)	(Runguphan et al., 2010)
Plant production/ *N. benthamiana*	7-chloro-tryptophan	77.8 ± 16.6 µg per gram fresh weight	4 weeks old plant + 4-6 days incubation after transformation	(Fräbel et al., 2016)
	6-chloro-tryptophan	70.3 ± 13.0 µg per gram fresh weight	4 weeks old plant + 4-6 days incubation after transformation	(Fräbel et al., 2016)

Production system/ production organism	**Product**	**Production**	**Production time**	**References**
	7-bromo-tryptophan	81.5 ± 2.9 µg per gram fresh weight	4 weeks old plant + 4-6 days incubation after transformation	(Fräbel et al., 2016)
	6-bromo-tryptophan	42.1 ± 21.4 µg per gram fresh weight	4 weeks old plant + 4-6 days incubation after transformation	(Fräbel et al., 2016)
Bacterial fermentation/ *C. glutamicum*	7-chloro-tryptophan	108 ± 2 mg L^{-1} (14 ± 1 mg per gram cell dry weight)	72 h	This study
	7-bromo-tryptophan	1.2 g L^{1} (65 mg per g cell dry weight)	72 h	This study

3.2 Strategies for metabolic engineering and optimization of *C. glutamicum* for improved production of halogenated L-tryptophan and indole

In the bacterial fermentative production with the halogenated Trp overproducing *C. glutamicum* strain HalT2, 0.3 g L^{-1} 7-Cl-Trp and 1.2 g L^{-1} 7-Br-Trp were produced (see chapter 2.2., 2.3). But in case of 7-Cl-Trp 3 g L^{-1} Trp and for 7-Br-Trp in total 0.9 g L^{-1} of Trp and anthranilate (Ant) accumulated. Additionally, in the indole overproducing *C. glutamicum* strain a complete conversion of Trp to indole was not observed. Hence, to achieve full conversion towards the products and higher production titers different bottlenecks could be improved, like the halogenation reaction, the tryptophanase reaction, the precursor supply, and the export system.

3.2.1 Optimization of the halogenation reaction

The halogenation of Trp with RebH occurs slowly since the enzyme activity is moderate. In crude extract of *C. glutamicum* the enzyme had a specific enzyme activity of 0.90 ± 0.01 mU mg^{-1} (see chapter 2.1). Compared to the purified enzyme the activity was 161 times lower (145 mU mg^{-1}) (Yeh et al., 2007). In this study, the gene expression of *rebH* was increased by an exchange of the ribosome binding site (see chapter 2.1). Hence, the production of 7-Cl-Trp was enhanced from 57 mg L^{-1} up to 108 mg L^{-1} (see chapter 2.1). For further improvement of the enzyme activity and the expression of *rebH* and *rebF* different approaches could be implemented. Often the heterologous expression of genes in bacteria leads to misfolding of the proteins and thus the degradation of the enzyme, which results in a low activity of the enzyme. The co-overexpression of chaperones facilitates the folding and maintain the solubility (Thomas et al., 1997). By co-overexpression of the chaperone GroES and GroEL genes with *rebH* in *E. coli* the protein solubility could be improved and the yield of RebH was 7 times higher compared to the expression without chaperones (Payne et al., 2013) (Fig. 3.2; Supplementary data table 3.1). Another option to improve the solubility and increase the activity of an enzyme was carried out for RebF. RebF was fused to a maltose-binding protein (MBP) (Cabrita et al., 2006) and the resulting RebF-MBP fusion protein was overproduced in *E. coli*. The turn over number of RebF-MBP for the reduction of FAD to $FADH_2$ was 2.5 times higher compared to RebF without fusion protein ($k_{cat,RebF}$=32 min^{-1};

$k_{cat,MBP\text{-}RebF}$=80 min^{-1}) (Payne et al., 2013) (Fig. 3.2; Supplementary data table 3.1). But the MBP fusion has not on every protein a positive effect. In case of RebH-MBP the activity was decreased compared to the wildtype RebH (Payne et al., 2013). However, in the work of Payne and co-workers only one functional fusion protein and fusion position was chosen. It is shown that the selection of the fusion position (C, N-terminal) and functional fusion proteins depends on the target protein (Lee and Kim, 2018). For example, the specific activity of the lipoxygenase of *Pseudomonas aeruginosa* was increased 2.8-fold by N-terminal fusion with self-assembling amphipathic peptides (Lu et al., 2013) and the overall catalytic efficiency of the chitinase D from *Serratia proteamaculans* was improved twice by the C-terminal fusion with auxiliary domains (Madhuprakash et al., 2015). Instead of fusing the target protein with an unfunctional protein, two target proteins could be fused together. The two proteins (for example RebH and RebF) could be fused by different linker sequences (Chen et al., 2013). For example, the expression of granulocyte colony stimulating factor and human serum transferrin was increased 11.2-fold in mammalian cells by the fusion by a suitable linker (Amet et al., 2009). Whether *rebH* and *rebF* are fused it is important to balance the expression. For example, Henke and co-workers improved the astaxanthin production with *C. glutamicum* by balancing the expression of two genes by testing different ribosome binding sites, spacing, and translational start codons (Henke et al., 2016b).

Since the specific enzyme activity of RebH is low and the improvement of the activity could enhance the efficiency of the halogenation an increased activity could be achieved by introducing mutation in the *rebH* gene sequence. Different direct evolution approaches are known to result in improved enzymes. One method is the error-prone PCR which creates random mutants by introducing base-pair errors during the PCR in the newly synthesized complementary DNA strand (McCullum et al., 2010). A library is generated, and the mutants are tested due to the requirement, like enhanced stability, solubility or activity. Poor and co-workers prepared a library of *rebH* mutants to screen them for higher thermostability and the substrate scope (Poor et al., 2014; Payne et al., 2015). Thus, they discovered mutants with a 5 °C higher temperature optimum compared to the wildtype and with an extended substrate scope (Poor et al., 2014; Payne et al., 2015). Moreover, mutants generated by error-prone PCR were discovered which showed higher activity compared to the wildtype version, for

example, the phytase from *Aspergillus niger* and the organophosphorus hydrolase *Pseudomonas diminuta* (Liao et al., 2012; Rezaie et al., 2018). Another approach of directed evolution is the site-saturation mutagenesis, where a small amount of active site residues are randomly mutated (Siloto and Weselake, 2012). For example, the catalytic efficiency of the β-fucosidase from β-galactosidase from *E. coli* was enhanced 180-fold by site-saturation mutagenesis (Parikh and Matsumura, 2005).

Another optimization approach is the change of the halogenase system. To our knowledge, no faster halogenase system than RebH and RebF, which halogenates Trp at the C7 position has yet been discovered. Until now, only the less efficient FAD-dependent halogenase PrnA and the NADH-dependent flavin reductase PrnF are well investigated (Keller et al., 2000; Dong et al., 2005; Lee and Zhao, 2007).

3.2.2 Enhanced co-factor supply and regeneration

A crucial step during the halogenation reaction is the co-factor regeneration. Two co-factors are required for the halogenation via RebH and RebF: $FADH_2$ (co-factor of the FAD-dependent halogenase) and NADH (co-factor of the NADH-dependent flavin reductase) (Yeh et al., 2005). NADH is provided by the oxidation of glucose and $FADH_2$ by the reduction of FAD catalyzed by the NADH-dependent flavin reductase. The NADH-dependent flavin reductase gene has to be expressed heterologously since *C. glutamicum* does lack a gene coding for a flavin reductase. In this study, it was shown, that the addition of flavin mononucleotide (FMN), the precursor of flavin adenine dinucleotide (FAD), yielded in higher production titers during the fermentative production of 7-Cl-Trp. With addition of FMN HalT1 produced 2-times more 7-Cl-Trp (see chapter 2.1). Consequently, the supply of the precursors of $FADH_2$ (riboflavin, FMN and FAD) is a limiting step during the halogenation in *C. glutamicum*. To increase the production of riboflavin and FMN different options could be applied. It was shown that due to the overexpression of the sigma factor H gene *sigH* or the deletion of the anti-sigma factor gene *rshA* (repressor of *sigH*) 50 genes were upregulated including the genes for the biosynthesis of riboflavin in *C. glutamicum* (Busche et al., 2012; Taniguchi and Wendisch, 2015). Only the bifunctional enzyme riboflavin kinase/FMN adenylyltransferase RibF, responsible for the

conversion of riboflavin to FAD, was not differentially expressed. However, by overexpression of *sigH* or deletion of *rshA* higher production of riboflavin was observed, but the concentration of FMN and FAD did not increase (Toyoda et al., 2014; Taniguchi and Wendisch, 2015) (Figure 3.2; Supplementary data table 3.1). To enhance the production of FMN and FAD *ribF* could be overexpressed. Moreover, Taniguchi and Wendisch showed that the balanced co-expression of *sigH* and *ribF* yielded in higher production of riboflavin and FMN. 19.8±0.3 μM riboflavin and 33.1±1.8 μM FMN were secreted extracellularly but FAD was not detected (Taniguchi and Wendisch, 2015). In eukaryotes, the two biosynthetic steps from riboflavin to FAD are catalyzed by two independent enzymes (Yatsyshyn et al., 2014). The conversion from riboflavin to FMN is catalyzed by a riboflavin kinase, for example, the FMN1 from *Candida famata* (Yatsyshyn et al., 2009). Further the FAD synthetases, for example, the FAD1 from *Saccharomyces cerevisiae* (Wu et al., 1995) or the FAD1 from *Debaryomyces hansenii* strain CBS 767 (Yatsyshyn et al., 2014), convert FMN to FAD. In the flavinogenic yeast *Candida famata* overproducing FMN (Yatsyshyn et al., 2009; Yatsyshyn et al., 2010) the overexpression of *FAD1* of *D. hansenii* CBS 767 led to production of FAD. After 40 h cultivation under optimized conditions, 451 mg L^{-1} FAD were produced (Yatsyshyn et al., 2014) (Fig. 3.2; Supplementary data table 3.1). Overexpression of *FAD1* (codon adjusted for prokaryotes) in *C. glutamicum* could lead to higher production of FAD and hence a higher supply of $FADH_2$ for the halogenation.

The second co-factor in the halogenation is NADH. NADH is oxidized by the NADH-dependent flavin reductase to reduce FAD to $FADH_2$ (Yeh et al., 2005). To enhance the NADH availability and thus prevention of NADH limitation, different approaches could be tested.

For the formation of L-lactate by reduction of pyruvate in *C. glutamicum* the NADH-dependent lactate dehydrogenase LdhA consumes NADH (Toyoda et al., 2009). Hence, by deletion of *ldhA* the NADH concentration could be increased (Blombach et al., 2009). Another option to increase the NADH concentration is the deletion of the H^+-ATPase and thus disruption of the oxidative phosphorylation of *C glutamicum*. Sawada and co-workers showed that the concentration of NADH was increased from 0.27 ± 0.05 mM to 0.53 ± 0.11 mM and the NAD^+/NADH ratio decreased from 13.0 to 5.4 (Sawada et al., 2012)

(Fig. 3.2; Supplementary data table 3.1). The increase of NADH is caused by higher glucose metabolism due to the defect of the H^+-ATPase (Sekine et al., 2001).

3.2.3 Improvement of the precursor supply for the biosynthesis of L-tryptophan

Trp is the direct precursor for the production of halogenated Trp and indole. In this study, *C. glutamicum* strain HalT2 produced around 2 - 3 g L^{-1} Trp (see chapter 2.1, 2.2). When a more efficient halogenation is available production of Trp could be a limiting step. Already, in the fed-batch fermentation the concentration of Trp was low (0.25 g L^{-1}) (see chapter 2.2) subsequently resulting in a low titer of 7-Br-Trp, even with improved halogenation reaction. Consequently, the production of Trp has to be improved.

The biosynthesis of Trp starts with the precursor phosphoenolpyruvate (PEP) and erythrose 4-phosphate (E4P) which both derive from glucose-6-phosphate. To increase the concentration of PEP and E4P various options could be applied. Since the phosphotransferase system (PTS), which is the major glucose uptake system in *C. glutamicum* is PEP dependent a PTS independent glucose transporter could increase the amount of PEP for the production of aromatic amino acids (Tang et al., 2013). An alternative sugar uptake system was proven by Linder and co-workers (Lindner et al., 2011). By overexpression of genes for the inositol permeases IolT1 and IolT2 together with a glucokinase gene from *C. glutamicum* in a PTS-deficient strain the growth in glucose was almost sustained (Lindner et al., 2011). This glucose uptake was improved by balancing the expression of the glucokinase from *B. subtilis* with IolT2 from *C. glutamicum* resulting in a slightly increased growth and production rate (Pérez-García et al., 2016). To further optimize the PEP supply several genes from the glycolysis could be considered as targets.

Moreover, to prevent by-product formation the following genes could be deleted (Fig. 3.2; Supplementary data table 3.1): i) 3-Deoxy-D-arabino-heptulosonate-7-phosphate (DHAP) phosphatase (encoded by *hpdA*), which dephosphorylates the Trp pathway intermediate DHAP to 1,3-dihydroxyacetone and it was already shown that the deletion maintained higher shikimate concentrations in *C. glutamicum* (Kogure et al., 2016), ii) pyruvate kinase (encoded by *pyk*) which transfers the phosphate group from PEP to ADP yielding pyruvate and ATP. By deleting *pyk* the PEP concentration was increased 5.6 times in *C. glutamicum*

(Sawada et al., 2015) and iii) NADH-dependent lactate dehydrogenase LdhA (encoded by *ldhA*). A deletion reduced the conversion of pyruvate to L-lactate, subsequently increasing the pyruvate concentration which can be further converted to PEP by the phenylphosphate synthase (encoded by *ppsA*) (Toyoda et al., 2009). Overexpression of *ppsA* in *E. coli* enhanced the DHAP production 1.8 times (Gosset et al., 1996). Additionally, it was shown that the overexpression of GAP dehydrogenase gene *gapA*, catalyzing the conversion of glyceraldehyde-3-phosphate to 1,3-bisphosphoglycerate, can enhance the concentration of shikimate in *C. glutamicum* (Kogure et al., 2016) (Fig. 3.2, Supplementary data table 3.1).

The concentration of the second Trp biosynthesis precursor E4P was increased by overexpression of the genes for transketolase (encoded by *tkt*) and transaldolase (encoded by *tal*) (Ikeda et al., 1999; Kogure et al., 2016; Mao et al., 2018). Additionally, the E4P concentration could be enhanced by feeding xylose as a carbon source to recombinant *C. glutamicum* (Mao et al., 2018). Xylose can be converted in the isomerase pathway via several steps to ribulose-5-phosphate an intermediate of the pentose-phosphate pathway (PPP). By overexpression of *xylA* from *Xanthomonas campestris* SCC1758 and *xylB* from *C. glutamicum* ATCC 13032 *C. glutamicum* utilized xylose as alternative carbon source (Meiswinkel et al., 2013) and thus the E4P concentration could be increased. Hence, co-feeding of xylose and glucose could increase the production of halogenated Trp by *C. glutamicum* since the concentration of PEP and E4P should be increased.

The next step to improve Trp production is the optimization of the shikimate pathway (Fig. 3.2; Supplementary data table 3.1). One option is to prevent the by-product formation of protocatechuate, which is generated by the 3-dehydroshikimate dehydratase (encoded by *qsuB*) from the Trp biosynthesis intermediate 3-dehydroshikimate. By deletion of *qsuB* the by-product formation was prevented (Purwanto et al., 2018). Another by-product formation was prohibited by the deletion of the shikimate 5-dehydrogenase (encoded by *qsuD*) which catalyzes the conversion from 3-dehydroquinate to quinate (Kubota et al., 2013; Kogure et al., 2016). Additionally, deletion of *qsuD* increases the shikimate concentration since the enzyme channels the flux in the opposite direction by hydrating shikimate to 3-dehydroshikimate as well (Purwanto et al., 2018). Further options to optimize the shikimate pathway is the overexpression of the pathway genes. It was already shown that

overexpression of a feedback resistant *aroG* (3-deoxy-D-arabino-heptulosonate 7-phosphate synthase gene) from *E. coli* prevented product inhibition by L-phenylalanine (Phe) and L-tyrosine (Tyr) in the Trp overproducing *C. glutamicum* strain Tp679 (Purwanto et al., 2018). Furthermore, overexpression of endogenous *aroBDE* (AroB: 3-dehydroquinate synthase; AroD: 3-dehydroquinate dehydratase; AroE: NADPH-dependent shikimate dehydrogenase) increased the shikimate concentration (Kogure et al., 2016). In addition, Kitade and co-workers improved the production of 4-hydroxybenzoic acid and shikimate in *C. glutamicum* by overexpression *aroCKB* (2-fold integration in the genome) and *aroG*, *aroD*, *aroE* and *aroA* from *C. glutamicum* and *ubiC* (chorismate pyruvate-lyase) from *P. rustigianii* (Kitade et al., 2018) (Fig. 3.2; Supplementary data table 3.1).

The product of the shikimate pathway is chorismate the precursor of all aromatic amino acids. Since the chorismate mutase was deleted in the Trp overproducing *C. glutamicum* strain the production of Phe and Tyr was prevented. Further *C. glutamicum* can convert chorismate to isochorismate (catalyzed by isochorismate synthase, *entC*) or to 4-amino-4-deoxychorismate (catalyzed by aminodeoxychorismate synthase, *pabAB*) a precursor of folate. Deletion of *pabAB* might lead to an increased chorismate concentration but it was shown that *C. glutamicum* became auxotroph for folate by this deletion, however, supplementing with 1 mM folate restored growth (Stolz et al., 2007). However, the effects of an *entC*-deletion in *C. glutamicum* are still unknown.

The last part of the Trp biosynthesis is the Trp pathway from chorismate to Trp. The genes of this pathway are encoded in the *trp* operon. The transcription of the *trp* operon is regulated by the transcriptional repressor LtbR and by attenuation (Herry and Dunican, 1993; Brune et al., 2007). Deletion of *ltbR* causes an increase of the *trp* operon expression (Brune et al., 2007). Furthermore, the Trp production was enhanced by the overexpression of the *trp* operon and a feedback-resistant 3-deoxy-D-arabino-heptulosonate 7-phosphate synthase (encoded by *aroII*) from a high-copy plasmid (Katsumata and Ikeda, 1993). As a result, the TrpE and the TrpD were strongly feedback inhibited by Trp resulting in a lower Trp production compared to the starting strain. To desensitize the enzymes mutagenesis was executed (*N*-methyl-*N*' -nitro-*N*-nitrosoguanidine as mutagen) with strains carrying the plasmid and the new mutated plasmids were retransformed in the starting strain. The resulting

strain produced 43 g L^{-1} Trp in a fed-batch fermentation and the K_i of TrpE and TrpD was increased 500-fold and 25-fold, respectively (Katsumata and Ikeda, 1993). This study showed as well, that TrpD was feedback inhibited by 7-Cl-Trp and 7-Br-Trp and thus, Ant accumulated in the culture medium (see chapter 2.1 and 2.2). To overcome this issue *trpD*s from *E. coli*, *B. subtilis* and *B. subtilis spizizenii* were overexpressed with an inducible expression vector and an optimized RBS for each *trpD*. Hence, the production of Trp was increased up to 3 g L^{-1} and Ant was completely converted (see chapter 2.3). In the last step of the Trp biosynthesis, TrpB requires L-serine as a co-substrate (Fig. 3.2; Supplementary data table 3.1). Ikeda and co-workers investigated the influence of higher L-serine concentration during the Trp biosynthesis and showed a 1.2-fold improved Trp production (Ikeda et al., 1994). In *C. glutamicum* the L-serine concentration was enhanced by i) deletion of the L-serine dehydratase which degrades L-serine to pyruvate, ii) regulation of *glyA* (L-serine hydroxymethyltransferase) via a chromosomal exchange of the native *glyA* promoter by an IPTG inducible promoter and, iii) overexpression of a feedback regulated *serA* (3-phosphoglycerate dehydrogenase gene), *serC* (Phosphoserine aminotransferase gene) and *serB* (Phosphoserine phosphatase gene) which yielded in a production of 86 mM L-serine (Peters-Wendisch et al., 2005). This concentration was enhanced up to 345 mM L-serine by deletion of *pabABC* (resulting in a folate depletion and therefore reduced GlyA activity, which made the IPTG dependent regulation dispensable) (Stolz et al., 2007). Taken together, by prevention of by-product formation and overexpression of specific genes the production of Trp could be increased by a multiple.

3.2.4 Export system identification

Until now only the import mechanism of Trp in *C. glutamicum* is known. The importer AroP (Aromatic amino acid transport protein) transports specifically Trp, as well as Phe and Tyr into the cell (Wehrmann et al., 1995). However, the latter aromatic amino acids can also be taken up by another system since they were still imported in an *aroP* deletion strain of *C. glutamicum* (Wehrmann et al., 1995). The deletion of *aroP* yielded in a 10 – 20 % higher Trp production (Ikeda and Katsumata, 1995) (Fig. 3.2; Supplementary data table 3.1). It is

yet unknown if AroP or another importer takes up halogenated Trp. Additionally, the export systems of both, Trp and the halogenated derivatives, are not identified so far. Lubitz and co-workers showed that overexpression of the exporter *lysE* (major export system for L-lysine, L-arginine and potentially L-citrulline) led to higher production of L-citrulline and deletion of *cgmR* (repressor of *cgmA, cgmA* exporter of putrescine and cadaverine and potentially for L-arginine) resulted in a 5% higher production of L-arginine (Lubitz et al., 2016). Hence, overexpression of the Trp or halogenated Trp exporter could lead to an increase of the halogenated Trp production. To identify the exporter several approaches are possible. One method is feeding with a dipeptide, for example, alanyl-tryptophan (Ala-Trp). Since *C. glutamicum* imports and hydrolyzes the dipeptide (Bröer and Krämer, 1991; Erdmann et al., 1993) the resulting monomeric L-alanine is easily catabolized but Trp is non-catabolizable (see chapter 2.1) which leads to an increased intracellular concentration of Trp and thus it has to be exported. The culture fed with Ala-Trp are harvest and analyzed with RNA-Seq in comparison to the non-fed cultures. In this work this feeding approach was tried out with 3 mM Ala-Trp, but in the RNA-Seq results no transport genes were upregulated. Additionally, the Trp and halogenated Trp overproducing *C. glutamicum* strains were cultivated and harvest in the exponential phase and analyzed by RNA-Seq, but the exporter(s) for Trp and halogenated Trp were not identified (data not shown). One reason that the exporter(s) were not identified may be that the intracellular Trp concentration was too low, so the exporter(s) genes were not upregulated. When Trötschel and co-workers identified the exporter of methionine (Met) of *C. glutamicum* by feeding 3 mM methionyl-methionine (Met-Met) they measured an intracellular concentration of 100 µmol Met per gram cell dry mass and around 2 mM Met extracellularly. In this study, extracellular concentrations of 0.12 mM and 0.6 mM Trp were measured in the Ala-Trp feeding and the Trp production experiment, respectively. Hence, the low concentration of exported Trp may be the reason that exporter(s) genes of Trp were not upregulated. Consequently, to achieve the upregulation of the exporter(s) genes *C. glutamicum* could be feed with higher concentration of Ala-Trp or a *C. glutamicum* strain which produces more and faster Trp could be used, so that already in the exponential phase around 2 mM Trp are produced and exported extracellularly.

3.2.5 Adaptive laboratory evolution (ALE)

Adaptive laboratory evolution (ALE) is a method for the analysis of evolutionary phenomena in a controlled laboratory settings (Dragosits and Mattanovich, 2013). Advantages of ALE with microorganisms are cultivation in the laboratory, mostly simple medium requirements and usually fast growth (Dragosits and Mattanovich, 2013). ALE can improve the growth rate (Pfeifer et al., 2017), product titers (Fong et al., 2005; Mahr et al., 2015) or the tolerance to stress (Lee et al., 2013; Oide et al., 2015). For the optimization of the fermentative production of halogenated Trp with *C. glutamicum* ALE could be a useful method. On the one hand, ALE could improve the growth rate and the production titer, on the other hand, stress tolerance to 7-Cl-Trp and 7-Br-Trp could be increased. For the first approach the halogenated producing *C. glutamicum* strain HalT2 could be grown in CGXII minimal medium (supplement with glucose and halide salts) and transferred to fresh medium by reaching the stationary phase. The process could be repeated until the growth rate and production of 7-Cl-Trp and 7-Br-Trp is enhanced. Since ALE could improve the whole production process starting from the sugar uptake and precursor supply until the halogenation at once it is a promising method. The tolerance of *C. glutamicum* wildtype to 7-Cl-Trp (K_i 0.1 mM, see chapter 2.1) and 7-Br-Trp (K_i 0.32 mM, see chapter 2.2) is low. To optimize its tolerance, *C. glutamicum* could be cultivated with 7-Cl-Trp and 7-Br-Trp. If *C. glutamicum* adapts to the substance (higher K_i) the concentration could be increased until an approved stress tolerance is reached. A disadvantage of the method is the high price of 7-Cl-Trp (e.g. abcr GmbH: 411.5 € per 250 mg (https://www.abcr.de/)) and 7-Br-Trp (e.g. Santa Cruz Biotechnology, Inc.: 153 € per 250 mg (https://www.scbt.com/home)) which have to be added to the medium. To reduce the cost the halogenated Trp could be produced in a fermentative production with *C. glutamicum* HalT2 in HSG medium and the product could be purified and isolated (description see chapter 2.2). To retrace adaption processes different omics analyses could be carried out. The resulting strains could be resequenced to evaluate the mutations that occured or screened in an RNA-Seq to determine the up- and downregulated genes (Choe et al., 2019).

3.2.6 Optimization of the indole production

The production of indole differs between microorganisms and plants. In microorganisms, Trp is converted by the tryptophanase to indole (see Fig. 2.4.1) and in plants indole-3-glycerol phosphate (IGP) is converted by the indole-3-glycerol phosphate lyase to indole (Frey et al., 1997; Lee and Lee, 2010) (Fig. 3.1).

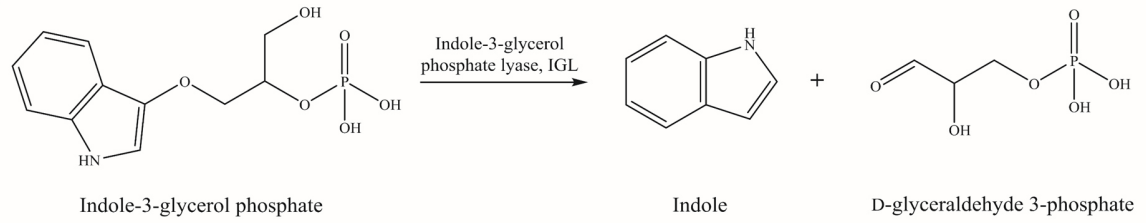

Figure 3.1: Schematic reaction of an indole-3-glycerol phosphate lyase. Indole-3-glycerol phosphate lyase is converted by the indole-3-glycerol phosphate lyase (IGL) to free indole, D-glyceraldehyde 3-phosphate.

In this study, indole was produced by the overexpression of tryptophanases genes (*tnaA*) from different microorganisms in the Trp overproducing *C. glutamicum* strain (see chapter 2.4). Additionally, optimization strategies, like enhanced *tnaA* expression or increased precursor supply were discussed (see chapter 2.4). But until now, it was not considered to transfer the plant indole production pathway to *C. glutamicum*. Since I3P is an intermediate in the Trp biosynthesis *C. glutamicum* could be metabolically engineered for the overproduction of IGP (see above: precursor supply, export system, ALE). To accumulate IGP and prevent the conversion to Trp the tryptophanase synthase (encoded by *trpBA*) could be deleted or downregulated, whereby deletion led to Trp auxotrophic strain (Swift and Stewart, 1991).

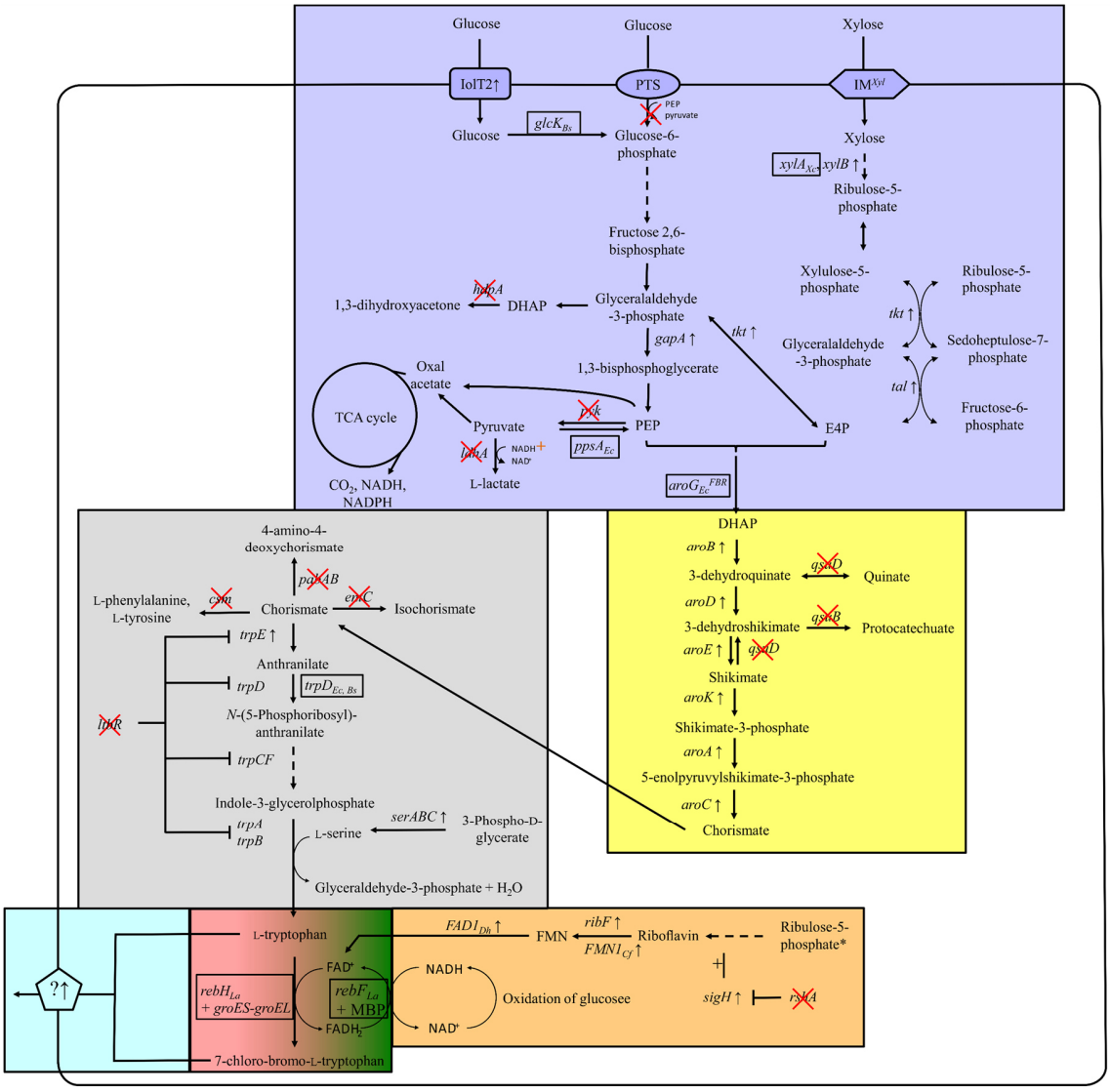

Figure 3.2: Schematic overview of strategies for metabolic engineering of *C. glutamicum* for an optimized halogenated L-tryptophan production. The optimization steps are divided in following improvements: PEP and E4P supply (purple), shikimate pathway (yellow), Trp pathway (grey), co-factor regeneration (orange), halogenation reaction (red-green) and the export (bright turquoise). Heterologously expressed genes are marked by black boxes, endogenously overexpressed genes are marked by ↑ and deleted genes are showed by red crosses. The question mark indicates a not identified exporter. These lines (┤) indicate transcriptional repression of the genes, + indicated transcriptional activation, red + indicated enhanced NADH concentration by deletion of *ldhA* and the * indicates that the riboluse-5-phoshate dirves from the pentose-phosphate pathway. Genes without further organism description derive from *C. glutamicum*. PEP and E4P supply (purple): glucokinase from *B. subtilis (*encoded by $glcK_{Bs}$), xylose isomerase from *X. campestris* (encoded by *xylA*), xylulokinase (encoded by *xylB*), transketolase (encoded by *tkt*), transaldolase (encoded by *tal*), DHAP phosphatase (encoded by *hdpA*), pyruvate kinase (encoded by *pyk*), NADH dependent lactate dehydrogenase (encoded by *ldhA*), phenylphosphate synthase (encoded by *ppsA*); Shikimate pathway (yellow): feedback resistant

3-deoxy-D-arabino-heptulosonate 7-phosphate synthase from *E. coli* (encoded by $aroG_{Ec}$), 3-dehydroquinate synthase (encoded by *aroB*) 3-dehydroquinate dehydratase (encoded by *aroD*) NADPH-dependent shikimate dehydrogenase (encoded by *aroE*) shikimate kinase (encoded by *aroK*) 5-enolpyruvylshikimate 3-phosphate synthase (encoded by *aroA*) chorismate synthase (encoded by *aroC*); Trp pathway (grey): chorismate mutase (encoded by *csm*), anthranilate synthase (encoded by *trpG, trpE*), anthranilate phosphoribosyltransferase (encoded by *trpD*),phosphoribosyl anthranilate isomerase (encoded by *trpF*), indole-3-glycerol phosphate synthase (encoded by *trpC*), tryptophan synthase (encoded by *trpB, trpA*), 3-phosphoglycerate dehydrogenase (encoded by *serA*), phosphoserine aminotransferase (encoded by *serC*), phosphoserine phosphatase (encoded by *serB*); co-factor regeneration (orange): anti-sigma factor (encoded by *rshA*), sigma factor H (encoded by *sigH*), bifunctional enzyme riboflavin kinase/ FMN adenylyltransferase (encoded by *ribF*), riboflavin kinase from *C. famata* (encoded by $FMN1_{Cf}$), FAD synthetase from *D. hansenii* (encoded by $FAD1_{Dh}$); halogenation reaction (red-green): FAD-dependent halogenase from *L. aerocolonigenes* (encoded by $rebH_{La}$), chaperones (encoded by *groES* and *groEL*), NADH-dependend flavin reductase from *L. aerocolonigenes* (encoded by $rebF_{La}$), maltose binding protein (MBP).

In *Zea mays* two indole-3-glycerol phosphate lyases are encoded, BXI and IGL, which catalyze the conversion of IGP to free indole (Frey et al., 1997; Frey et al., 2000). *In vitro* BX1 and IGL had a catalytic efficiency of 215 $mM^{-1}s^{-1}$ and 23 $mM^{-1}s^{-1}$, respectively (Frey et al., 2000). Until now, overexpression of indole-3-glycerol phosphate lyase genes in an IGP overproducing *C. glutamicum* strain was not described, however, it could lead to indole production.

3.3 Expansion of the genetic code by halogenated L-tryptophan derivatives

For a long time, peptide and protein engineering was restricted to 20 standard proteinogenic L-amino acid. In the 1950s the first incorporation of non-canonical (non-natural) amino acids (ncAAs) by replacing the canonical amino acid (cAA) counterparts in *E. coli* was established (Cowie and Cohen, 1957). In 1989 for the first time Schultz and co-workers reported the introduction of ncAAs into specific positions in the protein by genetic code expansion expanding the functions of proteins (Noren et al., 1989). In different *in vitro* and *in vivo* studies various new peptides and proteins with a wide range of properties were observed (Blaskovich, 2016; Zhou et al., 2016; Zambaldo et al., 2017). To incorporate ncAAs *in vivo* in the peptide or protein two methods are known: the genetic code engineering (or supplementation-based incorporation method (SPI)) and the genetic code expansion (or stop codon suppression (SCS)) (Hoesl and Budisa, 2012; Zhou et al., 2016). In the genetic code engineering method canonical amino acids (cAAs) are replaced by the ncAAs during

translation in a cAA analogous auxotrophic strain. This is only feasible with isostructural ncAAs because they are recognized by the host cell machinery and are loaded to endogenous tRNA synthetases (Yoshikawa et al., 1994). Isostructural ncAAs are isosteric to their cAAs analogs, for example, by single-atom substitutions such as H for F, S for CH2, or H for OH (Budisa et al., 1998). Orthogonal ncAAs cannot be used since they cannot precipitate in the usual translation (Zhou et al., 2016) For the antibiotic lichenicidin, the genetic code engineering method was chosen (Oldach et al., 2012). Plasmids encoding for the synthesis of the prepropeptides Bliα and Bliβ and a fosmid encoding the posttranslational lantibiotic biosynthesis machinery were overexpressed in Trp, methionine (Met) and proline (Pro) auxotrophic *E. coli* strains. The resulting strains were cultivated with the isostructural ncAAs, which yielded in lichenicidin incorporated with ncAAs (Oldach et al., 2012). Hence, the endogenous tRNA synthetase recognizes the added ncAAs. Furthermore, isostructural Trp analogs, like 5-fluoro-tryptophan, 5-hydroxy-tryptophan or 5-methyl-tryptophan were accepted by the tryptophanyl-tRNA synthetase from *Lactococcus lactis* (Zhou et al., 2016). These Trp analogs were introduced in the antimicrobial peptide nisin A at the Trp encoding codon (nisin naturally does not encode Trp residues, by engineering the nisin A gene four Trp residues were introduced) (Zhou et al., 2016). By the incorporation of the Trp analogs, the antimicrobial activity of nisin A remained the same or decreased dramatically.

In case of the genetic code expansion method ncAAs are inserted to the amino acid repertoire by site-specific incorporation in response to stop or quadruplet codons by heterologous expressing orthogonal aminoacyl-tRNA synthetase:tRNA pairs (o-pairs) which recognize the ncAAs (Hoesl and Budisa, 2012). This approach can use orthogonal as well as isostructural ncAAs (Zhou et al., 2016). The genetic code expansion method was carried out for example by Xie and co-workers, which incorporate *p*-iodo-L-phenylalanine in the bacteriophage T4 lysozyme in *E. coli* by overexpressing *Methanococcus jannaschii* tyrosyl-tRNA synthetase (TyrRS):$tRNA^{Tyr}_{CUA}$ pair (Xie et al., 2004). In this study, the orthogonal ncAAs 7-Cl-Trp and 7-Br-Trp were produced fermentatively by *C. glutamicum* (see chapter 2.1, 2.2, 2.3). Thus, this ncAAs could be introduced in the peptide and protein biosynthesis of *C. glutamicum* to generate new peptides and proteins. Since 7-Cl-Trp and 7-Br-Trp are

orthogonal an orthogonal aminoacyl-tRNA synthetase:tRNA pair which accepts this ncAAs have to be overexpressed. A promising pair is the phenylalanyl-tRNA synthetase (yPheRS (T415G)) with the mutant yeast amber suppressor tRNA ($ytRNA^{Phe}_{CUA\_UG}$) (Kwon and Tirrell, 2007). Kwon and co-workers showed, that by overexpressing this o-pair the Trp analogs 6-bromo-tryptophan, 6-chloro-tryptophan, 5-bromo-tryptophan and benzothienylalanine (BT) were incorporated into a protein. They placed at the 38^{th} position of the murine dihydrofolate reductase (mDHFR) an amber stop codon to enable the incorporation of the Trp analogs. Indeed the mDHFR incorporated with 6-bromo-trpytophan showed the highest expression yield but the highest catalytic efficiency was observed by mDHFR with 6-chloro-tryptophan (Kwon and Tirrell, 2007). To establish the same system in *C. glutamicum* the o-pair yPheRS (T415G):$ytRNA^{Phe}_{CUA\_UG}$ and a gene encoding for a protein harboring an amber codon could be overexpressed in the halogenated Trp producing strain. In this case it has to be considered that if the concentration of halogenated Trp is too low an incorporation of Trp instead of halogenated Trp could take place. Thus, the expression of the target gene could be induced if the concentration of halogenated Trp reached the necessary concentration. Hence, with this system 7-Cl-Trp and 7-Br-Trp could be introduced at a specific position (amber codon) in a chosen target protein. The incorporation of orthogonal ncAA in all cAA analog codons, for example, orthogonal halogenated Trp in the Trp codon, by genetic code engineering, has not been described yet, since it is not investigated if an aminoacyl-tRNA synthetase:tRNA pair exists which accepts orthogonal halogenated Trp to introduce it at the Trp codon. Thus, it is unlikely that *C. glutamicum* introduce 7-Cl-Trp and 7-Br-Trp random in the protein instead of Trp during the halogenated Trp production process or by extracellular added 7-Cl-Trp and 7-Br-Trp.

Nevertheless, random mutations in an endogenous tRNA synthestase:tRNA pair of *C. glutamicum* triggered by the halogenated Trp could lead to an introduction of 7-Cl-Trp and 7-Br-Trp in the Trp codons. This could be investigated by amino acid composition analysis of the whole proteome of *C. glutamicum* after feeding halogenated Trp or after the production process. The analysis method consists of two steps: hydrolysis of the substrate and chromatographic separation and detection of the amino acid residues (Fountoulakis and

Lahm, 1998). Based on the amino acid composition the incorporation of halogenated Trp could be proven.

Incorporation of ncAAs, by genetic code engineering or genetic code expansion in different peptides and proteins have various effects, as described for the lipase of *Thermoanaerobacter thermohydrosulfuricus*, where isostructural Met, Pro, Phe or Tyr analogs were incorporated (Hoesl et al., 2011). By the incorporation of the ncAA *meta*-fluorophenylalanine the enzyme activity and the substrate tolerance were enhanced up to 20% or 40%, respectively. In addition, the temperature and pH optimum differ up to 20°C and pH 3, respectively, with different ncAAs (Hoesl et al., 2011). Another effect of the isostructural incorporation can be the increased stability of a protein shown for ubiquitinin which contained (2S,4R)-4-fluoroproline (Crespo and Rubini, 2011). A disadvantage of the genetic code engineering is that only the isostructural ncAAs are introduced and hence the effect of only a few ncAAs can be investigated. In comparison the genetic code expansion can introduce the isostructural and the orthogonal ncAAs. Additionally, in this approach one specific position is targeted which allows selective analysis of protein parts and if the ncAAs are located at accessible positions further reactions, like cross-couplings are feasible. Brustad and co-workers used this approach for single-molecule fluorescence resonance energy transfer (smFRET) (Brustad et al., 2008). In the bacteriophage T4 lysozyme *p*-acetylphenylalanine was incorporated at position D72 and hydroxylamine-containing fluorophore was added. The dye reacts with the ketone amino acid and fluorescence was measure. This method was used to construct dual-labeling of the lysozymes to investigate their folding with smFRET (Brustad et al., 2008). Since the cross-coupling reactions Suzuki-Miyaura (Roy et al., 2008) and Mizoroki–Heck (Gruß et al., 2019) worked with 7-Cl-Trp and 7-Br-Trp they could be used in this approach, for example for the purification of the protein. 7-Cl-Trp and 7-Br-Trp could be used as ncAAs in the genetic code expansion to place them at the specific surface position from a protein such that the cross-coupling reaction could be carried out. Due to this cross-coupled substitute the protein could be purified from the crude extract and further analyzed without complex purification steps. Taken together, the substitution of Trp residues by orthogonal halogenated Trp in a protein

has not been described yet. But the incorporation of 7-Cl-Trp and 7-Br-Trp at specific position in a protein could be carried out and used for purification or labeling of proteins.

3.4 Processing halogenated L-tryptophan to expand the halogenated product portfolio

In this study, 7-Cl-Trp and 7-Br-Trp were produced by fermentation with recombinant *C. glutamicum*. These products could serve as precursors for the production of other halogenated substances. Hence, the product portfolio of *C. glutamicum* based on 7-Cl-Trp and 7-Br-Trp could be extended by various approaches: i) Trp is a starting substrate for the production of several substances such as serotonin, indigo, and indirubin. Instead of using Trp, 7-Cl-Trp and 7-Br-Trp (or other halogenated Trp) could be used as precursor creating, for example, new-to nature halogenated products, ii) since the production of C7 halogenated Trp by *C. glutamicum* was established in this study the *de novo* synthesis of C5 and C6 halogenated Trp by *C. glutamicum* could be investigated. The resulting products could be implemented instead of 7-Cl-Trp in the biosynthesis of rebeccamycin and pyrrolnitrin, and iii) 7-Br-Trp could be incorporated in the biosynthesis of rebeccamycin and pyrrolnitrin to receive the brominated forms of these compounds. Thus, various genes could be expressed in *C. glutamicum* to achieve production of new halogenated products. Although, it is not known for all described enzymes whether they accept halogenated compounds as substrate.
For the first expansion approach, halogenated Trp could be used instead of Trp as precursor to achieve new halogenated compounds.
A new product reachable by one catalysis step is 7-chloroindole and 7-bromoindole (Fig. 3.3). The tryptophanase from *E. coli* accepts beside his natural product Trp, various Trp derivatives, like chloro-tryptophan and methyl-tryptophan (Snell, 1975). In this study, three tryptophanases were tested on their substrate spectrum (see chapter 2.4). It was shown for the tryptophanases from *E. coli* and *P. vulgaris* that they accept either 7-Cl-Trp as well as 7-Br-Trp as substrate. Further, indole could be processed by enzymes to the dyes indigo (dark blue) or indirubin (red-violet) (Fig 3.3). Indirubin is the structure-isomer of indigo and the biosynthetic pathway of both is similar. The precursors indoxyl and 2-hydroxyindole derive by different pathways (Ma et al., 2018), for example, i) a naphthalene dioxygenase (NDO)

transfers two oxygen atoms to the indole resulting in *cis*-indole-2,3-dihydrodiol which is spontaneously converted to indoxyl, or ii) a flavin-containing monooxygenase (FMO) transfers under consumption of NADPH an oxygen atom to indole yielding in 2-hydroxyindole or indoxyl (Ensley et al., 1983; Han et al., 2013; Jung et al., 2018). To yield indigo two indoxyl molecules are dimerized (Ensley et al., 1983). Indirubin is dimerized from different precursors, depending on the production pathway of the substrates: i) if only indoxyl is produced (NDO pathway) indirubin is synthesized from indoxyl and isatin (indoxyl derivative) (Berry et al., 2002), or ii) it is dimerized from 2-hydroxyindole and indoxyl deriving from the FMO pathway (Han et al., 2013) (Fig. 3.3). Overexpression of the NDO from *Pseudomonas putida* in an *E. coli* (natural indole producer) yielded in indigo production (Ensley et al., 1983; Berry et al., 2002). Indirubin production in *E. coli* was achieved by overexpression of the FMO from *Methylophaga aminisulfidivorans* (Han et al., 2013). By integration of the genes for the production of, for example, indirubin in the halogenating *C. glutamicum* strain the halogenated indirubin derivatives could be produced, which have potency as anti-cancer substance (Ji and Zhang, 1985; Ferandin et al., 2006).

Furthermore, Trp is a starting substrate for the production of serotonin and melatonin. First Trp is decarboxylated to tryptamine (Fig. 3.3) which is catalyzed by various tryptophan decarboxylases. A promising candidate for the decarboxylation of halogenated Trp is the tryptophan decarboxylase from *C. roseus* since the enzyme accepts halogenated Trp as substrate (Fräbel et al., 2016). Tryptamines occur in several biological active products and in pharmaceuticals (Kochanowska-Karamyan and Hamann, 2010). Halogenated tryptamines have potential as antibiotics or radiopharmaceuticals (Tymiak et al., 1985; Dragulska and Kańska, 2014). The next interesting compound, the neurotransmitter serotonin, derives from tryptamine or 5-hydroxytryptophan depending on the organism. In plants, Trp is first decarboxylated to tryptamine and this is hydroxylated to serotonin by the tryptamine-5-decarboxylase (Schröder et al., 1999). In animals, Trp is hydroxylated to 5-hydroxyl-tryptophan and the carboxyl group is eliminated by the aromatic L-amino acid decarboxylase (Welford et al., 2016). Halogenated serotonin is not well investigated. But it was shown, that another neurotransmitter dopamine is highly stable in the chlorinated form and has the potential as detection agent for the study of Parkinson's disease patients

(Kalogiannis et al., 2016). By conversion of serotonin the hormone melatonin is synthesized in humans and mammals. It regulates circadian rhythms such as the sleep-wake rhythm or neuroendocrine rhythms (Hastings, 1991; Brzezinski, 1997). Two melatonin biosynthetic pathways are described. In the plant, pathway serotonin is *O*-methylated to 5-methoxytryptamine by the *N*-acetylserotonin *O*-methyltransferase. Further, 5-methoxytryptamine is *N*-acetylated by the serotonin *N*-acetyltransferase to melatonin (Byeon et al., 2016; Tan et al., 2016). In the pathway occurring in animals, the *N*-acetyltransferase converts serotonin to *N*-acetylserotonin which is converted to melatonin catalyzed by the *N*-acetylserotonin *O*-methyltransferase (Kang et al., 2013). Halogenated melatonin, which has potential as anti-reproductive agent, could be produced in the 7-Cl-Trp and 7-Br-Trp producing *C. glutamicum* strain by implementation of the genes for the melatonin pathway (Clemens et al., 1980; Richardson et al., 1983).

Further on, to expand the product portfolio genes from the plant *C. roseus* (see chapter 3.1), which accept halogenated compounds, could be integrated in *C. glutamicum* to produce halogenated alkaloids (12-chloro-19,20-dihydroakuammicine and 12-bromo-19,20-dihydroakuammicine), which derive from halogenated tryptamine (Runguphan et al., 2010). Products containing akuammicine have pharmaceutical applications (Menzies et al., 1998).

In addition, 7-Cl-Trp and 7-Br-Trp could be used as substrate for a second functionalization reaction, for example, methylation (Fig. 3.3). Other functionalizations beside the halogenation could lead to new properties of the product. In a recombinant *C. glutamicum* it was shown, that the wildtype *N*-methyl-L-amino acid dehydrogenase (DpkA) from *Pseudomoanas putida* catalyzed the *N*-methylation of pyruvate to *N*-methyl-L-alanine (Mindt et al., 2018) or the *N*-methylation of glyoxylate to sarcosine (Mindt et al., 2019b). By rational enzyme engineering of the DpkA (resulting in $DpkA^{F117L}$) the production of sarcosine was accelerated (Mindt et al., 2019a). Since DpkA and the mutant version $DpkA^{F117L}$ have a wide substrate spectrum (Mihara et al., 2005; Mindt et al., 2019a) they may accept halogenated Trp as substrate. Another enzyme, which could be used for the methylation of halogenated Trp is the cobalamin dependent radical *S*-adenosylmethionine methylase TsrM which methylates various Trp derivates such as 6-chloro-tryptophan, 6-fluoro-tryptophan or 7-methyl-tryptophan at the C2 position (Blaszczyk et al., 2017).

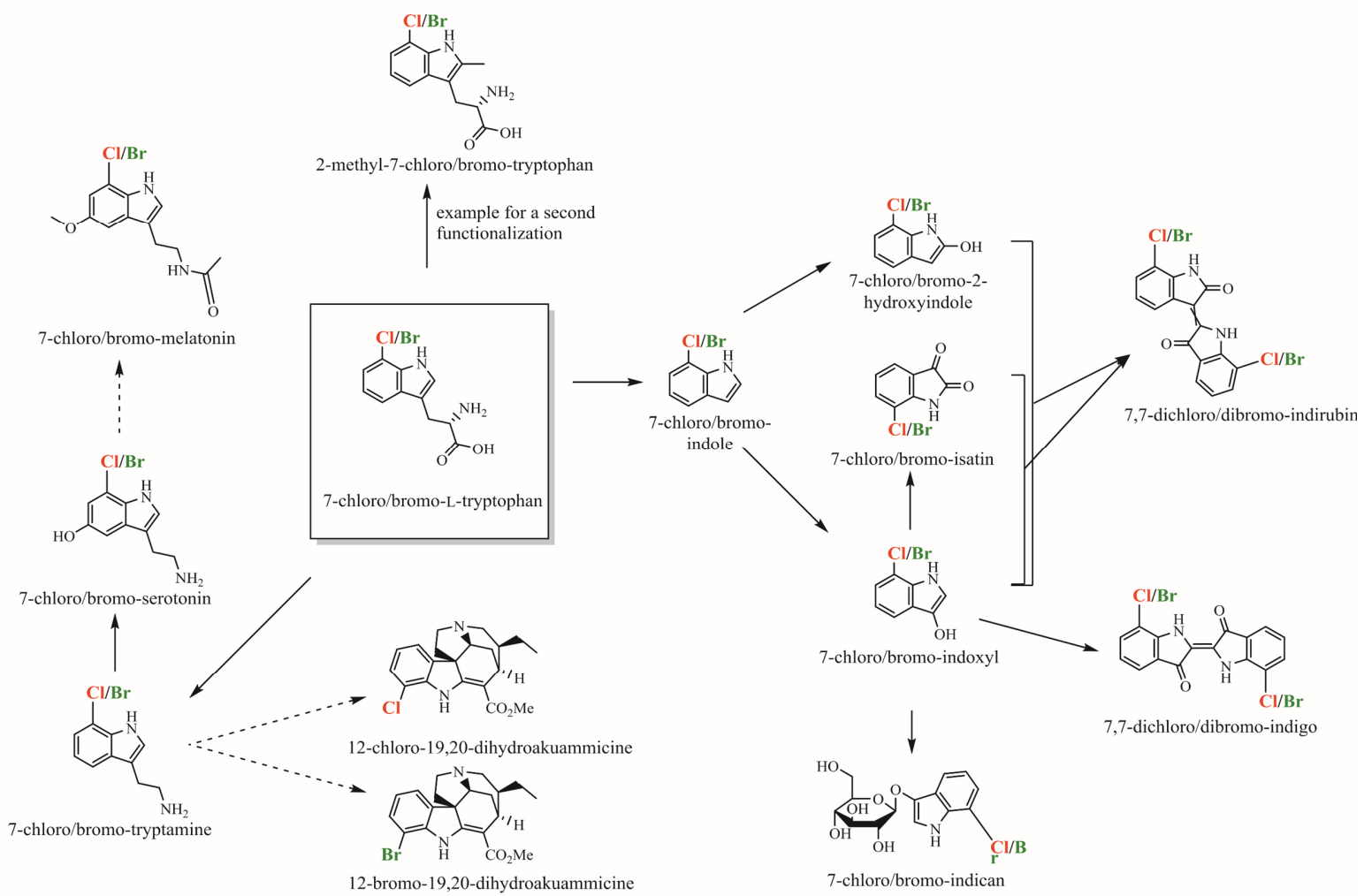

Figure 3.3: Schematic overview of possible halogenated compounds deriving from 7-Cl-Trp and 7-Br-Trp. The overview is related to the products deriving from Trp. All shown conversion steps are carried out via enzymatic steps. It is not known if each enzyme accepts halogenated Trp and the halogenated intermediates.

The second expansion approach is the implementation of the C5 and C6 halogenated Trp in the biosynthesis of rebeccamycin and pyrrolnitrin. Sánchez and co-workers substituted *rebH* by *pyrH* encoding for the FAD-dependent 5-halogenase from *Streptomyces rugosporus* LL-42D005 or by *thal* encoding for the FAD-dependent 6-halogenase from *Streptomycesalbogriseolus* (Sánchez et al., 2005) and overexpressed them with the *rebODCP* genes encoding for the enzymes catalyzing the next steps in the rebeccamycin biosynthesis. Thus, the produced 5-chloro-tryptophan (produced by PyrH) was converted by RebOD to 9-chloro-chromopyrrolic acid and 9,9´-dichloro-chromopyrrolic acid but in the next step, only the monochlorinated 3-chloro-arcyriaflavin instead of the dechlorinated 3,3´-dichloro-arcyriaflavin was produced by RebCP. When 6-chloro-tryptophan (produced by Thal) was the starting substrate already the first conversion step failed and only the monochlorinated 10-chloro-chromopyrrolic acid was produced (Sánchez et al., 2002) (Fig. 3.4). Hence, the production of C5 and C6-substituted rebeccamycin is unfeasible by overexpressing the natural *reb* operon with *pyrH* and *thal*. To achieve a pyrrolnitrin analog, *thal* was overexpressed in the pyrrolnitrin producing strain *Pseudomonas chlororaphis* ACN (Seibold et al., 2006). The first catalytic step, the ring arrangement and decarboxylation of 6-chloro-tryptophan catalyzed by PrnB, was successfully yielding in 3-(2'-Amino-4'-chlorophenyl)pyrrole (Kirner et al., 1998; Seibold et al., 2006) (Fig. 3.4).
The following steps catalyzed by PrnC and PrnD were not carried out since the enzymes did not accept the new intermediate as substrate. Hence, production of C5 and C6 substituted rebeccamycin and pyrrolnitrin is not feasible with the natural *reb* and *prn* genes. By enzyme engineering, the Reb and Prn enzymes could be optimized regarding their substrate spectrum (Payne et al., 2015). The optimized genes could be overexpressed in *C. glutamicum* together with the genes coding for the C5 and C6 FAD-dependent halogenase to produce C5 and C6 substituted rebeccamycin and pyrrolnitrin.
The third expansion approach is the exchange of 7-Cl-Trp by 7-Br-Trp for the production of rebeccamycin and pyrrolnitrin. In nature different kinds of halogenases were discovered, whereby chlorinating and brominating halogenases are the most common ones (Gribble, 2004). Nevertheless, for several halogenases, it was observed that they accept more than one halogen. For example, the FAD-dependent halogenases RebH and PrnA accept chlorine as

well as bromine (Van Pée et al., 1983; Yeh et al., 2005). Hence, the supplementation of bromine in the biosynthesis of rebeccamycin and pyrrolnitrin could lead to new brominated products. In this study, it is shown that the addition of sodium bromide facilitated the halogenated Trp producing *C. glutamicum* strain production of 7-Br-Trp (see chapter 2.2), whereby the concentration of bromide ions was 150 times higher than of chloride ions in the cultivation since RebH prefers chlorination over bromination (Yeh et al., 2005). Lam and co-workers showed in addition, that all following enzymes in the biosynthetic production of rebeccamycin accept the brominated substrates as well. They cultivated the rebeccamycin producing strain *L. aerocolonigenes* with potassium bromide which resulted in the production of the rebeccamycin analog bromorebeccamycin (Lam et al., 1991) (Fig. 3.4). The antitumor activity of rebeccamycin does not differ between the chlorinated or the brominated analog (Lam et al., 1991). The same observations were done for pyrrolnitrin, when sodium bromide was added to the cultivation of the pyrrolnitrin producing strain *Pseudomonas aureofaciens* ATCC 15926 the brominated analog was produced (Van Pée et al., 1983) (Fig. 3.4). Hence, the production of the brominated analogs of rebeccamycin and pyrrolnitrin could enable in *C. glutamicum* by overexpression of the *reb* or the *prn* operon, respectively.

All in all 7-Cl-Trp and 7-Br-Trp are promising precursors for several new products, which can have applications in the chemical, pharmaceutical or agrochemical industries. Since all conversion steps are enzymatically catalyzed or spontaneously the pathways could be transferred to the halogenated Trp producing *C. glutamicum* strain to investigate the production of various derivatives of halogenated 7-Cl-Trp and 7-Br-Trp (or other halogenated Trp).

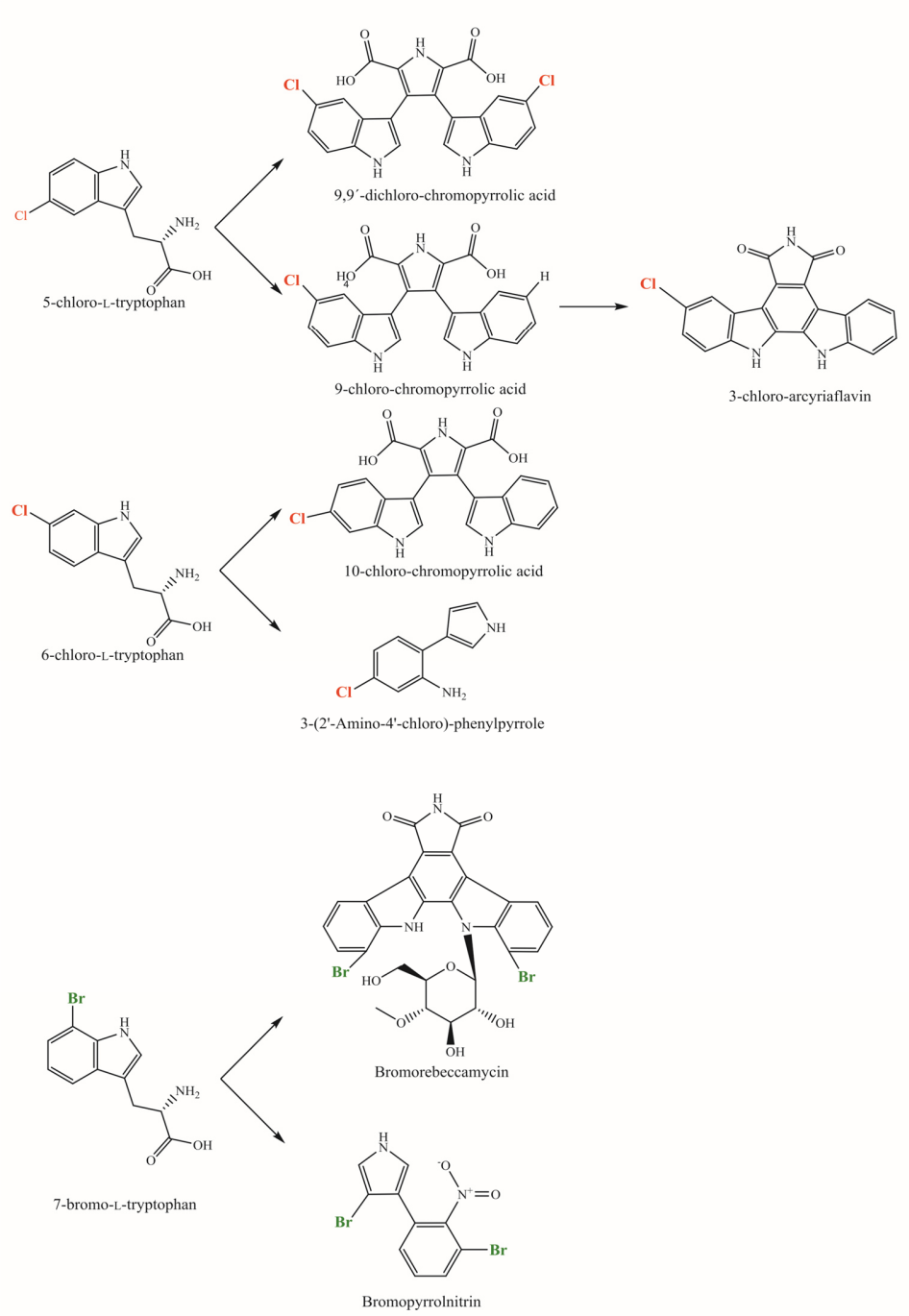

Fig. 3.4: Schematic overview of the rebeccamycin and pyrrolnitrin analogs. The first intermediate of the biosynthesis of rebeccamycin and pyrrolnitrin 7-Cl-Trp was exchanged by 5-Cl-Trp, 6-Cl-Trp, and 7-Br-Trp. The chemical structures of the resulting analogs are displayed.

Taken together, the fermentative production of halogenated Trp and indole with *C. glutamicum* is environmentally friendly and efficient. Consequently, it is a promising

initiation step for a wide range of prospects: i) indole and halogenated Trp could be further processed by *C. glutamicum* for expansion of the product portfolio, ii) the investigation of the other C-substituted Trp´s is promising since the production of 7-Cl-Trp and 7-Br-Trp is established, and iii) 7-Cl-Trp and 7-Br-Trp could be incorporated as ncAAs in peptides and proteins for proteomic studies. Hence, fermentative production of halogenated Trp and indole by *C. glutamicum* opens the possibilities to expand the product portfolio to new halogenated compounds by bacterial fermentation.

3.5 References

Amet, N., Lee, H.-F., and Shen, W.-C. (2009). Insertion of the designed helical linker led to increased expression of Tf-based fusion proteins. Pharm. Res. 26**,** 523. doi:10.1007/s11095-008-9767-0.

Berry, A., Dodge, T.C., Pepsin, M., and Weyler, W. (2002). Application of metabolic engineering to improve both the production and use of biotech indigo. J. Ind. Microbiol. Biotechnol. 28**,** 127-133. doi:10.1038/sj/jim/7000228.

Binder, D., Frohwitter, J., Mahr, R., Bier, C., Grünberger, A., Loeschcke, A., et al. (2016). Light-controlled cell factories: Employing photocaged isopropyl-β-D-thiogalactopyranoside for light-mediated optimization of *lac* promoter-based gene expression and (+)-valencene biosynthesis in *Corynebacterium glutamicum*. Appl. Environ. Microbiol. 82**,** 6141-6149. doi:10.1128/AEM.01457-16.

Blaskovich, M.A.T. (2016). Unusual amino acids in medicinal chemistry. J. Med. Chem. 59**,** 10807-10836. doi:10.1021/acs.jmedchem.6b00319.

Blaszczyk, A.J., Wang, B., Silakov, A., Ho, J.V., and Booker, S.J. (2017). Efficient methylation of C2 in L-tryptophan by the cobalamin-dependent radical S-adenosylmethionine methylase TsrM requires an unmodified N1 amine. J. Biol. Chem. 292**,** 15456-15467. doi:10.1074/jbc.M117.778548.

Blombach, B., Arndt, A., Auchter, M., and Eikmanns, B.J. (2009). L-Valine production during growth of pyruvate dehydrogenase complex-deficient *Corynebacterium glutamicum* in the presence of ethanol or by inactivation of the transcriptional regulator SugR. Appl. Environ. Microbiol. 75**,** 1197-1200. doi:10.1128/AEM.02351-08.

Blombach, B., Riester, T., Wieschalka, S., Ziert, C., Youn, J.-W., Wendisch, V.F., et al. (2011). *Corynebacterium glutamicum* tailored for efficient isobutanol production. Appl. Environ. Microbiol. 77**,** 3300-3310. doi:10.1128/AEM.02972-10.

Bröer, S., and Krämer, R. (1991). Lysine excretion by *Corynebacterium glutamicum*: 1. Identification of a specific secretion carrier system. Eur. J. Biochem. 202**,** 131-135. doi:10.1111/j.1432-1033.1991.tb16353.x.

Brune, I., Jochmann, N., Brinkrolf, K., Hüser, A.T., Gerstmeir, R., Eikmanns, B.J., et al. (2007). The IclR-type transcriptional repressor LtbR regulates the expression of leucine and tryptophan biosynthesis genes in the amino acid producer *Corynebacterium glutamicum*. J. Bacteriol. 189**,** 2720-2733. doi:10.1128/JB.01876-06.

Brustad, E.M., Lemke, E.A., Schultz, P.G., and Deniz, A.A. (2008). A general and efficient method for the site-specific dual-labeling of proteins for single molecule fluorescence resonance energy transfer. J. Am. Chem. Soc. 130**,** 17664-17665. doi:10.1021/ja807430h.

Brzezinski, A. (1997). Melatonin in humans. N. Engl. J. Med. 336**,** 186-195. doi:10.1056/nejm199701163360306.

Budisa, N., Huber, R., Golbik, R., Minks, C., Weyher, E., and Moroder, L. (1998). Atomic mutations in annexin V: thermodynamic studies of isomorphous protein variants. Eur. J. Biochem. 253**,** 1-9. doi:10.1046/j.1432-1327.1998.2530001.x.

Busche, T., Šilar, R., Pičmanová, M., Pátek, M., and Kalinowski, J. (2012). Transcriptional regulation of the operon encoding stress-responsive ECF sigma factor SigH and its anti-sigma factor RshA, and control of its regulatory network in *Corynebacterium glutamicum*. BMC genomics 13**,** 445. doi:10.1186/1471-2164-13-445.

Byeon, Y., Lee, H.J., Lee, H.Y., and Back, K. (2016). Cloning and functional characterization of the *Arabidopsis N*-acetylserotonin *O*-methyltransferase responsible for melatonin synthesis. J. Pineal Res. 60**,** 65-73. doi:10.1111/jpi.12289.

Cabrita, L.D., Dai, W., and Bottomley, S.P. (2006). A family of *E. coli* expression vectors for laboratory scale and high throughput soluble protein production. BMC Biotechnol. 6**,** 12. doi:10.1186/1472-6750-6-12.

Cabrita, M.T., Vale, C., and Rauter, A.P. (2010). Halogenated compounds from marine algae. Mar. Drugs 8**,** 2301-2317. doi:10.3390/md8082301.

Cantillo, D., and Kappe, C.O. (2017). Halogenation of organic compounds using continuous flow and microreactor technology. React. Chem. Eng. 2**,** 7-19. doi:10.1039/C6RE00186F.

Chen, X., Zaro, J.L., and Shen, W.-C. (2013). Fusion protein linkers: property, design and functionality. Adv. Drug Deliv. Rev. 65**,** 1357-1369. doi:10.1016/j.addr.2012.09.039.

Choe, D., Lee, J.H., Yoo, M., Hwang, S., Sung, B.H., Cho, S., et al. (2019). Adaptive laboratory evolution of a genome-reduced *Escherichia coli*. Nat. Commun. 10**,** 935. doi:10.1038/s41467-019-08888-6.

Clemens, J.A., Flaugh, M.E., Parli, J., and Sawyer, B.D. (1980). Inhibition of luteinizing hormone release and ovulation by 6-chloro-and 6-fluoromelatonin. Neuroendocrinology 30**,** 83-87. doi:10.1159/000122980.

Cowie, D.B., and Cohen, G.N. (1957). Biosynthesis by *Escherichia coli* of active altered proteins containing selenium instead of sulfur. Biochim. Biophys. Acta 26**,** 252-261. doi:10.1016/0006-3002(57)90003-3.

Crespo, M.D., and Rubini, M. (2011). Rational design of protein stability: effect of (2S, 4R)-4-fluoroproline on the stability and folding pathway of ubiquitin. PloS One 6**,** e19425. doi:10.1371/journal.pone.0019425.

Dandekar, A.M., and Fisk, H.J. (2005). Plant transformation: Agrobacterium-mediated gene transfer, in Transgenic Plants: Methods and Protocols. Springer. 35-46.

De Luca, V., Marineau, C., and Brisson, N. (1989). Molecular cloning and analysis of cDNA encoding a plant tryptophan decarboxylase: comparison with animal dopa decarboxylases. Proc. Natl. Acad. Sci. 86**,** 2582-2586. doi:10.1073/pnas.86.8.2582.

Dong, C., Flecks, S., Unversucht, S., Haupt, C., Van Pee, K.-H., and Naismith, J.H. (2005). Tryptophan 7-halogenase (PrnA) structure suggests a mechanism for regioselective chlorination. Science 309**,** 2216-2219. doi:10.1126/science.1116510.

Dragosits, M., and Mattanovich, D. (2013). Adaptive laboratory evolution–principles and applications for biotechnology. Microb. Cell. Fact. 12**,** 64. doi:10.1186/1475-2859-12-64.

Dragulska, S., and Kańska, M. (2014). Enzymatic synthesis of tryptamine and its halogen derivatives selectively labeled with hydrogen isotopes. J. Radioanal. Nucl. Chem. 299**,** 759-763. doi:10.1007/s10967-013-2816-0.

Elvers, B. (2014). Ullmann's fine chemicals. Wiley-VCH, Weinheim, Germany).

Ensley, B.D., Ratzkin, B.J., Osslund, T.D., Simon, M.J., Wackett, L.P., and Gibson, D.T. (1983). Expression of naphthalene oxidation genes in *Escherichia coli* results in the biosynthesis of indigo. Science 222**,** 167-169. doi:10.1126/science.6353574.

Erdmann, A., Weil, B., and Krämer, R. (1993). Lysine secretion by wild-type *Corynebacterium glutamicu*m triggered by dipeptide uptake. Microbiology 139**,** 3115-3122. doi:10.1099/00221287-139-12-3115.

Ferandin, Y., Bettayeb, K., Kritsanida, M., Lozach, O., Polychronopoulos, P., Magiatis, P., et al. (2006). 3 '-Substituted 7-halogenoindirubins, a new class of cell death inducing agents. J. Med. Chem. 49**,** 4638-4649. doi:10.1021/jm060314i.

Fong, S.S., Burgard, A.P., Herring, C.D., Knight, E.M., Blattner, F.R., Maranas, C.D., et al. (2005). In silico design and adaptive evolution of *Escherichia coli* for production of lactic acid. Biotechnol. Bioeng. 91**,** 643-648. doi:10.1002/bit.20542.

Fountoulakis, M., and Lahm, H.-W. (1998). Hydrolysis and amino acid composition analysis of proteins. J. Chromatogr. A 826**,** 109-134. doi:10.1016/S0021-9673(98)00721-3.

Fräbel, S., Krischke, M., Staniek, A., and Warzecha, H. (2016). Recombinant flavin-dependent halogenases are functional in tobacco chloroplasts without co-expression of flavin reductase genes. Biotechnol. J. 11**,** 1586-1594. doi:10.1002/biot.201600337.

Fräbel, S., Wagner, B., Krischke, M., Schmidts, V., Thiele, C.M., Staniek, A., et al. (2018). Engineering of new-to-nature halogenated indigo precursors in plants. Metab. Eng. 46**,** 20-27. doi:10.1016/j.ymben.2018.02.003.

Frese, M., Guzowska, P.H., Voss, H., and Sewald, N. (2014). Regioselective Enzymatic Halogenation of Substituted Tryptophan Derivatives using the FAD-Dependent Halogenase RebH. ChemCatChem. 6**,** 1270-1276. doi:10.1002/cctc.201301090.

Frese, M., and Sewald, N. (2015). Enzymatic Halogenation of Tryptophan on a Gram Scale. Angew. Chem. Int. Ed. 54**,** 298-301. doi:10.1002/anie.201408561.

Frey, M., Chomet, P., Glawischnig, E., Stettner, C., Grün, S., Winklmair, A., et al. (1997). Analysis of a chemical plant defense mechanism in grasses. Science 277**,** 696-699. doi:10.1126/science.277.5326.696.

Frey, M., Stettner, C., Paré, P.W., Schmelz, E.A., Tumlinson, J.H., and Gierl, A. (2000). An herbivore elicitor activates the gene for indole emission in maize. Proc. Natl. Acad. Sci. 97**,** 14801-14806. doi:10.1073/pnas.260499897.

Goddijn, O.J.M., Lohman, F.P., de Kam, R.J., and Hoge, J.H.C. (1994). Nucleotide sequence of the tryptophan decarboxylase gene of *Catharanthus roseus* and expression of *tdc-gusA* gene fusions in *Nicotiana tabacum*. Mol. Gen. Genet. 242**,** 217-225. doi:10.1007/bf00391016.

Gosset, G., Yong-Xiao, J., and Berry, A. (1996). A direct comparison of approaches for increasing carbon flow to aromatic biosynthesis in *Escherichia coli*. J. Ind. Microbiol. 17**,** 47-52. doi:10.1007/BF01570148.

Gribble, G.W. (1996). Naturally occuring organohalogen compounds—a comprehensive survery, in Progress in the chemistry of organic natural products. Springer. 1-423.

Gribble, G.W. (2004). Natural production of organohalogen compounds. Springer.

Gruß, H., Belu, C., Bernhard, L.M., Merschel, A., and Sewald, N. (2019). Fluorogenic Diversification of Unprotected Bromotryptophan by Aqueous Mizoroki–Heck Cross-Coupling. Chem. Eur. J. 25**,** 5880-5883. doi:10.1002/chem.201900437.

Han, G.H., Gim, G.H., Kim, W., Seo, S.I., and Kim, S.W. (2013). Enhanced indirubin production in recombinant *Escherichia coli* harboring a flavin-containing monooxygenase gene by cysteine supplementation. J. Biotechnol. 164**,** 179-187. doi:10.1016/j.jbiotec.2012.08.015.

Hastings, M.H. (1991). Neuroendocrine rhythms. Pharmacol. Ther. 50**,** 35-71. doi:10.1016/0163-7258(91)90072-T.

Henke, N., Heider, S., Peters-Wendisch, P., and Wendisch, V. (2016a). Production of the marine carotenoid astaxanthin by metabolically engineered *Corynebacterium glutamicum*. Mar. Drugs 14**,** 124. doi:10.3390/md14070124.

Henke, N.A., Heider, S.A.E., Peters-Wendisch, P., and Wendisch, V.F. (2016b). Production of the marine carotenoid astaxanthin by metabolically engineered *Corynebacterium glutamicum*. Mar. Drugs 14**,** 124. doi:10.3390/md14070124.

Herry, D.M., and Dunican, L.K. (1993). Cloning of the *trp* gene cluster from a tryptophan-hyperproducing strain of *Corynebacterium glutamicum*: identification of a mutation in the *trp* leader sequence. Appl. Environ. Microbiol. 59**,** 791-799.

Hoesl, M.G., Acevedo-Rocha, C.G., Nehring, S., Royter, M., Wolschner, C., Wiltschi, B., et al. (2011). Lipase congeners designed by genetic code engineering. ChemCatChem. 3**,** 213-221. doi:10.1002/cctc.201000253.

Hoesl, M.G., and Budisa, N. (2012). Recent advances in genetic code engineering in *Escherichia coli*. Curr. Opin. Biotechnol. 23**,** 751-757. doi:10.1016/j.copbio.2011.12.027.

Hughes, E.H., Hong, S.B., Shanks, J.V., San, K.Y., and Gibson, S.I. (2002). Characterization of an inducible promoter system in *Catharanthus roseus* hairy roots. Biotechnol. Prog. 18**,** 1183-1186. doi:10.1021/bp025603o.

Ikeda, M., and Katsumata, R. (1995). Tryptophan production by transport mutants of Corynebacterium glutamicum. Biosci. Biotechnol. Biochem. 59**,** 1600-1602. doi:10.1271/bbb.59.1600.

Ikeda, M., Nakanishi, K., Kino, K., and Katsumata, R. (1994). Fermentative Production of Tryptophan by a Stable Recombinant Strain of *Corynebacterium glutamicum* with a Modified Serine-biosynthetic Pathway. Biosci. Biotechnol. Biochem. 58**,** 674-678. doi:10.1271/bbb.58.674.

Ikeda, M., Okamoto, K., and Katsumata, R. (1999). Cloning of the transketolase gene and the effect of its dosage on aromatic amino acid production in *Corynebacterium glutamicum*. Appl. Microbiol. Biotechnol. 51**,** 201-206. doi:10.1007/s002530051382.

Ishaq, M.S., Afsheen, Z., and Khan, A. (2018). Disinfection Methods, in Photocatalysts-Applications and Attributes. IntechOpen.

Ji, X.J., and Zhang, F.R. (1985). Studies on antineoplastic action of indirubin derivatives and analogs and their structure-activity relationships. Acta Pharm. Sin. 20**,** 137-139.

Jia, H., Li, H., Zhang, L., and Xu, D. (2018). Development of a novel gene expression system for secretory production of heterologous proteins via the general secretory (Sec) pathway in *Corynebacterium glutamicum*. Iran J Biotechnol. 16. doi:10.21859/ijb.1746.

Jung, H.S., Jung, H.B., Kim, H.S., Kim, C.G., and Lee, J.H. (2018). Protein Engineering of Flavin-containing Monooxygenase from *Corynebacterium glutamicum* for Improved Production of Indigo and Indirubin. J. Life Sci. 28**,** 656-662. doi:10.5352/JLS.2018.28.6.656.

Kalogiannis, M., Delikatny, E.J., and Jeitner, T.M. (2016). Serotonin as a putative scavenger of hypohalous acid in the brain. Biochim. Biophys. Acta (BBA)-Molecular Basis of Disease 1862**,** 651-661. doi:10.1016/j.bbadis.2015.12.012.

Kang, K., Lee, K., Park, S., Byeon, Y., and Back, K. (2013). Molecular cloning of rice serotonin *N*-acetyltransferase, the penultimate gene in plant melatonin biosynthesis. J. Pineal Res. 55**,** 7-13. doi:10.1111/jpi.12011.

Katsumata, R., and Ikeda, M. (1993). Hyperproduction of tryptophan in *Corynebacterium glutamicum* by pathway engineering. Bio/Technology 11**,** 921. doi:10.1038/nbt0893-921.

Keller, S., Wage, T., Hohaus, K., Hölzer, M., Eichhorn, E., and van Pée, K.H. (2000). Purification and partial characterization of tryptophan 7-halogenase (PrnA) from *Pseudomonas fluorescens*. Angew. Chem. Int. Ed. 39**,** 2300-2302. doi:10.1002/1521-3773(20000703)39:13<2300::AID-ANIE2300>3.0.CO;2-I.

Kirchner, O., and Tauch, A. (2003). Tools for genetic engineering in the amino acid-producing bacterium *Corynebacterium glutamicum*. J. Biotechnol. 104**,** 287-299. doi:10.1016/S0168-1656(03)00148-2.

Kirner, S., Hammer, P.E., Hill, D.S., Altmann, A., Fischer, I., Weislo, L.J., et al. (1998). Functions encoded by pyrrolnitrin biosynthetic genes from *Pseudomonas fluorescens*. J. Bacteriol. 180**,** 1939-1943.

Kitade, Y., Hashimoto, R., Suda, M., Hiraga, K., and Inui, M. (2018). Production of 4-hydroxybenzoic acid by an aerobic growth-arrested bioprocess using metabolically engineered *Corynebacterium glutamicum*. Appl. Environ. Microbiol. 84**,** e02587-02517. doi:10.1128/AEM.02587-17.

Kochanowska-Karamyan, A.J., and Hamann, M.T. (2010). Marine indole alkaloids: potential new drug leads for the control of depression and anxiety. Chem. Rev. 110**,** 4489-4497. doi:10.1021/cr900211p.

Kogure, T., Kubota, T., Suda, M., Hiraga, K., and Inui, M. (2016). Metabolic engineering of *Corynebacterium glutamicum* for shikimate overproduction by growth-arrested cell reaction. Metab. Eng. 38**,** 204-216. doi:10.1016/j.ymben.2016.08.005.

Kubota, T., Tanaka, Y., Hiraga, K., Inui, M., and Yukawa, H. (2013). Characterization of shikimate dehydrogenase homologues of *Corynebacterium glutamicum*. Appl. Microbiol. Biotechnol. 97**,** 8139-8149. doi:10.1007/s00253-012-4659-y.

Kwon, I., and Tirrell, D.A. (2007). Site-specific incorporation of tryptophan analogues into recombinant proteins in bacterial cells. J. Am. Chem. Soc. 129**,** 10431-10437. doi:10.1021/ja071773r.

Lam, K.S., Schroeder, D.R., Veitch, J.M., Matson, J.A., and Forenza, S. (1991). Isolation of a bromo analog of rebeccamycin from *Saccharothrix aerocolonigenes*. J. Antibiot. 44**,** 934-939. doi:10.7164/antibiotics.44.934.

Lausberg, F., Chattopadhyay, A.R., Heyer, A., Eggeling, L., and Freudl, R. (2012). A tetracycline inducible expression vector for *Corynebacterium glutamicum* allowing tightly regulable gene expression. Plasmid 68**,** 142-147. doi:10.1016/j.plasmid.2012.05.001.

Lee, J.-H., and Lee, J. (2010). Indole as an intercellular signal in microbial communities. FEMS Microbiol. Rev. 34**,** 426-444. doi:10.1111/j.1574-6976.2009.00204.x.

Lee, J.-K., and Zhao, H. (2007). Identification and characterization of the flavin: NADH reductase (PrnF) involved in a novel two-component arylamine oxygenase. J. Bacteriol. 189**,** 8556-8563. doi:10.1128/JB.01050-07.

Lee, J.-Y., Seo, J., Kim, E.-S., Lee, H.-S., and Kim, P. (2013). Adaptive evolution of *Corynebacterium glutamicum* resistant to oxidative stress and its global gene expression profiling. Biotechnol. Lett. 35**,** 709-717. doi:10.1007/s10529-012-1135-9.

Lee, M.J., and Kim, P. (2018). Recombinant protein expression system in *Corynebacterium glutamicum* and its application. Front. Microbiol. 9**,** 2523. doi:10.3389/fmicb.2018.02523.

Liao, Y., Zeng, M., Wu, Z.-f., Chen, H., Wang, H.-n., Wu, Q., et al. (2012). Improving phytase enzyme activity in a recombinant *phyA* mutant phytase from *Aspergillus niger* N25 by error-prone PCR. Appl. Biochem. Biotechnol. 166**,** 549-562. doi:10.1007/s12010-011-9447-0.

Lindner, S.N., Seibold, G.M., Henrich, A., Krämer, R., and Wendisch, V.F. (2011). Phosphotransferase system-independent glucose utilization in *Corynebacterium glutamicum* by inositol permeases and glucokinases. Appl. Environ. Microbiol. 77**,** 3571-3581. doi:10.1128/AEM.02713-10.

Lu, X., Liu, S., Zhang, D., Zhou, X., Wang, M., Liu, Y., et al. (2013). Enhanced thermal stability and specific activity of *Pseudomonas aeruginosa* lipoxygenase by fusing with self-assembling amphipathic peptides. Appl. Microbiol. Biotechnol. 97**,** 9419-9427. doi:10.1007/s00253-013-4751-y.

Lubitz, D., Jorge, J.M.P., Pérez-García, F., Taniguchi, H., and Wendisch, V.F. (2016). Roles of export genes *cgmA* and *lysE* for the production of L-arginine and L-citrulline by *Corynebacterium glutamicum*. Appl. Microbiol. Biotechnol. 100**,** 8465-8474. doi:10.1007/s00253-016-7695-1.

Ma, Q., Zhang, X., and Qu, Y. (2018). Biodegradation and biotransformation of indole: advances and perspectives. Front. Microbiol. 9. doi:10.3389/fmicb.2018.02625.

Madhuprakash, J., El Gueddari, N.E., Moerschbacher, B.M., and Podile, A.R. (2015). Catalytic efficiency of chitinase-D on insoluble chitinous substrates was improved by fusing auxiliary domains. PloS One 10**,** e0116823. doi:10.1371/journal.pone.0116823.

Mahr, R., Gätgens, C., Gätgens, J., Polen, T., Kalinowski, J., and Frunzke, J. (2015). Biosensor-driven adaptive laboratory evolution of L-valine production in *Corynebacterium glutamicum*. Metab. Eng. 32**,** 184-194. doi:10.1016/j.ymben.2015.09.017.

Mao, Y., Li, G., Chang, Z., Tao, R., Cui, Z., Wang, Z., et al. (2018). Metabolic engineering of *Corynebacterium glutamicum* for efficient production of succinate from lignocellulosic hydrolysate. Biotechnol. Biofuels 11**,** 95. doi:10.1186/s13068-018-1094-z.

McCoy, E., and O'Connor, S.E. (2006). Directed biosynthesis of alkaloid analogs in the medicinal plant Catharanthus roseus. J. Am. Chem. Soc. 128**,** 14276-14277. doi:10.1021/ja066787w.

McCullum, E.O., Williams, B.A.R., Zhang, J., and Chaput, J.C. (2010). Random mutagenesis by error-prone PCR, in In vitro mutagenesis protocols. Springer. 103-109.

Meiswinkel, T.M., Gopinath, V., Lindner, S.N., Nampoothiri, K.M., and Wendisch, V.F. (2013). Accelerated pentose utilization by *Corynebacterium glutamicum* for accelerated production of lysine, glutamate, ornithine and putrescine. Microb Biotechnol. 6**,** 131-140. doi:10.1111/1751-7915.12001.

Menzies, J.R.W., Paterson, S.J., Duwiejua, M., and Corbett, A.D. (1998). Opioid activity of alkaloids extracted from *Picralima nitida* (fam. *Apocynaceae*). Eur. J. Pharmacol. 350**,** 101-108. doi:10.1016/S0014-2999(98)00232-5.

Mihara, H., Muramatsu, H., Kakutani, R., Yasuda, M., Ueda, M., Kurihara, T., et al. (2005). *N*-Methyl-L-amino acid dehydrogenase from *Pseudomonas putida*: A novel member of an unusual NAD (P)-dependent oxidoreductase superfamily. FEBS J. 272**,** 1117-1123. doi:10.1111/j.1742-4658.2004.04541.x.

Mindt, M., Hannibal, S., Heuser, M., Risse, J.M., Sasikumar, K., Nampoothiri, K.M., et al. (2019a). Fermentative production of *N*-alkylated glycine derivatives by recombinant *Corynebacterium glutamicum* using a mutant of imine reductase DpkA from Pseudomonas putida. Front. bioeng. biotechnol. 7**,** 232. doi:10.3389/fbioe.2019.00232.

Mindt, M., Heuser, M., and Wendisch, V.F. (2019b). Xylose as preferred substrate for sarcosine production by recombinant *Corynebacterium glutamicum*. Bioresour. Technol. 281**,** 135-142. doi:10.1016/j.biortech.2019.02.084.

Mindt, M., Risse, J.M., Gruß, H., Sewald, N., Eikmanns, B.J., and Wendisch, V.F. (2018). One-step process for production of *N*-methylated amino acids from sugars and methylamine using recombinant *Corynebacterium glutamicum* as biocatalyst. Sci. Rep. 8**,** 12895. doi:10.1038/s41598-018-31309-5.

Noren, C.J., Anthony-Cahill, S.J., Griffith, M.C., and Schultz, P.G. (1989). A general method for site-specific incorporation of unnatural amino acids into proteins. Science 244**,** 182-188. doi:10.1126/science.2649980.

O'Connor, S.E., and Maresh, J.J. (2006). Chemistry and biology of monoterpene indole alkaloid biosynthesis. Nat. Prod. Rep. 23**,** 532-547. doi:10.1039/B512615K.

Oide, S., Gunji, W., Moteki, Y., Yamamoto, S., Suda, M., Jojima, T., et al. (2015). Thermal and solvent stress cross-tolerance conferred to *Corynebacterium glutamicum* by adaptive laboratory evolution. Appl. Environ. Microbiol. 81**,** 2284-2298. doi:10.1128/AEM.03973-14.

Oldach, F., Al Toma, R., Kuthning, A., Caetano, T., Mendo, S., Budisa, N., et al. (2012). Congeneric lantibiotics from ribosomal in vivo peptide synthesis with noncanonical amino acids. Angew. Chem. Int. Ed. 51**,** 415-418. doi:10.1002/anie.201106154.

Parikh, M.R., and Matsumura, I. (2005). Site-saturation mutagenesis is more efficient than DNA shuffling for the directed evolution of β-fucosidase from β-galactosidase. J. Mol. Biol. 352**,** 621-628. doi:10.1016/j.jmb.2005.07.020.

Payne, J.T., Andorfer, M.C., and Lewis, J.C. (2013). Regioselective Arene Halogenation using the FAD-Dependent Halogenase RebH. Angew. Chem. 125**,** 5379-5382. doi:10.1002/anie.201300762.

Payne, J.T., Poor, C.B., and Lewis, J.C. (2015). Directed Evolution of RebH for Site-Selective Halogenation of Large Biologically Active Molecules. Angew. Chem. Int. Ed. 54**,** 4226-4230. doi:10.1002/anie.201411901.

Pérez-García, F., Peters-Wendisch, P., and Wendisch, V.F. (2016). Engineering *Corynebacterium glutamicum* for fast production of L-lysine and L-pipecolic acid. Appl. Microbiol. Biotechnol. 100**,** 8075-8090. doi:10.1007/s00253-016-7682-6.

Peters-Wendisch, P., Stolz, M., Etterich, H., Kennerknecht, N., Sahm, H., and Eggeling, L. (2005). Metabolic engineering of *Corynebacterium glutamicum* for L-serine production. Appl. Environ. Microbiol. 71**,** 7139-7144. doi:10.1128/AEM.71.11.7139-7144.2005.

Pfeifer, E., Gätgens, C., Polen, T., and Frunzke, J. (2017). Adaptive laboratory evolution of *Corynebacterium glutamicum* towards higher growth rates on glucose minimal medium. Sci. Rep. 7**,** 16780. doi:10.1038/s41598-017-17014-9.

Poor, C.B., Andorfer, M.C., and Lewis, J.C. (2014). Improving the stability and catalyst lifetime of the halogenase RebH by directed evolution. ChemBioChem 15**,** 1286-1289. doi:10.1002/cbic.201300780.

Purwanto, H.S., Kang, M.-S., Ferrer, L., Han, S.-S., Lee, J.-Y., Kim, H.-S., et al. (2018). Rational engineering of the shikimate and related pathways in *Corynebacterium glutamicum* for 4-hydroxybenzoate production. J. Biotechnol. doi:10.1016/j.jbiotec.2018.07.016.

Rezaie, E., Latifi, A.M., and Mirzaei, M. (2018). Activity improvement of organophosphorus hydrolase enzyme by error prone PCR method. J. Appl. Biotechnol. Rep. 5**,** 100-104. doi:10.29252/JABR.05.03.03.

Richardson, B.A., Vaughan, M.K., Petterborg, L.J., Johnson, L.Y., King, T.S., Smith, I., et al. (1983). Natural and synthetic analogues of melatonin and related compounds I. Effects on the reproductive system of the male Syrian hamster. J. Neural Transm. 56**,** 187-197. doi:10.1007/BF01243277.

Roy, A.D., Goss, R.J.M., Wagner, G.K., and Winn, M. (2008). Development of fluorescent aryltryptophans by Pd mediated cross-coupling of unprotected halotryptophans in water. Chem. Commun. 39**,** 4831-4833. doi:10.1039/B807512C.

Runguphan, W., and O'Connor, S.E. (2013). Diversification of monoterpene indole alkaloid analogs through cross-coupling. Org. Lett. 15**,** 2850-2853. doi:10.1021/ol401179k.

Runguphan, W., Qu, X., and O'connor, S.E. (2010). Integrating carbon–halogen bond formation into medicinal plant metabolism. Nature. 468**,** 461. doi:10.1038/nature09524.

Saikia, I., Borah, A.J., and Phukan, P. (2016). Use of bromine and bromo-organic compounds in organic synthesis. Chem. Rev. 116**,** 6837-7042. doi:10.1021/acs.chemrev.5b00400.

Sánchez, C., Butovich, I.A., Braña, A.F., Rohr, J., Méndez, C., and Salas, J.A. (2002). The biosynthetic gene cluster for the antitumor rebeccamycin: characterization and generation of indolocarbazole derivatives. Chem. Biol. 9**,** 519-531. doi:10.1016/S1074-5521(02)00126-6.

Sánchez, C., Zhu, L., Braña, A.F., Salas, A.P., Rohr, J., Méndez, C., et al. (2005). Combinatorial biosynthesis of antitumor indolocarbazole compounds. Proc. Natl. Acad. Sci. 102**,** 461-466. doi:10.1073/pnas.0407809102.

Sawada, K., Kato, Y., Imai, K., Li, L., Wada, M., Matsushita, K., et al. (2012). Mechanism of increased respiration in an H^+-ATPase-defective mutant of *Corynebacterium glutamicum*. J. Biosci. Bioeng. 113**,** 467-473. doi:10.1016/j.jbiosc.2011.11.021.

Sawada, K., Wada, M., Hagiwara, T., Zen-in, S., Imai, K., and Yokota, A. (2015). Effect of pyruvate kinase gene deletion on the physiology of *Corynebacterium glutamicum* ATCC13032 under biotin-sufficient non-glutamate-producing conditions: Enhanced biomass production. Metab. Eng. Commun. 2**,** 67-75. doi:10.1016/j.meteno.2015.07.001.

Schmittinger, P., Florkiewicz, T., Curlin, L.C., Lüke, B., Scannell, R., Navin, T., et al. (2000). Chlorine. Ullmann's Encyclopedia of Industrial Chemistry. doi:10.1002/14356007.a06_399.

Schröder, P., Abele, C., Gohr, P., Stuhlfauth-Roisch, U., and Grosse, W. (1999). Latest on enzymology of serotonin biosynthesis in walnut seeds, in Tryptophan, Serotonin, and Melatonin. Springer. 637-644.

Seibold, C., Schnerr, H., Rumpf, J., Kunzendorf, A., Hatscher, C., Wage, T., et al. (2006). A flavin-dependent tryptophan 6-halogenase and its use in modification of pyrrolnitrin biosynthesis. Biocatal. Biotransform. 24**,** 401-408. doi:10.1080/10242420601033738.

Sekine, H., Shimada, T., Hayashi, C., Ishiguro, A., Tomita, F., and Yokota, A. (2001). H^+-ATPase defect in *Corynebacterium glutamicum* abolishes glutamic acid production with enhancement of glucose consumption rate. Appl. Microbiol. Biotechnol. 57**,** 534-540. doi:10.1007/s002530100.

Siloto, R.M.P., and Weselake, R.J. (2012). Site saturation mutagenesis: Methods and applications in protein engineering. Biocatal. Agric. Biotechnol. 1**,** 181-189. doi:10.1016/j.bcab.2012.03.010.

Snell, E.E. (1975). Tryptophanase: structure, catalytic activities, and mechanism of action. Adv. Enzymol. Relat. Areas Mol. Biol 42**,** 287-333.

Speight, J.G. (2017). Chapter 3 - Industrial Organic Chemistry, in Environmental Organic Chemistry for Engineers*,* ed. J.G. Speight. Butterworth-Heinemann. 87-151.

Stansen, C., Uy, D., Delaunay, S., Eggeling, L., Goergen, J.-L., and Wendisch, V.F. (2005). Characterization of a *Corynebacterium glutamicum* lactate utilization operon induced during temperature-triggered glutamate production. Appl. Environ. Microbiol. 71**,** 5920-5928. doi:10.1128/AEM.71.10.5920–5928.2005.

Stolz, M., Peters-Wendisch, P., Etterich, H., Gerharz, T., Faurie, R., Sahm, H., et al. (2007). Reduced folate supply as a key to enhanced L-serine production by *Corynebacterium glutamicum*. Appl. Environ. Microbiol. 73**,** 750-755. doi:10.1128/AEM.02208-06.

Swift, S., and Stewart, G.S.A.B. (1991). The molecular biology of tryptophan synthase: A model for protein-protein interaction. Biotechnol. Genet. Eng. 9**,** 229-294. doi:10.1080/02648725.1991.10647882.

Tan, D.X., Hardeland, R., Back, K., Manchester, L.C., Alatorre-Jimenez, M.A., and Reiter, R.J. (2016). On the significance of an alternate pathway of melatonin synthesis via 5-methoxytryptamine: comparisons across species. J. Pineal Res. 61**,** 27-40. doi:10.1111/jpi.12336.

Tang, J., Zhu, X., Lu, J., Liu, P., Xu, H., Tan, Z., et al. (2013). Recruiting alternative glucose utilization pathways for improving succinate production. Appl. Microbiol. Biotechnol. 97**,** 2513-2520. doi:10.1007/s00253-012-4344-1.

Taniguchi, H., and Wendisch, V.F. (2015). Exploring the role of sigma factor gene expression on production by *Corynebacterium glutamicum*: sigma factor H and FMN as example. Front. Microbiol. 6**,** 740. doi:10.3389/fmicb.2015.00740.

Thomas, J.G., Ayling, A., and Baneyx, F. (1997). Molecular chaperones, folding catalysts, and the recovery of active recombinant proteins from *E. coli*. Appl. Biochem. Biotechnol. 66**,** 197-238. doi:10.1007/bf02785589.

Toyoda, K., Teramoto, H., Inui, M., and Yukawa, H. (2009). The *ldhA* gene, encoding fermentative L-lactate dehydrogenase of *Corynebacterium glutamicum*, is under the control of positive feedback regulation mediated by LldR. J. Bacteriol. 191**,** 4251-4258. doi:10.1128/JB.00303-09.

Toyoda, K., Teramoto, H., Yukawa, H., and Inui, M. (2014). Expanding the Regulatory Network Governed by the ECF-family Sigma factor σ^H in *Corynebacterium glutamicum*. J. Bacteriol.**,** JB-02248. doi:10.1128/JB.02248-14.

Tymiak, A.A., Rinehart Jr, K.L., and Bakus, G.J. (1985). Constituents of morphologically similar sponges: *Aplysina* and *Smenospongia* species. Tetrahedron 41**,** 1039-1047. doi:10.1016/S0040-4020(01)96471-3.

Van Pée, K.-H., Salcher, O., Fischer, P., Bokel, M., and Lingens, F. (1983). The biosynthesis of brominated pyrrolnitrin derivatives by Pseudomonas aureofaciens. J. Antibiot. 36**,** 1735-1742. doi:10.7164/antibiotics.36.1735.

Wehrmann, A., Morakkabati, S., Krämer, R., Sahm, H., and Eggeling, L. (1995). Functional analysis of sequences adjacent to *dapE* of *Corynebacterium glutamicum* reveals the

presence of *aroP*, which encodes the aromatic amino acid transporter. J. Bacteriol. 177**,** 5991-5993.

Welford, R.W.D., Vercauteren, M., Trébaul, A., Cattaneo, C., Eckert, D., Garzotti, M., et al. (2016). Serotonin biosynthesis as a predictive marker of serotonin pharmacodynamics and disease-induced dysregulation. Sci. Rep. 6**,** 30059. doi:10.1038/srep30059.

Wendisch, V.F., Brito, L.F., Lopez, M.G., Hennig, G., Pfeifenschneider, J., Sgobba, E., et al. (2016). The flexible feedstock concept in industrial biotechnology: metabolic engineering of *Escherichia coli*, *Corynebacterium glutamicum*, *Pseudomonas*, *Bacillus* and yeast strains for access to alternative carbon sources. J. Biotechnol. 234**,** 139-157. doi:10.1016/j.jbiotec.2016.07.022.

Wu, M., Repetto, B., Glerum, D.M., and Tzagoloff, A. (1995). Cloning and characterization of *FAD1*, the structural gene for flavin adenine dinucleotide synthetase of *Saccharomyces cerevisiae*. Mol. Cell. Biol. 15**,** 264-271. doi:10.1128/mcb.15.1.264.

Xie, J., Wang, L., Wu, N., Brock, A., Spraggon, G., and Schultz, P.G. (2004). The site-specific incorporation of *p*-iodo-L-phenylalanine into proteins for structure determination. Nat. Biotechnol. 22**,** 1297. doi:10.1038/nbt1013.

Yatsyshyn, V.Y., Fedorovych, D.V., and Sibirny, A.A. (2014). Metabolic and bioprocess engineering of the yeast *Candida famata* for FAD production. J. Ind. Microbiol. Biotechnol. 41**,** 823-835. doi:10.1007/s10295-014-1422-7.

Yatsyshyn, V.Y., Fedorovych, D.V., and Sibirny, A.A. (2010). Medium optimization for production of flavin mononucleotide by the recombinant strain of the yeast *Candida famata* using statistical designs. Biochem. Eng. J. 49**,** 52-60. doi:10.1016/j.bej.2009.11.010.

Yatsyshyn, V.Y., Ishchuk, O.P., Voronovsky, A.Y., Fedorovych, D.V., and Sibirny, A.A. (2009). Production of flavin mononucleotide by metabolically engineered yeast *Candida famata*. Metab. Eng. 11**,** 163-167. doi:10.1016/j.ymben.2009.01.004.

Yeh, E., Blasiak, L.C., Koglin, A., Drennan, C.L., and Walsh, C.T. (2007). Chlorination by a Long-Lived Intermediate in the Mechanism of Flavin-Dependent Halogenases. Biochem. 46**,** 1284-1292. doi:10.1021/bi0621213.

Yeh, E., Garneau, S., and Walsh, C.T. (2005). Robust in vitro activity of RebF and RebH, a two-component reductase/halogenase, generating 7-chlorotryptophan during rebeccamycin biosynthesis. Proc. Natl. Acad. Sci. U. S. A. 102**,** 3960-3965. doi:10.1073/pnas.0500755102.

Yoshikawa, E., Fournier, M.J., Mason, T.L., and Tirrell, D.A. (1994). Genetically engineered fluoropolymers. Synthesis of repetitive polypeptides containing *p*-fluorophenylalanine residues. Macromolecules 27**,** 5471-5475. doi:10.1021/ma00097a029.

Zambaldo, C., Luo, X., Mehta, A.P., and Schultz, P.G. (2017). Recombinant macrocyclic lanthipeptides incorporating non-canonical amino acids. J. Am. Chem. Soc. 139**,** 11646-11649. doi:10.1021/jacs.7b04159.

Zehner, S., Kotzsch, A., Bister, B., Süssmuth, R.D., Méndez, C., Salas, J.A., et al. (2005). A regioselective tryptophan 5-halogenase is involved in pyrroindomycin biosynthesis in *Streptomyces rugosporus* LL-42D005. Chem. Biol. 12**,** 445-452. doi:10.1016/j.chembiol.2005.02.005.

Zeller, W.E. (2001). Bromine in E-EROS Encyclopedia of Reagents for Organic Synthesis. Chichester: Wiley).

Zeng, J., and Zhan, J. (2011). Characterization of a tryptophan 6-halogenase from *Streptomyces toxytricini*. Biotechnol. Lett. 33**,** 1607-1613. doi:10.1007/s10529-011-0595-7.

Zhou, L., Shao, J., Li, Q., van Heel, A.J., de Vries, M.P., Broos, J., et al. (2016). Incorporation of tryptophan analogues into the lantibiotic nisin. Amino acids. 48**,** 1309-1318. doi:10.1007/s00726-016-2186-3.

3.6 Supplementary data

Table 3.1: Summery of feasible optimization steps to improve the production of 7-Cl-Trp and 7-Br-Trp and indole.

	Organism	Target compounds	Gene(s) (over)-expressed	Gene(s) knock-out	Final production/ Improvement	References
Halo-genation reaction	*E. coli*	Halo-genated Trp	Co-overexpression *groES-groEL*$_{Ec}$ with rebH		7 times higher expression of *rebH* (RebH: 15 mg L^{-1}; RebH + GroEL, GroES: 111 mg L^{-1})	(Payne et al., 2013)
	E. coli	Halo-genated Trp	Fusion protein (MBP) connected with ReF		2.5 times higher catalytic efficiency ($k_{cat,RebF}$=32 min^{-1}; $k_{cat,MBP-RebF}$=80 min^{-1})	(Payne et al., 2013)

	Organism	Target compounds	Gene(s) (over)-expressed	Gene(s) knock-out	Final production/ Improvement	References
Co-factor supply and regeneration ($FADH_2$ and NADH)	*C. glutamicum*	Riboflavin	*sigH*$_{Cg}$		32.4 ± 1.8 µM (12.9 ± 0.7 mg L^{-1})	(Taniguchi and Wendisch, 2015)
	C. glutamicum	Riboflavin, FMN	*sigH*$_{Cg}$, *ribF*$_{Cg}$		Riboflavin: 19.8 ± 0.3 µM (7.4 ± 0.1 mg L^{-1}) FMN: 33.1 ± 1.8 µM (15.1 ± 0.8 mg L^{-1})	(Taniguchi and Wendisch, 2015)
	C. glutamicum	Riboflavin, FAD		*rshA*	Riboflavin (intracellular): 1.1 mM/$OD_{610;}$ Riboflavin (extracellular): 8 mM (3 g L^{-1}); FAD (extracellular): 0.15 mM (0.12 g L^{-1})	(Toyoda et al., 2014)
	Candida famata	FMN	*FMN1*$_{Dh}$		231±4.11 mg L^{-1}	(Yatsyshyn et al., 2009)

	Organism	Target compounds	Gene(s) (over)-expressed	Gene(s) knock-out	Final production/ Improvement	References
	Candida famata	FAD	*FMN1*$_{Dh}$, *FAD1*$_{Dh}$		451 mg L^{-1}	(Yatsyshyn et al., 2014)
	C. glutamicum	NADH		*ldhA*	unknown	(Blombach et al., 2011)
	C. glutamicum	NADH		H+-ATPase	0.53 ± 0.11 mM (0.35 ± 0.07 g L^{-1})	(Sawada et al., 2012)
Precursor supply Trp biosynthesis	*C. glutamicum*	Sugar uptake	*iolT2*$_{Cg}$, *glcK*$_{Bs}$		Growth rate: WT: 0.32 ± 0.01 h^{-1} WT + iolT2$_{Cg}$ + *glcK*$_{Bs}$: 0.37 ± 0.01 h^{-1}	(Pérez-García et al., 2016)

	Organism	Target compounds	Gene(s) (over)-expressed	Gene(s) knock-out	Final production/ Improvement	References
	C. glutamicum	Shikimate	tkt_{Cg}, tal_{Cg}, $aroG^{S180F}{}_{Cg}$, $aroBDE_{Cg}$, $iolT1_{Cg}$, $glks_{Cg}$ ($glk1_{Cg}$, $glk2_{Cg}$, $ppgk_{Cg}$), $gapA_{Cg}$	*ptsH, aroK, qsuB, qsuD (hdpA)*	With *hdpA*:480 ± 68.3 mM (84 ± 12 g L^{-1}) Deleted *hdpA*: 536 ± 61.0 mM (93 ± 11 g L^{-1})	(Kogure et al., 2016)
	C. glutamicum	PEP		*pyk*	21432,5 pmol 20ODmL^{-1}	(Sawada et al., 2015)
	E. coli	DHAP	$ppsA_{Ec}$		1.37 ± 0.30 mmol DAHP gCDW^{-1}	(Gosset et al., 1996)

	Organism	Target compounds	Gene(s) (over)-expressed	Gene(s) knock-out	Final production/ Improvement	References
	C. glutamicum	E4P	tal_{Cg}, tkt_{Cg}	*aroK, qsuB, qsuD*	unknown	(Kogure et al., 2016)
	C. glutamicum	E4P	$xylAB_{Xc}$		unknown	(Mao et al., 2018)
	C. glutamicum	Shikimate	$aroG^{FBR}{}_{Ec}$, $aroF^{FBR}{}_{Ec}$, $ubiC^{FBR}{}_{Ec,}$ $qsuC_{Cg}$, $aroCKB_{Cg}$	*trpE, csm, pobA, vdh, qsuABCD*	0.80 ± 0.13 g L^{-1}	(Kitade et al., 2018)
	C. glutamicum	Shikimate	tkt_{Cg}, tal_{Cg}, $aroG^{S180F}{}_{Cg}$, $aroBDE_{Cg}$	*aroK, qsuB, qsuD*	291 ± 15 mM (51 ± 3 g L^{-1})	(Kogure et al., 2016)
Improved Trp biosynthesis	*C. glutamicum*	Trp		*ltbR*	Enhanced expression of the *trp* operon	(Brune et al., 2007)

Organism	Target compounds	Gene(s) (over)-expressed	Gene(s) knock-out	Final production/ Improvement	References
C. glutamicum	Trp	*aroI/II, trp* operon (after muta-genesis)		43 g L^{-1}	(Katsumata and Ikeda, 1993)
C. glutamicum	L-serine	Regulated *glyA*, $serA^{FBR}{}_{Cg,}$ $serB_{Cg}$, $serC_{Cg}$	*sdaA, (pabABC)*	With *pabABC* 86 mM (9 g L^{-1}) Deleted *pabABC* 345 mM (36 g L^{-1})	(Peters-Wendisch et al., 2005; Stolz et al., 2007)
C. glutamicum	Trp	*aroI/II, trp* operon (after muta-genesis), *serA*		50 g L^{-1}	(Ikeda et al., 1994)

	Organism	Target compounds	Gene(s) (over)-expressed	Gene(s) knock-out	Final production/ Improvement	References
Transport system	*C. glutamicum*	Trp		*aroP*	10 – 20 % increased production	(Ikeda and Katsumata, 1995)

Danksagung

Mein Dank gilt vor allem Herrn Prof. Dr. Volker Wendisch für die Überlassung dieses spannenden Themas, für die gute Betreuung und ständige Bereitschaft zum Gespräch sowie für die Förderung und Unterstützung.

Danken möchte ich auch apl. Prof. Dr. Jörn Kalinowski für die freundliche Übernahme des Koreferats.

Vielen Dank an Dr. Petra Peters Wendisch, Dr. Melanie Mindt und Tatjana Walter für das Korrektur lesen und hilfreichen Anregungen.

Mein Dank gilt Prof. Dr. Jin-Ho für die Überlassung der rekombinanten Coryne-Stämme. Auch danke ich Dr. Joe Max Risse und Thomas Schäffer für die Hilfe bei der Durchführung der Bioreaktor-Prozesse, sowie Hannah Minges, Steffen Dachwitz und Dr. Christian Schnepel für die Hilfe bezüglich chemischer und biochemischer Fragestellungen.

Meinen Laborkollegen Anastasia, Kerstin und Marina danke ich für die tolle Atomasphäre im Labor und die gegenseitige Unterstützung. Lieben Dank an meine Büropartner Kerstin, Melanie und Silvin für die tollen Gespräche.

Lieben Dank an die ganze “genpro”-Gruppe: Anastasia, Arthur, Ayham, Carina, Carlos, Carsten, Elvira, Fernando, Florian, Giu, Guido, Ina, Irene, João, Kerstin, Lenny, Luciana, Marina, Marta, Melanie, Mila, Nadja, Nour, Petra K, Petra PW, Pierre, Sabine, Silvin, Susanne und Tatjana. Außerdem danke ich meinen Studenten Anastasia, Anja, Konstantin, Max, Pascal und Sascha.

Danken möchte ich natürlich meinen Freunden und besonders meiner Familie für die Unterstützung und den Zuspruch.

Ein besonderer Dank geht an André für die große Unterstützung, die Geduld und das Verständnis.

Erklärung

Hiermit erkläre ich, dass ich die vorliegende Dissertation eigenständig und ohne unerlaubte Hilfsmittel angefertigt habe. Ich versichere, dass ich keine anderen als die angegebenen Quellen und Hilfsmittel benutzt, sowie Zitate kenntlich gemacht habe. Diese Dissertation wurde in der vorgelegten oder in ähnlicher Form noch bei keiner anderen Institution eingereicht. Ich habe bisher keine erfolglosen Promotionsversuche unternommen.

Bielefeld, den 21.11.2019

_____

Kareen Hildegard Veldmann